中国科学院上海应用物理研究所

年 报

2003—2004

（第 21 卷）

《中国科学院上海应用物理研究所年报》
编辑委员会

内容简介

本刊为 2003—2004 年度中国科学院上海应用物理研究所年报。该年报介绍了全所各科研机构两年的主要科研工作进展。内容按照上海光源、核物理、核分析技术、纳米生物医药、应用加速器、辐射技术、放射性药物、先进探测仪器、环境治理技术、核技术的开发和产业化顺序以中英文两种文字进行介绍。附录记载了 2003—2004 年度所学术活动、人才培养、国际交流的情况。

本年报供上海应用物理研究所的上级主管中国科学院和上海市各有关部门的领导及各类管理人员阅读；供各科研院所中相关领域的科研人员、高等院校师生，以及本所的科研人员及研究生阅读、参考。

前　言

把握机遇，重点突破，谋求跨越式发展

2003—2004 年，我所在中国科学院的领导下，学习和贯彻中国共产党十六大精神，贯彻中国科学院新时期发展战略，以所的更名为契机，以上海光源工程的立项和建设为全所工作的重中之重，积极争取科研任务，认真执行在研项目，大力开展实验平台建设，扩大学术交流与合作，着力建设创新人才队伍，努力提升研究生教育工作水平，不断完善研究所运行机制，进一步推进园区建设，深入开展创新文化建设，推动科技企业改制重组，为我所的“创新跨越、持续发展”奠定了坚实的基础。

一、明确发展目标，凝炼学科方向，完善学科布局

2003 年，我所经中国科学院批准更名为“中国科学院上海应用物理研究所”。所的更名标志着我所学科方向的重大调整，即从传统的核技术科学研究为主，转向以第三代同步光源、新型自由电子激光和先进离子束装置的研制及其相关的学科研究为主要学科方向。以此为契机，我所提出了“面向世界科学前沿开展科学平台的建设和运行及相关应用研究，面向国家社会经济需求开展核技术应用研究及其产业化”的中长期发展规划，进一步明确所的定位和学科发展方向，确立了建设我院上海多学科研究中心和一流研究所的发展目标。在重点学科的方向调整中，瞄准国家目标和领域前沿，召开所级专题学术研讨会 4 次，部署了 7 项纳米科学、T-ray 应用导向性研究项目以及所学科创新战略行动计划项目“研制超短电子束实验装置及相干红外光源”。2004 年，借助上海光源正式立项开工建设的大好机遇，按照所中长期发展规划“两个面向”的战略构想，进一步提出了我所在新阶段及未来十五年的创新体系与学科建设框架。这是一个以两个园区的有机整合为核心的发展框架，其学科布局及与之相应的科研结构包括上海光源大型科学平台建设与运行、基于先进光源与核技术的交叉学科研究、核物理研究、核技术科学的应用研究，其发展目标是建设我院上海多学科综合研究中心和一流的研究所；在此基础上，基本确定了我所创新三期方案的框架，启动新一轮学科目标的凝炼和科研结构的调整。在全力推动上海光源工程各项工作的同时，按照我所创新试点实施方案的要点，建设“一大装置”——上海光源、“两个园区”——嘉定园区和张江园区”，全面推进知识创新试点工作。

二、上海光源国家重大科学工程立项开工

2003 年，在中国科学院和上海市的领导下，我所以举所体制，领导分工把关，各研究室和职能部门密切协同，全力推动上海光源的立项工作，于 2004 年 1 月获得国务院正式批准项目建议书，上海光源国家重大科学工程正式立项。作为工程承担单位和项目法人单位，我所将上海光源工程列为本所“重中之重”的工作，确保工程节点计划和年度任务按时完成。2004 年 6 月，完成工程可行性研究报告；6 月 29 日，工程领导小组第一次会议审定工程可行性研究报告，并决定了上海光源工程领导组织机构；7 月，通过了国家发展和改革委员会委托中国国际工程咨询公司组织的专家评估。10 月 25 日，工程科学技术委员会举行会议，就工程初步设计、光束线站建设等问题提出了咨询意见。11 月，工程可行性研究报告获得国家发展改革委批复；同期，工程经理部完成了工程初步设计，并先后通过了中科院与上海市共同组织的初步设计预评审、国家发展改革委组织的评估；12 月 24 日，初步设计及开工报告获得批准。12 月 25 日，上海光源（SSRF）国家重大科学工程开工典礼在浦东张江隆重举行，上海光源工程正式破土动工。

三、积极争取科研项目，加快科技成果产出

2003—2004 年，共争取科研项目 46 项，包括上海光源国家重大科学工程、国家 973 项目 1 项、国家发展改革委专项 2 项、国家杰出青年基金 1 项、基金委重大项目 1 项等。其中，973 项目“基于超导加速器的 SASE 自由电子激光物的关键物理及技术问题的研究”共有 8 个子课题，我所承担其中的 4 个，我所赵振堂研究员任该项目副首席科学家。全所经费收入较往年有大幅度的提高，两年分别为 1.02 亿元和 1.05 亿元。部署领域前沿项目 10 项、所级创新项目 11 项。

两年内，共申请专利 37 项，已获授权专利 14 项；发表论文 381 篇，其中 SCI 收录论文 172 篇；组织完成科研项目结题验收 25 项。“现代核分析技术在生态系统中若干前沿问题的研究”获 2004 年度上海市科技进步三等奖。

多项重大科研项目的研究工作取得可喜的成果和进展。上海同步辐射装置预制研究项目通过国家组织的验收；烟气脱硫超大功率电子加速器研制成功，指标达到 700keV、300mA；研制出浸没式平片滤膜元件，填补了国内空白；1200mm 量程的新型长程面形仪通过验收，综合性能指标达到国际先进水平。100MeV 电子直线加速器以及上海 EBIT 装置如期完成总装，并于 2004 年底顺利出束；973 项目“放射性核束物理与核天体物理”和 RHIC-STAR 国际合作研究取得多项创新成果；深紫外自由电子激光（DUV-FEL）的研究、THz 技术及应用研究、DNA 单分子操纵与蛋白结晶的研究、微束在团簇中的输运机制及相关效应研究等重大项目取得可喜进展。

四、发挥特色，推进实验室及实验平台建设

仪器与设备的研制和改造、实验方法学的研究是我所的特色。截至 2004 年底，已建成 PC-FARM 集群计算系统、高电压实验室、生化实验室、T-ray 实验室、X 射线成像实验室，并投入使用。上海市低温超导高频腔技术重点实验室、分子标记及核素分子显像实验技术平台的建设也取得了阶段性的成果。与上海世龙科技有限公司联合建立了电池隔膜研究联合实验室，进一步提高民用非动力核技术的研究水平。在 2004 年中国科学院组织的院重点实验室的评估中，核分析重点实验室经过多方面的努力最终评为“B”，下一目标是争取建设成为国家重点实验室。在推进实验室及试验平台建设的同时，加强实验室的管理，在 2003 年出台了所大型共用仪器设备及公用实验室管理办法。

五、积极扩大国际国内学术交流与合作

以与国际上拥有同步辐射装置的国家在装置建设、运行、应用研究、科研人员学术交流等方面实行全面合作为主，同时开展多领域、多元化的国际合作。两年间，分别与韩国浦项光源（PLS）、德国罗森道夫研究所（FZR）、瑞士保罗•谢尔研究所（PSI）、日本佐贺大学同步辐射光应用中心（Saga University Synchrotron Light Application Center）签订所际合作协议。2004 年 8 月在日本 Spring-8 召开 SSRF 光束线站设计研讨会，在北京主办了“QCD 和 RHIC 物理”国际研讨会；以我为主开展高水平国际合作与交流，2004 年在所学术活动中心举办了我所系列国际学术研讨会“纳米与离子束间相互作用国际研讨会”（IWINP），主办世界华人物理大会卫星会议“储存环束流稳定性与不稳定性学术研讨会”。在扩大科研方面国际合作的同时，推进研究所管理和工程项目管理工作的国际化，2003 年首次组织管理人员访问日本 JASRI 和 KEK；2004 年 6 月邀请国际、国内的科学工程管理专家主讲，举办了上海光源工程项目管理培训暨研讨会。

六、推进科技企业改革和产业发展规划

自 2003 年确定所属科技企业改制与发展框架以来，不断加快与社会资源结合的步伐，加强与国外知名企业的合作，强化投资企业制度化管理的建设，为促进我所科技产业未来规模发展创造了良好的基础。2003 年完成上海科兴公司的工商注册登记，2004 年正式改制更名为安盛科兴药业

有限公司，美国 GE 公司持有其 70%的股权，原所编职工顺利完成了身份置换；所属全资公司上海核技术开发公司于 2004 年 4 月改制为上海日环科技投资有限公司;所后勤服务中心顺利完成改制，定名为“上海日环科技服务有限公司”，由所控股，公司管理骨干个人参股。2004 年，以研究所为依托，以所属企业为主体，争取到国家发改委“民用非动力核技术高技术产业化” 的两个项目；研究所与企业联建“电池隔膜联合实验室”，并设立了“电池隔膜联合实验室实验基地”，为提高企业的研发能力、提升企业的研发水平、加快科技成果的转化速度搭建了一个良好的平台。试行企业经营者年薪制，并在企业年度经营考核指标的选取、计划的制定、中期经营状况的跟踪及报告规范、年度考核等方面建立了一系列制度并加以完善，强化企业的年度审计，在企业的制度化管理上走出了坚实的一步。2003—2004 年，全所科技产业销售总收入均为 9300 万元左右，与往年相比基本持平；利润 400 万元左右，较 2002 年有显著提高；辐射改性材料、辐照装置、体内放射性药物的市场销售一直保持较快的增长，盈利能力也保持较高的水平。

七、健全人才政策体系，加快人才队伍建设

2003—2004 年，结合本所学科调整，采取特殊措施，讲求实效，引进和培养相应人才。进一步完善人才引进与管理、岗位聘任与考核的制度体系，相继出台了招聘“百人计划”三年计划、研究生招生计划、紧缺人才引进实施方案、“百人计划”管理细则、博士后流动站管理办法、新职工住房补贴、研究生导师条例、再就业中心管理补充规定等政策性文件，建立起一套符合我所特点的政策体系框架。在此基础上，以上海光源工程为重点，根据所中心工作的需要调整业务骨干（中层干部）的配置，进一步优化人力资源结构，加速进行我所的人才队伍建设。为确保上海光源工程建设任务的完成，已向中国科学院报告上海光源工程和我所创新三期人才队伍建设的方案。调整工程组织结构，推行矩阵管理模式，初步完成队伍组建和设岗聘任。同时积极创造条件，落实相关配套政策，通过现有队伍的培养提高、引进急需的工程技术骨干、加强国际合作和兄弟单位间的合作、长期或短期项目聘任、试行秘书制等手段，多渠道、多途径解决工程建设队伍的人员需求。2003—2004 年，我所包括上海光源工程共引进“百人计划”8 人、博士 43 人；招收博士生 89 人、硕士生 110 人；聘请诺贝尔奖获得者李政道先生为我所名誉教授；先后聘请 6 名杰出海外华人科学家为我所客座研究员。

完善研究生教育制度，试行弹性学制与学位论文“盲评”制度，提高教育质量。研究生招生数量与质量逐年上升，2003—2004 年共招收研究生 192 名，其中博士研究生 82 名。至 2004 年年底，在读研究生总数为 232 人，其中博士生 110 人。抓住入学教育、学位课程学习、学位论文开题、中期考核、预答辩、答辩等环节搞好培养工作，研究生教育成绩显著。两年中获得中国科学院院长奖学金优秀奖 3 人，“刘永龄”奖学金 2 人，中国科学院博士学位优秀论文 2 篇，上海市研究生优秀成果 1 项。

八、逐步完善管理体制，推进创新文化建设

2003—2004 年，我所进一步规范管理，努力营造创新与开放的文化氛围。制订或修订各类规章制度 61 项、废止 47 项，逐步建立和完善了一套适应于科技创新活动客观需求的管理制度体系。2003 年，以调整完善聘任制度为主，建立了管理岗位按需设岗、公开招聘、竞争上岗、择优聘任的机制，建立了科研岗位的设置、调整机制以及技术支撑岗位聘任制度，形成了科研、管理、技术支撑三个系列较为完整的聘任体系；制订和完善科研人员量化考核办法、科技企业量化考核办法并在全所试行。根据形势发展，及时调整所的科研管理和财务管理制度，修订了财务支付管理办法、课题管理办法、科研基金管理条例等规章制度，完善部门预算制度，以预算管理为抓手，加强研究所财务管理。

提升所的外部形象，扩大对外宣传。完成了研究所形象标识和视觉识别系统（VIS）的设计，

一个全新的、以创新和开放为核心价值观的形象标识系统已在全所推广。积极组织参加全国和上海市的大型群众性科普活动，参加上海国际工业博览会、全国科普活动周，组织并接待千余名大、中、小学生科普参观，进行相关核科学知识及科学发展观的宣传教育。加快所嘉定园区的建设步伐，成果显著。2003—2004 年相继完成了学术活动中心、102 综合楼、道路和绿化景观（改造）、实验工厂（所自筹）、113 实验楼、105 实验楼、信息中心楼的改造，启动了 109 实验楼、行政楼及所南大门、研究生宿舍的改造工程。嘉定园区“成为环境优美、安全宁静、宜于科研人员工作和休息的‘科学花园’”的建设目标已初具模样。

开展 “文明部门”评选活动，总结、交流各部门在创新文化建设方面的经验；在党员、干部和科研骨干中开展政治理论和管理知识的系列培训，由所党政主要领导作系列讲座，着重解决长期以来阻碍我所发展的观念问题；召开研究生思想政治工作研讨会，结合研究生思想状况调查报告，研讨当前青年思想教育工作的思路和方法。根据我所的实际情况，通过各种会议和多种形式的活动，加强思想道德建设，提升了职工对创新文化和科学发展观的理解。

2003—2004 年，我所在学科方向调整、科研任务争取、人才队伍建设、体制机制改革、创新文化建设等各个方面都取得了可喜的成绩，上海光源国家重大科学工程的开工建设更是给我所的发展带来了前所未有的大好机遇。历经艰辛筑成的发展道路已在我们面前展开，而前行中将面临的各种考验才刚刚开始。我们必须在今后的几年内，再接再厉，全力以赴，按时、优质地完成上海光源工程的建设和其他科研任务，同时，建设高水平的人才队伍，不断提升研究生教育水平，为尽早实现将我所建成国际化一流研究所的目标而努力工作。

2001 年－2005 年所领导成员

所　　长　徐洪杰

副 所 长　陆晓峰　朱志远　赵振堂

顾　　问　曹珊珊

所长助理　李　燕　马余刚　陈勋远　周福根

第 3 届学术委员会

主　任　杨福家

副主任　徐洪杰　沈文庆　李民乾　汪勇先

秘　书　李　燕

委　员　（以姓氏汉语拼音为序）

冯　军　顾嘉辉　归寿造　胡　钧　李德明　李民乾　李民熙
李文新　李　燕　陆晓峰　马余刚　钱春梁　邱士龙　沈天健
沈文庆　盛康龙　汪勇先　徐洪杰　许晓明　杨福家　姚思德
张桂林　赵小风　朱德彰　朱志远

目 次

上海光源

核物理

核分析技术

纳米生物医药

应用加速器

辐射技术应用

放射性药物

先进探测仪器

新技术中心

核技术开发和产业化

附　录

上海光源

Shanghai synchrotron radiation facility

上海光源简介

● **加速器物理与射频技术部：**加速器物理高频部主要从事与同步辐射光源相关的先进加速器物理及电类技术研究。本部下设加速器物理、高频技术、直线加速器等 3 个专业组，本部现有专业技术人员 46 人，职工共 30 人,在读研究生 16 人。目前该部主要承担 SSRF 相关部分的加速器物理设计与调试、高频与微波技术系统的研制、SSRF 100MeV 电子直线加速器的调试、10 MeV 皮秒电子加速器的改造、30 MeV 飞秒电子加速器及高亮度相干 T-ray 源的研制等研究任务。

● **束流测量与控制技术部**

● **机械工程部：**本部包括四个专业组：真空，磁铁，机械和低温。现有人员 21 人，其中研究员 5 人，副研及高工 5 人，博士研究生 3 人，硕士研究生 4 人。专业领域： 精密大型磁铁的设计制造；三维复杂电磁场计算、精密磁场测量；低温超导高频技术、超导高频腔设计和制造技术；大型无油超高真空的获得与测量技术、先进真空方法和技术跟踪、检漏技术、真空压强分布计算；大型复杂真空室的设计制造、精密和特种真空部件的制作；精密三维微动支架和平台的设计制造、三维计算机辅助机械设计；精密准直测量和校准技术，复杂系统的总体设计和加工制造。工作进展：(1)上海光源机器机械部分的总体设计制造和总装以及各系统设计，包括真空、磁铁、支架、低温。已完成有关初步设计，正在进行优化设计。(2) SDUV-FEL 高能量电子束团压缩物理与技术研究，已完成物理设计，开始进行工程设计。(3)负责上海 EBIT 真空、机械准直、低温超导、注入引出等系统的设计、制造、安装、调试。(4)参与 100 MeV 直线加速器建造。(5)其他实验装置：10 MeV 皮秒电子加速器的改造、30MeV 飞秒电子加速器及高亮度相干 THz 光源的研制。

● **电源技术部：**本部包括磁铁电源组和高压脉冲组。磁铁电源专业方向为大功率高稳定度特种磁铁电源的设计与制造，其研究领域包括大功率开关电源技术、数字化电源技术，和设备级计算机控制技术。现完成了 100MeV 直线加速器电源系统和超短电子束实验装置电源系统的建立任务，以及 SSRF 磁铁电源系统初步设计任务。电源组目前承担 SSRF 电源系统的建造任务。电源组拥有各种精密电学测量仪器和大功率电源设备试验场所，并拥有一支精干的研究队伍，为各类电源设备的研制和培养年轻人提供了良好的平台。高压脉冲组的专业方向为高压大电流快脉冲技术、新一代同步加速器的注入引出技术、高功率微波开关技术。具体的研究内容包括高性能大功率脉冲调制器、快冲击磁铁和切割磁铁及其电源的研制等等。近两年来完成了 110MW 脉冲调制器的研制，超短电子束实验装置脉冲功率源的恢复和优化改造等任务和 SSRF 注入引出系统的初步设计任务。目前的主要工作任务为 SSRF 储存环和增强器的注入引出系统及直线加速器的脉冲调制器的研制。

● **共用设施技术部**

● **同步辐射实验室与束线工程部：**部门主要任务围绕上海光源光束线站建设及其同步辐射应用研究。主要研究方向为： 同步辐射光束线技术及相关光学检测技术；同步辐射实验新方法以及在生命科学、材料科学、环境科学、成像、超快等领域的应用。过去的二年中，完成了上海光源首批光束线站设计和光学检测仪器研制（LTP）项目，并在 X 射线成像及蛋白质晶体学研究等方面开展了一系列工作，取得了较好的进展，逐步建立了一支以年轻科研骨干为主体的研究队伍。

SDUV-FEL 系统中基于 CORBA 组件的三层数据库应用初步设计

孙小影　沈立人　戴志敏

关键词　数据库，公共对象请求代理规范，自由电子激光

分析了加速器系统中常用的二层数据库结构存在的不足。对正在开发的上海深紫外自由电子激光（SDUV-FEL）数据库系统进行了探讨，提出了一种基于公共对象请求代理规范 (CORBA) 组件技术、用 C++构建中间件模型来实现三层数据库结构的方案， 并用一个简单的磁铁信息的例子说明了 CORBA 组件的设计过程。

Design of multi-tiered database application based on CORBA component in SDUV-FEL system

SUN Xiaoying　SHEN Liren　DAI Zhimin

Keywords　Database, Common object request broker architecture (CORBA), Free electron laser

In this paper, the drawback of usual two-tier database architecture was analyzed and the Shanghai Deep Ultraviolet-Free Electron Laser database system under development was discussed. A project for realizing the multi-tiered database architecture based on common object request broker architecture (CORBA) component and middleware model constructed by C++ was presented. A magnet database was given to exhibit the design of the CORBA component.

上海同步辐射装置中所用电子枪

盛树刚　林国强　顾 强　李德明

关键词　热离子枪，EGUN 程序

上海同步辐射装置电子枪是一台输出电子束能量 100 keV 的栅控电子枪，是上海同步辐射装置直线加速器的电子源。为了和上海同步辐射装置的储存环的运行模式相一致，该电子枪有两种工作模式：单束团模式和多束团模式。本文主要介绍了该电子枪的两种工作模式的性能和一些主要部件。

Electron gun for SSRF

SHENG Shugang LIN Guoqiang GU Qiang LI Deming

Keywords Thermionic gun, EGUN

A 100 kV triode-electron-gun has been designed and manufactured for the Linac of Shanghai Synchrotron Radiation Facility (SSRF). In this paper the performance of the gun and some key components are described.

储存环部分填充情况下的纵向耦合不稳定性

赵振堂 姜伯承

关键词 储存环，纵向耦合不稳定性，虚部阻抗

本文通过解析的方法分析了储存环在部分填充情况下的纵向耦合不稳定性，给出了不稳定性增长率和同步振荡频移的表达式。得到了一个有趣的结果：虚部阻抗对不稳定性的增长率也有贡献。这一点和均匀填充情况是不一样的。

Longitudinal coupled bunch instability in fractionally filled storage rings

ZHAO Zhentang JIANG Bocheng

Keywords Storage ring, Longitudinal coupled bunch instability, Imaginary part of impedance

Longitudinal coupled bunch instability in fractionally filled storage rings is studied in this paper. An analytic method is used to achieve the growth rate of the instability as well as the synchrotron oscillation frequency shift. An interesting phenomenon has been found that imaginary part of impedance makes contribution to the growth rate of the coupled bunch instability. This phenomenon is never observed in symmetrical cases.

SSRF 储存环轨道稳定性研究

戴志敏　刘桂民　黄　楠[1]

关键词　同步辐射光源，储存环，轨道控制

本文报告了 SSRF 储存环束流轨道稳定性分析和束流轨道反馈研究初步结果。束流轨道稳定性分析表明，储存环中束流水平轨道运动幅度小于束流水平轨道稳定性要求，但束流垂直轨道运动幅度远超过束流垂直轨道稳定性要求。我们提出了一个动态束流垂直轨道校正方案以减小储存环中束流垂直轨道运动幅度。该束流轨道校正系统由 38 个具有高同频带的空心线圈和 38 个高稳定的束流位置探测器组成。数值模拟结果表明，该束流轨道校正系统能够有效地抑制 100 Hz 内束流垂直轨道运动。

1 中国科学院高能物理研究所

Study of orbit stability in the SSRF storage ring

DAI Zhimin　LIU Guimin　HUANG Nan[1]

Keywords　Synchrotron radiation light source, Electron storage ring, Beam orbit control

In this paper, analysis of the beam orbit stability and conceptual study of the dynamic orbit feedback in the SSRF storage ring are presented. It is shown that beam orbit motion at the photon source points is smaller than the orbit stability requirements in horizontal plane, but exceeds the orbit stability requirements in vertical plane. A dynamic global orbit feedback system, which consists of 38 high-bandwidth air-coil correctors and 40 high-stable BPMs, is proposed to reduce the vertical orbit motion. Numerical simulations show that this dynamic orbit feedback system can stabilize the vertical orbit motion in the frequency up to 100 Hz.

1 Institute of High Energy Physics, the Chinese Academy of Sciences

SSRF 储存环磁聚焦结构设计

戴志敏　刘桂民　黄　楠

关键词　同步辐射光源，电子储存环，磁聚焦结构

上海同步辐射装置（简称 SSRF）是一台拟建的第三代同步辐射光源，其设计能量为 3.5 GeV。SSRF 由 20 个 DBA 单元组成，周长 396 m，自然发射度约 10 nm·rad。它可提供 10 个 7.24 m 的长直线节和 10 个 5.0 m 长的短直线节，用以安装插入件、高频腔及注入系统等。SSRF 的磁聚焦结构十分灵活，它的工作点和包络函数都可以在较大范围内调解以满足不同用户的需求，包括高包络函数模式和混合模式以及直线节消色散和不消色散模式等。本文报告 SSRF 的线性磁聚焦光学和动力学孔径研究结果。

Design of the SSRF storage ring magnet lattice

DAI Zhimin LIU Guimin HUANG Nan

Keywords Synchrotron radiation light source, Electron storage ring, Magnet lattice

The Shanghai Synchrotron Radiation Facility (SSRF) is a proposed 3rd generation light source with 3.5 GeV in energy. It is composed of 20 DBA cells resulting in a ring that is about 10 nm·rad in emittance and 396 m in circumference, and provides 10 straight sections of 7.24 m and 10 straight sections of 5.0 m for the inclusion of insertion devices, injection components and RF cavities. The lattice has high flexibility, and the tunes and beta functions can be easily adjusted within a wide range to meet the requirements for different operation modes, including high beta mode and hybrid beta mode with and/or without dispersion in straight sections. In this paper, the results of linear optics design and dynamic aperture study are presented.

多线程通信方法在高频幅度控制中的应用

张建兵 王 芳

关键词 高频系统，环路控制，激励电平，串口通信

高频系统幅度控制环路开环时，束流将会在腔上引入与正常工作腔压可比的场，流强升高时束流要从腔得到更多功率，此时腔自身消耗的功率保持不变，这就要求高频幅度控制发挥作用，满足束流和腔功率的要求。作为高频系统监控程序的一个组成部分，本文采用了多线程串口通信的方法实现对 SSRF 高频系统激励电平的控制。

Application of multi-threading communication in RF amplitude control

ZHANG Jianbing WANG Fang

Keywords RF system, Loop control, Driver low-level, Serial communication

When the amplitude loop of the RF system is opening, the beam will introduce a field that can compare with the working cavity voltage. As the beam energy is higher, the beam needs more power from the cavity and the dissipated power on the cavity should keep unchanged. The RF amplitude control is consequently necessary to meet requirements for beam current and cavity power. As a constituent of the monitor programs, a method of multi-threading serial communication to control the driver low-level of the RF system in SSRF is introduced.

500MHz 高频腔自动调谐控制系统

王 芳 陆建法 王光伟[1]

关键词 腔体，调谐，PLC 控制

上海同步光源(SSRF)的储存环中使用 8 个 500MHz 的高频加速腔。这些腔中的每一个腔的调谐过程都靠一个调谐器控制系统。调谐器控制系统将弥补相位漂移和腔内的扰动并保持在所希望的调谐环境，失谐相位角的误差不超过 1°。调谐控制系统使用了较为先进的 PLC 控制，以保证频率的稳定性，进而达到自动调谐的目的。该系统经过高功率实验运行，性能指标达到了设计要求。

1 中国科学院高能物理研究所

The phase servo tuner control system of the SSRF 500MHz cavity

WANG Fang LU Jianfa WANG Guangwei[1]

Keywords Cavity, Tune, PLC control

Eight 500MHz cavities are designed in the storage ring of the SSRF (Shanghai Synchrotron Radiation Facility). For each cavity, a control system is required to keep the cavity in tune during operation. The tuning is performed between the drive signal and the cavity probe signal. The error signal is amplified and used to drive a stepping motor which in turn moves a metallic plunger by PLC in or out of the cavity to achieve tuning. The tune speed is 1kHz/sec.

1 Institute of High Energy Physics, the Chinese Academy of Sciences

SSRF 高频低电平系统预制研究

王 芳 王光伟

关键词 低电平，反馈环路

工作频率为 500MHz 的高频加速系统，主要由三部分构成：谐振加速腔、微波功率源和 180kW 速调管、低电平控制与连锁保护。SSRF 预研阶段已经完成了一套低电平控制系统，它主要由 500MHz 信号源、三个反馈控制环路和连锁保护构成。本文重点介绍三个反馈环路的设计、调试测量结果。

Low level RF control system for SSRF

WANG Fang WANG Guangwei

Keywords Low level, Feedback, Control loop

One set of low level control system was developed in the R&D stage of SSRF. It consists of a 500 MHz signal generator, three feedback loops, an interlock and a protection system. This paper describes the design, commissioning and measurement results of this system, placing emphasis on the three feedback loops.

双波荡器自由电子激光理论

戴志敏

关键词 自由电子激光，双波荡器

给出了双波荡器自由电子激光器的通用理论。在双波荡器自由电子激光器中，引入了一个周期长度非常接近主波荡器中电子束感应加速振荡周期的附加波荡器。推导出了一套自洽方程组描述双波荡器中自由电子激光场演变过程，并分别给出了低增益、高增益和饱和三种情况下的解析解。研究表明，适当选择附加波荡器的参数，可以提高自由电子激光器的增益或转换效率。

Theory of a double-undulator free-electron laser

DAI Zhimin

Keywords Free-electron laser, Double undulator

In this paper, we present a general theory of the double-undulator free-electron laser, in which an additional undulator with period close to the beam electron betatron oscillation period in the main undulator is introduced. A set of self-consistent equations is developed to describe the evolution of the optical wave in this device. The basic nonlinear equations are analyzed in the low-gain regime, the high-gain regime, and the saturation regime, respectively. By properly selecting parameters of the additional undulator, it may enhance the gain or efficiency of the free-electron laser.

上海高增益谐波放大深紫外自由电子激光实验装置

赵振堂　戴志敏　赵小风　刘德康　周巧根

何多慧[1]　贾启卡[1]　陈森玉[2]　戴建枰[2]

关键词　高增益谐波放大，自由电子激光，深紫外

上海深紫外自由电子激光实验装置（简称 SDUV-FEL）是以高增益谐波放大模式产生最短波长达 88nm 的高功率激光。从 2000 年开始 SDUV-FEL 的设计与预制研究。目前，150MeV 电子直线加速器作为 SDUV-FEL 的第一段高亮度电子束注入器正在建造中。本文介绍 SDUV-FEL 的设计研究和预制研究情况。

1 中国科技大学国家同步辐射实验室

2 中国科学院高能物理研究所

The Shanghai high-gain harmonic generation DUV free-electron laser

ZHAO Zhentang　DAI Zhimin　ZHAO Xiaofeng　LIU Dekang　ZHOU Qiaogen

HE Duohui[1]　JIA Qika[1]　CHEN Senyu[2]　DAI Jianping[2]

Keywords　High-gain harmonic generation, Free-electron laser, Deep ultraviolet

The Shanghai deep ultraviolet free-electron laser source (SDUV-FEL) is an HGHG FEL facility designed for generating coherent output with wavelength down to 88 nm. The design and the relevant R&D of this HGHG FEL source have been under way since 2000. Currently, a 150 MeV S-band electron injector is under construction as the first linac section to produce a high brightness beam. The design study and the present R&D status of the SDUV-FEL have been presented in this paper.

1　NSRL, University of Science and Technology of China

2　Institute of High Energy Physics, the Chinese Academy of Sciences

用于增强器 Ramping 的任意波形发生器

沈国保 冷用斌 郑丽芳 陆承蒙 刘松强

关键词 EPICS，Ramping，任意波形发生器

在 EPICS 环境下，利用商业硬件模块以及 VxWorks 实时操作系统，采用软件方式实现用于增强器 Ramping 的任意波形发生器，详细分析了其结构，并给出了原理性测试结果。该任意波形发生器不仅可以用在增强器磁铁电源的控制中，而且可以用于加速器的高频系统腔压的动态控制。

An arbitrary function generator for the ramping of booster synchrotron

SHEN Guobao LENG Yongbin ZHENG Lifang LU Chengmeng LIU Songqiang

Keywords EPICS, Ramping, Arbitrary function generator

This paper describes the design and implementation of an arbitrary function generator (AFG), which will be used in the control system of Shanghai Synchrotron Radiation Facility. The AFG is constructed with COTS hardware modules and VxWorks real-time operating system and works under EPICS software environment. The AFG can be used to ramp booster's energy for power supply system, and to control the radio-frequency system as well.

基于 PC/104 的 EPICS 设备控制器

沈国保 冷用斌 郑丽芳 陆承蒙 刘松强

关键词 控制系统，EPICS，设备控制器，PC/104

介绍了采用 PC/104 的 EPICS 设备控制器的设计，详细分析了其软硬件结构，并给出了原理性测试结果。该控制器兼具输入输出控制器和设备控制器的功能，在简化 EPICS 应用体系结构方面做出了成功的尝试。

PC/104-based EPICS device controller

SHEN Guobao LENG Yongbin ZHENG Lifang LU Chengmeng LIU Songqiang

Keywords Control system，EPICS，Device controller，PC/104

This paper describes the design and implementation of a device controller by using PC/104 computer, which is supposed to be used in the control system of Shanghai Synchrotron Radiation Facility. The device controller is also used as I/O controller under EPICS architecture.

基于 EPICS 的加速器联锁保护系统

郑丽芳　沈国保　陆承蒙　刘松强

关键词　控制系统, EPICS, PLC 联锁

介绍一个在 EPICS 软件环境下实现的用于加速器的联锁保护系统。系统由 PowerPC CPU 和 VxWorks 实时操作系统组成的 VME 前端计算机（IOC）与高性能可编程逻辑控制器 PLC-5 共同组成。

An EPICS-based accelerator interlock and protection system

ZHENG Lifang　SHEN Guobao　LU Chengmeng　LIU Songqiang

Keywords　Control system, EPICS , PLC Interlock

This paper describes a machine interlock and protection system used for accelerators. The system is composed of a VME front-end computer and an Allen-Bradley programmable logic controller PLC-5. The software is developed in the EPICS (Experimental Physics and Industrial Control System) environment.

EPICS 系统中 CORBA 接口技术的研究

沈国保 郑丽芳　刘松强

关键词　EPICS，CORBA，控制系统

介绍了被称为软总线的中间件（middleware）CORBA 与分布式控制系统软件工具 EPICS 的接口技术。CORBA 接口技术能极大地改善大型实验物理装置的系统建模、仿真和机器运行等高水平物理应用软件的开发环境，提高软件可重用性、可维护性以及可移植性。

Study of CORBA interface for EPICS system

SHEN Guobao　ZHENG Lifang　LIU Songqiang

Key words　EPICS, CORBA, Control system

This paper describes a method for interfacing the middleware CORBA to EPICS-based distributed control system.　EPICS interfaced with CORBA will greatly facilitate the design and development of high-level application software, improve software reusability and maintainability and provide an easy way to transplant software for modeling, simulation and machine operation analysis.

采用实时校正技术的时间数字化测量方法

沈国保 丁建国 刘松强

关键词 TDC 数字延迟线 微控制器 实时校正 数字化测量

在综述各种时间数字化变换(TDC)方法的基础上，重点介绍了采用数字延迟线的 TDC 及刻度原理。以及采用嵌入微控制器来实现实时刻度的方法。

Time to digital conversion by using real-time calculation

SHEN Guobao DING Jianguo LIU Songqiang

Keywords TDC，Delay line，Microcontroller

This paper describes a TDC method by using integrated delay line. An embedded microcontroller is used for real-time calibration.

用于数字反馈研究的 Hall 电路

郑丽芳 李纪堂 刘松强

关键词 加速器，数字反馈，Hall 元件

介绍加速器数字反馈研究仿真实验平台中的 Hall 电路，该电路不仅用于磁场反馈，其电流输入电路又被用作系统的噪声注入电路。

A noise injector circuit for digital feedback study

ZHENG Lifang LI Jitang LIU Songqing

Keywords Accelerator, Digital feedback, Hall device

This paper describes a circuit for Hall device, which is applied in a digital feedback study system for accelerator control. The circuit can be used not only as a feedback device but also as a noise injector.

上海同步辐射装置平移长线圈磁测机的研制

张继东 曹 瓒 任芳林 周巧根 张丽华 李 宇 赵玉彬 阎和平

关键词 二极磁铁，积分场，平移长线圈

描述了上海同步辐射装置（SSRF）平移长线圈磁测机的设计和制造。磁测机包括的硬件主要有：测量线圈、直线运动平台、高精度数字积分仪、步进电机控制卡、高稳定度电源、直流电流传感器、6 位半数字电压表、GPIB 接口卡、及高精度编码器等。磁场测量和数据分析程序采用 LabVIEW 编制。该磁测机已测量了 SSRF 储存环二极磁铁的样机，效果良好，能做到灵活、快速和自动化地测量积分场。

Design and fabrication of a long coil magnetic measurement system

ZHANG Jidong CAO Zan REN Fanglin ZHOU Qiaogen ZHANG Lihua LI Yu ZHAO Yubin YAN Heping

Keywords Dipole magnets, Integral field, Moving long coil

A long coil magnetic measurement system has been built at SSRC to measure the storage ring dipole magnet prototypes of SSRF. The system consists of a 2.2m long coils and a control system. The basic design concept is to build a reliable, precise, fast and automatic system for the integral magnetic field measurement. A multifunction LabVIEW application program was developed on a main control unit of personal computer, with Microsoft Windows 98/2000. Several personal computer slot interface cards communicate with, and control various devices. The control system is designed to be versatile, modular, expandable, maintainable, quick and easily reconfigurable in both hardware and software. The system is accurate enough to characterize the magnetic field quality of the storage ring dipole magnet prototypes.

三维磁场测量特斯拉计的研制

张继东 阎和平 周巧根 赵玉斌

关键词 磁铁，测量，特斯拉计，非线性补偿

本文描述了一台新颖的测量加速器磁铁和插入件三维场分布的高精度特斯拉计。它由三维正交的磁场传感器探杆， 温度探头，恒流源，HP34970A 多通道数据采集器和 PC 机组成。软件采用 LabVIEW 编写，独有的软件温度补偿和非线性校正算法使仪器能够被校正到±100 μT 的精度。上海应用物理研究所（SINAP）的核磁共振仪和校正磁铁能够把仪器校正的上限提高到 1 T。

A teslameter for triaxial magnetic measurements

ZHANG Jidong YAN Heping ZHOU Qiaogen ZHAO Yubin

Keywords Magnet, Measurement, Teslameter, Nonlinearity compensation

A high precision system for measuring the three-dimensional distribution of magnetic fields with large volume, such as those produced by accelerator magnets and the undulator device, has been designed and commissioned. The meter consists of a triaxial magnetic field transducer, a temperature sensor, a constant current source, a HP34970A data acquisition/switch unit and PC. Both hardware and calibration software are inventions of SINAP, and the software includes the temperature and nonlinearity compensation. This instrument can be calibrated to a precision of ±100μT for a magnetic field up to 1T by means of an NMR system.

非蒸散型吸气剂对混合气体的抽气行为的研究

陈丽萍 蒋迪奎

关键词 NEG，混合气体，抽气性能

NEG 抽除混合气体的行为不同于抽单纯气体。测试了 SAES 公司的 NEG 组件 ST707WP1250 对由 80%H_2 和 20%CO 组成的混合气体的抽气性能，并和抽纯气性能进行了比较。混合气体中的 NEG 对 H_2 的抽速受 CO 影响，随 H_2 吸气量的增加而明显下降。混合气体中的 NEG 对 CO 的抽速不受 H_2 影响。研究结果为 SSRF 储存环真空系统设计提供了重要依据。

Pumping characteristics of mixed gases with non-evaporation getter

CHEN Liping JIANG DiKui

Keywords Non evaporation getter, Mixed gases, Pumping characteristics

Mixed gaseous (80% H_2 and 20% CO) were pumped by activating a non evaporation getter (NEG) to see how different it behaves when used to pump a pure gas. We found that NEG significantly reduces the pumping speed of H_2 with an increase of H_2 absorption, whereas it little affects the pumping speed of CO. Our finding is of some technical interest in designing the vacuum system of the storage ring in Shanghai Synchrotron Radiation Facility (SSRF).

可变椭圆极化波荡器相干太赫兹辐射的模拟计算

周巧根　戴志敏　徐洪杰

关键词　相干太赫兹辐射，飞秒电子束，极化光，波荡器

中国科学院上海应用物理研究所正在研制的相干太赫兹辐射装置是一台利用飞秒电子束团通过可变椭圆极化波荡器产生高亮度水平线极化光、垂直线极化光或各种椭圆极化光的强相干太赫兹辐射光源。本文描述了这种相干太赫兹辐射的光通量密度空间分布、光谱、极化特性和相干性等的计算方法和模拟计算结果。计算结果表明，对于能量为 20MeV、发射度为 1.5 π mm·mrad、束团长度为 200fs、电荷量为 50pC 的电子束团，在距离 0.6m 长的波荡器中心 1m 处可获得光通量密度峰值达 2×10^{9}photons/mm^{2}/0.1%BW 量级的太赫兹水平线极化光或圆极化光。

Simulation of the coherent THz radiation from a variable elliptically polarized undulator

ZHOU Qiaogen　DAI Zhimin　XU Hongjie

Keywords　Coherent THz radiation, Femto-second electron beam, Polarized light, Undulator

A new type of coherent THz light source is building in SINAP. It will use the femto-second electron beam passing through a variable elliptical polarized undulator to produce high brightness THz radiation with various linear, elliptical or circular polarization. The paper describes the computation methods and the simulation results of the flux density, spectrum, polarization and coherence for this kind of radiation. For an electron beam with the energy of 20 MeV, the emmitance of 1.5 πmm·mrad, the beam length of 200 fs and the electric charge of 50 pC, the THz radiation with horizontal linear polarization or circular polarization with the maximum flux density of 2×10^{9} photons/mm^{2}/0.1%BW can be obtained at the distance of 1 m from the center of an undulator 0.6 m long.

10(-10)Pa 溅射离子泵和非蒸散型吸气剂的复合泵

蒋迪奎　陈丽萍　殷立新

关键词　溅射离子泵，非蒸散型吸气剂，SIP+NEG 复合泵

不改变商用 SIP 的基本结构，把 NEG 组件 WP1250 装入 SIP，构成 NEG+SIP 的 XHV 复合泵。它使 NEG 和 SIP 的特点互补。NEG 激活前，SIP 单独抽气，极限压强 1.1×10^{-8} Pa；NEG 激活后，复合泵的极限压强降到 7×10^{-10}Pa。抽速稳定的范围更广，标称抽速是 SIP 抽速的 2.5 倍。

Integration of commercial sputtering ion pumps with non-evaporative getter

JIANG DiKui CHEN Liping YIN Lixin

Keywords Sputtering ion pump (SIP), Non evaporative getter (NEG), (SIP+NEG) pump combination

A novel type of extra-high-vacuum (XHV) pump has been successfully developed by installing components of non evaporative getter (NEG), WP1250, into a commercial sputtering ion pumps (SIP) without altering its frame. The strengths of the new pump include: 1. The upper limit of 1.1×10^{-8} Pa of SIP is not a problem, the ultimate pressure can reach 7×10^{-10} Pa after activating NEG; 2. Its constant pumping speed doubles that of SIP by activating NEG.

非蒸散型吸气剂（NEG）的性能特点和实际应用问题

蒋迪奎 陈丽萍

关键词 非蒸散型吸气剂，性能特点，应用

根据文献和实际经验，综述了非蒸散型吸气剂 ST707 和 ST101 的性能特点以及 NEG 在实际使用中要注意的问题。

Performance of non-evaporation NEGs and their applications

JIANG Dikui CHEN Liping

Keywords NEG, Performance, Application

Introduces the characteristics and performances of the non-evaporation getters NEGs St707 and St101 and some problems are proposed to deal with in their applications, based on relevant literatures and experience got from practice.

Investigation of mechanical stability of SSRF girder medsi 2004 (ESRF)

WANG Xiao YAN Zhongbao DU Hanwen YIN Lixin

Keywords **V**ibration, FEA, Beam stability

Beam stability is a major concern for the construction of a 3rd generation light source. Mechanical vibration of the storage ring components is one of the contributing factors to electron beam instability. In order to improve the performance of the girder developed in the R&D period of Shanghai Synchrotron Radiation Facility project, an optimization for the girder design has been started recently. The number of the girders in a lattice cell is modified from 3 to 5 to increase the first eigenfrequency of the magnet-girder assembly. For improving stiffness and stability, the structure of the girder and support has been redesigned and studied. The FEA results show that the static and dynamic performance has been improved significantly.

Design of a variable elliptically polarized undulator for coherent THz light source

ZHOU Qiaogen ZHANG Jidong ZHANG Honghui OUYANG Lianhua

Keywords Coherent THz light source, Elliptical polarization, Undulator

Coherent THz light source will be built in Shanghai Institute of Nuclear Research (SINR), the Chinese Academy of Sciences. A variable elliptically polarized undulator with Apple-II structure was designed to produce the linear polarized as well as various elliptically polarized THz radiations. The structure of the undulator corresponds to four standard Halbach-type magnet rows which consist of two pairs of planar permanent magnet rows above and below the electron orbit plane. The two rows at one diagonal can move along the longitudinal direction to provide various polarization modes. The period and the gap are 100 mm and 36 mm respectively and the number of period is five. This paper describes the magnet design, the force calculation and the stress analysis of the undulator. The magnetic fields will be optimized for horizontal linear polarization mode and circular polarization mode.

高精度磁铁稳流电源智能化接口的研制

许瑞年　赵黎颖　陈焕光　曹红萍　李德明

关键词　智能化接口，微处理器，高精度，稳流电源

介绍一台专用于高精度稳流电源的智能化接口的设计方案及样机的研制结果。该接口用单片机作为核心实现对大功率、高精度的磁铁电源进行智能化的本地控制并具有作为远程遥控接口的功能。它具有运行参数的设定、运行状态的检测、故障报警及记录、运行数据的保存及与计算机的通讯等功能。采用了主控机箱与操作面板分离的两体方案，主机与面板之间用串行数字信号进行连接。

Development of intelligent interface for high precision magnet power supply

XU Ruinian　ZHAO Liying　CHEN Huanguang　CAO Hongping　LI Deming

Keywords　Intelligence interface, MCU, High precision, Magnet power supply

A prototype interface device with an MCU core used for controlling a high-stability switch-mode huge power supply with high precision has been developed in our institute. This interface adopts a structure of the main case separated from the panel. The main functions include current setting and acquisition, detecting of running status and error, and communication with computer. In this paper, the structure of the device, both hardware and software design, and test results are described.

单片机在高精度磁铁稳流电源智能化接口中的应用

许瑞年　李德明

关键词　单片机，稳流电源，智能化，接口

介绍了自行研制的高精度稳流电源智能化接口中单片机的应用。将高容量、多功能、高输出能力的 PIC16F877 单片机分别应用在大功率高精度磁铁电源接口的主控模块和操作面板上，可以大幅度提高智能化接口的性能。研制成功的两体式智能化接口具有体积小、造价低、抗干扰能力强、可嵌入到电源机箱内等优点。

Application of MCU to intelligent interface of high precision magnet power supply

XU Ruinian LI Deming

Keywords Intelligent interface, MCU, High precision, Magnet power supply

Application of the high-capability MCU in the intelligent interface is introduced in this paper. A prototype of intelligent interface for high precision huge magnet power supply was developed successfully. This intelligent interface was composed of two parts: operation panel and main board, both of which adopt an MCU of PIC16F877 respectively. The interface has many advantages, such as small size, low cost and good interference immunity.

110MW 脉冲调制器控制器设计

周凡 谷鸣 陈志豪 傅禄新 范学荣

关键词 脉冲调制器，控制器，监控

为确保 110MW 脉冲调制器运行稳定可靠、维修安全和人员安全，同时满足中国科学院上海应用物理研究所 100MeV 直线加速器总体控制对调制器的要求，通过分析 110MW 脉冲调制器设备电路、工作原理和元器件特性，结合其硬件电路设计特点，描述了 110MW 脉冲调制器的设备控制器的监控方法和设计。通过调试、模拟运行和测试，控制器设计达到对调制器进行安全可靠的控制和保护的要求。

Design of 110MW pulse modulator’s controller

ZHOU Fan GU Ming CHEN Zhihao FU Luxin FAN Xuerong

Keywords Modulator, Controller, Monitoring

Based on analyzing the modulator’s hardware and the characters of the circuit, the 110MW pulse modulator’s controller has been designed. And the purpose of this work was to ensure the modulator’s stability, credibility and safety, and to make the modulator accord with the control-demand of the 100MeV linear accelerator. After being debugged and tested, the design was found to meet the requirement for controlling and guarding the modulator safely.

用电机能耗制动实现感应调压器电压的精密控制

陈焕光 李 瑞 卢宋林

关键词 感应电动机，能耗制动，电压控制

实现了交流感应电机能耗制动，介绍了制动原理，为交流感应电机快速制动应用提供了一种实用的方法。

Accurate voltage control of induction regulator on the principle of energy dissipation braking of electromotors

CHEN Huanguang LI Rui LU Songlin

Keywords Induction motor, Energy dissipation braking, Voltage control

The energy dissipation braking for AC induction motors is realized. The principle of the equipment is described. Obviously, it provides one way of fast braking the AC induction motors.

基于 LabVIEW 的电源智能接口控制

曹红萍 陈焕光 许瑞年 李德明

关键词 LabVIEW，接口控制，数据处理

磁铁电源智能接口测控系统利用 LabVIEW 数据采集、处理和智能控制等功能设计，通过 Serial Port Init.vi 初始化串口，将收到的数据和本/遥（RL）的设置分别存入 While loop。以 200ms 间隔发送查询命令，100ms 间隔读数据、检测 RL 电流值的改变。通过事件触发将数据在独立的 while loop 实现读写、显示、分析和监控。用局域变量控制 loop 实现同步开关、数据的出列和存档并通过以太网对故障信号进行远程监控。

Control of intelligent power interface based on LabVIEW

CAO Hongping CHEN Huanguang XU Ruinian LI Deming

Keywords LabVIEW, Interface control, Data processing

The interface control of a magnet power through serial communication based on LabVIEW is described. Serial COM is initialized by Serial Port Init.vi module, and the received data are saved in While loops with the shift register respectively. The demand command is sent out every 200ms, and data are read and checked every 100ms at the same time. Data independent of While loops are read, displayed, analyzed and controlled when trigger events take place. The local variants are used to synchronize the switches, save the data and send out the error information to Internet.

Shanghai synchrotron radiation facility and its medical applications

XIAO Tiqiao HE Jianhua XU Hongjie

Keywords Synchrotron radiation X-ray imaging, Beamline design, Medical application

Approved on January 7, 2004, Shanghai Synchrotron Radiation Facility (SSRF), a third generation synchrotron radiation light source, will be incommission in 2009. The main purpose of SSRF project is to establish a multidisciplinary platform for both researches in frontier sciences and R&D of high technology in China. The electron energy in the storage ring will be 3.5GeV, emittance 3.0nm.rad. It will be able to supply light beam with photon energy ranging mainly from 0.1 to 40keV, which will open new research opportunities for life science, material science, earth and environmental science and many other fields. Medical application of synchrotron radiation is becoming more and more important in recent years. The outstanding characteristics of SSRF ensure high brightness and high flux output at photon energy range larger than 4keV, which is well suited for medical applications. Among the initial suite of SSRF beamlines, one beamline named “imaging and medical application” will take precedence over the others, the budget for which will be covered by the whole project. Light source is a 1.8 Tesla wiggler, which covers the photon energy range of 8-120keV. Two endstations will be constructed with the first located inside the experimental hall and the second located at a satellite building. The second endstation mainly aims at large size imaging and potential clinical applications. Imaging modalities including in-line phase contrast imaging (IL-PCI), diffraction enhanced imaging (DEI), microtomography (MCT) will be developed. Some preliminary experiments concerning medical imaging have been carried out using BSRF and an in-house microfocus X-ray source, which will benefit the development of new imaging techniques at the endstation.

Effect of spatial coherence on application of in-line phase contrast imaging to synchrotron radiation mammography

XIAO Tiqiao[1,3] BERGAMASCHI A[1] DREOSSI D[1] LONGO R[1] OLIVO A[1]
PANI S[1] RIGON L[1] ROKVIC T[1,2,3] VENANZI C[1] CASTELLI E[1]

Keywords Spatial coherence, Phase contrast imaging, Mammography, Synchrotron radiation

Effect of spatial coherence on the application of in-line phase contrast imaging (IL-PCI) to synchrotron radiation (SR) mammography is investigated experimentally at SYRMEP/ELETTRA. Factors related to spatial coherence and IL-PCI image quality, including source-emittance difference in vertical and horizontal direction, photon energy, slit width, sample-to-detector distance (SDD) and detector resolution, are investigated respectively. The preliminary experimental results demonstrate that better IL-PCI image quality could be achieved in the vertical direction of the beam. As to slit width, the

horizontal spatial coherence remains almost the same until the slit width is gradually close to 5 mm. For mammography applications of IL-PCI, slit width of 100mm could be employed with acceptable image quality. Lower photon energies result in better coherence and correspondingly better IL-PCI image quality. As a result of compromising between dose and image quality, photon energy of ~19keV is recommended for SR mammography. To preserve the edge enhancement resulted from good coherence of SR, an appropriate SDD and an applicable detector should be selected. The optimum SDD highly depends on the detector resolution. For high resolution film, the best IL-PCI image quality could be obtained at a much smaller SDD while an SDD of ~1.5 m is needed to achieve optimum image quality for X-ray CCD with pixel size of 14 μm. A relatively large pixel size of the detector will deteriorate the edge enhancing efficiency and results in lower IL-PCI image quality. In practice, a compromise for detectors should be made between the spatial resolution and the sensitivity.

---

1 Dipartimento di Fisica, Università di Trieste e INFN, Sezione di Trieste, Italy

2 Faculty of Physics, University of Belgrade, Belgrade, Serbia and Montenegro

3 Supported by ICTP TRIL program

一种新型 X 射线相衬成像实验室系统

肖体乔　徐洪杰　陈 敏　杜国浩　魏 逊　骆玉宇　刘丽想

关键词　相衬成像，空间相干性，纳聚焦 X 射线管

目前的 X 射线相衬成像研究大都采用同步辐射光源。光源点尺寸达微米量级的 X 射线管辐射具有较好的空间相干性，也可用于相衬成像研究。本文报道了一种基于纳聚焦 X 射线管的新型相衬成像实验室系统，光源点尺寸可达 500 nm。实验结果表明，该系统可对低 Z 样品如生物软组织、有机样品等的内部结构成清晰像，分辨率可达微米量级。与已有系统相比较，其空间分辨率和有效通量都有相当大的提高。锥形光束张角约为 30°，通过纵向扫描机构调节样品与光源点间距可调整投影放大率，从而降低对探测器分辨率的要求。适用于大样品研究，且可实现样品的横向二维扫描。在医学、生物学、材料科学及化学反应动力学等领域有重要应用前景。

A new type of laboratory system for X-ray phase-contrast imaging

XIAO Tiqiao　XU Hongjie　CHEN Min　DU Guohao　WEI Xun

LUO Yuyu　LIU Lixiang

Keywords　Phase-contrast imaging, Spatial coherence, Nanofocus X-ray tube

Up to now, X-rays employed for phase-contrast imaging mostly come from synchrotron radiation facility. Radiation from X-ray tubes with source size of the order of micrometer is also applicable for X-ray phase-contrast imaging (XPCI), because of its fairly good spatial coherence. In this paper, a new type of laboratory system for XPCI, based on a nanofocus X-ray tube with source size of 500 nm, is

reported. The experimental results show that this XPCI lab system is applicable for high resolution imaging to the inner structure of low *Z* samples, such as soft tissues, organic materials, etc.. Resolution of a few micrometers was achieved. Compared to the system reported earlier, spatial resolution and effective flux for the new one have been greatly improved. Open angle for the cone-shaped X-ray beam is about 30°. Distance between the sample and source can be easily adjusted to meet the specified magnification ratio through projection, so that the limits to the resolution of X-ray detectors can be reduced. It is possible for the system to be employed for the investigation of samples with relatively large size, while a mechanic system is designed to ensure the transverse 2-d scanning of them. Important application potentials for the XPCI lab system can be found in the fields of clinical medicine, biology, material science, chemical reaction dynamics, etc.

基于位相衬度的软组织内部结构 X 射线无损成像

肖体乔　张桂林　徐洪杰　田玉莲[1]　黄万霞[1]　朱佩平[1]

关键词　无损成像，位相反衬，同步辐射，临床诊断

利用北京同步辐射装置开展了基于位相衬度的软组织内部结构 X 射线无损成像研究。对原有光束线结构作了改动以扩大束斑尺寸，从而可以对更大的样品成像。实验中采用了 X 射线位相反衬同轴成像方式。给出了一系列样品的研究结果。金鱼内部软组织结构成像分辨率优于 50μm。以 SD 大鼠为动物模型开展了肿瘤早期诊断研究，观察到了尺寸约为 100μm 的早期肿瘤。最后讨论了该技术在医学临床诊断中的应用。

1 中国科学院高能物理研究所

Nondestructive X-ray imaging of inner structure of soft tissues in phase contrast

XIAO Tiqiao　ZHANG Guilin　XU Hongjie　TIAN Yulian[1]

HUANG Wanxia[1]　ZHU Peiping[1]

Keywords　Nondestructive imaging, Phase contrast, Synchrotron radiation, Clinic diagnosis

Nondestructive X-ray imaging of inner structure of soft tissues in phase contrast is investigated with Beijing Synchrotron Radiation Facility (BSRF). Modification to the beamline setup is made to enlarge the X-ray beam size and consequently larger samples can be imaged. In-line setup is employed for experiments. Results on a serial of samples are given and soft-tissue details of less than 50 μm inside a fresh goldfish are obtained. Diagnosis of tumor in its early stage is also investigated taking SD rat as the model. Tumor at the size of ~100 μm is observed. Potential of this technique in clinic diagnosis is discussed.

1　Institute of High Energy Physics, the Chinese Academy of Sciences

X 射线相衬成像用于生物碱沉淀研究的可行性

魏 逊 肖体乔 陈 敏 骆玉宇 席再军 刘丽想 杜国浩 徐洪杰
田玉莲[1] 朱佩平[1] 黄万霞[1] 袁清习[1]

关键词 X 射线相衬成像，生物碱，沉淀，结构

生物碱与一些特殊的试剂作用生成沉淀。这些反应可用于生物碱的检测和精制。本文分别在同步辐射装置和微聚焦 X 射线成像系统上用 X 射线相衬成像（XPCI）方法研究了三种不同类型的生物碱沉淀的结构。结果显示：Hager 试剂作用下，有机胺类的秋水仙碱沉淀呈针状，吡啶类的槟榔碱沉淀呈胶团体，异喹啉类的小檗碱沉淀呈花瓣状，与目测或在光学显微镜下观察到的形态有很大差别。本文为今后用 XPCI 方法研究更复杂的化学反应体系提供了一定的参考和依据。

1 中国科学院高能物理研究所

Feasibility of using X-ray phase-contrast imaging to study alkaloidial precipitates

WEI Xun XIAO Tiqiao CHEN Min LUO Yuyu XI Zaijun
LIU Lixiang DU Guohao XU Hongjie TIAN Yulian[1]
ZHU Peiping[1] HUANG Wanxia[1] YUAN Qingxi[1]

Keywords X-ray phase-contrast imaging, Alkaloid, Precipitate, Structure

The alkaloids are organic nitrogenous bases found mainly in plants, which deposit with certain reagents in water. These precipitation reactions can be used to determine the alkaloids' existence and to refine them. The present paper studied three different types of alkaloidal precipitates by X-ray phase-contrast imaging (XPCI) based both on Beijing Synchrotron Radiation Facility (BSRF) and on a nanofocus X-ray tube laboratory system. The XPCI results reveal the needle precipitate of colchicines (amine alkaloid), the micelle precipitate of arecoline (pyridine alkaloid) and the petal precipitate of berberine (isoquinoline alkaloid). Comparisons of the results obtained by different methods are made to verify the feasibility of XPCI's future application to more complicated chemical systems.

1 Institute of High Energy Physics, the Chinese Academy of Sciences

顺态相钛酸钡内部微观极化团簇的皮秒观测

邰仁忠 NAMIKAWA K[1] SAWADA A[2] KISHIMOTO M[3] TANAKA M[3]
陆培祥[4] NAGASHIMA K[3] MARUYAMA H[5] ANDO M[6]

关键字 X 射线散斑，极化团簇，软 X 射线激光，铁电，顺电，动态团簇

基于皮秒软 X 射线激光散斑技术，铁电体材料钛酸钡铁电相与顺电相内存在的极化团簇被首次观测到。这些动态团簇连续变化通过居里温度点 T_c。团簇间平均距离随温度线形变化、团簇大小无明显变化。居里温度 T_c 上方 5 度处团簇内极化值最大。当温度朝 T_c 冷却时，团簇间短距离相关强度按（T-T_c）$^{-0.41\pm0.02}$ 随温度演化。

Picosecond view of microscopic-scale polarization clusters in paraelectric $BaTiO_3$

TAI Renzhong NAMIKAWA K[1] SAWADA A[2] KISHIMOTO M[3] TANAKA M[3]
LU Peixiang[4] NAGASHIMA K[3] MARUYAMA H[5] ANDO M[6]

Keywords Speckles, Polarization clusters, Soft X-ray laser, Ferroelectrics, Paraelectrics, Dynamic cluster

The polarization clusters existing in both the ferroelectric and the paraelectric phase of $BaTiO_3$ are directly observed and characterized for the first time by a picosecond soft X-ray laser speckle technique. These dynamic clusters appear continuously across the Curie temperature T_c. The clusters' distance increases approximately linearly with temperature, while their mean size does not change significantly. The polarization exhibits a maximum at a temperature about 5℃ above T_c. The clusters' short-range correlation strength diverges as $(T-T_c)^{-0.41\pm0.02}$ as temperature decreases toward T_c.

---

1 Tokyo Gakugei University, 2 Okayama University, 3 Advance Photon Research Center, JAERI,
4 Huangzhong University of Science and Technology, 5 Hiroshima University, 6 PF,KEK

利用瞬态 X 射线散斑技术观测铁电体材料

邰仁忠 NAMIKAWA K[1] KISHIMOTO M[2] TANAKA M[2] SAWADA A[3]
HASEGAWA N[2] KAWACHI T[2] SUKEGAWA K[2] KADO M[2] OCHI Y[2]
NISHIKINO M[2] NAGASHIMA K[2] DAIDO H[2] KATO Y[2]
MARUYAMA H[4] ANDO M[5]

关键词 X 射线散斑，X 射线激光，钛酸钡，瞬态

利用简单的装置完成了皮秒 X 射线散斑实验。光源是小型的等离子体 X 射线激光，波长为 13.9nm, 脉宽为 7 皮秒。样品是具有 a/c 多电畴结构的单晶钛酸钡。物质相关函数包含了散射体（电畴）的统计信息，通过反卷积过程直接从散斑图样中得到。瞬态 X 射线散斑将非常有利于探测常规手段观测不到的快速微观过程。

Observation of ferroelectric material with instantaneous X-ray laser

TAI Renzhong NAMIKAWA K[1] KISHIMOTO M[2] TANAKA M[2]
SAWADA A[3] HASEGAWA N[2] KAWACHI T[2] SUKEGAWA K[2] KADO M[2]
OCHI Y[2] NISHIKINO M[2] NAGASHIMA K[2] DAIDO H[2] KATO Y[2]
MARUYAMA H[4] ANDO M[5]

Keywords X-ray speckles, X-ray laser, $BaTiO_3$

Picosecond X-ray speckles experiment has been conducted with a simple setup. The source was a compact silver-plasma-based X-ray laser, with a wavelength of 13.9nm and pulse duration of 7ps. The sample was a single crystal of $BaTiO_3$, with ferroelectric multi-domain structure (*a/c* domains). The matter correlation function, including statistical information of those randomly distributed scatterers (domains here) within the sample, was extracted by deconvolution of the speckle pattern. The instantaneous X-ray speckle technique has proved to be particularly efficient to be used to observe fast microscopic-scale phenomena that are hard to access with other methods currently.

1 Tokyo Gakugei University, 2 Advance Photon Research Center, JAERI, 3 Okayama University,
4 Hiroshima University, 5 PF,KEK

用 X 射线激光作为相干光源来表征铁电体材料特性

郜仁忠 NAMIKAWA K[1] KISHIMOTO M[2] TANAKA M[2]
KADO M[2] SUKEGAWA K[2] HASEGAWA N[2] KAWACHI T[2] 陆培祥[3]
NISHIKINO M[2] OCHI Y[2] NAGASHIMA K[2] DAIDO H[2] SAWADA A[4]
MARUYAMA H[5] ANDO M[6] KATO Y[2]

关键词 电畴结构，X 射线激光，动态极化团簇

利用 X 射线瞬态散斑技术实验表征了铁电体材料钛酸钡的瞬态电畴结构。结果显示：升温过程中相关电畴尺寸按幂指数规律减小。与准静态电畴相比，高温相的动态团簇也被实验首次证实存在并被表征。

Characterization of material properties using X-ray laser as a coherent X-ray source

TAI Renzhong NAMIKAWA K[1] KISHIMOTO M[2] TANAKA M[2]
KADO M[2] SUKEGAWA K[2] HASEGAWA N[2] KAWACHI T[2] LU Peixiang[3]
NISHIKINO M[2] OCHI Y[2] NAGASHIMA K[2] DAIDO H[2] SAWADA A[4]
MARUYAMA H[5] ANDO M[6] KATO Y[2]

Keywords Domain structure, X-ray laser, Dynamic polarization cluster

The transient ferroelectric domain structures of barium titanate were characterized near its critical temperature T_c by means of picosecond X-ray laser speckles. The results show that the correlated domain size decreases in a power law as temperature rising toward T_c. Compared to this quasi-static polarization domains existing below T_c, the dynamic polarization clusters were also confirmed to exist in this crystal above T_c and characterized for the first time by the same technique.

1 Tokyo Gakugei University,
2 Advance Photon Research Center, JAERI,
3 Huangzhong University of Science and Technology,
4 Okayama University,
5 Hiroshima University,
6 PF,KEK

硅烷化云母表面对蛋白质晶体生长过程的作用

唐 琳 黄一波 刘德泉 李俊玲 茅 恺 刘 琳
程中军 龚为民 胡 钧 何建华

关键词 硅烷化云母，蛋白质，结晶化

用 3-aminopropyl triethoxysilane 硅烷化后的云母表面具有大面积平整，表面疏水性可控并带有一定量的正电荷等特点。在本文中，这种经过特殊工艺处理后的云母表面被用作溶菌酶、天花粉和其他三种结构未知的蛋白质的晶体生长基底（我们使用的结晶方法是悬滴蒸汽扩散法）。实验结果表明：和对照实验中使用的硅烷化盖玻片相比较，这种特殊的硅烷化云母表面能够明显地改善蛋白质的结晶过程：明显降低了溶菌酶晶体生成所需的时间；在增大天花粉蛋白质晶体尺度的同时减少了晶体数目；明显地提高了三种结构未知蛋白质晶体的质量和衍射能力。

Effects of the silanized mica surface on protein crystallization

TANG Lin HUANG Yibo LIU Dequan LI Junling MAO Kai LIU Lin
CHENG Zhongjun GONG Weimin HU Jun HE Jianhua

Keywords Silanized mica, Protein, Crystallization

The freshly cleaved mica surface silanized by 3-aminopropyl triethoxysilane possesses the flatness in a large area, a controlled hydrophobilicity and some amount of positive charges. In this paper, this specially treated silanized mica has been used as a surface for the crystallization of lysozyme, trichosanthin and other three kinds of proteins with unknown structures. Crystallization experiments have been carried out by hanging drop vapor diffusion method and the results indicate that this kind of silanized mica can ameliorate protein crystallization process considerably as compared with the silanized glass cover slip control. For lysozyme, the induction time required for the crystal growth decreases markedly. For trichosanthin on the silanized mica surface, the crystal size is obviously larger and the number of crystals grown is much less. And for the three kinds of proteins with unknown structures, the diffraction ability of the crystals grown on this kind of mica has been improved considerably.

利用原子力显微镜原位观察α-Synuclein 积聚纤维的解聚过程

唐 琳 李洪涛[1] 吉丽娜 杜海宁[1] 张 峰 胡晓芳[2] 李民乾 胡红雨[1] 胡 钧[2]

关键词 α-synuclein 蛋白纤维，原位原子力显微镜

本文利用原子力显微镜在溶液中对α-Synuclein 积聚纤维的解聚过程进行了原位观察。观察结果表明：当α-Synuclein 积聚纤维稀释到一定程度后，它在溶液中能够自发地逐步解聚。解聚过程一般开始于纤维的中间，长纤维先解聚成短纤维，短纤维再进一步解聚成大小不同的颗粒。我们的实验结果还表明，盐酸胍能够明显地促进纤维的解聚。

---

1 中国科学院上海生物化学与细胞研究所, 2 上海交通大学生命科学研究中心

Direct visualization of disaggregation of human α-synuclein fibrils by in situ atomic force microscopy

TANG Lin LI Hongtao[1] JI Lina DU Haining[1] ZHANG Feng
HU Xiaofang[2] LI Minqian HU Hongyu[1] HU Jun[2]

Keywords Human α-synuclein fibrils, In situ atomic force microscopy

The in situ atomic force microscopy (AFM) has been used to study the process of disaggregation of

α-synuclein fibrils in solution. It was found that α-synuclein fibrils could disaggregate step by step on mica surface in solutions when diluted to some extent. The disaggregation usually started randomly at the middle of the fibrils, and the long fibrils could disaggregate into short fragments and protein particles with various sizes. It was observed directly that guanidinium chloride could dissolve the long α-synuclein fibrils quickly.

1 Laboratory of Proteomics, Institute of Biochemistry and Cell Biology

2 Nanobiology Laboratory of Bio-X Life Science Research Center

原子力显微镜在α-Synuclein 积聚和解聚研究中的应用

唐 琳 李洪涛 杜海宁 吉丽娜 张 峰 李民乾 胡红雨 胡 钧

关键词 α-synuclein 蛋白纤维，积聚，原子力显微镜

研究α-Synuclein 蛋白纤维的积聚和解聚过程对于帕金森症等神经退化性疾病的预防和治疗有着重要意义。本文利用原子力显微镜对α-Synuclein 的积聚过程的不同阶段进行了研究，并在此基础上对已经积聚形成的α-Synuclein 纤维在溶液中的解聚过程进行了原位观察。实验结果表明：α-Synuclein 积聚过程包括单体→寡聚体→短纤维→长纤维这几个阶段；而α-Synuclein 纤维在浓度降低的情况下，会发生解聚，解聚是从纤维的中间发生断裂开始，经过一段时间后，长的蛋白纤维会解聚成为一些短纤维和很多蛋白颗粒。

Application of atomic force microscopy in studying α-synuclein's aggregation and disaggregation

TANG Lin LI Hongtao DU Haining JI Lina ZHANG Feng

LI Minqian HU Hongyu HU Jun

Keywords α-synuclein fibril, Aggregation, Atomic force microscopy

Studying the aggregation and disaggregation processes of α-synuclein fibrils is very meaningful for the therapy of some neurodegenerative diseases, such as Parkinson's disease and Alzheimer's disease. In this paper, the α-synuclein at different stages of its aggregation process was observed by atomic force microscopy. And the disaggregation process of α-synuclein fibrils was monitored by *in situ* atomic force microscopy in solution. It was found that the process of α-synuclein fibrillization included several stages: (a) oligomerization from monomers; (b) formation of short fibrils; (c) maturation of fibrils; and that α-synuclein fibrils could disaggregate step by step in solution when diluted to some extent. The disaggregation usually started at the middle of the fibrils, and as time went by, the long fibrils could disaggregate into some short fragments and particles with different sizes. Relevant mechanism has been discussed.

块体非晶合金 $Zr_{55}Cu_{30}Al_{10}Ni_5$ 玻璃转变温度附近晶化的同步辐射 X 光小角散射研究

柳 义 柳林[1] 王俊[2] 董宝中[2]

关键词 同步辐射，X 光小角散射，块体非晶合金，玻璃转变，等温退火

应用同步辐射 X 光小角散射法对块体非晶合金 $Zr_{55}Cu_{30}Al_{10}Ni_5$ 在玻璃转变温度附近的晶化进行研究。实验表明：在 400—442 ^{o}C 的退火温度范围内, 样品中已有结晶颗粒析出，析出颗粒的大小差别不明显，但析出颗粒的数量与退火温度及退火时间有关。 退火时间一定时, 析出的颗粒数量随退火温度的升高而增多; 退火温度一定时, 析出的颗粒数量随退火时间的增加而增多。

1 华中科技大学材料学院，2 中国科学院高能物理研究所

Study on crystallization of $Zr_{55}Cu_{30}Al_{10}Ni_5$ bulk amorphous alloy near glass transition temperature by SAXS

LIU Yi LIU Lin[1] WANG Jun[2] DONG Baozhong[2]

Keywords Synchrotron radiation, Small angle X-ray scattering, Bulk amorphous alloy, Glass transition, Isothermal annealing

The crystallization of $Zr_{55}Cu_{30}Al_{10}Ni_5$ bulk amorphous alloy near the glass transition temperature has been investigated by synchrotron radiation X-ray small angle scattering (SAXS). The experimental results show that crystal particles in amorphous matrix are formed during the annealing of 400℃—442℃ which is near glass transition temperature. It is found that there are no obvious differences in the size of precipitated crystal particles and that the number of precipitated particles increases with the increase of annealing time at the given annealing temperature, or increases with the increase of annealing temperature in the given annealing time.

1 Department of Materials Science and Engineering, Huazhong University of Science & Technology

2 Institute of High Energy Physics, the Chinese Academy of Sciences.

BSRF-3B3 中能光束线聚焦镜压弯机构离线测试

朱 毅 傅 远 夏绍建 朱佩平[1] 周泗忠[2]

关键词 聚焦镜，压弯机构，离线测试，成像规律

聚焦镜是光束线中重要部件,将从储存环中引出的同步辐射光在水平和垂直两个方向上聚焦，以缩小像斑，提高光子密度。聚焦镜的聚焦性能好坏直接影响到光束线的成像性能。目前，国际

上对聚焦镜压弯机构的性能测试，有些是采用长程面型仪（LTP），从微观上测量聚焦镜的面型，而非从宏观的角度涉及聚焦镜成像性能的测试；另外，对于聚焦镜成像性能及规律的测试，也大多采用在线测试的方法。在线测试，一方面浪费大量的同步光机时，另一方面对测试人员的身体造成一定的伤害。为此，在 BSRF-3B3 中能光束线安装调试过程中，我们设计出一套完整的离线测试方法。这种方法采用激光模拟同步辐射光，测试聚焦镜压弯机构性能，并通过观察焦点处光斑变化规律测试压弯机构性能，摸索压弯成像规律；另一方面，记录压力传感器读数，为今后在线调试提供参考依据。

1 中国科学院高能物理研究所, 2 中国科学院西安光学精密机械研究所

Testing of four-point bender for cylindrical mirror of BSRF-3B3 beamline

ZHU Yi FU Yuan XIA Shaojian ZHU Peiping[1] ZHOU Sizhong[2]

Keywords Toroidal mirror, Bender, Off-line testing, Imaging rule

The toroidal mirror coated with nickel on the fused silicon substrate is an important part at the BSRF-3B3 beamline, which focuses a beam of synchrotron radiation from the bending magnet on the sample in both vertical and horizontal directions. Here, a Four-Point Bender is used to bend a cylindrical mirror coated nickel on the fused silica substrate. In the past, a long trace profiler (LTP) was used to test performance of the Four-Point Bender, but this technique couldn't test the cylindrical mirror's macro-performance of imaging. So, we have designed a new method: using a laser beam instead of a beam of synchrotron radiation to off-line test the performance of the Four-Point Bender, and grope for the rule of imaging by observing the imaging of the beam focused. In this paper, we introduce details of the testing method.

1 Institute of High Energy Physics, the Chinese Academy of Sciences.

2 Xi'an Institute of Optics and Precision Mechanics

新型大量程 LTP 控制系统及数据处理系统

杜国浩 肖体乔 夏绍建 温 利 徐洪杰

关键词 面阵 CCD，线性导轨，位相板，质心法，衍射图像

讨论了最近研制成功的新型大量程长程面形仪（LTP）中精密线性导轨扫描、定向移动以及高精度任意步长等运动的控制；采用面阵CCD获取准直激光束通过位相板形成的衍射图像、经采集卡数字化，由计算机完成数据处理。数据处理中实现了MATLAB与VC++程序间的通信，采用质心法分离测量光斑以及参考光斑，并利用MATLAB中神经网络算法求取位相板衍射图像中暗线位置，达到了设计要求的精度。

Control system and data processing system of the novel LTP

DU Guohao XIAO Tiqiao XIA Shaojian WEN Li XU Hongjie

Keywords Area scan CCD camera, Linear guided stage, Phase plate diffraction, Centroidal method, Diffraction picture

The control of linear guided stage and image capturing system in the novel Long Trace Profiler (LTP) are discussed. Diffraction pattern capturing and data processing are completed through area scan CCD camera, frame grabber and computer. Communication between the Matlab and VC++ is established. The measuring pattern and reference pattern are separated by the law of centroidal method. Higher precision of the light spot determination is obtained using Neural Networks Algorithms.

微聚焦管硬 X 射线位相衬度成像

陈 敏 肖体乔 骆玉宇 刘丽想 魏 逊 杜国浩 徐洪杰

关键词 位相衬度成像，微聚焦管 X 线源，吸收衬度成像，光学传递函数

利用微聚焦管硬 X 射线光源进行同轴位相衬度成像实验，所用的光源聚焦尺寸最小可达 0.5 μm。根据硬 X 线管的光学传递函数对光源尺寸、相干长度等因素对成像分辨率的影响进行了分析。对新鲜的未经任何处理的生物样品进行了位相衬度成像，分辨率在 10 μm 左右，并和吸收衬度成像进行了对比。实验结果表明利用微聚焦管作为硬 X 线光源，多色硬 X 线位相衬度成像可以得到比吸收衬度成像高得多的分辨率。

Phase-contrast imaging with microfocus X-ray source

CHEN Min XIAO Tiqiao LUO Yuyu LIU Lixiang WEI Xun

DU Guohao XU Hongjie

Keywords Phase-contrast imaging, Microfoucus X –ray source, Absorption-contrast imaging, Optical transfer function

Experimental results of the in-line phase-contrast imaging with a microfocus X-ray source are reported. The minimized focused spot size of the X-ray source is about 0.5μm. According to the optical transfer function of the microfocus, the effects of both X-ray source's size and the coherent length of X-ray on the imaging resolution are discussed. The phase-contrast images of fresh biomaterials are obtained with 10μm resolution. Compared with the absorption-contrast image, the fine-structure of fresh biomaterials can be observed in the phase-contrast image with much higher resolution.

核 物 理

Nuclear physics

核物理室简介

上海应用物理研究所核物理室主要开展放射性核束物理实验与理论研究，中高能及极端相对论能量的重离子碰撞（RHIC）反应的实验和理论研究，基于同步辐射加速器的亚 GeV 及 MeV 量级 BCS γ 束的产生及其在多学科研究领域和应用领域的探索性研究。另外，我们还从事碳纳米管与合成机制、分子动力学及其可能应用的研究，DNA 的物理性质、生物流体及流体相关的计算方法等。在研国家重点基础研究发展规划项目（973）1 项，国家基金委重点项目 1 项，中国科学院知识创新工程重要交叉方向项目 1 项，国家杰出青年基金海外类 1 项,国家自然科学基金 5 项等。现有中国科学院院士 1 名，国家杰出青年基金获得者 1 人，中国科学院百人计划 1 人，海外客座研究员 2 人，及其他中高级研究人员 10 人，研究生 30 多人。主要承担国家 973 计划、国家基金委重点项目和中科院创新方向性项目等。2003 年发表论文 49　篇，2004 年发表 SCI 论文 52 篇。其中合作发表的 Phys Rev Lett 12 篇。

利用 BUU 模型研究核反应总截面的入射能量和同位旋依赖性

蔡翔舟 沈文庆 钟 晨 马余刚 方德清 张虎勇
魏义彬 郭威 陈金根 王鲲 马国亮

关键词 BUU 模型，反应总截面，同位旋

我们利用 BUU 模型研究了核反应总截面的入射能量依赖性和同位旋依赖性，计算中使用了方型的和 HO-型的密度分布，密度分布的宽度参数通过拟合相对论能量下核反应总截面的实验数据得到，上述 BUU 模型的计算可以比采用光学限近似的 Glauber 模型的计算结果更好地拟合实验数据，消除了对高能归一下中能核反应总截面的系统低估。研究表明核反应总截面是对核状态方程(EOS)敏感的物理量，定义的差异因子可以实验数据作为是否存在晕或皮结构的一个辅助判据。

Study of incident energy and isospin dependencies of total reaction cross section via the BUU model

CAI Xiangzhou SHEN Wenqing ZHONG Chen MA Yugong FANG Deqing
ZHANG Huyong WEI Yibin GUO Wei CHENG Jingen WANG Kun MA Guolian

Keywords BUU model, Total reaction cross section, Isospin

The incident energy and isospin dependencies of total reaction cross sections σ_R were studied using the Boltzmann–Uehling–Uhlenbeck (BUU) model. When the width parameter of square-type or HO-type density distribution is obtained by fitting the σ_R at relativistic energies, the calculated result with BUU-model can reproduce the experimental data at intermediate energies better than that with Glauber-model of optical limit approximation. The systematical underestimation of σ_R at intermediate energy was removed out by BUU calculation framework. It is found that σ_R is sensitive to nuclear equation of state (EOS). It is also found that the difference factor (d) defined in text is sensitive to the nuclear structure such as neutron halo and neutron skin, etc.

利用 BUU 模型研究 ^{11}Li 的核反应总截面和双中子剥去截面

蔡翔舟 沈文庆 钟 晨 马余刚 张虎勇 魏义彬
陈金根 周星飞 郭 威 王鲲 马国亮

关键词 中子晕, 核反应总截面, 双中子剥去截面

发展了 BUU 模型，使能够同时研究双中子晕结构核 ^{11}Li 引起反应的核反应总截面和双中子剥去截面，计算中使用软的核物质状态方程和 0.8 倍的核子-核子碰撞截面，相对论平均场模型计算的中子和质子密度被引入 BUU 模型，用来代替通常使用的方密度分布，计算结果可以很好地拟合不同反应系统实验数据。假定对于晕核及其核芯核，彼此的核反应总截面与相互作用截面之

间的差别相同，那么 ^{11}Li 的双中子剥去截面可以表示成 ^{11}Li 及其核芯核 ^{9}Li 引起反应的核反应总截面之差，研究结果表明这一假定可以适用于高能，对于中能核反应，需要更多实验数据来检验。

Boltzmann-Uehling-Uhlenbech calculation of total reaction cross-section and fragmentation cross-section

CAI Xiangzhou SHEN Wenqing ZHONG Chen MA Yugang ZHANG Huyong
WEI Yibin CHEN Jingen ZHOU Xingfei GUO Wei WANG Kun MA Guoliang

Keywords Neutron halo, Total reaction cross section, 2n-removal reaction cross section

The σ_R and σ_{-2n} have been calculated via the BUU model by using soft EOS and $0.8\times Cug$. The density distribution obtained from RMF model has been introduced to replace the commonly used square-type distributions in BUU calculation. The calculated results can reproduce the experimental data well for various reaction systems. Here σ_{-2n} is calculated as the difference between σ_R of halo nucleus and core nucleus, by assuming $\sigma_{corr}\cong 0$. It indicates that this assumption works very well at high energy in the BUU calculation. More experimental measurements are necessary to test the validity of this assumption at intermediate energy.

基于同步辐射加速器的康普顿背散射光源性质及其应用研究

蔡翔舟 顾嘉辉 郭 威 马余刚 沈文庆

关键词 光束线站，康普顿背散射，同步辐射装置，高功率激光器

我们介绍了利用康普顿背散射（BCS）产生 γ 射线的原理，并以 SSRF 储存环电子运行参数为例，给出了利用 BCS 方法产生 MeV 量级 γ 射线束的计算结果，预期该光子束具有高强度、高极化度、单色性、方向性好等优点。同时对国际上已运行和拟建的高能和低能 γ 束线站的装置和性能作了简要介绍，并分别探讨了高能和低能准单色极化 γ 射线在核物理和核天体物理研究中的广泛应用前景。文中对基于正对以及离轴几何条件下，采用直线加速器加速的电子同短脉冲强激光发生 Compton/Thomson 散射的激光同步辐射源作了初步探讨，这一方法为我们构建超短脉冲的高亮度、准单色、可调谐的 X - γ 射线源开辟了一条新途径。

Studies on property and application of compton back-scattering γ-ray source based on synchrotron radiation facility

CAI Xiangzhou GU Jiahui GUO Wei MA Yugang SHEN Wenqing

Keywords γ-Ray beam line, Compton back-scattering, Synchrotron radiation facility, High power laser

We present an outline of Compton back-scatering (BCS) theory and properties of BCS γ-rays of 1—25MeV with numerical compution based on major parameters of SSRF(Shanghai Synchrotron Radiation Facility) storage ring. It predicted that the high intensity quasi-monochromatic BCS γ-rays with high linear or circular polarization will be produced. We briefly introduce the facilities and properties of present and proposed γ-ray beam lines in the world. They can be widely applied to fundamental researches of nuclear physics, nuclear astrophysics and related applications. We also present some preliminary results of a Laser Synchrotron Source (LSS) based on Compton/Thomson scattering of the electrons of a linac and high-power laser beams in head-on and off-axis geometry. This approach opens a new route toward ultra-short, high-brightness, quasi-monochromatic tunable X-ray/ γ-ray source.

RHIC 200 GeV d+Au 碰撞中 K^0s, ϕ, Λ和 Ξ 粒子的产额研究

蔡翔舟　马余刚　沈文庆　黄焕中　（STAR 实验合作组）

关键词　横向动量谱，核修正因子，氘-金碰撞

我们给出了 RHIC-STAR 探测器测量得到的能量为 200 GeV 的 d+Au 碰撞中K^0s, ϕ, Λ和Ξ粒子横向动量分布的初步结果，测量的横向动量谱可以用双指数函数很好地拟合。通过二元碰撞数的归一可以得到 p_t 范围到 6GeV/c 的粒子产额的中心度依赖函数（R_{CP}），结果表明，K^0s, ϕ, Λ 和Ξ粒子的 R_{CP} 遵循粒子种类的依赖性，和 parton recombination 模型关于强子形成的预言一致，表明 Cronin 效应及其粒子种类依赖性可能并不仅仅来源于初始状态下的部分子散射。

Production of K^0s, ϕ, Λ and Ξ from 200 GeV d+Au collisions at RHIC

CAI Xiangzhou　MA Yugang　SHEN Wenqing　HUANG Huanzhong

for the STAR Collaboration

Keywords　Transverse momentum spectra, Rcp, d+Au collisions

We present a preliminary measurement of K^0s, ϕ, Λ and Ξ transverse momentum (p_t) distribution from $sqrt(s_{NN})$=200 GeV d+Au collisions at RHIC. The measured spectra can be described by using a double exponential fit. The centrality dependence of the particle yield with respect to the number of binary collision scaling (R_{CP}) will be presented for a p_t up to 6 GeV/c. The particle dependence of the R_{CP} among K^0s, ϕ, Λ and Ξ is consistent with expectations from parton recombination models for hadron formation. The Cronin effect and its particle dependence appear not due to initial parton scatterings alone as previously assumed in models.

轻核中激发态的质子晕或皮

陈金根[1] 蔡翔舟 张虎勇 沈文庆 任中洲[2] 蒋维洲
马余刚 钟 晨 魏义彬 郭 威 周星飞 马国亮 王 鲲

关键字 轻核，激发态，相对论平均场，质子晕（皮）

本文用相对论平均场理论（NLZ 和 NL3 势）研究了 ^{13}N、^{15}N 和 ^{9}B 的基态和激发态特性。计算显示理论计算的结合能与相应的实验值非常接近，结果发现：^{13}N 和 ^{9}B 的第一激发态以及 ^{15}N 的第二激发态都是弱束缚的。特别是对 ^{13}N 和 ^{15}N，它们的质子密度分布在激发态时有一个长的尾巴，而且这些核的最外层的质子均方根半径与他们相应的物质均方根半径相比非常大。所以我们预测在 ^{13}N 的第一激发态和 ^{15}N 第二激发态分别存在质子晕结构；而在 ^{9}B 的第一激发态存在质子皮结构。

1 浙江林学院理学院
2 南京大学物理系

Proton halo or skin in the excited states of light nuclei

CHENG Jingen[1] CAI Xiangzhou ZHANG Huyong SHEN Wenqing
REN Zhongzhou[2] JIANG Weizhou MA Yugang ZHONG Chen WEI Yibing
GUO Wei ZHOU Xingfei MA Guoliang WANG Kun

Keywords Light nuclei, the excited states, Relativistic mean-field, proton halo (skin)

The properties of nuclei ^{13}N, ^{15}N and ^{9}B are investigated in the relativistic mean-field theory with NLZ and NL3 force parameters. The calculated binding energies are very close to the experimental ones. The calculations show that the first excited state ($1p_{1/2}$) in ^{9}B, the first excited state ($2s_{1/2}$) in ^{13}N and the second excited state ($2s_{1/2}$) in ^{15}N are weakly bound. Especially for ^{13}N and ^{15}N, the proton density distributions in the two above excited states have a long tail and the RMS radii of the last proton are greatly larger compared with their respective matter radii. It is predicted that there exists a proton halo in the first excited state of ^{13}N and in the second excited state of ^{15}N, respectively. It also indicates that the first excited state in ^{9}B is a proton skin state.

1 College of Sciences, Zhejiang Forestry University
2 Department of Physics, Nanjing University

相对论平均场对大形变核 ^{23}Al 的奇异结构研究

陈金根[1] 蔡翔舟 张虎勇 王庭太 马余刚 任中洲[2]
方德清 钟 晨 魏义彬 郭 威 周星飞 王 鲲 马国亮
田文栋 左嘉旭 马春旺 陈金辉 颜廷志 沈文庆

关键字 四极形变，能级倒转，质子晕，相对论平均场

我们用 NL075 势的相对论平均场模型对质子晕候选核 ^{23}Al 进行了研究，在研究过程中运用了约束计算方法。约束计算结果表明 ^{23}Al 有一个大的长轴形变，在此大形变条件下，由于 $1d_{5/2}$ 和 $2s_{1/2}$ 能级比较靠近，从而发生了能级倒转，这种倒转可能会有利于晕的形成。我们能自洽给出外层核子占有几率，计算预测 ^{23}Al 的 $2s_{1/2}$ [211]和 $1d_{5/2}$ [202]能级上的质子都是弱束缚的，它们的质子占有数分别为 0.56 和 0.29。另外，计算结果显示 ^{23}Al 的物质分布半径与实验结果相一致，而且质子和中子均方根半径之差非常大。这些都表明在 ^{23}Al 中存在质子晕结构。

1 浙江林学院理学院
2 南京大学物理系

Investigation of exotic structure of the deformed nucleus ^{23}Al

CHENG Jingen[1] CAI Xiangzhou ZHANG Huyong WANG Tingtai MA Yugang
REN Zhongzhou[2] FANG Deqing ZHONG Chen WEI Yibing GUO Wei ZHOU
Xingfei WANG Kun MA Guoliang TIAN Wendong ZUO Jiaxu MA Chunwang
CHEN Jinhui YAN Tingzhi SHEN Wenqing

Keywords Quadrupole deformation, Inversion of energy levels, Proton halo, Relativistic mean-field

The candidate for proton halo nucleus ^{23}Al is investigated base on the constrained calculations in the framework of deformed relativistic mean field (RMF) model with the NL075 parameter set. It is shown by the constrained calculations that, the deformation of ^{23}Al. With that large deformation, the non-constrained RMF calculation predicts that there has an inversion between the $2s_{1/2}$ [211] and $1d_{5/2}$ [202] shells and the valence protons in the two above shells are weakly bound. The calculated RMS radius for matter is in agreement with the experimental one. It is also predicted that the difference between the proton RMS radius and the neutron one is very large. It is suggested that there exists a proton halo in ^{23}Al.

1 College of Sciences, Zhejiang Forestry University
2 Department of Physics, Nanjing University

$\sqrt{S_{NN}}$ = 200 GeV 重离子碰撞中 Φ 介子的椭圆流

陈金辉 马余刚 马国亮 蔡翔舟 左嘉旭 贺泽君 龙家丽 沈文庆 钟 晨
陈金根 方德清 郭 威 马春旺 苏前敏 田文栋 王 鲲 魏义彬 颜廷志

关键词 Φ 介子，椭圆流，多相输运模型

通过 Φ---k^+ + k^- 衰变道，应用多相输运模型（AMPT），我们重构了质心系能量为 200 GeV 的金金碰撞中 Φ 介子的椭圆流。结果表明，Φ 介子的椭圆流和其它介子椭圆流的实验结果有相似的行为。我们给出了椭圆流和横向动量的函数关系，在此基础上研究了碰撞中心度的依赖性和强子过程的再散射效应。

Elliptic flow of Φ-meson at top RHIC energy

CHEN Jinhui MA Yugang MA Guoliang CAI Xiangzhou ZUO Jiaxu
HE Zejun LONG Jiali SHEN Wenqing ZHONG Chen CHEN Jingen
FANG Deqing GUO Wei MA Chunwang SU Qianmin
TIAN Wendong WANG Kun WEI Yibin YAN Tingzhi

Keywords Φ-meson, Elliptic flow, AMPT model

Based on a multiple transport (AMPT) model, the elliptic flow V_2 of Φ-meson at relativistic heavy ion collision (RHIC) energy has been presented where the Φ is reconstructed from k^+k^- pair. The V_2 of Φ-meson seems to give a similar behavior as that of other mesons compared with the experimental results. The dependences of transverse momentum p_T and of centrality of V_2 is obtained. In addition, the rescattering effect is also investigated for Φ.

中能下碎片椭圆流的核子数标度律研究

颜廷志 马余刚 蔡翔舟 陈金根 陈金辉 方德清 郭 威
贺泽君 龙家丽 马春旺 马国亮 沈文庆 苏前敏
田文栋 王 鲲 魏义彬 钟 晨 左嘉旭

关键词 椭圆流，核子数标度律

最近在相对论能区的 RHIC 实验中发现了强子椭圆流与横动量的关系存在着组分夸克数的标度律现象，即不同组分夸克数目的强子对应不同的椭圆流曲线，但每组分夸克数目的强子椭圆流曲线则重合。与此类比，我们考虑中能区的椭圆流对碎片质量数 A 是否也存在标度律现象。我们用 IQMD 模型对该现象进行了初步研究。选择的碰撞系统为 ^{86}Kr+^{112}Sn、^{86}Kr+^{124}Sn，分别对软势、

硬势、同位旋相关与否进行了研究。发现轻质量碎片的椭圆流、快度分布、动量分布等也类似于相对论能区那样存在的标度率，即存在着对碎片质量数 A 的标度律现象，即每核子的椭圆流、快度密度、动量分布曲线在误差范围内也是重合的。对中能区碎片的椭圆流的核子数标度率的理解有助于理解 RHIC 能区椭圆流的物理起源。

Nucleon number scaling of elliptic flow in intermediate energy heavy ion collisions

YAN Tingzhi MA Yugang CAI Xiangzhou CHEN Jingen CHEN Jinhui
FANG Deqing GUO Wei HE Zejun LONG Jiali MA Chunwang MA Guoliang
SHEN Wenqing SU Qianmin TIAN Wendong WANG Kun
WEI Yibin ZHONG Chen ZUO Jiaxu

Keywords Elliptic flow, Nucleon number scaling

The number-of-constituent-quark (NCQ) scaling of elliptic flow of hadrons has been found at relativistic heavy ion collisions recently, namely the elliptic flow of hadrons formed by different number of quarks is different, but the elliptic flow per constituent quark is the same. In parallel, we want to explore if there exists the number-of-nucleon scaling (NN) of elliptic flow of fragments at intermediate energy heavy ion collisions. To this end, ^{86}Kr+^{112}Sn and ^{86}Kr+^{124}Sn collisions have been simulated by Isospin Quantum Molecular Dynamics model. In our preliminary results, we found that there are also NN scaling phenomena for the elliptic flow, rapidity distribution and transverse momentum distributions of light fragments. The coalescence model of fragment formation can explain the NN scaling of elliptic flow, rapidity distribution and transverse momentum distribution of fragments.

^{23}Al 的单质子晕结构研究

方德清 马春旺 马余刚 蔡翔舟 陈金根 陈金辉 郭 威
田文栋 王 鲲 魏义彬 颜廷志 钟 晨 左嘉旭 沈文庆

关键词 核反应总截面，Glauber 模型，质子晕

我们采用 Glauber 理论对丰质子核 ^{23}Al 的核反应总截面进行了研究。假设 ^{23}Al 的结构为核芯加一个价质子。核芯的密度分布采用 HO 形式的分布，而价质子的密度分布通过求解 Woods-Saxon 势的本征值方程得到。通过对炮弹和靶的密度分布进行多高斯展开，我们得到了计算穿透函数的解析表达式。在模型中库仑力和有限力程效应都考虑了，从而使得修正后的 Glauber 模型适合研究晕核的反应总截面。 我们的计算表明 ^{23}Al 的最后一个质子主要处于 s 轨道，这说明它具有质子晕结构。

Study on the one-proton halo structure in ^{23}Al

FANG Deqing MA Chunwang MA Yugang CAI Xiangzhou CHEN Jingen
CHEN Jinhui GUO Wei TIAN Wendong WANG Kun WEI Yibin
YAN Tingzhi ZHONG Chen ZUO Jiaxu SHEN Wenqing

Keywords Reaction cross section,Glauber model, Proton halo

The Glauber theory has been used to investigate the reaction cross section of proton-rich nucleus ^{23}Al. A core plus a proton structure is assumed for ^{23}Al. HO-type density distribution is used for the core while the density distribution for the valence proton is calculated by solving the eigenvalue problem of Woods-Saxon potential. The transparency function in an analytical expression is obtained adopting multi-Gaussian expansion for the density distribution. Coulomb correction and finite-range interaction are introduced. This modified Glauber model is apt for halo nuclei. A dominate s-wave is suggested for the last proton in ^{23}Al from our analysis which is possible in the RMF.

^{21}Na 的动量分布与核反应总截面研究

方德清 马余刚 蔡翔舟 沈文庆 孙志宇[1] 任中洲[2] 郭 威 魏义彬 王 鲲
颜廷志 马春旺 陈金根 陈金辉 马国亮 苏前敏 田文栋 钟 晨 左嘉旭
Hosoi M[3] Izumikawa T[4] Kanungo R[5] Nakajima S[3] Ohnishi T[5] Ohtsubo T[4]
Ozawa A[6] Suda T[5] Sugawara K[3] Suzuki T[3] Takisawa A[4]
Tanaka K[5] Yamaguchi T[3] Tanihata I[5]

关键词 动量分布，核反应总截面

在 RIKEN 的放射性束流线（RIPS）上，用 135A MeV ^{28}Si 主束轰击 Be 靶产生次级束 ^{21}Na。实验测量了 64A MeV ^{21}Na 打 C 靶的单质子擦去反应以及核反应总截面。用飞行时间（TOF）的方法测量了从 ^{21}Na 产生 ^{20}Ne 碎片的动量分布。分析得到了 ^{21}Na 产生 ^{20}Ne 的动量分布半高宽（FWHM）初步结果为（221±15） MeV/c，在误差范围内与 Goldhaber 模型的预言基本一致。核反应总截面数据的分析以及相关理论研究正在进行之中。

---

1 近代物理研究所

2 南京大学物理系

3 Department of Physics, Saitama University

4 Department of Physics, Niigata University

5 日本理化学研究所

6 Department of Physics, Tsukuba University

Study on the momentum distribution and reaction cross section for ^{21}Na

FANG Deqing MA Yugang CAI Xiangzhou SHEN Wenqing SUN Zhiyu[1]
REN Zhongzhou[2] GUO Wei WEI Yibin WANG Kun YAN Tingzhi
MA Chunwang CHEN Jingen CHEN Jinhui MA Guoliang SU Qianmin
TIAN Wendong ZHONG Chen ZUO Jiaxu Hosoi M[3] Izumikawa T[4] Kanungo R[5]
Nakajima S[3] Ohnishi T[5] Ohtsubo T[4] Ozawa A[6] Suda T[5] Sugawara K[3] Suzuki T[3]
Takisawa A[4] Tanaka K[5] Yamaguchi T[3] Tanihata I[5]

Keywords Momentum distribution, Reaction cross section

The one-proton removal reactions as well as reaction cross sections for ^{21}Na on carbon target have been studied by using 135A MeV ^{28}Si primary beam on RIPS in RIKEN. The longitudinal momentum distributions of ^{20}Ne fragments from ^{21}Na breakup have been measured at 64A MeV by means of direct time-of-flight method. FWHM of the distributions have been determined to be 221±15 MeV/c, which is consistent with the Goldhaber Model's prediction within the error bars. The detailed analysis of reaction cross sections and theoretical study are in progress.

1 Institute of Modern Physics
2 Department of Physics, Nanjing University
3 Department of Physics, Saitama University
4 Department of Physics, Niigata University
5 The Institute of Physical and Chemical Research (RIKEN), Japan
6 Department of Physics, Tsukuba University

^{15}C 的中子晕结构研究

方德清 Yamaguchi T 郑 涛[1] Ozawa A[1] Chiba M[1] Kanungo R[1]
Kato T[1] Morimoto K[1] Ohnishi T[1] Suda T[1] Yamaguchi Y[1]
Yoshida A[1] Yoshida K[1] Tanihata I[1]

关键词 动量分布，核反应总截面，Glauber 模型

在 RIKEN 的放射性束流线（RIPS）上，用 110A MeV ^{22}Ne 主束轰击 Be 靶产生次级束 ^{14,15}C。实验测量了 80A MeV ^{14,15}C 打 C 靶的单中子或双中子擦去反应，以及核反应总截面。用飞行时间(TOF)的方法测量了从 ^{15}C 产生 ^{13,14}C 碎片和从 ^{14}C 产生 ^{13}C 碎片的横向动量分布。分析得到了 ^{15}C

产生 ^{14}C 和 ^{13}C 的动量分布半高宽（FWHM）分别为（71±9） MeV/c 和（223±28） MeV/c，而 ^{14}C 产生 ^{13}C 的动量分布半高宽为（195±21） MeV/c。从 ^{15}C 和 ^{14}C 产生的 ^{13}C 的动量分布宽度与 Goldhaber 模型的预言基本一致。而 ^{15}C 产生 ^{14}C 的动量分布宽度却要比该模型计算小得多，这一结果与 MSU 和 GANIL 的测量一致。同时观测到 ^{15}C 的核反应总截面比相邻核有反常增加。在 Glauber 模型的框架中，对实验测得的动量分布和核反应总截面进行了探讨。动量分布和核反应总截面分析结果同时显示 ^{15}C 的最后一个中主要处于 $s_{1/2}$ 态，具有中子晕结构。

1 日本理化学研究所

One-neutron halo structure in ^{15}C

FANG Deqing Yamaguchi T ZHENG Tao[1] Ozawa A[1] Chiba M[1] Kanungo R[1]
Kato T[1] Morimoto K[1] Ohnishi T[1] Suda T[1] Yamaguchi Y[1] Yoshida A[1]
Yoshida K[1] Tanihata I[1]

Keywords Momentum distribution,Reaction cross section,Glauber model

The one or two-neutron removal reactions as well as reaction cross sections for $^{14,15}C$ on carbon target have been studied by using 110A MeV ^{22}Ne primary beam on RIPS in RIKEN. The longitudinal momentum distributions of $^{13,14}C$ fragments from ^{15}C, and ^{13}C fragments from ^{14}C breakup have been measured at 83A MeV by means of direct time-of-flight method. FWHM of the distributions have been determined to be （71±9） MeV/c and （223±28） MeV/c for ^{14}C and ^{13}C from ^{15}C, and （195±21） MeV/c for ^{13}C from ^{14}C. The FWHM for ^{13}C fragments from ^{15}C and ^{14}C breakup are consistent with the Goldhaber Model's prediction. The FWHM of ^{14}C fragments from ^{15}C is much smaller, which confirms the experimental results from MSU and GANIL. An anomalous enhancement from its neighbors has been observed in the measured reaction cross section of ^{15}C. The experimental data are discussed in the framework of the Glauber model. The analysis of both the fragment momentum distributions and reaction cross sections indicate a dominant s-wave component in the ground state of ^{15}C.

1 The Institute of Physical and Chemical Research (RIKEN), Japan

谁主导了微米（纳米）尺度下单根 DNA 分子附近水的流体行为

张 益 李华兵 雷晓玲 陆杭军 艾小白 胡 钧 陈十一 方海平

关键词 流动性，DNA，纳米尺度

实验上用水流作用在拉直的 DNA 分子上得到波形结构，通过与实验比较，发现纳米尺度的 DNA 与水的相互作用可以用宏观理论来讨论。

What governs the fluidic behavior of water near single DNA molecules at the micro/nano scale?

ZHANG Yi LI Huabing LEI Xiaoling LU hangjun AI Xiaobai HU Jun
CHEN Shiyi FANG Haiping

Keyword Fluidic behaviour, DNA, Micro/nano scale

The fluidic behavior of water at the micro/nano scale is studied by using of single DNA molecules as a model system. Stable curved DNA patterns with spans about one micron were generated by using of water flows, and observed by Atomic Force Microscopy. By rigorously comparing the numerical simulation results with these patterns, it is suggested that macroscopic hydrodynamics stillwork quantitatively well on the fluid flows at the nanoscale. Our observation is also helpful to understand of the dynamics of biomolecules in solutions from nanoscale to microscale.

可控纳米水通道的开关效应

万荣正 李敬源 陆杭军 方海平

关键词 纳米碳管，水通道，分子动力学

运用分子动力学方法研究了连续形变的单壁纳米碳管（SWNT）中的水分子的动力学行为，发现当形变在 2.0 Å 以内时，管中的净流量和水分子平均数目都没有太大变化，但形变进一步增加 0.6 Å 时，这两个值迅速下降。由此发现这一纳米通道具有可以过滤噪音同时又对有效信号非常敏感的特性，可以作为极好的通道开关。生物水通道的类似良好特性可能也来自于两者内部相似的水密度的驻波型分布。而使这一通道由开转变到关状态所需的最小外力正好处于目前实验手段所能达到的范围内，这就为发展基于单壁纳米碳管的纳米器件提供了可能。

Controllable water channel gating of nanometer dimensions

WAN Rongzheng LI Jingyuan LU Hangjun FANG Haiping

Keywords Carbon nanotube, Water channel, Molecular dynamics

The dynamics of water molecules in a single-walled carbon nanotube (SWNT) under continuous deformations was studied with molecular dynamics simulations. The flux and occupancy remain almost fixed within a deformation of 2.0Å but decreases sharply for a further deformation of 0.6Å. The nanopore is an excellent on-off gate that it is both effectively resistant to deformation noises and sensitive to available signals. Biological water channels are expected to share this advantage due to similar wavelike water distributions. The minimal external force required for triggering an open-close transition falls within the working range of many available experimental facilities, which provides possibility of developing SWNT-based nanoscale devices.

碱基水平单个 DNA 分子的动力学模拟

雷晓玲　王晓峰　胡 钧　方海平

关键词　模拟，DNA，碱基层面

基于 DNA 的统计模型（Phys. Rev. Lett. 82，4560 (1999)），提出了一个碱基层面介观尺度双链 DNA 的离散模型。数值模拟结果完全符合了 DNA 单分子操纵实验中出现的从相对拉伸 1.1 到 1.65 区域的 65pN 平台，并且数值模拟不同的超螺旋程度下的力拉伸曲线可以和实验数据比拟。数值模拟还发现大沟和小沟对 DNA 拉伸实验影响很小。我们的模型利于研究 DNA 短片段的行为，在统计模型和原子尺度的模型之间架起了一座桥梁。

Dynamic simulation of single DNA molecule at the base level

LEI Xiaoling　WANG Xiaofeng　HU Jun　FANG Haiping

Keywords　Simulation, DNA, Base level

A mesoscopic discrete dsDNA model at the base level is proposed based on the statistical model (Phys. Rev. Lett. 82, 4560 (1999)). The numerical simulations reproduce the 65pN plateau and those on the force vs extension for different supercoiling degrees are favorable with the experimental data. It is found that the existence of the major grooves and minor grooves play a negligible role in the stretching. Our model has potential applications on the study of short DNA segments and provides a bridge between the statistical models and atomic modelling.

纳米尺度液滴的接触角与液滴大小的相关性

郭宏凯　方海平

关键词　接触角，纳米尺度，非极性，液体氩

我们用分子动力学方法研究了纳米尺度下静止在固体基底上的非极性氩液滴的接触角。结果发现接触角随着液滴大小的变化关系跟液体分子和固体基底分子之间的相互作用强度密切相关。这一发现跟以前的许多理论和实验结果相一致。

Drop size dependence of the contact angle of nanodroplets

GUO Hongkai　FANG Haiping

Keywords　Contact angle，Nanosized, Non-polarized, Liquid argon

The contact angle of nanosized non-polarized argon sessile droplets on a solid substrate is studied

by using of molecular dynamics simulations. It is found that the drop size dependence of the contact angle is sensitive to the interaction between the liquid molecules and solid molecules. This observation is consistent with many of the previous theoretical and experimental results.

SARS 传播中超级传播者的根本机理

方海平　陈纪修　胡 钧　徐学敏

关键词　蒙特卡罗模型，超级传播者

我们在一个时空蒙特卡罗模型的基础上，发现超级传播者具有很高的频率。而潜伏期对超级传播者出现的频率起至关重要的作用。

On the origin of the super-spreading events in the SARS epidemic

FANG Haiping　CHEN Jixiu　HU Jun　XU Lisa

Keywords　SARS, Super-spreading events

“Super-spread events” (SSEs), which have been observed in Singapore, HongKong in China and many cities all over the world, usually have a large influence on the early course of the epidemics. The understanding of these SSEs is critical to the containment of SARS. In this Letter it is shown that the possibility of SSEs is still high enough even when the virulences are equal for all the infective individuals, based on a simple spatial-relevant Monte-Carlo model (SEIR). The long latent periods play a critical role in the appearance of SSEs. The heterogeneity of the activities of infective cases can also increase the possibility.

单个带电颗粒在牛顿流体中的晶格玻尔兹曼模拟

万荣正　方海平　林志方　陈十一

关键词　格子玻尔兹曼方法，带电颗粒

运用格子玻尔兹曼方法研究了单个带电圆柱颗粒在二维充满牛顿流体中的管道中的沉降过程。当液体的介电常数小于管壁的介电常数时，颗粒和管壁之间存在的是静电吸引力，在低雷诺数下，流体作用力将颗粒推向管道中心，在这两种方向相反的力的共同作用下，对应于每一个距离管壁足够远的初始位置，存在一个临界的线电荷密度 q_c，当颗粒的线电荷密度为 q_c 时，它将在离开中心线的地方垂直下降，这是不同于沿中心线下降这一稳定态的一个亚稳态。此时颗粒本身的旋转对维持这一亚稳态的稳定性起着重要作用。当颗粒的线电荷密度大于或小于 q_c 时，颗粒将最终落到管壁上或回到中心线。这一模拟方法和发现的新现象将对进一步研究多颗粒悬浮液有很大帮助。

Lattice boltzmann simulation of a single charged particle in a newtonian fluid

WAN Rongzhen FANG Haiping LIN Zhifang CHEN Shiyi

Keywords Lattice Boltzmann simulation, Charged particle

The lattice Boltzmann method is used to study the sedimentaion of a single charged circular cylinder in a two-dimensional channel in a Newtonian fluid. When the dielectric constant of the liquid is smaller than that of the walls, there are attractive forces between the particle and the walls. The hydrodynamic force pushes the particle towards the centerline at low Reynolds numbers. Due to the competition between the Coulomb force and the hydrodynamic force in opposite directions, there is a critical linear charge density q_c at which the particle will fall vertically off-centerline, which is a metastable state in addition to the stable state on centerline, for any initial position of the particle sufficiently far from the proximal wall. It is found that the rotation of the particle plays an important role in the stability of such metastable states. The particle hits on the wall or falls on the centerline when the linear charge density on the particle is greater or less than q_c. The simulation method and the new phenomena are also helpful in the study of charged multi-particle suspensions.

二维狭窄动脉管中悬浮粒子的晶格玻尔兹曼模拟

李华兵 方海平 林志方 徐世雄 陈十一

关键词 格子玻尔兹曼方法，悬浮粒子，动脉狭窄

用晶格玻尔兹曼方法研究悬浮粒子流过一个模型化的动脉狭窄。狭窄是由平面管道中的两个圆柱构成，使狭窄处的缝隙大于 d 小于 $2d$，d 是粒子的直径。开始时只有一个粒子被放在偏中心线上，经过狭窄之后粒子将迁移到偏中心线的位置，在狭窄处速度比在平面管道里要大得多。只有当两个粒子被放置在中心线两侧对称性很高的位置，它们才能完全把狭窄堵塞。一个非常小的不对称将会在狭窄口前被放大，其中一个粒子将会后退，留出空间让一个粒子先过去，以至于不会堵塞狭窄。当这个狭窄取在两个临界值之间时，可以观察到粒子之间以及粒子和最近的鼓包之间有吸引力的迹象。通过多粒子悬浮研究压积的分布，我们发现狭窄的缝隙对粒子在远离狭窄部分的平管中的压积有很大的影响。

Lattice Boltzmann simulation on particle suspensions in a two-dimensional symmetric stenotic artery

LI Huabing FANG Haiping LIN Zhifang XU Shixiong CHEN Shiyi

Keywords Lattice Boltzmann simulation**,** Particle suspensions, Stenotic artery

The technique of lattice Boltzmann simulation has been applied to the study of two-dimensional

particle suspensions through a modeled arterial stenosis. The stenosis model consists of two-side symmetric semicirculars in a planar channel with the width of the stenosis throat larger than d and less than 2d, where d is the diameter of the particles. When only one particle is positioned off-centerline initially, the particle migrates off-centerline after passing the stenosis and the velocity at the stenosis throat is much larger than that in a flat tube. Only when two particles are positioned symmetrically to the centerline to a very high accuracy can the flow be blocked by two particles completely. A very small asymmetry will be amplified proximal to the stenosis throat in that one of the particles goes back to leave space to let the other particle passing the stenosis first so that the particles cannot be blocked. An evidence of attractive interactions between the particles as well as a particle and a proximal protuberance is observed when the asymmetry is very small and the width at the stenosis throat is between two critical values. The hematocrit distribution of the particles is studied by simulating multiparticle suspensions. It is found that the width of the stenosis throat has a significant influence on the hematocrit distribution of the particles in the flat tubes far from the stenosis.

二维情况下在晶格玻尔兹曼方法中流体对运动边界作用力的计算方法

李华兵　吕晓阳　方海平　钱跃红

关键词　格子玻尔兹曼方法，流体力

在二维情况下我们研究了在晶格玻尔兹曼方法中流体对曲线边界和运动边界的作用力的两种计算方法：动量交换法和压力交换积分法。得到以下结论：

（1）对静止流体中的倾斜边界和圆弧边界，压力张量积分法的结果和解析解精确吻合，而动量交换法在边界比较短的时候误差比较大；

（2）用压力张量积分法来计算流体对边界的作用力来模拟圆柱在二维管道中的沉降，结果和二阶运动边界有限元方法精确吻合；

（3）用压力张量积分法发现圆柱在 Poiseuille 流中将迁离中心线，和 Segré-Silberberg 效应一致。

总之，在有弹性边界和运动边界的情况下，压力张量积分法将是一个比较好的选择。

Force evaluations in lattice Boltzmann simulations with moving boundaries in two dimensions

LI Huabing　LU Xiaoyang　FANG Haiping　QIAN Yuehong

Keywords　Lattice Boltzmann simulations, Hydrodynamic forces

Two techniques, based on the exchange of momentum and the integration of stress tensor, for the evaluation of the hydrodynamic forces in the lattice Boltzmann simulations are investigated on the

curved and moving boundaries in two dimensions. The following results are obtained by numerical simulations: (i) the hydrodynamic forces on an inclined boundary and arc in liquid without flow computed by the stress-integration method agree with analytical predictions to a very high accuracy, while those by the momentum-exchange method have considerable errors for small segments; (ii) the simulation results of the sedimentation of a circular cylinder in a two-dimensional channel with the stress-integration method for hydrodynamic forces are in excellent agreement with those by a second-order moving finite-element method; (iii) the particle migrated from the centerline is found to occur in the simulations of a circular cylinder in a Poiseuille flow by the stress-integration method, consistent with the Segré-Silberberg effect. In conclusion, the stress-integration method can be a good candidate to evaluate the hydrodynamic forces on the elastic boundaries and moving particles in fluid.

用晶格玻尔兹曼方法模拟横波在 Maxwell 粘弹流中的传播

李华兵　谭惠丽　方海平

关键词　晶格玻尔兹曼方法，粘弹流

建立了一个模拟 Maxwell 粘弹流的 9 速晶格玻尔兹曼方法，模拟了横波在 Maxwell 粘弹流中的传播。波形和横向速度的衰减与解析解精确吻合。

Lattice Boltzmann simulation of transverse wave in Maxwell viscoelastic fluid

LI Huabing　TAN Huili　FANG Haiping

Keywords　Lattice Boltzmann method, Viscoelastic fluid

A 9-speeds lattice Boltzmann method for Maxwell viscoelastic fluid flow is proposed. Traveling of transverse wave in Maxwell viscoelastic fluid flow is simulated. The wave shape, transverse speed and decay rate are agree with theoretic results very well.

晶格玻尔兹曼方法模拟膜在流体中的形变

李华兵　方海平　林志方

关键词　格子玻尔兹曼方法，表面膜

建立了模拟二维膜的晶格玻尔兹曼方法，事实模拟表明膜的张力存在一个临界值，此时，膜的暂态的形状看起来象一个柱波，当这个膜相对更软或更硬时，它将演变到一个稳定的状态，变成一条直线。

Lattice Boltzmann simulation of deformable membrane in fluid

LI Huabing FANG Haiping LIN Zhifang

Keywords Lattice Boltzmann simulation, Deformable membrane

A lattice Boltzmann method is proposed to simulate the two-dimensional membrane. Numerical simulation shows that at a critical value of membrane tension, the pattern of the membrane at transient state behaves like a standing wave with a node staying at rest. In addition, when the membrane is relatively soft or stiff , it will evolve into a steady-state close to its initial straight pattern.

用晶格玻尔兹曼方法模拟多个悬浮颗粒在准二维对称狭窄动脉管中的流动行为

李华兵 吕晓阳 方海平 林志方

关键词 晶格玻尔兹曼方法，多粒子悬浮，数值模拟，有狭窄的动脉

用三维晶格玻尔兹曼方法研究钢性粒子悬浮流过一个准二维的模型化的狭窄，仅当两个粒子高度对称地位于中心线的两侧时，粒子才会完全堵塞狭窄口。当狭窄口的宽度 $b<2d$，粒子趋向于集中在管道中心线上。和红细胞趋向于血管的中心的观察结果相一致。目前的研究表明用准二维方法研究三维悬浮粒子在有狭窄的动脉中的行为非常有效。

Simulation of multi-particle suspensions in a quasi-two-dimensional symmetric stenotic artery with Lattice Boltzmann method

LI Huabing LU Xiaoyang FANG Haiping LIN Zhifang

Keywords Lattice Boltzmann model, Multi-particle suspensions, Numerical simulations, Stenotic artery

The three-dimensional Lattice Boltzmann model has been applied to the study of rigid particle suspensions through a quasi-two-dimensional modelled arterial stenosis. Only when two particles are positioned symmetrically to the centerline to an extremely high accuracy, the particles can be blocked completely at the stenosis throat. Particles incline to gather near the centerline for a stenosis throat width b<2d, consistent with the observation that red blood cells tend to concentrate near the center of the vessel. The present study shows that the quasi-two-dimensional system is an effective model to study the behaviour of three-dimensional multi-particle suspension in stenotic arteries.

单壁纳米管的 THz 波段光电导

韩家广　朱志远　廖 怡　王震遐　孙立涛　王庭太

关键词　纳米管，THz，光电导

利用有效介质模型对单壁纳米管的THz电导性质进行理论研究。结果符合最近的实验且预言了电导随频率减小。同时，也给出了单壁纳米管的非对角电介质函数。

Optical conductivity of single walled nanotube films in the terahertz region

HAN Jiaguang　ZHU Zhiyuan　LIAO Yi　WANG Zhenxia

SUN Litao　WANG Tingtai

Keywords　Single walled nanotube, THz, Optical conductivity

A theoretical investigation for the conductivity of single walled nanotube films is carried out with an effective medium model in the terahertz region. The results are compared with the recent experiment and a decrease of the real conductivity with increasing frequency is predicted. Meanwhile, the off-diagonal components of the dielectric function of single-walled carbon nanotube films based on the magneto optical effects are also shown.

球形空腔中的 Casimir 效应

韩家广　余礼平　王震遐　朱志远

关键词　Casimir 效应，球形腔，单一球体

真空零点能导致 Casimir 效应。一个球形空腔可以被分为三个区域，我们对每个区域进行了分析，给出了 Casimir 能的通解。Zeta 函数归一化被用来消除求和的发散。最后，我们发现一个单一球体的 Casimir 效应能够包含在我们的结果中。

The electromagnetic Casimir effect of spherical cavity

HAN Jiaguang　YU Liping　WANG Zhenxia　ZHU Zhiyuan

Keywords　Casimir effect, Spherical cavity, Single sphere

The Casimir effect results from the zero-point energy of vacuum. A spherical cavity can be divided into three regions, and we make an analysis of every region and then give a formal solution of Casimir energy, The zeta-function regularization is also used to dispel the divergence of the summation. At the end, we can see the Casimir effect of a single sphere is include in our results.

在单壁纳米管 THz 磁光效应中的新的震荡

韩家广 朱志远 廖 怡 王震遐 张 伟 孙立涛 王庭太

关键词 新的震荡，单壁纳米管，磁光效应

基于 Drude 模型，我们对单壁纳米管在 THz 波段的磁光效应进行了研究。计算表明纳米管磁光 Kerr 效应起源于等离子震荡。我们指出这种震荡正比于外加磁场并且震荡周期随圆频率增大。这些性质和单壁纳米管的朗道能级有关。反射谱和 FOM 谱揭示这种震荡对磁光 Kerr 效应起了决定作用。同时在不动外磁场下我们看到了 Kerr 转角的移动。

New oscillation in terahertz magneto-optical effect of single-walled carbon nanotubes film

HAN Jiaguang ZHU Zhiyuan LIAO Yi WANG Zhenxia ZHANG Wei

SUN Litao WANG Tingtai

Keywords New oscillation, SWNTs, Magneto-optical effect

The magneto-optical Kerr effect of single-walled carbon nanotubes (SWNTs) film in the Terahertz region is theoretically studied by means of the Drude model. The calculation shows a new oscillation occurring near the plasma frequency as the origin of the magneto-optical Kerr effect for the single-walled nanotubes film. We propose that the amplitude of this near plasma frequency oscillation is directly proportional to the external magnetic field and its period increases with increasing cyclotron frequency. We consider these features of this oscillation of SWNTs are related to the Landau energy of SWNTs. The reflectivity and figure of merit (FOM) spectrum also reveal that this oscillation is the dominant mechanism for the magneto-optical Kerr effect of SWNTs film. Meanwhile, the shift and large enhancement of Kerr rotation under different external magnetic fields is explained.

InSb 的 THz 磁光 Kerr 效应

韩家广 朱志远 廖 怡 王震遐 余礼平 张 伟 孙立涛 王庭太

关键词 InSb，磁光Kerr效应，THz

我们对 InSb 在 THz 波段的磁光效应进行了研究。 结果表明在室温和低温下 Kerr 谱在 THz 波段有很强的增加。这种增加来自于等离子体的边缘效应。同时， 在不同外磁场的情况下我们讨论了 InSb 的磁光 Kerr 谱。在不动外磁场和温度下看到了 Kerr 转角的移动。

The magneto-optical kerr effect of InSb in terahertz region

HAN Jiaguang ZHU Zhiyuan LIAO Yi WANG Zhenxia YU Liping
ZHANG Wei SUN Litao WANG Tingtai

Keywords InSb, Magneto-optical kerr effect**,** THz

A theoretical investigation for the magneto-optical Kerr effect of InSb in Terahertz region is carried out. The results show an enhancement of Kerr effect both at room temperature and a low temperature in Terahertz region. The enhancement of Kerr spectrum due to the plasma edge effect is put forward. Meanwhile, the magneto-optical Kerr effect spectrum of InSb in the different external magnetic fields are discussed. The peak shifts of the Kerr rotation under different external magnetic fields and temperatures are discussed.

萘，α 萘酚，β 萘酚，联苯和蒽的 THz 光谱

韩家广 徐 慧 朱志远 余笑寒 李文新

关键词 THz光谱，振动模式，Lorentz模型

对萘，α 萘酚，β 萘酚，联苯和蒽的远红外 THz 光谱进行了测量。我们对被测样品的低频振动模式包括他们的特性和共性进行了讨论。 同时测得复介电函数。 用 Lorentz 模型对实验结果进行了拟合。

Terahertz spectroscopy of naphthalene, a-naphthol, b-naphthol, biphenyl and anthracene

HAN Jiaguang XU Hui ZHU Zhiyuan YU Xiaohan LI Wenxin

Keywords THz spectroscopy, Vibrational modes, Lorentz model

The far-infrared THz spectra of naphthalene, α-naphthol, β-naphthol, biphenyl and anthracene have been measured using THz time-domain spectroscopy. The low-energy vibrational modes of measured molecules are discussed based on their characteristic and common features. The complex dielectric functions are obtained. Meanwhile, it is shown that the experimental results can be well fitted by a standard Lorentz model.

单壁纳米管在 THz 波段内的电导性质

韩家广 朱志远 王震遐 张 伟 余礼平 孙立涛 王庭太 何 锋 廖 怡

关键词 Maxwell–Garnett模型，Drude– Lorentzian 模型，电导率

基于 Maxwell–Garnett (MG) and Drude– Lorentzian (DL) 模型对单壁纳米管在 THz 波段内的电导性质进行了研究。理论研究指出电导随频率增加会减小。同时也在理论上给出了电介质函数的实部。

The conductivity of single walled nanotube films in Terahertz region

HAN Jiaguang ZHU Zhiyuan WANG Zhenxia ZHANG Wei YU Liping
SUN Litao WANG Tingtai HE Feng LIAO Yi

Keywords Maxwell–Garnett model，Drude– Lorentzian model，Conductivity

The conductivity of single-walled nanotube films is investigated with a combination of Maxwell–Garnett (MG) and Drude– Lorentzian (DL) model in terahertz region. A theoretical investigation for the recent experiment is given and a decrease of the real conductivity with increasing frequency is predicted. Meanwhile, the real part of dielectric function of single-walled carbon nanotube films is displayed.

单壁纳米管薄膜的 THz 电导性质

韩家广 朱志远 何 锋 廖 怡 王震遐 张 伟 余礼平 孙立涛 王庭太

关键词 THz电导，纳米管薄膜，不同样品

单壁纳米管在 THz 波段内的电导性质被进行了研究基于 Maxwell–Garnett (MG) and Drude–Lorentzian (DL) 模型。 理论拟合了 Jeon 的实验结果并预言了电导随频率增加会减小。同时对不同样品进行了理论上的讨论。

Terahertz conductivity of single walled nanotube films

HAN Jiaguang ZHU Zhiyuan HE Feng LIAO Yi WANG Zhenxia
ZHANG Wei YU Liping SUN Litao WANG Tingtai

Keywords THz conductivity, Single walled nanotube film, Different samples

The conductivity of single walled nanotube films is investigated with a combination of the

Maxwell-Gernett model and the Drude-Lorentz model in the Terahertz region. A theoretical fit for Jeon's experiment is given and a decrease of the real conductivity with increasing frequency is predicted. Meanwhile, the MG and DL models are also discussed for different samples.

GaN 的 THz 磁光效应

韩家广　朱志远

关键词　GaN，磁光效应，THz

我们利用 Drude 模型对 GaN 在 THz 波段的磁光效应进行了研究。晶格振动同时被考虑在理论计算中。同时，在不同载流子浓度和外磁场的情况下我们讨论了 GaN 的磁光 Kerr 谱。我们也给出了 3 维 Kerr 转角和平均的反射谱。

Terahertz frequency magneto-optical effect of GaN thin film

HAN Jiaguang　ZHU Zhiyuan

Keywords　GaN, Magneto-optical effect, THz

The magneto-optical Kerr effect of GaN in Terahertz region is calculated by means of the Drude model. The influence of lattice vibration on the Kerr spectrum of GaN is theoretically discussed. Meanwhile, the change of Kerr rotation under different carrier densities and external magnetic fields is numerically analyzed. The 3D profile view of Kerr rotation and the average reflectivity are also presented.

单壁纳米管薄膜在 THz 波段的电导性质

韩家广　朱志远　王震遐　余礼平　张 伟　孙立涛　王庭太

关键词　有效介质模型，光电导，THz

利用有效介质模型理论进行了单壁纳米管薄膜的太赫兹波段的光导理论的计算，解释了最近的实验结果并发现了纳米管薄膜的电导随入射光频率增加而减小，同时也计算了不同填充因子下单壁纳米管薄膜材料在太赫兹波段的电导函数。

THz conductivity of singled walled nanotube films

HAN Jiaguang　ZHU Zhiyuan　WANG Zhenxia　YU Liping

ZHANG Wei　SUN Litao　WANG Tingtai

Keywords　Effective medium model, Optical conductivity, THz

The conductivity of single-walled nanotube films is investigated with an effective medium model in terahertz region. A theoretical investigation for the recent experiment is given and a decrease of the real conductivity with increasing frequency is predicted. Meanwhile, the real part of conductivity of single-walled carbon nanotube films is displayed for different filling factors.

THz 在金属模板中的传输

韩家广　张 伟　朱志远　王震遐　余礼平　孙立涛　王庭太

关键词　THz，传输，金属模板

我们理论论证了 THz 在金属模板的传播性质。计算出可能发生传播的频率以及能量透射率。给出了在不同入射频率和不同几何参数的条件下能量透射率的曲线图。同时发现了依赖于模板长度和传播频宽的透射率的振动。

Terahertz propagation in metal templates

HAN Jiaguang　ZHANG Wei　ZHU Zhiyuan　WANG Zhenxia

YU Liping　SUN Litao　WANG Tingtai

Keywords　THz, Propagation, Metal templates

Terahertz (THz) propagation in a metal template has been theoretically demonstrated. The possible propagating frequencies and power transmittance have been calculated. The power transmittance curves are displayed with different incident frequency and different geometric parameters. The oscillations of transmittance dependent on length of the template and the theoretical propagating bandwidth have been found.

同心无限柱环导体腔中的量子电动力学效应

蒋维洲　王震遐　傅德基　艾小白　朱志远

关键词　Casimir 效应，柱环腔体，零点能，量子电动力学，

不带电导体空腔存在可用真空零点能解释的宏观量子效应。本工作研究以同轴不同半径柱面围成的导体柱环腔体中电磁场真空零点振动模式所给出的宏观量子效应。零点振动模式通过求解柱环空腔边界条件下无源的 Maxwell 方程组获得。得到了双柱面同心柱环中单位长度和单位面积的且是有限的真空能量即 Casimir 能量。这有限的 Casimir 能量可以分解为独立而且收敛的三部分，它们分别来自内柱面、外柱面和柱环之中。对多柱面同心柱环，Casimir 能量可分解为独立的（2n-1）部分（n 为柱面数）。柱环是类似于平行板的几何结构。但柱环所给出的 Casimir 能量和 Casimir 势能系数是随着柱环间隔变化的，不同于平行板是常数的情况。这相对于平行板几何具非平凡性质的 Casimir 能量将产生一个平行板几何中所没有的附加的一项 Casimir 力。

Casimir energy of concentric and infinite cylindrical shells of perfect conductor

JIANG Weizhou WANG Zhenxia FU Deji AI Xiaobai ZHU Zhiyuan

Keywords Casimir effect, Cylindrical ring cavity, Zero-point energy, Quantum electro-magnetic dynamics

We investigate the Casimir energy, due to the zero-point vacuum fluctuations, in a space which is cut into parts by the concentric and infinite cylindrical shells which are perfectly conductive. The Casimir energy turns out to be convergent. A interesting decomposition for the Casimir energy is found during the renormalization with the Zeta function regularization. For the double-layer shells it is decomposed into three independent and convergent parts that are from the interior, exterior cylindrical shells and between them, respectively. One of three parts, from between the two shells, has the property that the coefficient of the Casimir energy varies with the shell interval, comparing to the constant coefficient for a topologically similar geometry, the parallel plates. For n-layer shells, the Casimir energy consists of (2n-1) parts all of which are convergent.

相对论平均场研究镍铜锌同位素高、超形变态的粒子稳定性

蒋维洲 王庭太 朱志远

关键词 核形变，相对论平均场

对 beta 稳定线附近镍铜锌的高、超形变二级极小态的性质用相对论平均场理论作了研究。揭示了二级极小态对中子和质子发射的稳定性。预言了 A<61 的铜同位素的二级极小态可发生质子发射； 预言了一个更可能发射质子发射的锌同位素 ^{59}Zn 的超形变二级极小态。

Particle stability of highly-and super-deformed states of Ni, Cu and Zn isotopes near beta-stability in relativistic mean-field Theory

JIANG Weizhou WANG Tingtai ZHU Zhiyuan

Keywords Nuclear deformation, Relativistic mean-field theory

The properties of secondary minima with highly-or super-deformations in Ni, Cu and Zn isotopes near beta-stability are investigated in the relativistic mean-field theory. The stability of the secondary minima against proton and neutron emission is revealed for these nuclei. The proton emission may possibly occur at secondary minima in Cu isotopes with A<61, for the predicted large emission energy. A more possible candidate for proton emission is predicted to be ^{59}Zn due to its very large emission energy.

形变的相对论平均场理论中的奇 A 碳同位素的奇特结构

蒋维洲[1] 任中洲[1,2] 朱志远[1]

关键词 晕核，相对论平均场理论

我们研究了 pion 介子和 Omega 介子的空间矢量部分在奇 A 碳同位素中的贡献。pion 介子和 Omega 介子的空间矢量部分在奇 A 核中提供吸引作用，对单粒子性质而不是大块性质产生影响。作为一个膺矢量，pion 介子能对中子和质子势井的相对深度作较小的移动，这跟 rho 介子的贡献相反。 对于一个同位素链一个一般的趋势是随着同位旋的增大，pion 介子和 Omega 介子的空间矢量部分的贡献减弱。从普通核到晕核，pion 介子和 Omega 介子的空间矢量部分的贡献存在反常的减弱，这可从 ^{19}C， ^{15}C 和 ^{21}C 中看出.

1 兰州重离子加速器国家实验室理论核物理中心

2 南京大学物理系

Exotic structures of odd-A Carbon isotopes in the deformed relativistic mean-field theory

JIANG Weizhou[1] REN Zhongzhou[1,2] ZHU Zhiyuan[1]

Keywords Halo nuclei, Relativistic mean-field theory

We study contributions of the pion meson and spatial component of the omega meson in the odd-A Carbon isotopes. The pion and spatial omega provide small attractions in odd-A nuclei, giving rise to considerable influences on the single-particle energies rather than the bulk properties such as total binding energies, and root-mean-square (rms) radii. As an isovector, the pion can shift slightly the relative potential depth of neutron and proton, contrary to the role of the rho meson. There is a general trend that both the pion and spatial omega fields reduce with the rise of isospin in the isotopic chain. From the normal nucleus to halo nucleus, an abnormal drop of the pion or spatial omega field may occur, as can been seen in ^{19}C, ^{15}C and ^{21}C.

1 Center of Theoretical Nuclear Physics, National Laboratory of Heavy Ion Accelerator

2 Department of Physics, Nanjing University

用相对论 Hartree 方法研究晕核中的两体关联贡献

蒋维洲 朱志远 邱锡钧 任中洲 沈文庆

关键词 两体关联，晕核，相对论 Hartree 方法

发展了折合相对论两体关联贡献的相对论密度依赖方法并用来研究晕核性质。通过考虑核势

由两体相互作用主导而重建晕核子－介子耦合顶角。研究了双中子晕核 ^{11}Li 和单中子晕核 ^{19}C。理论产生了它们各自的分离能，均方根半径和晕尾巴。提供必要吸引的关联贡献对保证 ^{11}Li 关系 $S_n > S_{2n}$ 的成立至关重要。

Two-body correlation contributions in halo nuclei with a relativistic Hartree approach

JIANG Weizhou ZHU Zhiyuan QIU Xijun REN Zhongzhou SHEN Wenqing

Keywords Two-body correlation, Halo nucleus, Relativistic Hartree approach

The relativistic density dependent Hartree framework, where the relativistic two-body correlations are properly incorporated, is developed to study properties of halo nuclei. The halo nucleon-meson vertex is reconstructed considering the nuclear potentials can be built dominantly from the two-body interactions. The two-neutron halo nucleus ^{11}Li, together with the one-neutron halo nucleus ^{19}C, is investigated. Separation energies, root-mean-square radii, and halo tails of above halo nuclei are nicely reproduced. The correlation contribution which provides essential attractions for halo neutrons is important to guarantee the relation $S_n > S_{2n}$ for ^{11}Li.

^{24}Al 的奇异性结构研究

马春旺 方德清 马余刚 蔡翔舟 沈文庆 孙志宇[1] 任中洲[2] 郭 威 魏义彬
王 鲲 颜廷志 陈金根 陈金辉 马国亮 苏前敏 田文栋 钟 晨 左嘉旭
Hosoi M[3] Izumikawa T[4] Kanungo R[5] Nakajima S[3] Ohnishi T[5] Ohtsubo T[4]
Ozawa A[6] Suda T[5] Sugawara K[3] Suzuki T[3] Takisawa A[4] Tanaka K[5]
Yamaguchi T[3] Tanihata I[5]

关键词 动量分布，核反应总截面，Glauber 模型

我们通过实验测量 ^{24}Al 的核反应总截面与其相邻核比较和测量 ^{24}Al 碎裂反应产物的动量分布的方法来检验其是否具有奇异（晕或皮）核结构。我们采用 $B\rho$-TOF-ΔE 的方法对靶前粒子进行鉴别和 TOF-ΔE-E 的方法对靶后粒子进行鉴别，已分析得到了初步的动量分布和核反应总截面。同时在理论计算中假定 ^{24}Al 为核芯加价质子结构，核芯密度分布假设为 HO 类型，价质子密度分布由 Woods-Saxon 势本征方程的解来计算。把实验结果与用修正的 Glauber 模型理论计算的核反应总截面和动量分布进行比较的深入研究正在进行之中。

1 近代物理研究所，2 南京大学物理系
3 Department of Physics, Saitama University
4 Department of Physics, Niigata University
5 日本理化学研究所
6 Department of Physics, Tsukuba University

Study of the Structure Exoticness of ^{24}Al

MA Chunwang FANG Deqing MA Yugang CAI Xiangzhou SHEN Wenqing
SUN Zhiyu[1] REN Zhongzhou[2] GUO Wei WEI Yibin WANG Kun YAN Tingzhi
CHEN Jingen CHEN Jinhui MA Guoliang SU Qianmin TIAN Wendong
ZHONG Chen ZUO Jiaxu Hosoi M[3] Izumikawa T[4] Kanungo R[5] Nakajima S[3]
Ohnishi T[5] Ohtsubo T[4] Ozawa A[6] Suda T[5] Sugawara K[3] Suzuki T[3]
Takisawa A[4] Tanaka K[5] Yamaguchi T[3] Tanihata I[5]

Keywords Momentum distribution, Total interaction cross section, Glauber model

To determine whether ^{24}Al has an exotic (halo or skin) structure or not,we measure the total interaction cross section (σ_R) and compare it with that of ^{24}Al's neighboring nuclei to see whether there is an abnormal increase; in addition, we measure the momentum distribution of the fragments from ^{24}Al to see whether it is narrow. Particles before and after the C target are identified by means of Bρ-TOF-ΔE and TOF-ΔE-E, respectively. The preliminary results of the momentum distribution and total interaction cross section have been obtained. In the theoretical calculation we assume that ^{24}Al is composed of a core plus a valence proton, and the density distribution of the core is assumed to be HO type while the density distribution of the valence proton is obtained by solving the eigen-value equation of the Woods-Saxon potential problem. The further work on experimental result and theoretical calculation is in progress.

1 The Institute of Modern Physics Research，2 Department of Physics, Nanjing University
3 Department of Physics, Saitama University，4 Department of Physics, Niigata University
5 The Institute of Physics and Chemical Research(RIKEN)，6 Department of Physics, Tsukuba University

超相对论离子碰撞的△-标度和信息熵

马国亮 马余刚 王 鲲 萨本豪 沈文庆 黄焕中 蔡翔舟 张虎勇
卢朝辉 钟 晨 陈金根 魏义彬 周星飞

关键词 △-标度，信息熵，相对论离子碰撞

△-标度的方法已经被应用于处理蒙特卡罗程序 LUCIAE3.0 产生的 p+p、C+Ca 和 Pb+Pb 的数据当中。△-标度的方法被发现对于一些物理量是有效的，例如带电粒子多重数，奇异粒子多重数以及两体核核碰撞的数目。我们应用这种方法于一个很宽的能量范围（实验系能量从 20 A GeV 到 200 A GeV）。另外我们还得到了多重数的信息熵随能量的依赖性。

Δ-scaling and information entropy in ultra-relativistic nucleus-nucleus collisions

MA Guoliang MA Yugang WANG Kun SA Benhao SHEN Wenqing
HUANG Huanzhong CAI Xiangzhou ZHANG Huyong
LU Zhaohui ZHONG Chen CHEN Jingen WEI Yibin ZHOU Xingfei

Keywords lta-scaling, Iformation entropy, Rlativistic ion collision

The **Δ**-scaling method has been applied to ultra-relativistic p+p, C+C and Pb+Pb collision data simulated using a high energy Monte Carlo package, LUCIAE 3.0. The **Δ**-scaling is found to be valid for some physical variables, such as charged particle multiplicity, strange particle multiplicity and number of binary nucleon-nucleon collisions from these simulated nucleus-nucleus collisions over an extended energy ranging from Elab = 20 to 200 A GeV. In addition we derived information entropy from the multiplicity distribution as a function of beam energy for these collisions.

158A GeV 的相对论重离子碰撞的强子快度分布及温度拟合

马国亮 马余刚 王 鲲 沈文庆 蔡翔舟 张虎勇
卢朝辉 钟 晨 陈金根 魏义彬 黄焕中 萨本豪

关键词 LUCIAE3.0，快度分布，横向动量分布，动力学温度，QGP 相变

针对最近 NA49 在 158A GeV 的实验（C+C，Si+Si，Pb+Pb）数据，应用 LUCIAE3.0 模型进行模拟，得到了强子的快度分布和横向动量分布，并与实验数据进行比较，发现基本与实验数据相吻合。并对横向动量分布进行温度拟合，给出了和实验数据吻合很好的结果，但是对于重系统或重强子 LUCIAE3.0 给出的结果相对较差。

Rapidity distributions and thermal fits for relativistic heavy-ion collisions at 158 A GeV

MA Guoliang MA Yugang WANG Kun SHEN Wenqing CAI Xiangzhou ZHANG Huyong LU Zhaohui ZHONG Chen CHEN Jingen WEI Yibin
HUANG Huanzhong SA Benhao

Keywords LUCIAE3.0, Rapidity distribution, Ttransverse momentum distribution, Kinetic temperature, QGP phase transition

LUCIAE3.0 model was used to simulate the relativistic heavy-ion collisions, namely C+C, Si+Si

and Pb+Pb, which were already performed experimentally by NA49 collaboration. The simulated results of rapidity and transverse momentum distributions of all kinds of hadrons were compared with the NA49 data and found that they can fit the experimental data mostly. The kinetic temperature was deduced by the thermal fits to the transverse mass distributions of hadrons. It is found that the temperatures of light systems or hadrons fit the experimental data well, however, those of heavy systems or hadrons deviate much from the data, which probably because that LUCIAE3.0 doesn't include the information of QGP phase transition.

相对论重离子碰撞的温度涨落与热容

马国亮 马余刚 萨本豪 王 鲲 蔡翔舟 魏义彬 张虎勇

卢朝辉 钟 晨 陈金根 龙家丽 贺泽君 沈文庆

关键词 重离子碰撞， 夸克胶子等离子体，统计理论和涨落，热容

使用 LUCIAE 3.0 模型模拟了 SPS 能区 Pb+Pb 和 C+C 在不同能量（E^{lab}=20—200AGeV）和不同中心度下的重离子碰撞。并通过逐个事件的粒子温度涨落提取出了相应粒子的热容，发现对于同一碰撞系统，单位发射粒子的热容随碰撞能量的升高而下降直至饱和，随着碰撞参数 b 的增大而减小，而且发现单位发射粒子的热容具有随粒子质量的变大而变大的关系。同时还发现不同碰撞系统中同一种粒子具有相同的单位发射粒子热容，并给出了相应的解释

Temperature Fluctuation and heat capacity in relativistic heavy-ion collisions

MA Guoliang MA Yugang SA Benhao WANG Kun CAI Xiangzhou

WEI Yibin ZHANG Huyong LU Zhaohui ZHONG Chen

CHEN Jingen LONG Jiali HE Zejun SHEN Wenqing

Keywords Heavy ion collision, Quark-gluon plasma, Statistical theory and fluctuations, Heat capacity

We used LUCIAE model to simulate the Pb+Pb and C + C in SPS energy .The heat capacity was then extracted from event by event temperature fluctuation. It is found that the heat capacity per hadron multiplicity decreases with the increasing of beam energy and impact parameter for a given reaction system. While with the increasing of hadron mass, the heat capacity per hadron multiplicity rises. In addition, we found that, for a given hadron, the heat capacity per hadron multiplicity is almost the same regardless the reaction system. Some discussions were also given.

62 GeV/c 金-金碰撞的 Φ 介子产生与椭圆流

马国亮　马余刚　蔡翔舟　陈金辉　左嘉旭　钟 晨　沈文庆　黄焕中

关键词　椭圆流，Φ 介子，62 GeV/c 金-金碰撞

使用来自于 ZDC 的最小偏畸的 trigger 选择并分析了 Au+Au $\sqrt{s}$=62 GeV 的实验数据。从 0—80%的 6.2 百万事件中得到 Φ 介子的产额和椭圆流 v_2。通过计算每一对 K^+和 K^-的不变质量，横向动量和快度去组建 Φ 介子。由于这样产生的不变质量分布含有大量背景，采用了混合事件的技术进行组建背景。一共分了 0—20%、 20%—40%、40%—60%、60%—80%、0—80%五个中心度。对其进行了效率修正后，我们使用指数函数对其进行拟合得到表观温度和 dN/dy。我们还研究了 $\langle p_T \rangle$ 和 Φ/k。发现表观温度 T，dN/dy，$\langle p_T \rangle$ 和 Φ/k 都随着带电粒子多重数的增长而增长。

另外，还使用混合事件的技术研究了 $\sqrt{s}$=62 GeV 的 Au+Au 碰撞中 Φ 介子的椭圆流 v_2。发现两个 K^+和 K^-之间的自关联会增长 Φ 介子的 v_2。当扣除掉它们之间的自关联后，发现 Φ 介子的 v_2 随着横向动量增加而增加，但是它的数值要小于 n， k p 的 v_2。

Φ Production and its Elliptic flow v_2 in Au+Au Collision at $\sqrt{s}$=62 GeV

MA Guoliang　MA Yugang　CAI Xiangzhou　CHEN Jinhui　ZUO Jiaxu

ZHONG Chen　SHEN Wenqing　HUAN Huanzhong

(for RHIC-STAR Collaboration)

Keywords　Elliptic flow, Phi meson, Au+Au at 62 GeV/c

$\sqrt{s}$=62 GeV Au+Au data are selected analyzed by a minimum bias trigger employing the ZDC's. Φ meson's production and elliptic flow v_2 results were presented from 6.2 million 0—80% Au+Au events.

Reconstruction of the Φ was accomplished by calculating the invariant mass (m_{inv}) of all permutations of candidate K^+ K^- pairs. The resulting invariant mass distribution consisted of the Φ signal on a large background that is predominantly combinatorial. The shape of the combinatorial background was calculated using the mixed-event technique. For the centrality measurement of production, five different centrality bins are divided such as 0—20%, 20%—40%,40%—60%, 60%—80%, 0—80%.After efficiency correction, the m_T spectra are obtained. After fiting them by an exponential function, we get the inverse slope T, dN/dy and $\langle p_T \rangle$. the Φ/k ratio are also investigated. it is found that they all increase with Nch.

In addition, the elliptic flow v_2 of Φ in 0—80% centrality bin at $\sqrt{s}$=62 GeV Au+Au collision is investigated by event-mixing technique. we find the auto-correlation between K^+ and K^- increases the value of v_2. When removing it, we find that Φ's v_2 increases with pT, but the value of v_2 is smaller than other particles such as n, k p etc.

格点气体模型下的同位旋标度率

马余刚 王 鲲 魏义彬 马国亮 蔡翔舟 陈金根
方德清 郭 威 沈文庆 田文栋 钟 晨

关键词 格点气体模型，同位旋标度行为，非对称核子-核子作用势

我们在格点-气体模型的框架下，讨论了质量数为 36 的热发射源的同位旋标度现象。发现当核子-核子之间的作用势是同位旋相关势时，同位旋的标度参数（α和β）随着温度的增加而减小；相反，当核子-核子之间的作用势是同位旋不相关势时，同位旋的标度参数（α和β）不随温度的变化而变化。另外，相对的中子或质子密度显示了随系统的中子-质子比的近似线性关系。

Isoscaling in the lattice gas model

MA Yugang WANG Kun WEI Yibin MA Guoliang CAI Xiangzhou CHEN Jingen
FANG Deqing GUO Wei SHEN Wenqin TIAN Wendong ZHONG Chen

Keywords Lattice gas model, Isoscaling behavior, Asymmetric nucleon-nucleon potential

Isoscaling behavior is investigated using the isotopic and isobaric yields from an equilibrated thermal source which is prepared by the lattice gas model (LGM) for lighter systems with A = 36. The isoscaling parameters α and β are observed to drop with temperature for the LGM with the asymmetric nucleon-nucleon potential. However, the isoscaling parameters do not show a temperature dependence for the LGM with the symmetric nucleon-nucleon potential. The relative neutron or proton density shows a nearly linear relation with the N/Z (neutron to proton ratio) of the system.

核液气共存态时的核碎片的发射的统计行为

马余刚 韩定定 沈文庆 蔡翔舟 陈金根 贺泽君 龙家丽
马国亮 王 鲲 魏义彬 余礼平 张虎勇 钟 晨 周星飞 朱志远

关键词 碎片发射，发射位垒，液气共存

在同位旋相关的格点气体模型和经典分子动力学的框架下，我们研究了核碎片的发射行为。我们发现除了在液气相变点附近外，对于重于质子的碎片的发射几乎满足泊松分布。而且从碎片的平均多重数与温度的倒数的关系中，存在着线性的 Arrhenius 律行为。从 Arrhenius 律的斜率可以提取核碎片的发射位垒。我们得到了不同电荷数和质量数的发射位垒，并用体现库仑能和表面能的公式进行拟合。发射位垒的值能很好地拟合低能区地条件位垒的数据。另外，我们还讨论了源的大小、库仑作用和冻结密度等物理因素对碎片发射的影响。

Statistical nature of cluster emission in nuclear liquid-vapour phase coexistence

MA Yugang HAN Dingding SHEN Wenqin CAI Xiangzhou CHEN Jingen
HE Zejun LONG Jiali MA Guoliang WANG Kun WEI Yibin YU Liping
ZHANG Huyong ZHONG Chen ZHOU Xingfei ZHU Zhiyuan

Keywords Cluster emission, Emission barrier, Liquid-vapor phase coexistence

The emission of nuclear clusters is investigated within the framework of isospin dependent lattice gas model and classical molecular dynamics model. It is found that the emission of individual cluster which is heavier than proton is almost Poissonian except near the transition temperature at which the system is leaving the liquid-vapor phase coexistence and the thermal scaling is observed by the linear Arrhenius plots which is made from the average multiplicity of each cluster versus the inverse of temperature in the liquid vapor phase coexistence. The slopes of the Arrhenius plots, i.e. the "emission barriers", are extracted as a function of the mass or charge number and fitted by the formula embodied with the contributions of the surface energy and Coulomb interaction. The good agreements are obtained in comparison with the data for low energy conditional barriers. In addition, the possible influences of the source size, Coulomb interaction and “freeze-out”ensity and related physical implications are discussed.

质量数 36 附近核的临界现象的实验证据

马余刚 Wada R[1] Hagel K[1] Wang J[1] Keutgen T[2] Majka Z[3] Murray M[1]
Qin L[1] Smith P[1] Natowitz J B[1] Alfaro R[4] Cibor J[5] Cinausero M[6] El Masri Y[2]
Fabris D[7] Fioretto E[6] Keksis A[1] Lunardon M[1] Makeev A[1] Arie N[8] Martin E[1]
Martinez-Davalos A[4] Menchaca-Rocha A[4] Nebbia G[7] Prete G[6] Rizzi V[7]
Ruangma A[1] Shetty D V[1] Souliotis G[1] Staszel P[3] Veselsky M[1] Viesti G[7]
Winchester E M[1] Yennello S J[1]

关键词 临界行为，液气相变，量热曲线

我们对 47 MeV/nucleon ^{40}Ar+Al，Ti 和 Ni 反应的实验研究表明，有许多的实验观测量同时说明质量数 36 附近的核在激发能（5.65±0.5）MeV、温度（8.4±0.5）MeV 时存在着最大的涨落行为。在这点最大的涨落处，存在着许多不同的定量的观测量表明了核的表观临界行为。核的量热曲线没有显示出核温度的平台，这是明显地有别于重系统中的量热曲线的行为。这可能说明了，

与重核的表观的一级液气相变行为相比较，这些很轻的系统可能出现了在临界点附近的二级的液气相变。

1 Cyclotron Institute，Texas A&M University，College Station，Texas 77843，USA

2 UCL，Louvain-la-Neuve，Belgium ，

3 Jagiellonian University，Krakow，Poland

4 Instituto de Fisica，UNAM，Mexico City，Mexico ，

5 Institute of Nuclear Physics，Krakow，Poland

6 INFN，Laboratori Nazionali di Legnaro，I-35020 Legnaro，Italy

7 INFN and Dipartimento di Fisica dell'Universitá di Padova，I-35131 Padova，Italy

8 LPC，IN2P3-CNRS，ISMRA et Université，F-14050 Caen Cedex，France

Evidence of Critical Behavior in the Disassembly of Nuclei with A～36

MA Yugang WADA R[1] Hagel K[1] WANG J[1] Keutgen T[2] Majka Z[3] Murray M[1] Qin L[1] Smith P[1] Natowitz J B[1] Alfaro R[4] Cibor J[5] Cinausero M[6] El Masri Y[2] Fabris D[7] Fioretto E[6] Keksis A[1] Lunardon M[1] Makeev A[1] Marie N[8] Martin E[1] Martinez-Davalos A[4] Menchaca-Rocha A[4] Nebbia G[7] Prete G[6] Rizzi V[7] Ruangma A[1] Shetty D V[1] Souliotis G[1] Staszel P[3] Veselsky M[1] Viesti G[7] Winchester E M[1] Yennello S J[1]

Keywords Critical behavior, Liquid gas phase transition, Caloric curve

A wide variety of observables indicate that maximal fluctuations in the disassembly of hot nuclei with A～36 occur at an excitation energy of （5.65±0.5）MeV and temperature of （8.4±0.5）MeV. Associated with this point of maximal fluctuations are a number of quantitative indicators of apparent critical behavior. The associated caloric curve does not appear to show a plateau such as that seen for heavier systems. This may indicate that, in contrast to similar signals seen for apparent first order liquid-gas transitions in heavier nuclei, the observed behavior in these very light nuclei may well be associated with a second order transition at the critical point.

1 Cyclotron Institute, Texas A&M University, College Station, Texas 77843, USA

2 UCL, Louvain-la-Neuve, Belgium

3 Jagiellonian University, Krakow, Poland

4 Instituto de Fisica, UNAM, Mexico City, Mexico

5 Institute of Nuclear Physics, Krakow, Poland

6 INFN, Laboratori Nazionali di Legnaro, I-35020 Legnaro, Italy

7 INFN and Dipartimento di Fisica dell'Universitá di Padova, I-35131 Padova, Italy

8 LPC, IN2P3-CNRS, ISMRA et Université, F-14050 Caen Cedex, France

核液气相变的新进展

马余刚　沈文庆

关键词　液气相变，Zipf 定律

我们评论了核液气相变的新进展，尤其是强调了在重离子碰撞中的液气相变的观测信号。这些观测信号包括幂指数律的质量分布、碎片的发射率、核的 Zipf 定律、双重性（Bimodality）、碎片的最大涨落、Δ-标度律、量热曲线、相共存曲线、临界温度、临界指数分析、负的比热和不稳定性等。我们还介绍了与作者有关的液气相变的实验和理论工作。

Recent progress of nuclear liquid gas phase transition

MA Yugang　SHEN Wenqin

Keywords　Liquid-gas phase transition, Zipf law

Recent progress on nuclear liquid gas phase transition (LGPT) has been reviewed, especially for the signals of LGPT in heavy ion collisions. These signals include the power-law charge distribution, cluster emission rate, nuclear Zipf law, bimodality, the largest fluctuation of the fragments, Δ -scaling, caloric curve, phase coexistence diagram, critical temperature, critical exponent analysis, negative specific heat capacity and spinodal instability etc. The systemic works of the authors on experimental and theoretical LGPT are also introduced.

RHIC 能量下夸克-胶子等离子体中的双轻子产生和化学平衡

龙家丽　贺泽君　马国亮　马余刚

关键词　夸克-胶子等离子体，化学平衡，双轻子产生

基于 Jüttner 部分子分布函数建立了正在进行化学平衡的具有有限重子数密度的夸克-胶子等离子体系统的演化模型。通过研究系统的双轻子产生，发现由于系统较高的初始温度、较大的胶子密度和中等质量区较大的胶子聚变和夸克湮灭反应截面，使得正反夸克对湮灭为双轻子的反应，以及胶子聚变和夸克湮灭为热粲夸克对的反应对中等质量区双轻子产生提供了占统治的贡献。

Dileptons from a chemically non-equilibrated quark-gluon plasma

LONG Jiali　HE Zejun　MA Guoliang　MA Yugang

Keywords　Quark-gluon plasma, Chemical equilibration , Dilepton production,

We have studied the evolution and dilepton production of a chemically equilibrating quark-gluon plasma system at finite baryon density. We found that due to the increase of the quark phase life-time

with increasing initial quark chemical potential, and other factors like higher initial temperature, larger gluon density and gluon fusion or quark annihilation cross section, thermal charmed quarks provide a dominant contribution to dilepton yield. This results in a significant enhancement of intermediate mass dilepton production.

相对论核-核碰撞中的奇异性产生

龙家丽　贺泽君　马余刚　马国亮

关键词　夸克-胶子等离子体，重子密度，奇异性

用描述胶子、夸克和 S 夸克化学平衡的具有有限重子密度的弛豫方程组，在夸克相到强子相的快速突变的图景中，研究了夸克相和强子相的奇异性产生。发现 K^-/π^-的比值增加了，是 PP 碰撞的 3 倍多。

Strangeness production in ultrarelativistic nucleus-nucleus collisions

LONG Jiali　HE Zejun　MA Yugang　MA Guoliang

Keywords　Quark-gluon plasma,　Baryon density, Strangeness

Based on relaxation equations describing the chemical equilibration of gluons, quarks and squarks at finite baryon density derived from Juttner distribution of partons, with the help of a rapid phase transition scenario from quark phase into hadron phase, we have calculated strangeness production in quark phase and hadron phase, found that K^-/π^- ratio is enhanced over that in pp collisions by about a factor 3.

具有有限重子密度的化学非平衡部分子气中单圈和双圈级的硬光子产生

龙家丽　贺泽君　马余刚

关键词　夸克-胶子等离子体，光子产生，化学平衡

研究了在化学非平衡的具有有限重子数密度的夸克-胶子等离子体系统中的单圈和双圈级的硬光子产生。发现光子产额是初始夸克化学势的增函数，它主要来自于快度 $y\leq 6$ 的贡献，以及初始时间段的贡献占统治地位。另外，来自于韧致辐射和 Compton 过程 $qg \to q\gamma$ 的贡献也很大。

Hard photon production from a chemically equilibrating quark-gluon plasma with finite baryon density at two-loop level

LONG Jiali HE Zejun MA Yugang

Keywords Quark-gluon plasma, Photon production, Chemical equilibration

We study hard photon production from a chemically non-equilibrated quark-gluon plasma with finite baryon density at one-loop and two-loop levels on the basis of Juttner distribution of partons of the system. We find that the photon yield is a strongly increasing function of the initial quark chemical potential, main contributions are given by rapidities $y \leq 6$, and photon production is ruled by early times. In addition, we note that contribution from bremsstralung and Conpton process $qg \to q\gamma$ dominates.

化学非平衡夸克-胶子等离子体中的奇异性

贺泽君 龙家丽 马余刚 马国亮

关键词 化学非平衡夸克-胶子等离子体，奇异性

我们基于部分子的 Juttner 分布，推导出描述胶子、夸克和 S 夸克化学平衡的具有有限重子密度的弛豫方程组，研究了奇异性的产生、化学平衡和演化。我们发现奇异性的产生敏感的依赖初始值，而且随初始夸克相寿命的增加显著的提高。此外，计算的奇异性与热力学平衡系统中的明显差别表明，在非平衡系统中研究奇异性是非常重要的。

Strangeness in a chemically non-equilibrated quark-gluon plasma

HE Zejun LONG Jiali MA Yugang MA Guoliang

Keywords Chemically non-equilibrated quark-gluon plasma, Strangeness

We study strangeness of a chemically equilibrating quark-gluon plasma at finite baryon density based on Juttner distribution of partons. We find that the strangeness production depends obviously on initial values, and will accelerates with the change of the initial system from a chemically non-equilibrated to a equilibrated quark-gluon plasma. We also find that the calculated strangeness is very different from the one in the thermodynamic equilibrium system, it shows that this study may help us to understand the formation of quark-gluon plasma via a chemically non-equilibrated evolution frame-work.

进行化学平衡的夸克-胶子物质中热粲夸克对双轻子的贡献

贺泽君 龙家丽 马余刚

关键词 双轻子，进行化学平衡的夸克-胶子等离子体

我们发现在进行化学平衡的富重子夸克-胶子物质中，由于系统慢的冷却、高的温度、大的胶子密度以及 $gg \Leftrightarrow c\bar{c}$ 大的聚变截面，反应 $gg \Leftrightarrow c\bar{c}$ 对双轻子提供了占统治的贡献，造成中等质量双轻子重大增强。

Thermal charmed quark contribution to dileptons in chemically equilibrating quark-gluon matter

HE Zejun LONG Jiali MA Yugang

Keywords Dilepton, Chemical equilibration quark-gluon plasma

We find that in achemically equilibrating baryon-rich quark-gluon matter, due to the slow cooling rate, high temperature, large gluon density as well as large fusion cross section of $gg \Leftrightarrow c\bar{c}$ in the intermediate mass region, the gluon fusion $gg \Leftrightarrow c\bar{c}$ provides a dominant contribution to dileptons with intermediate masses, resuting in the significant enhancement of intermediate mass dileptons.

^{76}Se 的低自旋新能级及其晕带能级结构的讨论

沈水法 李 燕 顾嘉辉

关键词 衰变，γ射线，能级，符合，投影壳模型，正宇称晕态

分别用反康谱仪和两个高纯锗探测器进行了单谱和符合谱测量，研究了 ^{76}Br 的衰变[1]。用 ^{75}As(α，3n)^{76}Br 和 ^{76}Se(p，n)^{76}Br 两种核反应生成了 ^{76}Br 核。实验结果证实了以前报道的属于 ^{76}Se 的能级和γ射线。首次发现了 39 条新γ射线和 15 个新能级。基于 logft 的计算值、所观测到的能态的退激发方式和一些核反应的实验结果，提出了新能级的自旋和宇称。建议了一个新的 ^{76}Br 衰变纲图。

我们在投影壳模型框架下对 ^{76}Br 的子体 ^{76}Se 的正宇称晕态进行了计算。首先用 4 点公式计算能隙参数Δ_p 和Δ_n[2]。 核的总结合能 B 取自文献[3]，并且如果有实验值的话尽量采用实验值。计算结果为Δ_p=1.71MeV 和Δ_n=1.7125MeV。在 Nilsson 势中出现的自旋-轨道力参数κ和μ取自 Zhang 等人的工作[4]， 它是在 Bengtsson 和 Ragnarsson 所提参数基础上的一个改版[5]。最近，在质子数和中子数为 28≤N≤40 的丰质子区，Sun 等人基于新的实验数据提出一组新的 Nilsson 参数[6]。考虑到现今研究的核其中子数是 42，我们认为这组新的参数不一定很适合于 ^{76}Se 核，尽管 Zhang 等所建议的参数是从 A≈120-140 区域推断出来的[4]。在 Subber 等人的工作中[7]，用动力学形变模型（DDM）计算了基态和第一激发态的形变值，它既符合于来自 p，p'实验的实验值[8]，又和从电磁跃迁几率推出值相一致[9]。因此，在下面的计算中，我们将在形变ε_2=0.30 处建立壳模型基。

此后，真空态$|\phi(\varepsilon_2=0.30)\rangle$写为$|0\rangle$。十六极形变参数$\varepsilon_4=0.053$ 取自 Möller 等人的文献[3]。在计算中，组态空间由取 N=4（N=4）主壳中接近费米面的中子（质子）准粒子态并由它们形成多准粒子态架构。^{76}Se 正宇称晕态的实验观测值和 PSM 预言的比较如文献[1]的图 4 所示。实验能级取自 Wells 等人的 ^{76}Se 核在束研究的结果[10]，可以发现，对 2^+ 能级的数据还可以粗略地加以描述。但对 $I\geq4$ 的能级就和实验结果不同，即 PSM 对 4^+以上能级符合得并不好。很明显理论计算值偏高。在这里，我们要强调的是所有的这些态都是经过一次性的对角化而获得，而没有对个别态进行任何的调整。

参考文献

1 SHEN Shuifa, LI Yan, HUANG Wenda, *et al.* J Phys Soc Jpn, 2004, **73**: 1180

2 Aage Bohr, Ben R M. Nuclear Structure,Vol. 1 (Benjamin, New York, Amsterdam, 1969), p. 169

3 Möller P, Nix J R, Myers W D, *et al*. Atom Data Nucl, Data Tables, 1995, **59**: 185

4 Zhang J Y, Xu N,Fossan D B, *et al*. Phys Rev, 1989, **C39**: 714

5 Bengtsson T, Ragnarsson T. Nucl Phys, **A436**(1985)14

6 Yang Sun, Jing-ye Zhang, Mike Guidry, *et al*. In: Phys Rev C62(2000)021601

7 Subber A R H, Robinson S H, Hungerford P, *et al.* J Phys G: Nucl Phys, 1987, **13**: 807

8 Matoba M, Hyakutake M, Koori N, *et al*. Nucl Phys, 1979, **A325**: 389

9 Matoba M. Phys Lett, 1979, **B88**: 249

10 Wells J C, Robinson R L Jr, Kim H J, *et al*. Phys Rev, 1980, **C22**: 1126

Decay of ^{76}Br and its daughter's level structure

SHEN Shuifa LI Yan GU Jiahui

Keywords Decay, γ-ray, Level, Coincidence, PSM, Positive-parity yrast states

The decay of ^{76}Br has been investigated by means of γ-ray spectroscopy[1]. The ^{76}Br nuclei were produced in two reactions, i. e., ^{75}As(α, 3n)^{76}Br and ^{76}Se(p, n)^{76}Br. The Compton-suppressed spectrometer and High-purity Ge detectors have been used singly and in coincidence, respectively, to study γ-rays in the β^++EC decay of ^{76}Br to ^{76}Se. 37 γ rays were observed for the first time among 138 γ-rays reported. A decay scheme of ^{76}Br including 15 new levels is proposed which accommodates 120 of these transitions. Spins and parities for new levels are proposed from calculated log*ft* values, modes on the observed decay, and some nuclear reaction experiment results.

In our calculations in the framework of the projected shell model, the pairing gap parameters are calculated using the four-point formula[2]. The values of the total nuclear binding energy B are taken from ref. [3], and the experimental data are adopted if only they can be supplied. The results are Δ_p=1.71 MeV and Δ_n=1.7125 MeV. The spin-orbit force parameters, κ and μ, appearing in the Nilsson potential are taken from the compilation of Zhang *et al.*[4] which is a modified version of Bengtsson and Ragnarsson[5] and has been fitted to the latest experimental data. It is supposed to apply over a sufficiently wide range of shells. These κ and μ are different for different major shells (N-dependent). Recently, based on available experimental data, a new set of Nilsson parameters is proposed by Sun *et*

al.[6] for proton-rich nuclei with proton or neutron numbers 28≤N≤40. Considering that nucleus studied in the present work has neutron numbers 42, so we think this new set is not very suitable to the nucleus ^{76}Se although the Nilsson parameter set proposed by Zhang *et al*.[4] is deduced for the A≈120-140. In the work of Subber *et al*[7], the deformation values of the ground and the first-excited states are calculated in the DDM, which show reasonable agreement with both experimental values obtained from the p, p' experiment[8] and those evaluated from electromagnetic transition probabilities[9]. In the following calculations, we thus construct the shell model basis at the deformation ε_2=0.30. The vacuum state $|\phi(\varepsilon_2 = 0.30)\rangle$ is hereafter written as $|0\rangle$. The hexadecapole deformation parameter ε_4=0.053 is taken from the compilation of Möller *et al*[3]. In the calculations, the configuration space is constructed by selecting the qp states close to the Fermi energy in the N=4 (N=4) major shell for neutrons (protons) and forming multi-qp states from them. The comparison of the experimentally observed positive-parity yrast states of ^{76}Se with the predictions of the PSM is given in Fig. 4 of ref. [1]. The experimental levels have been taken from the in-beam study of the nucleus ^{76}Se by Wells *et al*. [10]. As can be seen, about 2^+ level, the datum is described roughly well. But the agreement with experiment of the levels I≥4 becomes worse. i. e., the PSM fitting above 4^+ is not good. Obviously the energies are overpredicted in ^{76}Se. We emphasize here that all these states have been obtained by a single diagonalization, without any adjustment for individual states.

References

1 SHEN Shuifa, LI Yan, HUANG Wenda, *et al.* J Phys Soc Jpn, 2004, **73**: 1180

2 Aage Bohr, Ben R M. Nuclear Structure,Vol. 1 (Benjamin, New York, Amsterdam, 1969), p. 169

3 Möller P, Nix J R, Myers W D, *et al*. Atom Data Nucl, Data Tables, 1995, **59**: 185

4 Zhang J Y, Xu N,Fossan D B, *et al*. Phys Rev, 1989, **C39**: 714

5 Bengtsson T, Ragnarsson T. Nucl Phys, **A436**(1985)14

6 Yang Sun, Jing-ye Zhang, Mike Guidry, *et al.* IN: Phys Rev, **C62**(2000)021601

7 Subber A R H, Robinson S H, Hungerford P, *et al.* J Phys G: Nucl Phys, 1987, **13**: 807

8 Matoba M, Hyakutake M, Koori N, *et al*. Nucl Phys, 1979, **A325**: 389

9 Matoba M. Phys Lett, 1979, **B88**: 249

10 Wells J C, Robinson R L Jr, Kim H J, *et al*. Phys Rev, 1980, **C22**: 1126

有限重子密度的非化学平衡夸克-胶子等离子体的演化方程

贺泽君 龙家丽 马余刚

关键词 进行化学平衡的夸克-胶子等离子体，驰豫方程

导致化学平衡的反应被假定为 $gg \Leftrightarrow ggg$ 和 $gg \Leftrightarrow q\bar{q}$。并假定弹性部分子散射足够快，能维持局域热平衡，则部分子密度的演化可用主方程描述。结合这些主方程和系统的能量-动量守恒方程和重子数守恒方程，得到一组描述系统温度、化学势以及夸克和胶子逃逸因子演化的驰豫方程组。

Evolution equation of a chemically non-equilibrated quark-gluon plasma at finite baryon density

HE Zejun LONG Jiali MA Yugang

Keywords Chemically equilibrating quark-gluon plasma, Relaxation equation

The dominant reactions leading to chemical equilibrium are assumed to be $gg \Leftrightarrow ggg$ and $gg \Leftrightarrow q\bar{q}$. Assuming that elastic parton scatterings are sufficiently rapid to maintain local thermal equilibrium, the evolution of the parton densities can be given by the master equations. Combining the master equations together with equation of energy-momentum conservation and equation of baryon number conservation, one can get a set of coupled relaxation equations describing evolutions of the temperature T, quark chemical potential μ_q and fugacities λ_q for quarks and λ_g for gluons on the basis of Juttner distribution of a chemically equilibrating quark-gluon plasma at finite baryon density.

奇-奇核 $^{80, 82, 84}$Rb 正宇称晕带旋称反转的机理

沈水法 顾嘉辉 沈文庆

关键词 旋称反转, 角动量投影壳模型, 晕带, 四极形变

在 A—80 区奇-奇核旋称反转问题上已提出几种机制，但没有一种理论推断是结论性的。在本工作中将角动量投影壳模型应用到 ^{80,82,84}Rb 核，对组态为$\pi g_{9/2}\otimes\nu g_{9/2}$的正宇称晕带和组态为$\pi(p_{1/2}, p_{3/2}, f_{5/2})\otimes\nu g_{9/2}$ 的负宇称晕带理论计算和实验结果进行了比较，特别是对正宇称晕带中的 signature 反转机制进行了探讨[1,2]。角动量投影壳模型计算显示正宇称晕带中的 signature 反转是原子核随自旋增加形状发生变化的信号，其间原子核从低自旋的长椭球变到高自旋的扁椭球。此外，还确定了此两带的原子核形状。

参考文献

11 SHEN Shuifa，GU Jiahui，SHI Shuanghui, *et al.* Phys Lett, 2003, **B554**: 115

12 SHEN Shuifa，GU Jiahui，SHEN Wenqing, *et al.* Prog Theor Phys，2004, **111**: 721

On the mechanism of signature inversion in the doubly odd nuclei $^{80, 82, 84}$Rb

SHEN Shuifa GU Jiahui SHEN Wenqing

Keywords Signature inversion, Projected shell model (PSM), Yrast state, Quadrupole deformation

Several mechanisms have been proposed for signature inversion in the structure of A ~80 odd-odd nuclei, but the corresponding theoretical calculations have not been conclusive. In the present work, the angular momentum projected shell model (PSM) is applied to the study of the nuclei $^{80, 82, 84}$Rb [1-2]. The

results of the calculations regarding the positive parity yrast band for the configuration $\pi g_{9/2}\otimes\nu g_{9/2}$ and the negative parity yrast band for the configuration $\pi(p_{1/2}$ or $p_{3/2}$ or $f_{5/2})\otimes\nu g_{9/2}$ are compared with experimental data. According to the interpretation provided by the projected shell model, the signature inversion displayed in the positive parity yrast band for these nuclei is a signal of a substantial quadrupole shape change that takes place with increasing spin: The nucleus evolves from a prolate shape at low spin through a triaxial shape to an oblate shape at high spin. In addition, we specify the nuclear shapes of these two bands in these two nuclei.

References

1 SHEN Shuifa, GU Jiahui, SHI Shuanghui, *et al*. Phys Lett, 2003, **B554** :115

2 SHEN Shuifa, GU Jiahui, SHEN Wenqing, *et al.* Prog Theor Phys, 2004, **111**: 721

用 Langevin 方程模拟核裂变碎片的同位旋标度

王 鲲 马余刚 魏义彬 蔡翔舟 陈金根 方德清 郭 威

马国亮 沈文庆 田文栋 钟 晨 周星飞

关键词 裂变动力学，同位旋标度，朗之万方程

我们使用结合 Langevin（朗之万）方程和统计衰变的模型模拟 ^{112}Sn＋^{112}Sn 和 ^{116}Sn+^{116}Sn 这两个同位旋相关的核裂变过程，使用蒙特卡罗高斯抽样的方法得到了对称和非对称裂变的产物分布，并对这两个系统的同位素和同中子异位素的产物分布进行了同位旋标度律研究，提取出同位旋标度律参数α和β，以及这两个参数同质子数和中子数的关联与碎片分布宽度的影响。我们发现，同位旋标度参数同入射能量和系统的粘滞系数是有关联的，同位旋标度可以作为研究裂变动力学的一个探针。

Isoscaling of fission fragments with langevin equation

WANG Kun MA Yugang WEI Yibin CAI Xiangzhou CHEN Jingen

FANG Deqing GUO Wei MA Guoliang SHEN Wenqing

TIAN Wendong ZHONG Chen ZHOU Xingfei

Keywords Fission dynamics, Isoscaling, Langevin equation

The Langevin equation is used to simulate the fission process of ^{112}Sn＋^{112}Sn and ^{116}Sn+^{116}Sn.The mass distribution of the fission fragments are given by assuming the process of symmetric fission or asymmetric fission with the Gaussian probability sampling. The isoscaling behaviour has been observed from the analysis of fission fragments of both reactions, and the isoscaling parameter α and β have been obtained. It seems that the isoscaling parameter α is sensitive to the width of fission probability, and it also depends on beam energy and reduced friction parameter. Therefore the isoscaling analysis of the fission data can be taken as a sensitive tool to investigate the fission dynamics.

合成 109 号超重元素的实验提议

王 鲲 马余刚 马国亮 魏义彬 蔡翔舟 陈金根 郭 威 钟 晨 沈文庆

关键词 超重核，统计蒸发模型

我们用一个统计蒸发模型（HIVAP）计算了轻核打锕系靶合成超重元素反应的生成截面，并与已有的实验数据对比，在此基础上提出了使用 $^{30}Si+^{243}Am$ 反应方式来合成 109 号元素的实验提议。并且对反应截面和最佳入射能量做了估算。计算的结果对兰州重离子加速器实验室合成超重核素的实验有一定的参考作用。

A Proposed reaction channel for the synthesis of the superheavy nucleus *Z*=109

WANG Kun MA Yugang MA Guoliang WEI Yibin CAI Xiangzhou

CHEN Jingen GUO Wei ZHONG Chen SHEN Wenqing

Keywords Superheavy nuclei, Statistical-evaporation model

We apply a statistical-evaporation model (HIVAP) to calculate the cross sections of superheavy elements, mainly about actinide targets and compare with some available experimental data. A reaction channel $^{30}Si+^{243}Am$ is proposed for the synthesis of the element Z=109 and the cross section and the suitable beam energy are estimated. This result can be used for refering to our national laboratory in Lanzhou (HIRFL).

超声合成纳米碳球

王震遐 余礼平 张 伟

关键词 超声处理，类洋葱碳球

超声处理去离子水中高序石墨形成了类洋葱纳米碳球。高分辨率透射电子显微镜（HRTEM）和电子衍射（ED）分析表明这些纳米球由无序的石墨晶格线组成，它们的尺寸大小在 10—200 nm 之间。另外，为了解释纳米碳球的生长机制，我们提出了一种两步生长机制：石墨屑（graphenes）先形核，然后以“滚雪球”方式长大。

Carbon spheres synthesized by ultrasonic treatment

WANG Zhenxia YU Liping ZHANG Wei

Keywords Ultrasound treatment, Onion-like nanosphere

Onion-like carbon nanospheres have been synthesized through ultrasound treatment on highly

oriented pyrolytic graphite (HOPG) material in deion water. High resolution transmission electron microscope (HRTEM) and electron diffraction (ED) analyses show that these nanospheres are composed of disordered lattice lines of graphene sheets and the size of them ranges from about 10nm to 200nm. In addition, to explain the growth mechanism of carbon nanospheres, one possible two-stage model was proposed of nucleus formation and “rolling snowball” growth of carbon nanospheres.

嵌 Ar-泡的类 Schwarzite 碳

王震遐　余礼平　张 伟

关键词　离子辐照，Ar-泡，类 Schwarzite 碳

镍氩离子先后注入石墨形成了含氩泡的类 Schwarzite 碳膜。用高分辨率透射电子显微镜（HRTEM）和 X 射线能量散射谱（EDS）分析辨别出碳和氩的完全相分离。而拉曼谱和电子衍射谱表明这种碳膜为类玻璃态的相结构材料。本文对这种嵌有氩泡的类 Schwarzite 纳米材料的可能的生长机制进行了初步探讨。

Schwarzite-like carbon entrapped argon bubbles

WANG Zhenxia　YU Liping　ZHANG Wei

Keywords　Ion irradiation, Ar-bubbles, Schwarzite-like carbon

Schwarzite-like carbon flakes with argon-bubbles were fabricated by using nickel and argon ions irradiation on graphite in proper order. Complete phase separation between carbon and argon was distinguished by high–resolution transmission electron microscopy (HRTEM) images and X-ray energy dispersive spectroscopy (EDS) measurements. Raman scattering and electron diffraction (ED) pattern reveals that as-grown flake has the phase structure of the glassy-carbon-like. Possible growth process of these nanoscale materials of Schwarzite-like carbon embedded Ar-bubbles was briefly discussed.

离子辐照产生无定形分子节结构

王震遐　余礼平　张 伟

关键词　离子束焊接，碳纳米线节

实验和分子动力学研究表明，电子辐照能在单壁碳纳米管的交叉处形成分子节。最近分子动力学计算机模拟预测离子辐照也能连接单壁碳纳米管。我们发现用碳离子辐照多壁碳纳米管后，碳纳米管转变成了无定形碳纳米线，更重要的是，在这一过程中，在多壁碳纳米管的交叉处通过焊接，形成了各种各样的无定形碳纳米线的分子节。这表明离子束辐照是对多壁纳米管焊接而形成纳米线分子节的一种有效方法。

Amorphous molecular junction produced by ion irradiation on carbon nanotubes

WANG Zhenxia YU Liping ZHANG Wei

Keywords Ion-beam welding, Carbon nanowire junction

Experiments and molecular dynamics have demonstrated that electron irradiation could create molecular junctions between crossed single-walled carbon nanotubes. Recently molecular dynamics computation predicted that ion irradiation could also join single-walled carbon nanotubes. Employing carbon ion irradiation on multi-walled carbon nanotubes, we find that these nanotubes evolve into amorphous carbon nanowires, more importantly, during the process of which various molecular junctions of amorphous nanowires are formed by welding from crossed carbon naotubes. It demonstrates that ion-beam irradiation could be an effective way not only for the welding of single-wall nanotubes but also for the formation of nanowire junctions.

离子辐照下碳纳米管的催化合成

王震遐 吴永庆 张 伟

关键词 碳纳米管，离子注入，透射电子显微镜

我们用双离子注入的方法成功获得了各种多壁碳纳米管（MWCNTs）。这是一种合成多壁碳纳米管的新方法。虽然生长机制和物理性质目前还不是很清楚。但这种方法也可能用于其他纳米材料的合成。

Catalytic synthesis of carbon nanotubes under ion irradiation

WANG Zhenxia WU Yongqing ZHANG Wei

Keywords Carbon nanotubes, Ion-implantation, TEM

We successfully obtained various multi-wall carbon nanotubes (MWCNTs) including bent or distorted nanotubes, using the double ion (Fe^+ and Ar^+) irradiation method. This approach is expected to form a new general route for synthesis of MWCNTs, the growth mechanism and physical properties of which are of great interest. This multi-ion irradiation idea may also be valid for other material and be used for fabricating nanostructures.

同位选相关的量子分子动力学模型(IQMD)的反应总截面研究

魏义彬 蔡翔舟 沈文庆[1,2] 马余刚[1] 张虎勇 钟 晨
郭 威 陈金根 马国亮 王 鲲

关键词 核反应总截面，同位旋相关的量子分子动力学

我们介绍了同位选相关的量子分子动力学模型（IQMD）的反应总截面研究结果。模型中的不变的核子相体积被随着能量而改变的相体积所代替。调整之后的 IQMD 模型能够很好的拟合稳定核以及奇异核所引起的中能区核-核反应总截面的实验数据。利用此模型探讨了 ^{11}Li 的不同密度分布对反应总截面的影响。结果显示，采用实验中提取的密度分布比利用 Skyrme-Hartree-Fock 计算的密度分布更好的拟合反应总截面的能量激发函数；此外，较高入射能量的反应总截面更加地依赖 ^{11}Li 的密度分布的尾巴部分。

1 高等科学技术中心
2 宁波大学物理系

Total reaction cross section in an isospin-dependent quantum molecular dynamics model

WEI Yibin CAI Xiangzhou SHEN Wenqing[1,2] MA Yugang[1] ZHANG Huyong
ZHONG Chen GUO Wei CHEN Jingen MA Guoliang WANG Kun

Keywords Total reaction cross section, Isospin-dependent quantum molecular dynamics

The isospin-dependent quantum molecular dynamics (IDQMD) model is used to study the total reaction cross section σ_R. The energy-dependent Pauli volumes of neutrons and protons have been discussed and introduced into the IDQMD calculation to replace the widely used energy-independent Pauli volumes. The modified IDQMD calculation can reproduce the experimental σ_R well for both stable and exotic nuclei induced reactions. Comparisons of the calculated σ_R induced by ^{11}Li with different initial density distributions have been performed. It is shown that the calculation by using the experimentally deduced density distribution with a long tail can fit the experimental excitation function better than that by using the Skyrme-Hartree-Fock calculated density without long tails. It is also found that σ_R at high energy is sensitive to the long tail of density distribution.

1 CCAST (World Laboratory), PO Box 8730
2 Department of Physics, Ningbo University

一种新的研究丰中子核素结构的探针-HBT 方法

魏义彬 马余刚[1] 沈文庆[1] 马国亮 王 鲲 蔡翔舟
钟 晨 郭 威 陈金根 周星飞

关键词 Hanbury-Brown-Twiss 方法，奇异结构

利用量子分子动力学（IQMD）模型作为核反应的事件发生器，我们给出了丰中子核导致的核反应中的中子-中子关联函数的 HBT 计算结果。对核反应中 ^{11}Li 发射的两晕中子的关联函数的计算结果非常好地拟合了实验数据。利用此方法，我们揭示了关联函数强度与核的单中子分离能之间的关系。研究结果显示利用关联函数方法研究丰中子奇异核内部结构是可行的。

1 高等科学技术中心

A new possible probe for investigating the exotic structure of neutron-rich nuclei by using hanbury-brown-twiss method

WEI Yibin MA Yugang[1] SHEN Wenqing[1] MA Guoliang WANG Kun
CAI Xiangzhou ZHONG Chen GUO Wei CHEN Jingen ZHOU Xingfei

Keywords Hanbury-Brown-Twiss Method, Exotic structure

Hanbury-Brown-Twiss (HBT) results of the nucleon-nucleon correlation function have been presented for the nuclear reactions with neutron-rich projectiles using an event-generator, i.e., the Isospin-dependent quantum molecular dynamics model. A good agreement of our calculation for the two-halo-neutron correlation function of ^{11}Li with the experimental data has been reached. In addition, we explore that the relationship between the single neutron separation energy and the strength of the HBT. Results show that it is feasible to investigate the exotic structure of neutron-rich nuclei with HBT method.

1 CCAST (World Laboratory), PO Box 8730

探索核素的 HBT 强度对核素结合能以及分离能的依赖性

魏义彬 马余刚[1] 沈文庆[1,2] 马国亮 王 鲲 蔡翔舟 钟 晨 郭 威 陈金根

关键词 Hanbury-Brown-Twiss 方法，结合能，分离能

利用同位旋相关的量子分子动力学（IQMD）模型，我们给出了 Be 同位素丰中子核导致的核反应的双中子关联函数的 HBT 研究结果。我们揭示了中子-质子关联函数在低相对动量区域的强

度与平均结合能之间的关系。我们还进一步探索了质子-晕中子关联函数强度与单中子分离能之间的关系。研究结果显示，中子-质子关联函数强度对核的分离能以及结合能非常敏感。

1 高等科学技术中心
2 宁波大学物理系

Exploring binding energy and separation energy dependences of HBT strength

WEI Yibei MA Yugang[1] SHEN Wenqing[1,2] MA Guoliang WANG Kun
CAI Xiangzhou ZHONG Chen GUO Wei CHEN Jingen

Keywords Hanbury-Brown-Twiss method, Binding energy, Separation energy

Hanbury Brown-Twiss (HBT) results of the nucleon-nucleon correlation function have been presented for the nuclear reactions with neutron-rich projectiles (Be isotopes) using an event-generator, the Isospin-Dependent Quantum Molecular Dynamics model. We explore that the relationship between the binding energy per nucleon of the projectiles and the strength of the neutron-proton HBT at small relative momentum. Moreover, we reveal the relationship between the single neutron separation energy and the strength of the halo neutron-proton HBT. Results show that neutron-proton HBT results are sensitive to binding energy or separation energy.

1 CCAST (World Laboratory), PO Box 8730
2 Department of Physics, Ningbo University

^{29}P 的碎裂产物 ^{28}Si 的纵向动量分布

魏义彬[1] 马余刚 蔡翔舟 钟 晨 陈金根[1] 张虎勇 方德清[1] 王 鲲[1] 马国亮[1]
郭威[1] 田文栋[1] 沈文庆 詹文龙[2] 肖国青[2] 徐瑚珊[2] 孙志宇[2] 李加兴[2]
郭忠言[2] 王 猛[2] 陈志强[2] 胡正国[2] 陈立新[2] 李 琛[2] 毛瑞士[2] 白 洁[2]

关键词 纵向动量分布，质子皮结构，^{29}P

我们测量了轰击 C 靶的 30.7 MeV/n 的 ^{29}P 的单质子剥离反应产物 ^{28}Si 的纵向动量分布。此动量分布的半高宽为 110.5(23.5) MeV/c。我们假设 ^{29}P 的内部结构为 ^{28}Si 加上一个价质子，并在此假设的基础上，利用成熟的 Glauber 模型验证了我们的实验结果。此模型中采用的 ^{29}P 的密度分布为 Skyrme-Hartree-Fock 的理论计算结果。我们的研究结果显示，在 ^{29}P 核素中可能存在着质子皮结构。

1 中国科学院研究生院，2 中国科学院近代物理研究所

Parallel momentum distribution of ^{28}Si fragments from ^{29}P

WEI Yibin[1] MA Yugang CAI Xiangzhou ZHONG Chen CHEN Jingen[1]
ZHANG Huyong FANG Deqing[1] WANG Kun[1] MA Guoliang[1] GUO Wei[1]
TIAN Wendong[1] SHEN Wenqing ZHAN Wenlong[2] XIAO Guoqing[2] XU Hushan[2]
SUN Zhiyu[2] LI Jiaxing[2] GUO Zhongyan[2] WANG Meng[2] ZHEN Zhiqiang[2]
HU Zhengguo[2] CHEN Lixin[2] LI Chen[2] MAO Ruishi[2] BAI Jie[2]

Keywords Parallel momentum distribution, Proton-skin structure, ^{29}P

Distribution of the parallel momentum of ^{28}Si fragments from the breakup of 30.7MeV/nucleon ^{29}P has been measured on C targets. The distribution has the FWHM with the value of 110.5(23.5)MeV/c which is consistent quantitatively with Glauber model calculation assuming by a valence proton in ^{29}P. The density distribution is also predicted by Skyrme-Hartree-Fock calculation. Results show that there might exist the proton-skin structure in ^{29}P.

1 Graduate School of the Chinese Academy of Sciences
2 Institute of Modern Physics, Chinese Academy of Scences

^{25}Si 丰质子核的反应截面和碎片动量分布的测量

颜廷志 马余刚 方德清 蔡翔舟 沈文庆 孙志宇[1] 任中洲[2] 郭 威 魏义彬
王 鲲 颜廷志 马春旺 陈金根 陈金辉 马国亮 苏前敏 田文栋 钟 晨
左嘉旭 Hosoi M[3] Izumikawa T[4] Kanungo R[5] Nakajima S[3] Ohnishi T[5]
Ohtsubo T[4] Ozawa A[6] Suda T[5] Sugawara K[3] Suzuki T[3] Takisawa A[4]
Tanaka K[5] Yamaguchi T[3] Tanihata I[5]

关键词 动量分布，核反应总截面，^{25}Si

2004 年 4 月核物理室重离子反应小组为进一步研究 ^{23}Al 的奇异结构，在日本 RIKEN 完成一项实验。该实验产生的次级束中同时包含有丰质子核 ^{25}Si，因此通过对该实验的数据分析可以为其是否存在质子皮结构提供实验上的判据。该实验采用了靶前 $B\rho$-TOF-ΔE、靶后 TOF-ΔE-E 的粒子鉴别方法，可以同时完成对反应总截面、单质子剥离截面以及碎片动量分布的测量。有关碎片动量分布和反应截面的初步结果已经得到，更细致的分析还在进行中。

1 近代物理研究所，2 南京大学物理系
3 Department of Physics, Saitama University
4 Department of Physics, Niigata University
5 日本理化学研究所，6 Department of Physics,Tsukuba University

Study on the momentum distribution and total reaction cross section for ^{25}Si

YAN Tingzhi MA Yugang FANG Deqing CAI Xiangzhou SHEN Wenqing SUN Zhiyu[1] REN Zhongzhou[2] GUO Wei WEI Yibin WANG Kun YAN Tingzhi MA Chunwang CHEN Jingen CHEN Jinhui MA Guoliang SU Qianmin TIAN Wendong ZHONG Chen ZUO Jiaxu Hosoi M[3] Izumikawa T[4] Kanungo R[5] Nakajima S[3] Ohnishi T[5] Ohtsubo T[4] Ozawa A[6] Suda T[5] Sugawara K[3] Suzuki T[3] Takisawa A[4] Tanaka K[5] Yamaguchi T[3] Tanihata I[5]

Keywords Momentum distribution, Total interaction cross section,^{25}Si

We performed an experiment at RIKEN, Japan in April 2004 for further study of the exotic structure of ^{23}Al. The secondary beam produced in the experiment also includes proton-rich nucleus ^{25}Si. Through the analysis of the experimental data, it is hopeful to obtain some evidence to the predicted one proton skin structure of ^{25}Si. We used Bρ-TOF-ΔE method before target and TOF-ΔE-E method after target to determine particles, and could measure total reaction cross section, one proton removal cross section and momentum distribution of fragmentations in this experiment. Some preliminary results of the momentum distribution and total interaction cross section have been obtained.

1 Institute of Modern Physics, Chinese Academy of Scences
2 Department of Physics, Nanjing University
3 Department of Physics, Saitama University
4 Department of Physics, Niigata University
5 The Institute of Physics and Chemical Research
6 Department of Physics,Tsukuba University

核素结合能的中子-质子关联函数依赖性的系统研究

魏义彬[1] 马余刚 沈文庆 马国亮[1] 王 鲲[1] 蔡翔舟 钟 晨 郭 威[1]
陈金根[1] 方德清 田文栋 周星飞[1]

关键词 中子-质子动量关联函数，结合能

利用 IQMD 模型作为事件发生器，我们给出了不同同位素（B，N，C，Li）系统导致的核反应中的核子-核子关联函数结果。对中子-中子关联函数在较低相对动量区域的强度与核素的平均每核子结合能之间的关系给出了系统的研究结果。结果显示，在不同的同位素系统导致的核反应中，其中子-质子关联函数的强度均对核素的平均结合能敏感。

1 中国科学院研究生院

Systematic studies of binding energy dependence of neutron-proton momentum correlation function

WEI Yibei[1] MA Yugang SHEN Wenqing MA Guoliang[1] WANG Kun[1]
CAI Xiangzhou ZHONG Chen GUO Wei[1] CHEN Jingen[1] FANG Deqing
TIAN Wendong ZHOU Xingfei

Keywords Neutron-proton momentum correlation function, Binding energy

Hanbury Brown-Twiss (HBT) results of the nucleon-nucleon correlation function have been systematically investigated for a series nuclear reactions with light projectiles (B, N, C, Li) with help of Isospin-Dependent Quantum Molecular Dynamics model. The relationship between the binding energy per nucleon of the projectiles and the strength of the neutron-proton HBT strength at small relative momentum has been obtained. Results show that neutron-proton HBT results are sensitive to binding energy per nucleon.

1 Graduate School of the Chinese Academy of Sciences

轻丰质子核中可能存在的奇异结构

张虎勇[1] 沈文庆[1] 马余刚 蔡翔舟 方德清 卢朝晖 钟 晨 魏义彬 陈金根
周星飞[1] 马国亮[1] 王 鲲 任中洲[2] 詹文龙[3] 郭忠言[3]
肖国青[3] 徐瑚珊[3] 王建松[3] 孙志宇[3]

关键词 反应总截面，动量分布，丰质子核

在兰州近代物理研究所 RIBLL 上，我们用 69 MeV/核子的 ^{36}Ar 初级束轰击 ^{9}Be 靶，通过炮弹碎裂反应产生放射性核束。我们用透射输运法测量了 30 MeV/核子左右的次级束轰击碳靶的反应总截面。结果显示 ^{23}Al 和 ^{27}P 的反应总截面相对邻近同位素有较大增大，而 ^{17}F 有一定增大。这说明 ^{23}Al 和 ^{27}P 有着较大的均方根半径，是质子晕核。我们还测得了 ^{31}Cl、^{32}Cl、^{33}Cl、^{28}S、^{29}S 的反应总截面和动量分布，实验数据还在分析中。通过用密度依赖的相对论平均场理论计算发现 ^{23}Al、^{27}P 和 ^{31}Cl 都有质子晕结构，^{17}F 和 ^{32}Cl 有质子皮结构。我们还提出了寻找新的质子滴线附近核素 ^{25}P 和 ^{26}S 的实验方案，并探讨了较轻质子晕、质子皮核测量研究的重要性。

1 宁波大学理学院
2 南京大学物理系
3 兰州近代物理研究所

Possible exotic structure in light proton-rich nuclei

ZHANG Huyong[1] SHEN Wenqing[1] MA Yugang CAI Xiangzhou FANG Deqing
LU Zhaohui ZHONG Chen WEI Yibin CHEN Jingen ZHOU Xingfei[1]
MA Guoliang[1] WANG Kun REN Zhongzhou[2] ZHAN Wenlong[3] GUO Zhongyan[3]
XIAO Guoqing[3] XU Hushan[3] WANG Jiansong[3] SUN Zhiyu[3]

Keywords Total reaction cross section, Mmomentum distribution, Proton-rich nuclei

Radioactive ion beams were produced through the projectile fragmentation induced by 69MeV/nucleon ^{36}Ar primary beam on a ^{9}Be target. Measurements of reaction cross section (σ_R) for some proton-rich nuclei on carbon target at intermediate energies around 30MeV/nucleon have been performed on RIBLL of HIRFL by transmission method and transmission plus transportation method. The experimental σ_R values for ^{23}Al and ^{27}P are abnormally large compared with their neighboring nuclei and that of ^{17}F has an enhancement compared with the neighboring isotopes. It suggests anomalously large matter root-mean-square radii and proton halo structure in ^{23}Al and ^{27}P. The experimental σ_R values and momentum distribution of fragmentation reaction product for ^{31}Cl, ^{32}Cl, ^{33}Cl, ^{28}S, ^{29}S were performed also on RIBLL by transmission and transportation method. These data are in analyzing. The calculation of relativistic density-dependent Hartree shows that the nuclei ^{23}Al, ^{27}P, ^{31}Cl may have proton-halo structure and ^{17}F, ^{32}Cl may have proton-skin structure. New experiment on the search for new nuclides ^{25}P and ^{26}S in proton drip line is also described. The significance of these measurements and possible proton halo and skin for light proton-rich nuclei has been discussed.

1 College of Sciences, Ningbo University

2 Department of Physics, Nanjing University

3 Institute of Modern Physics, Chinese Academy of Scences

Al 同位素中对关联的同位旋效应

张虎勇[1] 沈文庆[1] 任中洲[2] 马余刚 蔡翔舟 卢朝晖 钟 晨
魏义彬 陈金根 周星飞[1] 马国亮[1] 王 鲲

关键词 对关联，同位旋效应，Skyrme-Hartree-Forck 方法，滴线核

我们用 Skyrme-Hartree-Forck 方法研究 Al 同位素的结合能，着重研究了对关联中的同位旋效应。计算结果表明，Skyrme-Hartree-Forck 能很好描述具有不能对关联形式的 Al 同位素的结合能。我们发现当 Al 同位素在靠近质子滴线时，对关联的同位旋效应扮演了一个重要的角色。

1 宁波大学理学院

2 南京大学物理系

Isospin effect of the pairing correlation in Al isotopes

ZHANG Huyong[1] SHEN Wenqing[1] REN Zhongzhou[2] MA Yugang
CAI Xiangzhou LU Zhaohui ZHONG Chen WEI Yibin CHEN Jingen ZHOU
Xingfei[1] MA Guoliang[1] WANG Kun

Keywords Skyrme-Hartree-Fock approach, Isospin effect, Dripline nuclei, Pairing correlation

The binding energies of Al isotopes are investigated by using the Skyrme-Hartree-Fock approach with the SKIII force parameter. Special emphasis is placed on the influence of the isospin effect of the pairing correlation on the neutron separation energy. Calculations show that the Skyrme-Hartree-Fock approach provides a good description of the binding energy of Al isotopes with different forms of pairing correlation. Meanwhile, it is found that the isospin effect of the pairing correlation plays a great role to the separation energy when the Al isotopes approach to the proton drip line.

1College of Sciences, Ningbo University，2 Department of Physics, Nanjing University

^{17}F、^{17}O 和 ^{17}Ne、^{17}N 的基态和第一激发态的结构

张虎勇[1] 沈文庆[1] 任中洲[2] 马余刚 陈金根 蔡翔舟 卢朝晖 钟 晨
郭 威 魏义彬 周星飞[1] 马国亮[1] 王 鲲

关键词 相对论平均场，激发态，质子晕，中子皮

我们用相对论平均场方法研究了 ^{17}F 和 ^{17}O 以及 ^{17}Ne 和 ^{17}N 的基态和第一激发态。研究发现，^{17}Ne 的基态和第一激发态具有双质子晕结构，^{17}N 的第一激发态具有双中子晕结构；^{17}F 和 ^{17}O 的第一激发态具有中子晕结构，^{17}F 和 ^{17}O 的基态具有中子皮结构。

1 宁波大学理学院，2 南京大学物理系

Structures of ^{17}F and ^{17}O, ^{17}Ne and ^{17}N in the ground state and the first excited state

ZHANG Huyong[1] SHEN Wenqing[1] REN Zhongzhou[2] MA Yugang
CHEN Jingen CAI Xiangzhou LU Zhaohui ZHONG Chen GUO Wei
WEI Yibin ZHOU Xingfei[1] MA Guoliang WANG Kun

Keywords Relativistic mean-field approach, Excited state, Proton halo, Neutron skin

The structures of two couples of mirror nuclei ^{17}F and ^{17}O, ^{17}Ne and ^{17}N in the ground state and in

the first excited state are investigated using the relativistic mean-field approach. Two-proton halo in ^{17}Ne in the first excited state and in the ground state and two-neutron halo in ^{17}N in the first excited state are suggested. Meanwhile, one-proton halo in ^{17}F in the first excited state and one-neutron halo in ^{17}O in the first excited state are also suggested. The skin structure appears in ^{17}F and ^{17}N in the ground state。

1 College of Sciences, Ningbo University

2 Department of Physics, Nanjing University

从核反应总截面实验测量的提取核半径

张虎勇[1] 沈文庆[1] 任中洲[2] 马余刚 陈金根 蔡翔舟 蒋维洲 钟 晨

郭 威 魏义彬 周星飞[1] 马国亮[1] 王 鲲[1]

关键词 相对论平均场，Glauber 模型，核半径，质子皮

我们用兰州近物所 RIBLL 上测得实验核反应总截面，结合 Glauber 模型提取了相应的核半径。同时，我们也用密度依赖的相对论平均场理论对核半径和考虑形变的参数化核半径经验化公式进行了理论计算。从得到的实验值和理论，我们提出 ^{23}Al、^{27}P 可能存在质子晕结构，^{24}Al 可能存在质子皮结构。并且我们发现在形变在核半径扮演了一个重要的角色。

1 宁波大学理学院，2 南京大学物理系

Nuclear radii extracted from experimental reaction cross sections

ZHANG Huyong[1] SHEN Wenqing[1] REN Zhongzhou[2] MA Yugang CHEN Jingen

CAI Xiangzhou JIANG Weizhou ZHONG Chen GUO Wei WEI Yibin

ZHOU Xingfei[1] MA Guoliang[1] WANG Kun[1]

Keywords Relativistic mean-field approach,Glauber model, Nuclear radius, Proton skin

We illustrate typical experimental reaction cross sections σ_R which have obtained on RIBLL at Heavy Ion Research Facility of the Institute of Modern Physics (IMP) at Lanzhou. The corresponding nuclear radii are extracted from the measured experimental σ_R using the Glauber model. Meanwhile, theoretical nuclear radii are also calculated using Relativistic density-dependent Hartree and spherical relativistic mean-field theory with Pauli blocking. For comparison, the nuclear radii of these nuclei are also calculated using the empirical radius format in which the deformation has been taken into account. From the given experimental and theoretical nuclear radii, we suggest that there may exist proton halo

structure in ^{23}Al, ^{27}P and may exist proton skin structure in ^{24}Al. We also find that the deformation plays a great role to the nuclear radii.

1 College of Sciences, Ningbo University

2 Department of Physics, Nanjing University

晕核散射中的碎片动量分布及核子逃逸截面

赵耀林　朱志远　马中玉 [1]

关键词　Glauber 理论，晕核，动量分布，核子逃逸截面

最近有关滴线核晕结构的研究已经越来越多地引起实验和理论上的重视。研究表明一些丰质子核具有一个或两个晕核子，而丰中子核有可能具有更多的晕核子形成晕中子集团。对晕核其反应截面和核子逃逸截面相比于它的稳定的同位素要大得多，并且散射后形成碎片的动量分布宽度很窄。我们应用少体 Glauber 理论，完整地给出了晕核散射的动量分布和核子逃逸截面，并将其推广到含有多个晕核子的晕核散射。其反应机理采用两种不同的方法处理，一种是在低能散射时考虑末态相互作用，末态晕核子波函数采用修正的自由粒子波函数；另一种是在高能散射时忽略了末态相互作用。这样我们就可以通过对实验上测量的反应截面、核子逃逸截面及动量分布三个物理量的同时分析，提取有关晕核结构更准确的信息。

1 中国原子能科学研究院

Momentum distribution of fragment and nucleon removal cross section in halo nuclei reaction

ZHAO Yaolin　ZHU Zhiyuan　MA Zhongyu[1]

Keywords　Glauber theory, Halo nuclei, Momentum distribution, Nucleon removal cross section

Recently the research on the halo structure of the drip-line nuclei has attracted much attention both in experiment and theory. They have shown some nuclei have one or more halo nucleons. Within the few body Glauber model, the momentum distribution of a fragment and nucleon removal cross section in halo nuclei reaction have been perfectly given and extended to about the halo nuclei having more halo nucleons. The reaction mechanism is treated in two different approachs. One is that the final-state interaction is considered. And the wave function of halo nucleon standing in finial state is taken as a modified free particle wave function. In another approach we neglect the finial-state interaction and don't do the modification. Thus through simultaneously studying the reaction cross section, momentum distribution and nucleon removal cross section within Glauber model, one could get more specified information on halo structure of the drip-line nuclei..

1 China Institute of Atomic Energy

模拟锆（Zr）的基体效应对 Ni_3Al-x at.% Zr 晶界内聚性的影响

郑里平

关键词 晶界浓度，偏析子与诱发子，基体效应

双粒子模型被用来研究微量元素锆（Zr）的基体效应对 Ni_3Al-x at.% Zr 晶界内聚性的影响。模型显示，x[锆(Zr)的基体浓度]从 0.1 增加到 0.5，在晶界 Zr 富集是增加的；Ni 富集和 Al 贫乏在 $x=0.3$ 时趋于最大。模型还显示，Ni_3Al-x at.% Zr 晶界的内聚性在 $x=0.3$ 时为最佳。

Monte Carlo simulations of the bulk effects of Zr on the cohesion of the Ni_3Al-x at. % Zr grain boundary

ZHENG Liping

Keywords Grain boundary concentrations, Inducing and segregating species, Bulk effects

The double species model has been employed to calculate dependence of the grain boundary cohesion on the Zr bulk concentration, for the Ni_3Al-x at. % Zr (100%Ni\100%Ni)[001]/∑5(210)/36.87° symmetric tilt grain boundary, at the equilibrium. Calculations show that when x (the Zr bulk concentration) increases from 0.1 to 0.5, the Zr enrichment increases, both the Ni enrichment and the Al depletion maximizes at $x=0.3$. The calculations also show the best cohesion of the grain boundary at $x=0.3$.

通过碳纳米管的粒子束流传输

郑里平 许子建 朱志远

关键词 碳纳米管，沟道效应，粒子束流传输

荷能粒子在碳纳米管里的(轴)沟道效应，显示大的沟道直径和微弱的退沟道因子。在粒子束物理的领域中，碳纳米管沟道的最迷人应用是，与在高梯度加速场里粒子加速的可能性相联系，和与建造 TeV 对撞机的可能性相联系。通过研究 450 GeV π^-介子、450 GeV 质子、450 GeV U^{+92} 和 10 GeV/c C^{+6} 离子等束流的实例，介绍了这应用研究的进展。

Transmission of particle beam through nanotubes

ZHENG Liping XU Zijian ZHU Zhiyuan

Keywords Nanotubes, Channeling, Transmission of particle beam

Channeling of energetic particle in nanotubes exhibits the large diameter of the channels and the

weak dechanneling factors. In particle-beam physics field, the most intriguing applications of the nanotubes-channeling are connected with the possibility of particle acceleration in high gradient accelerating fields, and with the possibility of construction of TeV colliders. The progress of these applications is introduced by studying 450GeV π^-, 450GeV proton, 450GeV U^{+92} and 10GeV/c C^{+6} beams.

用 Boltzmann-Uehling-Uhlenbeck 模型研究轻核引起的核反应总截面

钟 晨　沈文庆　蔡翔舟　张虎勇　魏义彬　方德清　马余刚

关键词　核反应总截面，BUU 模型，轻核

用 Boltzmann-Uehling-Uhlenbeck（BUU）模型可以很好的描述中能重离子核反应动力学。Ingemarsson 测量了大量由 α 粒子、氘以及质子等轻核引起的核反应总截面。我们成功应用 BUU 模型计算了由这些轻核引起的核反应总截面。

Study on the total reaction cross sections induced by light nuclei via the boltzmann-uehling-uhlenbeck model

ZHONG Chen　SHEN Wenqing　CAI Xiangzhou　ZHANG Huyong

WEI Yibin　FANG Deqing　MA Yugang

Keywords　Total reaction cross section, BUU model, Light nuclei

Boltzmann-Uehling-Uhlenbeck (BUU) Model can describe successfully intermediate energy heavy ion collision dynamics. Ingemarsson *et al*. measured the total reaction cross sections of intermediate energyα-particles, deuterons and protons on targets from ^{9}Be to ^{208}Pb. This work can reproduce calculate the total reaction cross section induced by these light nuclei using BUU Model.

用修正的统计擦碎模型研究 $^{40/36}$Ar+^{9}Be 系统蒸发前和蒸发后碎片的同位旋标度现象

钟 晨　马余刚　方德清　蔡翔舟　王 鲲　田文栋　魏义彬　陈金根　郭 威

周星飞　马国亮　苏前敏　陈金辉　颜廷志　左嘉旭　马春旺　沈文庆

关键词　同位旋标度，统计擦碎模型，蒸发

实验测得约 60 MeV/核子 ^{40}Ar+^{9}Be 和 ^{36}Ar+^{9}Be 反应的同位素分布，用修正的同位素擦碎模型能很好拟合实验数据。从计算中提取了同位旋标度 (Isoscaling) 参数 α 和 $|\beta|$，研究发现蒸发前后

|β|变化不大，而 α 有较大变化。但是蒸发后 α 和 $|\beta|$却大致相等。同时我们还发现同位旋标度参数能够表征同位旋消失现象。

Study on isoscaling behavior of pre-fragments and fragments from the collision of ^{40,36}Ar+^{9}Be with modified statistical abrasion-ablation model

ZHONG Chen MA Yugang FANG Deqing CAI Xiangzhou WANG Kun
TIAN Wendong WEI Yibin CHEN Jingen GUO Wei ZHOU Xingfei
MA Guoliang SU Qianmin CHEN Jinhui YAN Tingzhi ZUO Jiaxu
MA Chunwang SHEN Wenqing

Keywords Isoscaling, Statistical abrasion-ablation model, Evaporation

Isotopic distribution for intermediate mass fragments have been measured for ^{40}Ar+^{9}Be and ^{36}Ar+^{9}Be at about 60MeV/nucleon. The isotopic distributions of the fragmentation reaction products were well reproduced by using a modified statistical abrasion-ablation model. From the data simulated by SAA model, we distill the isoscaling parameters α and |β|. Before the evaporation and after the evaporation, |β| is roughly equal with each other and α has changed a lot relatively. For fragments, a monotonic increase of α and |β| with the increase of Z and N is observed, andα≈ |β|. It has been discussed the relation between isoscaling parameters and the disappearance of the isospin effect of fragmentation.

62.4 GeV Au + Au 中 K^0_S 介子的产生

左嘉旭 蔡翔舟 马余刚 马国亮 陈金辉 钟 晨 沈文庆（STAR 实验合作组）

关键词 62.4 GeV/c 金-金碰撞， K^0_S

对在 RHIC 上进行的 62.4 GeV Au + Au 碰撞实验中 K^0_S 横动量分布进行了测量。在实验中，运用 V_0 衰变拓扑方法，通过衰变道 $K^0_S \to \pi^+ + \pi^-$ 来重构 K^0_S 介子。得到的 K^0_S 粒子产额谱可以用指数函数或波尔兹曼函数来很好地拟合，从而得到不同碰撞中心度下的 dN/dy 和温度参数。利用对二体碰撞粒子数归一化的不同中心度下粒子的产额，我们可以测量中心碰撞对周边碰撞的粒子产额比（R_{CP}）。其横动量可测量达到 6.6GeV/c 的范围。实验结果表明 K^0_S 的 R_{CP} 和 Φ 的比较接近，这意味着在中间横动量区域 R_{CP} 具有粒子种类的相关性。

Production of Ks^0 from 62.4 GeV Au + Au collisions at RHIC

ZUO Jiaxu CAI Xiangzhou MA Yugang MA Guoliang CHEN Jinhui

ZHONG Chen SHEN Wenqing (for the STAR Collaboration)

Keywords 62.4 GeV/c Au+Au, Ks^0

We present the preliminary measurement of Ks^0 transverse momentum (p_T) distribution from $\sqrt{s_{NN}}$ =62.4 GeV Au + Au collisions at RHIC. The Ks^0 particle is reconstructed via its decay channels to charged daughter particles through the V_0 decay topology method, $Ks^0 \rightarrow \pi^+ + \pi^-$. The measured spectra can be described by using an exponential fit or a Boltzmann fit. Then the dN/dy and the temperature can be deduced for different centrality bins. The centrality dependence of the particle yield with respect to the number of binary collision scaling (R_{CP}) will be presented for a transverse momentum up to 6.6GeV/c. The R_{CP} of Ks^0 is closed to that of ϕ, which imply the particle type dependence of R_{CP} at intermediate pt.

核分析

Nuclear analysis techniques

康普顿γ成像仪及其数据的重建

潘强岩 Y. Gono[1] S. Motomura[1] S. Enomoto[2] Y. Yano[2]

关键词 康普顿γ成像仪， 数据重建

康普顿γ成像仪 (Compton Camera) 是人们正在开发的一种新的造影仪器。数据重建是开发康普顿γ成像仪、实现其商品化的关键技术问题之一，具有挑战性。我们用国际上通用的粒子 (射线) 与物质的相互作用的模拟程序—GEANT4 对γ射线在探测器中的散射和吸收的全过程作了模拟，对其中的数据重建方法作了一些探索。

图 1(a) 是用背投影法重建的点源图像，其中像素的大小为 0.5 mm×0.5 mm。放射源 ^{137}Cs 位于康普顿γ成像仪的对称轴上，距离散射探测器的中心位置为 60 mm。这里我们选用了一通过放射源的位置并垂直于成像仪的对称轴的平面作为成像面。图上的椭圆是其中一个圆锥表面在成像面上的投影。图 1(a) 中除了清晰显示位于中心位置的放射源外，其他位置的记数 (本底) 也相当可观，特别是越接近源的位置本底越高。高本底会带来两个严重的问题：首先，影响了成像仪的本征空间位置分辨。从点源的二维造影垂直剖面 (图 1(d)) 得到位置分辨 (FWHM) 只有 5.6mm。其次，就某一康普顿γ散射事件对应于成像面上的椭圆而言，除了其中的一点代表了γ射线的起源位置外，其余部分都贡献给了其他像素，干扰了对其他位置的造影。在实际应用中人们是需要对立体物体进行造影，这种高本底的数据重建方法将是无法容忍的，也是行不通的。

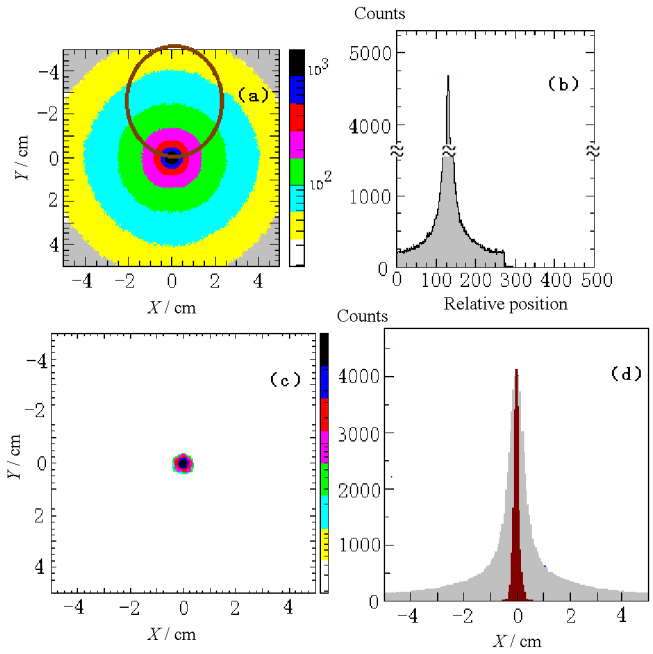

图 1.

Fig.1 (a) X-Y coordinates of a point source reconstructed by using the back-projection method. One of the ellipses is also shown; (b) Density distribution of the selected Compton scattering event; (c) X-Y coordinates of a point source reconstructed by using the TSBP method; (d) Slices of the images.

针对背投影法所存在的问题，我们提出了图像重建的改进方法。作为例子，还是以点源为例。在背投影法的基础上，如果选出其中的一个康普顿γ散射事件 (图 1(a) 中的椭圆)，将沿着它在

成像面上的椭圆轨迹进行展开作为 x 轴，由通过该椭圆轨迹上的每一点的其它椭圆的数目作为 y 轴构成的位置谱 (图 1(b)所示)。从图 1(b)可以清楚地看到该事件最有可能来源自该位置谱的峰值所对应的空间位置。这样，只取位置谱上的峰值所对应的空间位置进行成像，就排除了该椭圆上的其他点，大大地了降低，获得了如图 1(c)所显示的一低本底的高质量图像。经过我们重新处理，图像的空间位置分辨 (FWHM)由原来的 5.6 mm 提高到 1.2 mm，同时，排除了背投影法中大量本底在不同位置之间的干扰而严重影响成像质量的问题。也就是说，这种新的图像重建方法克服了背投影法中的高本底的问题，为康普顿 γ 成像仪的数据重建提供了一种简单、有效的新方法，我们暂时定名为“背投影峰位法”。图 1(d)给出了背投影法和背投影峰位法的点源垂直剖面图。

1 Department of Physics, Kyushu University, Fukuoka 812-8581, Japan

2 Cyclotron Center, RIKEN, Saitama 351-0198, Japan

Compton camera and its image reconstruction

PAN Qiangyan Y. Gono[1] S. Motomura[1] S. Enomoto[2] Y. Yano[2]

Key words Compton camera, Image reconstruction

A Compton camera always consists of two detectors whose front and rear ones are called a scatter and an absorption detector, respectively. The original position of a γ-ray source can be obtained by using kinematics of Compton scattering and position information of a γ-ray interaction points in the two detectors. Therefore, a Compton camera does not require the lead collimator, which is inevitable for SPECT, resulting an increase of efficiency of a γ-ray detection. The data reconstruction is one of the big challenges for the development of a Compton camera. In this article, a new image reconstruction method, which is made based on the back-projection procedure, is proposed. A simulation shows that the position of a point source can be identified with an accuracy of less than 0.02 mm using this new method.

We describe a Compton camera consisting of two position sensitive planar Ge's of 20 mm thick. The cathodes of these Ge's are divided into 25 segments of an equal size, 10×10 mm. The signals from these segments give the interaction positions as well as the energy information. Two detectors are placed parallel to each other and the distance between them is 60 mm.

In order to simplify the mathematical procedure, one can use an image plane, which is placed in parallel to a scatter detector at a certain distance and defined as x-y plane, to carry out a two-dimensional imaging. Distances between planes and a scatter detector are selected in the region, which is determined as a most likely region of the source location by checking a simple back-projection. A z-axis is defined as a perpendicular axis with respect to a detector surface. If a single point source of activity is considered, a succession of Compton scattering events will generate a number of ellipses which have a common point of intersection as shown as the dark point in Fig.1(a), thereby defining the image point. This method, which is known as a back-projection method, can reproduce the source location. However the image background is also high, because the entire back-projected ellipse was recorded to reconstruct the image. Actually, only one point of each projected ellipse is at the origin of the incoming gamma ray. All the other recorded points form a huge background. Thus, the

back-projection method has two major drawbacks: Limitation of spatial resolution and blurring the other image position.

In our new method, a second step is introduced to select one point for each ellipse. After an image is made in the first step, each ellipse is overlapped with the image. Then a density of points is projected along the whole ellipse and the peak point position of the density is only selected for final image reconstruction. By applying this procedure for all ellipses one gets an image with far lower background comparing with that made by only the first step. We call this method as a two steps back-projection (TSBP) method. This procedure is shown in Fig.1. A selected ellipse is overlapped with a first step image shown in Fig.1 (a). Fig.1 (b) displays a density distribution along the selected ellipse.

Here, an example resulted by the TSBP method for the reconstruction of a point source of ^{137}Cs is shown in Fig.1(c). The source was placed at 60 mm apart from a surface of the scatter detector. An FWHM of the peak is (1.35±0.15) mm. By using a peak fitting procedure, an accuracy of about 0.02 mm may be obtained for a position determination. Fig.1(a) shows a result of a simple back-projection (SBP). An FWHM of the peak is about 6 mm. It is clear that both a position resolution and a background are significantly improved with the new reconstruction method.

In summary, a new image reconstruction method, TSBP, was proposed. An image made by TSBP was significantly improved both in a position resolution and a background reduction comparing with that obtained by SBP. The computer simulation was made for the Compton camera that consists of two segmented Ge's. This camera has a high energy resolution enough for a multitracer usage.

1 Department of Physics, Kyushu University, Fukuoka 812-8581, Japan

2 Cyclotron Center, RIKEN, Saitama 351-0198, Japan

水热条件下碳纳米管的氧化过程研究

吴小利 岳 涛 陆荣荣 朱德彰 朱志远

关键词 碳纳米管，水热反应，修饰

碳纳米管自发现以来因其优良的力学、电学和热学特性受到广泛地关注[1]。在碳纳米管的应用研究过程中，表面修饰逐渐成为一个新的研究领域，通过碳纳米管的表面修饰可以增加它在结构复合材料中的分散性，改良碳纳米管光学复合材料的发光特性，制备基于碳纳米管的生物探针等。[2] 碳纳米管的氧化在碳纳米管表面修饰过程中有相当重要的作用，在氧化过程中引入的羟基、羧基等官能团可以使碳纳米管进一步与其它化学试剂进行反应，如：用带有羧基的碳纳米管与胺基化合物反应得到的功能化碳纳米管可以用作化学纳米探针[3-4] 以及结构复合材料的添加剂[5]等。水热条件是材料制备的一种重要的手段，它能够为化学反应提供均一的反应条件。

我们在水热条件下不同的时间和温度下用各种氧化剂对碳纳米管进行了表面修饰，并利用红外和 X 射线光电子能谱表征了氧化后样品的化学结构，并用拉曼光谱研究了它的物理结构。结果表明：在水热条件下，除了可以在一定程度上纯化碳管以外，各种氧化剂都可以成功的功能化碳纳米管，在这一过程中，引入了羧基，羟基等化学官能团。在功能化过程中，碳纳米管管壁上 C 的 sp^3 杂化结构随着功能化程度的增强而增加。通过控制反应的条件如：温度，填充度，时间等参数可以改变引入官能团的数量。

The functionalization of the carbon nanotubes by hydrothermal treatment

WU Xiaoli YUE Tao LU Rongrong ZHU Dezhang ZHU Zhiyuan

Keywords Carbon nanotube, Hydrothermal treatment, Functionalization

Since its first discovery, carbon nanotube (CNT) has attracted great interest of researchers in many fields with their numerous potential applications. Most of these applications require targeted chemical functionalization of the carbon nanotubes and the oxidation process is a critical step in the chemical functionalization of CNTs, which can introduce the initial functional groups, such as hydroxyl, carbonyl, and carboacidic groups, to the surface of CNTs. With these groups, the carbon nanotubes can be further

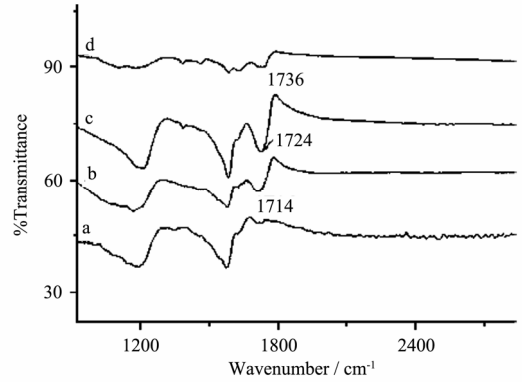

Fig.1 FT-IR spectrum of CNTs oxidized by different reagents: (a)the raw CNTs;(b)$KMnO_4$;(c)HNO_3; (d) H_2O_2

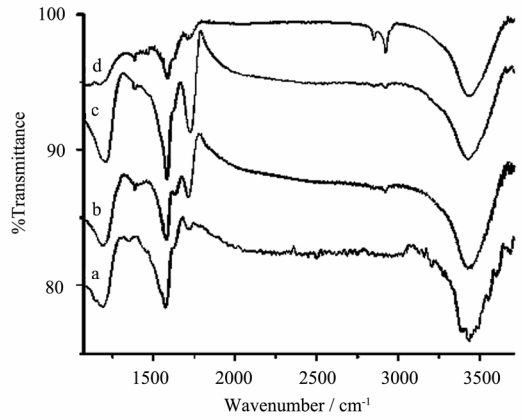

Fig.2 FT-IR spectrum of CNTs oxidized by diluted nitric acid during different treatment time: (a)the raw CNTs; (b) 3h; (c) 6h; (d) 10h

modified by amines, alcohols or other chemical reagents. We report here on the functionalization of CNTs through hydrothermal treatment which could provide the necessary conditions for chemical functionalization. The results revealed that the CNTs could be oxidized successfully by different kinds of reagents under hydrothermal conditions, and several kinds of chemical groups such as $-OH$, $-C=O$, -COOH were introduced to the CNTs surface. During the process of the oxidation the structure of CNTs was affected and the sp^3 structure became more abundant. The amount and types of chemical groups resulted on the surface of CNTs could be controlled by choosing different reaction conditions.

双离子(Fe^+和Ar^+)注入合成碳纳米管

吴永庆　陆荣荣　王震遐　朱德彰　巩金龙　李玉兰　朱志远

关键词　离子注入，碳纳米管

自 1991 年以来，碳纳米管 (CNTs) 以其独特的结构、性能和潜在应用前景引起了各国科学家的广泛关注。目前，合成碳纳米管的方法主要有电弧放电法、激光蒸发法和气相沉积法 (CVD) 法三种。近年来，荷能离子辐照法也在碳纳米结构的合成及相变研究中得到了应用。单离子辐照石墨产生碳纳米管已见报道，但是该法得到的碳纳米管不仅数量极少，而且管壁缺陷较多，远不如 CVD 法制备得到的碳纳米管。因此，本论文采用双离子辐照 (Fe 离子和 Ar 离子)法实现了纳米管的合成。

首先，用 60 keV 的 Fe^+注入石墨，束流强度 5 μA/cm^2，总剂量 5×10^{17}ions/cm^2，靶室真空 2×10^{-6}Torr。其次，在不破坏靶室真空条件下，进行 Ar^+注入，实验条件同前。制备得到样品用扫描电子显微镜 (SEM，Leo 1530VP 型)、高分辨率透射电子显微镜 (HRTEM，Philips CM-200) 进行观察和分析。实验发现有大量的碳纳米管生成，其形貌和结构与 CVD 法制备的碳纳米管极为相似。这是离子注入催化剂来合成碳纳米管的实例。为研究纳米管合成新方法，进一步探索催化作用机制开辟了新的思路。

双离子注入石墨合成 CNTs 的过程是：(1)Fe^+注入碳靶后形成了碳化铁催化颗粒前体 (precursors)；(2)随后 Ar^+注入不仅促使催化颗粒成长到具有催化 CNTs 生长活性的尺寸，而且制造了提供碳源的合适环境，满足了碳管的催化生长条件。

Catalytic synthesis of carbon nanotubes under double ion (Fe^+ and Ar^+) irradiation

WU Yongqing　LU Rongrong　ZHU Dezhang　GONG Jinlong

LI Yulan　ZHU Zhiyuan

Keywords　Ion irradiation, Carbon nanotube

The discovery of carbon nanotubes (CNTs) has motivated intense interest in the study of their peculiar structure, physical properties, synthesis methods and formation mechanism, and the potential technological applications. CNTs were prepared typically by DC arc discharge method, laser vaporization of graphite and chemical vapor deposition (CVD). Recently, ion beams have been also used in CNTs synthesis and phase transition of carbon nanostructures. It was reported that carbon nanotubes could be synthesized by Ar^+ irradiation to the carbon plate in spite of tiny yield and many defects. Our focus here is whether the direct formation of nanotubes by implanting catalytic element such as iron or other elements will be realized or not. Therefore we decided to investigate the formation of CNTs using Fe^+ ion bombardment on the carbon plate surface before Ar^+ irradiation. A quite surprising result emerging from the double ions (catalytic ion and impacted ion) irradiation experiments was that CNTs were found on the surface of graphite target under such sequence irradiation conditions. The morphologies and structures of as-grown nanotubes were dependent on ion irradiation characteristic

features.

CNTs were prepared using the double ion irradiation in a proper order. First, the amorphous carbon was implanted by 60 keV Fe^+ ions (dose: $5\times10^{17}cm^{-2}$) at room temperature. The as-implanted sample was then implanted by Ar^+ ion in the same above experimental conditions. The morphology of CNTs was characterized by a LEO-1530-VP field-emission scanning electron microscope (FE-SEM) with accelerating voltage of 10 kV. The microstructures of CNTs were studied with a Philips CM200 EFG model high-resolution transmission electron microscope (HR-TEM) operated at the accelerating voltage of 160 KV.

The growth mechanism of various carbon nanotubes in the present work is not clearly understood. It is commonly believed that localizability in space and discontinuity in time caused by random injection of innumerable ions will result in a growth change of nanotube structure in site and time during growth process. Here is a possible mechanism for the formation of carbon nanotubes in double ions irradiation. On one hand, during Ar^+ irradiation of Fe-implanted samples, cascaded-atoms in the locally melted region produced by the cascade thermal spike occurrs. This behavior leads to considerable carbon atom clustering and motion around the nanoparticles. On the other hand, the presence of the Fe-nanoparticles can catalyze the carbon atoms and/or clusters transformation towards graphitic layers which encircle catalytic particle in a similar way, as in CCVD growth.

基于同步辐射 X 射线荧光分析的大气气溶胶单颗粒源解析

岳伟生　李晓林　余笑寒　邓 彪　刘江峰　万天敏　张桂林　李 燕

黄宇营[1] 何 伟[1] 华 巍[1]

关键词　同步辐射，大气气溶胶，指纹，源解析

同步辐射微束 X 射线荧光分析 (micro-SXRF) 是在传统的 X 射线荧光分析法基础上发展起来的一种先进分析技术。由于同步辐射光源具有高亮度、高极化、高准直等特点，所以与传统的 X 射线荧光分析相比，以同步辐射 X 射线为激发源的荧光分析法具有高的灵敏度 (绝对探测限可达 1fg) 和良好的空间分辨率，因此这种方法在生命科学、材料科学、地球环境科学等领域获得了广泛的应用。在环境科学研究方面，由于同步辐射光的优异性能，micro-SXRF 是研究大气气溶胶的一种理想手段。Sz.Török 等人用同步辐射 X 射线微束分析了直径为 1—200 μm 的电厂飞灰颗粒物的元素和一些元素的价态。Maria Caterina Camerani 等人用 micro-SXRF 分析了单个飞灰颗粒的元素和元素在颗粒物上的分布。这些工作没有开展对颗粒物的来源追踪。

本工作将北京同步辐射装置 (BSRF) 微束用于上海市大气气溶胶单颗粒的研究，并对空气中 PM_{10} (空气动力学直径 <10 μm) 来源作了追踪。基本做法是：首先，收集造成上海市大气污染的污染源，用 micro-SXRF 分析污染源样品单颗粒，获取颗粒物的 micro-SXRF 能谱，把单颗粒的 micro-SXRF 能谱作为污染源颗粒的“指纹”特征存入到计算机，建立污染源单颗粒指纹数据库；然后，用同样的实验条件分析环境空气监测样品，获取其单颗粒 micro-SXRF 能谱；最后，利用模式识别程序将环境空气监测样品颗粒物的能谱与数据库中污染源单颗粒指纹进行对比，从而识别出环境空气监测样品的来源。结果表明同步辐射微束是研究大气气溶胶单颗粒的理想手段。将单颗粒的 micro-SRXRF 能谱与模式识别技术相结合，识别出上海市吴淞工业区某交通要道采样点

PM_{10}主要来源于钢铁工业(26%)、土壤(16%)、无铅汽油汽车尾气(15%)、燃煤(10%)、水泥(10%)和助动车尾气(8%)。

1 中国科学院高能物理研究所

Source identification of PM_{10} collected at a heavy traffic roadside by analyzing individual particles using synchrotron radiation

YUE Weisheng LI Xiaolin YU Xiaohan DENG Biao LIU Jiangfeng
WAN Tianmin ZHANG Guilin LI Yan HUANG Yuying[1] HE Wei [1] HUA Wei [1]

Keywords Synchrotron radiation, Aerosol, Fingerprints, Source apportionment

PM_{10} (particular matter with aerodynamic diameter≤10μm) is considered to be a health hazard since it can reach the lower respiratory tract where they are phagocytized by alveolar macrophages. Thus, abatement of PM_{10} pollution is necessary for identifying pollution sources of PM_{10} pollution, where control measures would have to be taken. Because of the advantages of synchrotron radiation source, micro-SXRF measurements can be carried out in air, non-conductive samples can be analyzed and non-destructive analysis is possible due to the lower thermal damage compared to charged particle excitation. By means of a micro-focused X-ray beam, micro-SXRF is a good tool for the analysis of individual particles with diameter of several micrometers. A particular advantage of micro-SXRF in comparison with conventional X-ray source and particle excitation methods is the extremely high brilliance achieved with synchrotron radiation (SR) source. Therefore, a spectrum of a single aerosol particle can be obtained in a short time and the analysis of large amount of particles is also possible. Micro-SXRF has been used successfully to determine the characterization of individual aerosol particles recently by Camerani and Camerani Piniani *et al*. In their work, the elemental composition and the distribution of some elements in the particles were determined. However, to our best knowledge, there is no report on the source apportionment PM_{10} analyzed by micro-SXRF.

In this work, the micro-SXRF of BSRF was applied to the study of single atmosphere aerosol particles. Sources of PM_{10} collected at a heavy traffic roadside in the heavy industrial area of Shanghai were also identified by the combination of micro-SXRF of single aerosol particle and pattern recognition. The identification was carried out as follows: First, a set of individual particles from 14 pollution sources were analyzed by micro-SXRF. Their micro-SXRF spectra were used to establish a fingerprint database for the pollution sources. Second, other individual aerosol particles collected at a busy traffic roadside located in the heavy industrial zone of Shanghai, were analyzed with same facilities. Last, these particles were identified for finding their origins by comparing their micro-SXRF spectrum pattern with those in the fingerprint database by pattern recognition technique. The results show that the particles analyzed are mainly from metallurgic industry (26%), unleaded gasoline automobile exhaust (15%), coal combustion (10%), cement dust (10%) and motorcycle exhaust (8%).

1 Institute of High Energy Physics, Chinese Academy of Sciences

催化裂解 C_2H_2 制备多壁碳纳米管的研究

吴永庆　陆荣荣　朱德彰　巩金龙　李玉兰　何绥霞　朱志远

关键词　催化裂解，多壁碳纳米管

碳纳米管 (CNTs) 自 1991 年被日本 Iijima 教授发现以来，因其独特的结构和奇异的物理化学性能以及所具有的诱人应用前景，倍受各国研究者的广泛关注。碳纳米管的制备通常有电弧法、催化裂解法和激光法三种方法，其中催化裂解法 (CVD) 是最为广泛应用的方法。为搞清楚催化裂解中反应温度、催化剂和反应气体组成及气体流量等参数对多壁碳纳米管 (MWNTs) 生长的影响规律，本实验室通过裂解乙炔制备 MWNTs，运用 SEM、TEM、HRTEM 及拉曼光谱对其形貌和微观结构进行了分析，对碳管生长机理也作了初步的探讨。结果表明：(1) 在使用乙炔为碳源气体时，铁镍复合催化剂的效果要好于单一催化剂，催化剂膜厚应小于 50 nm；(2) 当反应温度为 650~700℃，反应气体为 N_2:C_2H_2:H_2 = 100:20:10 (sccm)，气压为 180Torr 时，可获得产量高、直径分布均匀、石墨程度高的多壁碳纳米管。

The study of carbon nanotubes synthesized by acetylene catalytic pyrolysis

WU Yongqing　LU Rongrong　ZHU Dezhang　GONG Jinlong

Li Yulan　ZHU Zhiyuan

Keywords　Catalytic Pyrolysis, Carbon Nanotube

Since its discovery by Iijima in 1991, carbon nanotube (CNT) is of great interest all over the world because of its complex structures, peculiar physical and chemical properties as well as its promising applications. Several synthetic approaches, such as arc discharge, laser vaporization and chemical vapor deposition (CVD), have been developed to grow carbon nanotubes. Among them, chemical vapor deposition has been intensively applied as a powerful method due to its ability to synthesize large-scaled CNTs with controlled diameter and length. In order to investigate the effects of the reaction temperature, catalysts, the compositions and flux of the reaction gases on the production of CNTs by CVD method, CNTs were prepared by acetylene catalytic pyrolysis in our lab and their morphologies and structures were studied using SEM, TEM, HRTEM and Raman methods. The growth mechanism of CNTs was briefly discussed as well.

Experiment results showed that,

1．When acetylene is used as carbon source, the compound catalyst of Fe and Ni is more suitable to grow CNTs than single element catalyst. The thickness of the compound catalyst (FeNi) should be less than 50 nm.

2．When the reaction temperature to grow CNTs is between 650℃and 700℃, the composition of reaction gas N_2:C_2H_2:H_2 = 100:20:10(sccm), the reaction gas pressure 180Torr, the as-grown CNTs exhibit a reasonably good graphitized tubular microstructure with high production and homogeneous diameter distribution.

多孔氧化铝模板中高度石墨化碳纳米管阵列的制备

俞国军 王 森 巩金龙 朱德彰 何绥霞 朱志远

关键词 碳纳米管，多孔氧化铝模板，石墨化

由于碳纳米管具有十分重要的基础研究和应用研究价值，一经发现就引起了科学界和企业界广泛的兴趣。其中，对于高度取向碳纳米管的研究一直以来就是热点。过去十年中，许多研究人员花费了大量精力用化学气相沉积的方法在多孔氧化铝模板的孔道中直接沉积得到碳纳米管，因为这种管子不仅高度取向，而且直径分布基本均一，其长度、内外壁直径均随模板可控。不过，这种管子有一个很大的缺点，那就是其晶化程度极低，管壁为无定型碳或玻璃碳结构，与用电弧放电法和过渡金属催化法生长的多壁碳纳米管的结构相差甚远。这给它的应用和研究带来很大的限制。

我们在前面工作的基础上，进一步研究了此种管子的生长机制，认为其实质是一种高温裂解碳在多孔氧化铝弱催化作用下的积碳效应，管子质量与氧化铝模板孔道的平滑程度密切相关。据此，结合氢氧自由基对于无定形碳的刻蚀原理，采用乙醇作为碳源，在 800ºC 低气压下，以化学气相沉积的方法在多孔氧化铝模板的孔道中直接沉积得到碳纳米管阵列。高分辨透射电镜显微镜成像表明，碳纳米管的管壁由基本平行排列的石墨壁构成，中间夹杂着一些无定形碳。在实验上第一次得到了完全由多孔氧化铝模板孔道制约，高度石墨化的碳纳米管阵列。

Observation of well multiwallized carbon nanotube arrays within anodic aluminum oxide template

YU Guojun WANG Sen GONG Jinlong ZHU Dezhang HE Suixia ZHU Zhiyuan.

Keywords Carbon Nanotube, Porous anodic aluminum oxide template, Graphitization

In the last decade, many research groups investigated the preparation of the CNT arrays by chemical vapor deposition (CVD) within porous anodic aluminum oxide (AAO) template, because these nanotubes were very uniform in diameter, highly ordered, and perfectly vertical with respect to the plane of the template. Unfortunately, the crystallinity of these nanotubes was much lower than the ones by other methods, such as arc discharge synthesis, and was far from a multiwall carbon nanotube structure, even was amorphous. Until now, there are no reports about this kind of highly multiwallized carbon nanotubes, since their first obtaining.

In this work, we have firstly observed the arrays of well multiwallized, uniform carbon nanotubes within the nano-channels of anodic aluminum oxide (AAO) template. In order to improve the multiwallization extent, ethanol as reactant gas was selected, and dilute phosphoric acid was used to smooth the channel walls of the AAO. The structure and morphology of CNTs were characterized by scanning electron microscope (SEM, LEO 1530 VP), conventional transmission electron microscopy (TEM) and high resolution transmission electron microscopy (HRTEM, JEOL JEM-2011).

多孔氧化铝模板与铝基体的分离

俞国军 王 森 巩金龙 朱德彰 何绥霞 朱志远

关键词 多孔氧化铝，铝基片，分离

制备具有超细、均一纳米尺度孔道的阵列材料是近十年来研究人员一直努力的方向。因为这种材料可用作纳米器件，如磁、电、光电纳米器件的衬底或模板，其极高的长径比是目前的平板印刷技术难以达到的。阳极氧化的多孔氧化铝膜作为典型的自组织纳米孔道材料，具有十分难得的合适结构。其孔道的直径、孔间距和孔深度等都可通过合适的电化学氧化条件控制。在通常情况下，这层膜与其下面的铝基体必须分开，以用于各自的用途。比如，为了得到具有表面纳米凹坑结构的铝基体，则用磷酸和铬酸的混合液溶解掉表面的氧化膜；为了得到表面的氧化膜，则须用氯化汞溶液腐蚀掉铝基体。这中间的过程不仅耗时，而且操作不慎容易对人体和环境造成伤害。

我们借鉴和改进了前人的技术，采用逆电剥离法把多孔氧化铝膜与铝基体直接分开，不仅省时省材，而且对环境和人体几乎没有任何威胁。为了得到结构完整的多孔氧化铝膜或铝基体，我们对于剥离的几个具体影响因素，如氧化温度，膜厚度，反向电压大小等作了比较。发现最适宜的氧化温度是 15ºC，临界膜厚度和临界反向电压分别为 20 μm 和 40 V。扫描电子显微镜 (SEM) 和原子力显微镜 (AFM) 都证实，用这种方法进行分离，对多孔氧化铝膜或铝基体不产生损伤和污染。

Separation of porous anodic alumina membrane from replicated aluminum sheet

YU Guojun WANG Sen GONG Jinlong ZHU Dezhang HE Suixia ZHU Zhiyuan

Keywords Porous Anodic Alumina Membrane, Al sheet, separation

Porous anodic alumina membrane (PAAM), a typical self-organized material with uniform nano-channels formed by electrochemical anodic oxidation of Al sheet in an appropriate acid solution, has attracted increasing interest as an important template or mask for fabrication of nanometer-scale structures. In most instances, the PAAM and the sandwiched Al sheet should be separated from each other for their respective purposes, such as preparation of monodispersed carbon nanotube or nanofibre arrays by CVD (chemical vapor deposition) for the PAAM, which could be obtained after etching away the Al sheet in saturated $HgCl_2$ solution, and fabrication of nanostructure metal surface by sputtering for the replicated Al sheet, which could be achieved by removing the PAAM with a mixed H_2CrO_4/H_3PO_4 solution. However, until now, there are few reports on the separation of the PAAM and the sandwiched Al sheet.

In this study, porous anodic alumina membrane (PAAM) and sandwiched Al sheet were separated from each other by an inverted DC voltage free of long time immerging of the samples in saturated $HgCl_2$ solution or mixed H_2CrO_4/H_3PO_4 solution. The images of the samples by scanning electronic microscopy (SEM) and atomtic force microscopy (AFM) showed that the unopened barrier layer of the PAAM or the surface of the separated Al sheet was not only ordered but also intact by this simple

method, and the separated Al sheet with ordered arrays of nano-notch could be utilized directly for several times after separation. Dependence of successful separation of the sandwiching PAAM/Al sheet on the PAAM thickness, the anodization temperature and the inverted voltage were investigated.

碳源和载气种类对于氧化铝模板法制备的碳纳米管石墨化程度的影响

俞国军　王 森　巩金龙　朱德彰　何绥霞　朱志远

关键词　碳源，载气，碳纳米管石墨化

用热化学气相沉积的手段在多孔氧化铝模板中得到了高度取向的碳纳米管阵列。实验表明，除了温度和模板本身的质地因素外，所用碳源和载气的种类对于此种碳纳米管的结构有重要影响，其中对于管壁的石墨化程度影响尤为明显。

在其他条件相同的情况下，我们比较了乙炔、苯、萘、和乙醇四种碳源对于碳管石墨化程度的影响。用 X 射线粉末衍射仪 (XRD)、拉曼光谱以及高分辨透射电子显微镜 (HRTEM) 成像表征后，发现乙醇较其他三种碳源在碳管石墨化方面具有明显的优势，乙炔次之。这可能是因为乙醇裂解得到的氢氧自由基对于无定形碳具有刻蚀作用，而乙炔在高温下则很容易产生乙炔三聚，最终形成多聚的六元环。载气方面，使用氩气比氮气效果好。这可能是因为氮气参与了碳纳米管的形成活动，在管壁中夹杂了极少量的氮元素。

但不论使用何种碳源或载气，除了使用乙醇得到了管壁结构接近于多壁的碳纳米管外，氧化铝模板法制备的碳纳米管的微观结构均与多壁碳纳米管结构相差甚远。

Effects of carbon sources and carrier gas on graphitization of carbon nanotubes within anodic aluminum oxide template

YU Guojun　WANG Sen　GONG Jinlong　ZHU Dezhang　ZHU Zhiyuan

Keywords　Carbon Source, Carrier Gas, Graphitization of Carbon Nanotube

Template-synthesis technique based on anodic aluminum oxide (AAO) template was applied for preparation of highly ordered carbon nanotube arrays by thermal chemical vapor deposition (CVD). It was found that carbon sources and carrier gas were of great importance for the fabrication and structure of carbon nanotube arrays within anodic aluminum oxide (AAO) template, particularly for their graphitization extent. Four kinds of carbon sources (acetylene, benzene, naphthalene, and ethanol) and two kinds of carrier gas (argon and nitrogen) were compared for the carbon nanotubes growth. We found that ethanol was the best carbon source among these four kinds of carbon sources for the graphitization of tubes. On the carrier gas hand, argon is better than nitrogen. X-Ray diffraction (XRD), Raman spectrum and high resolution transmission electron microscopy (HRTEM) were used to characterize the tubes' structures.

一种用于 SPM 分析的大气气溶胶单颗粒样品的制备方法

岳伟生　李晓林　王永其　张桂林　李 燕

关键词　SPM，单颗粒，制备方法

单颗粒靶样的制备是用扫描质子微探针 (SPM) 分析单颗粒大气气溶胶的关键技术之一。目前，国内外已报道 “悬浮液法”、“抖落法”等几种制备单颗粒样品的方法。这些方法在大气气溶胶单颗粒分析中起着重要的作用，但是它们在对颗粒物样品原始信息的保持方面还存在着一些不足。本工作在这些工作的基础之上，摸索出另外一种制备大气气溶胶单颗粒样品的方法，我们称它为“直接法”。

在本工作中，先后试验了几种材料做颗粒物支撑膜，最后认为聚乙烯醇缩丁醛 (PVB) 是做颗粒物支撑膜的理想材料。做法是：(1) 将 58 mg 白色聚乙烯醇缩丁醛粉末放入小烧杯，向烧杯中加入 6 mL 异丁醇，轻微振荡，使聚乙烯醇缩丁醛粉末溶解。(2) 取约 0.1 mL 聚乙烯醇缩丁醛溶液，滴入去离子水中。溶液在水面扩散形成薄膜。(3) 用预先制好的铝框从水中撩起薄膜。(4) 将带有薄膜的铝框晾干，这样，有 PVB 薄膜的铝框便可以用于直接采集颗粒物了。在采集大气颗粒物样品的时候，将有 PVB 薄膜的铝框放入采样器中，就可以将颗粒物直接采在膜上。取出样品，便可以用于 SPM 分析。通过控制采样的空气流量，就可以控制颗粒物在膜上分布的疏密程度。实验的结果表明用“直接法”制备的大气气溶胶单颗粒样品适合于 SPM 测量。用 PVB 做成的薄膜透明度高，机械性能较好，具有较好的抗冲击性能。用“直接法”制成的单颗粒样品，更好地保持了颗粒物原始信息。空气中颗粒物浓度在 100—180 μg/m^3 之间时，采样的空气流量为 1 m^3，可以得到合适的颗粒物分布密度。

A sample preparation method of individual aerosol particles for SPM analysis

YUE Weisheng　LI Xiaolin　WANG Yongqi　ZHANG Guilin　LI Yan

Keywords　SPM, Single particle, Preparation

Sample preparation of individual aerosol particle in SPM analysis is critical. Several methods were reported before, but they have some limitations in keeping physical and chemical information of individual particles. A new method for the preparation of individual aerosol particle in SPM analysis was developed in this work. Ideally, for optimum PIXE sensitivities, the substrates should be as thin and as clear as possible and the substrate should be rug enough to withstand the air pressure. Several materials were tested for the substrate, but none of them satisfied the requirements mentioned above. Then, the polyvinyl butyral (PVB) film was tested. The preparation of the sample was as follows: First, 58 mg PVB powder was dissolved in 6mL isobutyl alcohol. Then, a droplet of the solution was dropped onto the surface of deionized water at room temperature. The droplet stretched and a very thin nylon foil (about 0.2μm) was formed on the water surface. The foil was taken out of the water by an aluminum frame. Finally, aerosol particles were collected directly on the polyvinyl butyral (PVB) foil by using air sampler. Microscopic observation indicates that the particles were separated completely and

the interval of particles was reasonable when collected 1 m^3 at particle concentration within 100—180 μg/m^3. The SPM experiment proves that the PVB foil has excellent stability under proton micro-beam bombardment and it is a suitable backing material for supporting the single particle for SPM analysis.

单壁碳纳米管的纯化和修饰

俞国军　巩金龙　朱德彰　岳 涛　吴小利　朱志远

关键词　单壁碳纳米管，纯化，修饰

自从碳纳米管的发现并报道以来，研究人员已经采用电弧法、激光法、催化裂解法等多种方法成功地实现了碳纳米管的生长。但无论何种方法，制备的单壁碳纳米管或多壁碳纳米管产物中，总有其他杂质存在，如金属催化剂颗粒、无定形碳、石墨碳碎片、碳纳米颗粒等，在很大程度上制约着对碳纳米管性能的研究和应用潜力的开发。因此，对碳纳米管产物进行纯化，提高产物纯度和改善结构显得相当重要。迄今为止，对碳纳米管产物进行纯化不外乎物理法和化学法，对此已有各种相关的报道，取得了较大进展。用化学法纯化碳纳米管主要是利用碳纳米管与碳纳米颗粒等杂质之间的氧化速率有差异来实现的。金属催化剂、无定形碳、石墨碎片、碳纳米颗粒等较碳纳米管容易氧化。碳纳米管主要由呈六边形排列的碳原子构成， 但端口、缺陷及弯曲部分还存在五元环和七元环等缺陷，因此，化学方法对结构有缺陷的碳纳米管有一定程度的破环，但在破坏的同时，实际上也对碳纳米管进行了修饰。

我们利用高锰酸钾在酸溶液中的强氧化作用来提纯商业购买的单壁碳纳米管。发现通过控制高锰酸钾、硫酸、碳纳米管产品之间的配比，以及回流温度和回流时间，不仅可以提纯单壁碳纳米管，而且可以定量的修饰单壁碳纳米管。初始产品和处理后的产物用扫描电子显微镜 (SEM)、高分辨透射电子显微镜 (HRTEM)、红外光谱以及拉曼光谱进行了表征。

Purification and modification of single wall carbon nanotubes

YU Guojun　GONG Jinlong　ZHU Dezhang　YUE Tao　WU Xiaoli　ZHU Zhiyuan

Keywords　Single wall carbon nanotubes, purification, modification

Commercial single wall carbon nanotubes (SWCNTs) were purified and modificated by refluxing in mixed solution of sulfuric acid and potassium permanganate. The SWCNTs could be modificated quantitatively by selecting reflux conditions, such as the ratio of sulfuric acid to potassium permanganate, the reflux time and the reflux temperature. The images by scanning electron microscope (SEM, LEO 1530 VP), conventional transmission electron microscopy (TEM) and high resolution transmission electron microscopy (HRTEM, JEOL JEM-2011) showed that the impurities (e.g. amorphous carbon) were efficiently removed. IR and Raman spectrums of the treated products indicated the SWCNTs were well modificated.

利用原子力显微镜对 ALG-2 积聚的研究

张 峰 吴 芳[1] 龚为民[1] 胡 钧 何建华

关键词 AFM，ALG－2，细胞凋亡

细胞凋亡是一种由遗传决定的通过激活细胞自杀程序而启动的细胞死亡形式。细胞凋亡发生时，细胞会发生一些显著的、有秩序的形态学变化，包括细胞萎缩，染色质凝聚，DNA 降解成寡聚核苷酸片断，最终细胞被裂解成一些不连续的膜泡 (被称作凋亡体) 而迅速被临近的细胞吞噬。在多细胞生物体的发育、完整性的维持和内环境的稳定方面，细胞凋亡 (或者细胞程序性死亡) 是一个非常重要的生物学过程，比如除去不必要的、损伤的或者老的细胞。所以，许多人类疾病的病因与异常的细胞凋亡有密切相关性。异常的抑制凋亡会造成自体免疫疾病或者癌症，而不必要的增强细胞凋亡也会导致慢性疾病的发生 (如神经退行性疾病)。

钙离子控制着许多细胞活动，包括肌肉收缩，细胞粘联，分泌，能动性，生长，分化，基因表达，细胞死亡，等等。在静息状态的真核细胞内，游离钙离子的浓度在细胞质中是 50－100 nmol/L， 而在胞外空间或者钙离子储存器 (如内质网，线粒体) 中的浓度在 2－5 mmol/L 之间。当有刺激作用时，钙离子在细胞质中的浓度会在短时间内升到 1 μmol/L，这种钙离子浓度的变化被称作第二信使。钙结合蛋白是这种活动的调控子，并且在上述提到的各种生理现象中通过一系列不同的机制起重要作用。一些酶 (如蛋白激酶 C 和磷脂酶 C) 都在含有钙离子结合位点，如钙调蛋白激酶可以结合钙离子或者钙调蛋白。根据配基结合区域的序列和三维结构，细胞内的钙离子结合蛋白被分为四大组：EF－手，C2，annexins，和产酸钙离子储存蛋白。

细胞凋亡相关蛋白 ALG-2 是一种分子量为 22 kDa 的钙结合蛋白，在正常脑中大量表达，属于戊-EF-手蛋白家族。ALG-2 参与不同来源癌组织中细胞凋亡的调控。ALG-2 在细胞增值与细胞死亡之间的调控作用是分子细胞生物学当前研究的热点。利用原子力显微镜研究了 ALG-2 与钙离子结合情况，在单分子水平上直观地观察了 ALG-2 蛋白与钙离子结合前后的形态变化。ALG-2 与钙离子结合后发生的积聚现象，说明了 ALG-2 在凋亡细胞内发挥信号传导作用的可能机制。

1 中国科技大学

Study of ALG-2 aggregation by atomic force microscopy

ZHANG Feng WU Fang[1] GONG Weimin[1] HU Jun HE Jianhua

Keywords ALG-2, AFM, Apoptosis

Apoptosis is a form of cell death resulting from the activation of a genetically determined cell suicide program. It is characterized by a distinctive and orchestrated sequence of morphological changes including cell shrinkage, chromatin condensation, subsequent nuclear segmentation, and eventual cellular disintegration into discrete membrane-bound vesicles called apoptotic bodies that are rapidly phagocytosed by neighboring cells. Apoptosis is a fundamentally important biological process that is required during development and maintaining the integrity as well as homeostasis of multi-cellular organisms, i.e., removing unnecessary, damaged or aged cells. Therefore, inappropriate apoptosis, however, underlies the etiology of many human diseases. Abnormal resistance towards

apoptosis may lead to autoimmune diseases or cancer, whereas unnecessary enhancement of apoptotic processes could favor chronic pathologies such as neurodegenerative disorders.

Calcium ions control a variety of cellular phenomena, including muscle contraction, adhesion, secretion, motility, growth, differentiation, gene expression, cell death, etc. In resting eukaryotic cells, concentration of free Ca^{2+} is between 50—100 nmol/L in the cytosol, whereas it is between 2—5 mmol/L in the extracellular space or in the Ca^{2+}storing organelles (endoplasmic reticulum, mitochondria). Upon stimulation it transiently increases up to 1 mmol/L in the cytosol, and this change of the Ca^{2+} concentration is transmitted as a signal of the intracellular second messenger. Ca^{2+}binding proteins are the mediators of the signal, and play pivotal roles in the above-mentioned cellular phenomena through a variety of different mechanisms. Some enzymes, such as protein kinase C and phospholipase C contain Ca^{2+}-binding sites within the enzyme, whereas calmodulin kinase binds the Ca^{2+} /calmodulin. Based on primary and 3-D structures of the ligand binding domains, the intracellular Ca^{2+}binding proteins are classified into four groups: EF-hand, C2, annexins and acidic Ca^{2+}storage proteins.

The apoptosis-linked protein ALG-2 is a 22 kDa, Ca^{2+}binding protein expressed in normal brain,which belongs to the penta-EF-hand protein family. ALG-2 participates in apoptotic regulatory events occurring in cancerous tissues of different origins. The regulatory role of ALG-2 at the interface between cell proliferation and cell death is hotly discussed in the field of molecular cell biology. We have studied the binding of ALG-2 and Ca^{2+} by atomic force microscopy and observed the morphological changes of both before and later of ALG-2 binding with calcium ions on the molecular lever in vitro. The phenomenon which ALG-2 aggregates after binding with calcium ions indicates the potential mechanism with which ALG-2 exerts its signal transduction function in apoptosis cell.

1. University of Science and Technology of China

GAV 肽(VGGAVVAGV)在体外自我积聚成细纤维并促进 α-Synuclein 纤维化

张 峰 杜海宁[1] 吉丽娜 李洪涛[1] 胡钧 胡红雨[1] 何建华

关键词 GAV 肽，α-Synuclein，积聚，纤维化

α-Synuclein，淀粉样β-蛋白和 prion 蛋白都是与一些神经退行性疾病相关的淀粉样蛋白。这三种蛋白包括一个被认为是与纤维化和毒性密切相关的保守序列——GAV 结构花样。为了更进一步了解纤维组装过程中 GAV 结构花样的作用，我们化学合成了 GAV 肽段——NH_2-VGGAVVAGV-$CONH_2$，并与野生型α-Synuclein 对比，研究了 GAV 肽段的纤维化性质及其纤维形态。结果显示这个 GAV 短肽可以自发积聚成纤维，而且此过程与 pH 和 GAV 肽的浓度密切相关。GAV 短肽形成的纤维高度大约 3.0 nm，而且比野生型的α-Synuclein 形成的纤维更长。另外，发现 GAV 肽也可以促进α-Synuclein 带电氨基酸突变体的纤维化进程，但是却不能促使 GAV 肽缺失的α-Synuclein 突变体纤维化。针对以上结论，提出了一个纤维形态和纤维组装的可能模型。

1 中国科学院上海生命科学研究院

The GAV peptide (VGGAVVAGV) Can Self-assemble into thin filaments and promote α-Synuclein fibrillization *in vitro*

ZHANG Feng DU Haining [1] JI Lina LI Hongtao [1] HU Jun
HU Hongyu [1] HE Jianhua

Keywords GAV peptide, α-Synuclein, AFM, Fibrillization

α-Synuclein, amyloid β-protein and prion protein are among the amyloidogenic proteins related to some neurodegenerative diseases. The three proteins contain a consensus sequence (GAV motif) that was proposed to be associated with the fibrillization and cytotocixity. To further understand the function of the GAV motif in fibril assembly, we chemically synthesized the GAV peptide, and investigated the fibrillization properties and filament morphologies in comparison with those of native α-Synuclein. The results show that the short peptide can self-assemble into filaments with the pH and concentration dependent processes. The filaments generated from the GAV peptide (2.2—3.3 nm in height) are thinner but longer than those from α-Synuclein. Moreover, the GAV peptide can also enable fibrillization of the charge-incorporated but not the GAV-deficient α-Synuclein mutants. A schematic model for the fibril assemblies and filament morphologies is presented.

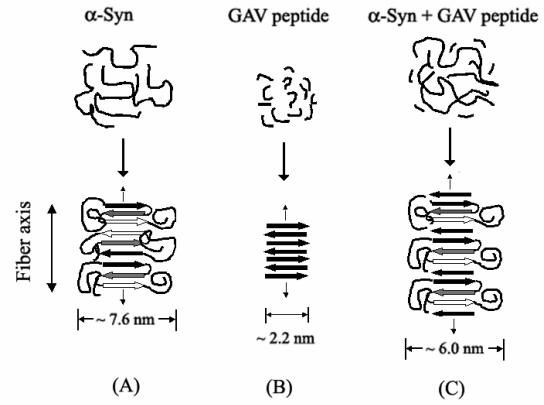

1. Shanghai Institutes for Biological Sciences.

由蛋白酶切实验推测的一个 α-synuclein 纤维模型

张 峰 吉丽娜 杜海宁 [1] 胡红雨 [1] 胡 钧 何建华

关键词 蛋白酶 K，α-Synuclein，AFM

α-Synuclein 在细胞内蛋白质的积聚 (路易小体和路易神经突) 是一些神经退行性疾病的主要症状，比如帕金森病，路易小体闹病以及老年痴呆症等。近年的免疫组化实验说明 α-Synuclein 的异常积聚可能是这些疾病的主要致病原因。然而， α-Synuclein 如何致病的分子机理至今还不太清楚。有趣的是 α-Synuclein 在生理条件下是一个天然的无规卷曲蛋白，几乎没有任何二级结构。那么这样一个没有结构的蛋白是怎么样转变成一个高度有序的纤维的呢？所以当前研究的焦

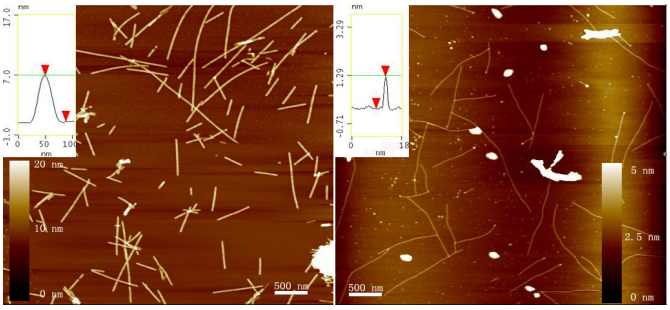

α-synuclein 纤维（没有酶切） α-synuclein 纤维（酶切后）

图 1

点就是探测 α-Synuclein 纤维的结构信息。我们利用蛋白酶 K 在 37°C 酶切培养 6 天的 α-Synuclein 纤维，结果发现 α-Synuclein 纤维没有被蛋白酶裂解成片断或寡聚体，而是变成了比没有酶切前更细的纤维，这里我们出示了 α-Synuclein 纤维在酶切前后的原子力显微镜图片（图 1），并且提出了一个蛋白酶 K 使得α-Synuclein 纤维变细的理论模型。

1 中国科学院上海生命科学研究院

A conjectural model of α-Synuclein fiber based on proteolysis experiment

ZHANG Feng JI Lina DU Haining[1] HU Hongyu[1] HU Jun HE Jianhua

Keywords α-Synuclein, Proteinase K, AFM

It was well known that intracellular proteinaceous aggregates (lewy bodies and lewy neurites) of α-Synuclein are hallmarks of neurodegenerative diseases such as Parkinson's disease, dementia with lewy body and Alzhiemer's disease etc. Recent immunohistochemical experiments indicated α-syncline's abnormal aggregation may be the main reason for these diseases. However, the molecular mechanisms underlying α-Synuclein remain unknown. An intriguing aspect of this problem is that α-Synuclein is a natively unfolded protein, with little or no ordered structure under physiological conditions. This raises the question of how an essentially disordered protein is transformed into highly organized fibrils. So, the current hotspot is focused on searching the structure information of α-Syncline'S fibrils.

We had used proteinase K to digest α-Synuclein fibers incubated for 6 days at 37 centigrade degree, and found that the resulting α-Synculein fibers were not cracked down by the proteinase K, but became thinner than before digested by proteinase K. Pictures of α-Synuclein fiber of both before and after digestion of proteinase K by atomic force microscopy were obtained. A model was supposed to describe the process of digestion which proteinase K made α-Synuclein fiber became thinner.

1. Shanghai Institutes for Biological Sciences.

单个 DNA 分子的纳米定位

李 宾 张 益 李民乾 胡 钧[1]

关键词 蘸笔，纳米刻蚀技术，单个 DNA 分子，纳米定位

在单分子水平上研究生物分子的相互作用是目前生命科学研究领域的热点之一[1,2]。原子力显微镜 (AFM) 是在单分子水平上研究生物大分子功能必不可缺的工具。它不但可在近生理环境中观察单个生物大分子，而且可用于操纵生物分子。

近年来发展起来了可用于操纵生物分子的 AFM 操纵技术—“蘸笔”纳米刻蚀技术 (DPN)。利用它，已经制作出了蛋白质纳米阵列和 DNA 纳米阵列。DPN 原理是基于 4 千多年前的“蘸笔”技术，只不过用纳米尺度的 AFM 针尖作为笔尖，固相衬底作为纸张，通过操纵 AFM 针尖将蘸在笔尖上的“墨水”转移到纸张上，以获得所设计的纳米级图案。

本文采用的 DPN 方法是通过直接切换 AFM 的工作模式 (接触模式和轻敲模式) 来实现纳米图形的“读”和“写”，全部过程仅使用同一个 AFM 针尖。用此方法我们将蘸在 AFM 针尖上的蛋白质溶液沉积到了单个拉直的 DNA 分子上，对单个拉直 DNA 分子进行了纳米定位。本文已可将沉积在 DNA 分子上蛋白质溶液点的大小、点与点的间距控制在 100 纳米以下。

参考文献

[1] H. Peter Lu, Luying Xun, X. Sunney Xie, Single-molecule enzymatic dynamics. Science 1998, 282, 1877-1882.

[2] F. Oesterhelt, D. Oesterhelt, M. Pfeiffer, et al, Unfolding Pathways of Individual Bacteriorhodopsins. Science 2000,288, 143.

1 上海交通大学 Bio-X 生命科学研究中心

Dip-pen nanolithography on single DNA molecules with protein “ink”

LI Bin ZHANG Yi LI Minqian HU Jun[1]

Keywords Dip-pen Nanolithography, single DNA molecules, Nanodepositing on solf materials

Investigation of interactions between biomacromolecules at the single-molecule level is one of the hotspots in the field of bioscience research. Atomic force microscopy (AFM) plays an important role in this field for it can be used not only to reveal the topographic structures of biomacromolecules but also to manipulate these molecules on surfaces.

Recently, an AFM-based Dip-pen Nanolithogrphy (DPN) has been developed to fabricate nanopatterns of biological and chemical “inks” on various surfaces. The DPN technique uses an AFM tip as a pen and a solid substrate as a piece of paper. It is believed that the ink molecules adsorbed on the pen are transferred to the paper through a water meniscus between the pen and the paper. Protein and DNA nanoarrays have been created by using the DPN technique.

Herein we present a novel DPN procedure for fabricating nanopatterns on soft surfaces. This method enables us to make nanopatterns even on single biomacromolecues. This ability was

demonstrated by depositing protein “ink” onto a stretched DNA molecule on mica substrate. This DPN procedure was achieved by directly switching the AFM operation mode between contact mode (which is good to deposit materials) and tapping mode (which is good to image soft materials) to write and read patterns in real time and in situ without change of AFM tips. The tapping mode AFM was used to locate and “read” the protein nanospots on the single DNA molecule, while the contact mode AFM was used to deposit protein molecules onto the DNA molecule. The size and the space of protein spots could be controlled at sub-100 nm level.

In addition to the ability of nanopatterning on soft materials, our method creates opportunities for studying AFM-directed site-specific interactions between DNA molecules and some reagents.

1. Bio-X Life Science Research Center, Shanghai Jiao-Tong University

Ar 离子束作用下 C_{60} 修饰单壁碳纳米管研究

岳 涛 黄建鸣 朱德彰

关键词 碳纳米管，富勒烯，离子束

自从 1991 年 Iijima 发现碳纳米管以来，由于其特有的 sp^2 成键方式，使其具有独特的机械性能、电学性能和化学性能，在场发射电极、催化剂载体、储氢材料和生物医用材料中具有广阔的应用前景。富勒烯 C_{60} 分子与碳纳米管有着类似的碳碳成键方式，它已经被用在电子设备、润滑剂及超导材料中，而且具有较高的化学活性，通过反应容易形成不同的衍生物，提高它的溶解与反应性。如果将碳纳米管与富勒烯 C_{60} 进行有效地结合，可能制备出一种新的纳米碳材料。将富勒烯 C_{60} 分子通过溶解填充的方式灌入碳纳米管的管腔，形成一种排列规则的“peapod”。采用固相机械化学研磨反应，也可把富勒烯 C_{60} 分子接在碳纳米管的管壁上。

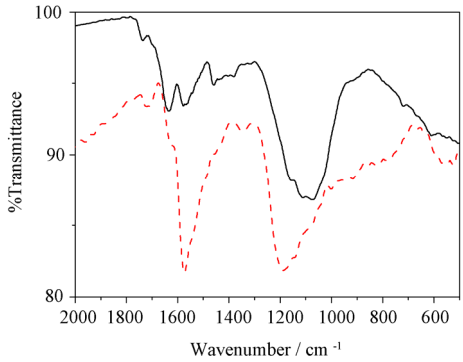

Fig.1 FT-IR spectra of pristine SWNT (dash line) and SWNT-C_{60} (solid line)

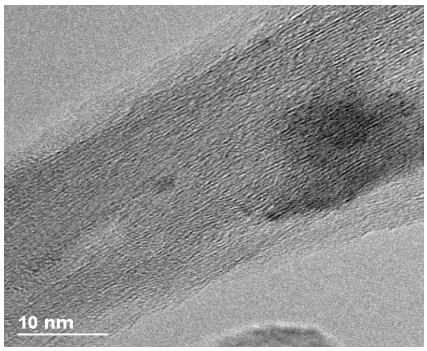

Fig.2 High-TEM image of SWNT-C_{60}

实验中我们将质量数比为 5:1 的富勒烯 C_{60} 分子与单壁碳纳米管在铜靶上制成混合物的膜，使用能量为 20keV 的 Ar 离子束进行辐照，剂量为 $10^{16}/cm^2$。反应产物用大量的甲苯、去离子水进行洗涤，除去未作用的 C_{60}。样品烘干后分别进行 FT-IR、Raman、UV-Vis 光谱和 TEM 表征。结果表明 C_{60} 与碳纳米管的混合物经过 Ar 离子束辐照后，碳原子间的共轭 π 键被打开，通过自身修复发生连接，形成 C_{60} 修饰的单壁碳纳米管。由于管壁上有 C_{60} 笼的存在，碳纳米管将具有更好的溶解与化学反应活性。

C_{60} modified single-walled carbon nanotubes with Ar ion beam

YUE Tao HUANG Jianming ZHU Dezhang

Keywords Carbon nanotube, Fullerene, Ion beam

Single-walled carbon nanotubes(SWNTs) have attracted much interest and excitement across a broad spectrum of science and technologies including engineering, biology and medicine. Meanwhile, fullerene C_{60} posses a good prospect to be applied in lubrication, non-linear optical device and electronic device. So it can be expected that modification of SWNTs using C_{60} to form a new carbon material will lead to novel electronic properties for potential application.

In this paper, we present an approach of C_{60} covalently modified SWNT via an Ar ion beam irradiation. The ion beam energy was 20keV, the ion beam current was held at 1μA and a dose was $1\times10^{16}cm^{-2}$. After irradiation, the reaction mixture was washed with a large excess of toluene followed by centrifugation until the excessive of C_{60} was removed. The irradiated samples have been characterized by FT-IR, Raman spectrum and TEM. The results indicated that the conjugated π bonds in C_{60} and SWNTs can be broken and then self-rectified the defects to form a new carbon material of C_{60} modified SWNTs.

上海市吴淞地区 $PM_{2.5}$ 的细胞毒性研究

王 伟 程 硕 谈明光 陆文忠 童永彭 张桂林 李 燕

关键词 $PM_{2.5}$，细胞毒性，大气颗粒物

颗粒物是一种重要的空气污染物，颗粒物的大小、形态和组成与健康密切相关。粒径大小不同，被吸入并沉积在呼吸系统的部位不同，对机体的危害也有差异。细颗粒物表面吸附大量的有毒有害物质，吸入后可沉积在肺泡，甚至可经过肺换气进入机体血液循环系统从而到达其他器官，最终造成呼吸系统和其他系统结构和功能的损害。国外大量流行病学研究资料提示细颗粒物浓度的上升与疾病的发病率、死亡率关系密切，尤其是呼吸系统疾病。大气颗粒物尤其是细颗粒物 $PM_{2.5}$ 的研究已受到国内外学者的普遍关注。

吴淞地区是上海市重工业区，有上钢一厂、上钢五厂、铁合金厂和宝山钢铁集团等大型工业污染源。本试验应用中流量采样器采集了上海市吴淞地区细颗粒物 $PM_{2.5}$，分别用水和二氯甲烷提取其无机和有机成分。将中国仓鼠肺成纤维细胞 (CHL) 以 5×10^4/mL 的浓度接种于 24 孔培养板，每孔 1.0 mL，37°C，5%CO_2 培养 24h，然后将提取的两种颗粒物以 10、50、100、200 μg/mL 的浓度染毒细胞 10 h，收集细胞培养液，检测细胞的代谢及氧化损伤情况。结果见下表。

结果显示随着 $PM_{2.5}$ 的两种提取成分染毒浓度 (10—200μg/mL) 的增加，细胞培养液中 MDA 水平呈上升趋势，而 SOD 呈下降趋势，由此提示细胞膜上的不饱和脂肪酸受到了的自由基的攻击，产生了脂质过氧化，进而导致 SOD 及代谢产物 MDA 含量的变化。自由基生成增多，使产生的脂质过氧化产物增多，不但引起细胞缺氧， 还可以进一步损伤组织细胞，使细胞通透性发生变化，因而引起细胞代谢指标 LD 及 LDH 水平发生相应的变化。

表 1 上海市吴淞地区 $PM_{2.5}$ 不同提取成分对细胞代谢及氧化损伤的影响

浓度 (μg/mL)	LDH(U/L)		LD(mmol/L)		MDA(nmol/mL)		SOD(U/mL)	
	H_2O	CH_2CL_2	H_2O	CH_2CL_2	H_2O	CH_2CL_2	H_2O	CH_2CL_2
0	71.30±6.21	71.30±6.21	0.27±0.07	0.27±0.07	0.22±0.06	0.22±0.06	54.82±6.88	54.82±6.88
10	86.41±8.92	75.83±5.88	0.28±0.03	0.27±0.04	0.28±0.02	0.27±0.07	52.52±2.46	52.46±4.03
50	128.32±8.92	121.01±7.22	0.31±0.04	0.32±0.03	0.39±0.07	0.41±0.08	46.78±2.58	47.30±2.78
100	222.23±9.17*	374.58±8.01*	0.34±0.04	0.35±0.03	0.67±0.10*	0.80±019*	35.91±1.72	33.90±1.20
200	152.65±10.16*	136.04±9.18*	0.41±0.06*	0.464±0.07*	0.91±0.24**	1.10±0.14**	27.03±2.37*	21.84±2.24*

注：H_2O 代表无机提取成分； CH_2CL_2 代表有机提取成分。

*与阴性对照组相比，$P<0.05$；**与阴性对照组相比，$P<0.01$。

结果表明上海市吴淞地区细颗粒物 $PM_{2.5}$ 的无机、有机提取成分对对细胞具有一定程度的氧化损伤毒性，并影响细胞的代谢活力。

Cytotoxicity of $PM_{2.5}$ in Wusong, Shanghai

WANG Wei CHENG Shuo TAN Mingguang LU Wenzhong TONG Yongpeng
ZHANG Guilin LI Yan

Keywords $PM_{2.5}$, Cytotoxicity, Ambient particulate matter

This study was undertaken to determine the cytotoxicity of various concentrations of fine particulate matter smaller than 2.5 μm in aerodynamic diameter ($PM_{2.5}$) in Wusong, Shanghai. Prior to test cellular oxidation and metabolism, both organic and non-organic fractions of $PM_{2.5,}$ varied from 10 to 200μg/ml, were incubated separately in vitro with the cell line CHL 10h. In all experiments, CHL were sensitive to both kinds of $PM_{2.5}$ exposure. Results from the laboratory test showed PM2.5 can oxidize and impire cell and cause cellular metabolic dysfunction.

DNA 单分子的纳米定位切割、分离与 PCR 扩增

吕军鸿 李海阔[1] 安红杰[1] 王国华 汪 颖 李民乾 张 益 胡 钧[1]

关键词 原子力显微镜 (AFM)，DNA 单分子，定位切割，拾取，PCR 扩增

报道了一种利用原子力显微镜 (AFM) 的定位切割和分离 DNA 单分子的技术。首先用分子梳技术将 DNA 拉直固定在经 3-氨基丙基三乙氧基硅烷修饰的云母基底上，再用 AFM 针尖从长链 DNA 分子中的特定位置切割制备 DNA 片段之后，通过精细控制原子力显微镜针尖与 DNA 样品之间的作用力，对 DNA 片段进行“推”和“折叠”，最后实现了拾取。成像、切割和分离的整个过程都是通过一个针尖完成的。所分离的 DNA 片段可以被单分子 PCR 试验成功地扩增。对其中的物理化学机制进行了讨论。

1 上海交通大学 Bio-X 生命科学研究中心

Positioning dissection, isolation, and PCR amplification of single DNA molecules with nanometer resolution

LÜ Junhong LI Haikuo [1] AN Hongjie [1] WANG Guohua WANG Ying LI Minqian ZHANG Yi HU Jun [1]

Keywords Atomic force microscopy (AFM), Single DNA molecules, Positional dissection, picking-up, PCR amplification

A technique for the positioning dissection and isolation of single DNA molecules by using the tips of atomic force microscope (AFM) has been demonstrated. DNA molecules were firstly stretched and deposited on a 3-aminopropyl triethoxysilane-coated mica substrate by Molecular Combing technique. Single fragments were dissected from a long stranded DNA molecule with the AFM tip from the desired positions, and then pushed and folded by precise control of the distance and the force between the tip and the sample, and finally picked up. All the process could be finished and repeated with a single tip. All the operations including imaging, dissection and isolation could be carried out with one AFM tip. The isolated DNA fragments could be successfully amplified by the single-molecule PCR experiments. Some of the physical and chemical origins of these observations have been discussed.

1. Bio-X Life Science Research Center, Shanghai Jiao-Tong University

树木年轮中的元素含量和铅同位素比值的分析研究

谈明光 陈建敏 李玉兰 李 燕 张桂林

关键词 树木年轮，铅同位素比，ICP-MS

树木是生态环境中的重要组成部分，它品种繁多，分布广泛， 与人类的生存环境密切相关。树木年轮具有定年准确、连续性强的特点，一般认为不同年代生成的年轮中记录着当时的大气环境的信息，测定年轮中的元素浓度和铅同位素比值的变化，可以帮助人们了解环境污染的历史和动态变化[1-2]。

本工作采集了一棵生长于上海市嘉定区的樟树的年轮样品，该树的树龄约四十年。样品在离根部 1 米处切开后，取出 2 cm 厚的年轮盘，利用目测定年法判定该树生长期为 1960－1999 年。将年轮盘沿直径轴切开后，用不锈钢刀取出逐年的样品，每年各取二份约 1 g 的平行样品。使用 $HNO_3+H_2O_2$ 微波消解法将样品处理成待测溶液后，使用 X-7 ICP－MS (Thermo Elemental) 测定了样品中的 Al、Cr、Mn、Co、Cu、Zn、As、Pb、Sr 和 Zn 等 15 种元素和 $^{206}Pb/^{207}Pb$ 的比值。在同位素比值测定时，使用了 NIST981 标准物质作质量歧视校正。分析结果表明：样品中的各元素的浓度都远低于气溶胶中相应元素的浓度， 它们虽然都呈一定波动变化，但规律性并不很强 (图 1)，$^{206}Pb/^{207}Pb$ 的比值的变化也很小，这可能与样品所跨越的年份有限有关。

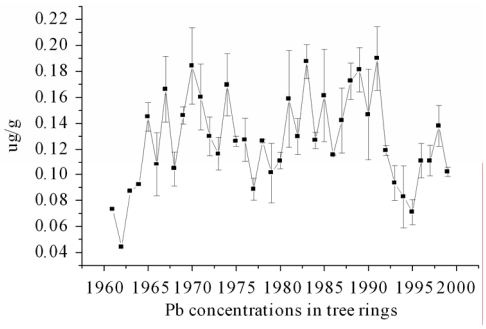

图 1

尽管人们对年轮的研究一直有很大兴趣，但对树木年轮能否有效记录环境变化历史一直存在着争论[3]。由于树木主要通过根部吸收外界物质，因此年轮中所积累的元素必然与树木生长的土壤和大气沉积都有关系，它不只单独反映大气环境的状况和变化。而且还有许多更复杂的因素影响着年轮中各元素的积累：如各种污染物的溶解度差异、不同离子从地表向根部迁移速度的不同、树木根系分别扎于土壤的不同深度并不断变化、年轮的生长速度受气候影响而变化、元素在年轮间可能的迁移等等，树木年轮能否作为大气环境的生物指示剂需要进一步探索。

参考文献

[1] K. L. Padilla, K. A. Anderson, Chemosphere, 2002, 49:575-585

[2] D. J. Bellis, K. Satake, M. Noda et al., Sci. Total Environ., 2002, 295:91-100

[3] R. Bindler, I. Renberg, J. Klaminder et al.., Sci. Total Environ., 2004, 319:173-183

Attempt of evaluating the historical pollution records in the annual growth rings

TAN Mingguang CHEN Jianmin LI Yuelan LI Yan ZHANG Guilin

Keywords Tree ring, Lead isotope ratio, ICP-MS

Trees are one of the most available specimens for historical monitoring the large scale environmental changes and anthropogenic activities. There is strong interest in dendrochemistry by analyzing trace element concentration changes in the annual growth tree rings to provide historical change in environmental pollution.

To study the utility of dendrochemistry to reserve past atmospheric pollution trends, contents of 15 heavy metals and $^{206}Pb/^{207}Pb$ in the annual growth tree rings of a 40－year-old *camphor* were analyzed by ICP mass spectrometry (X7, Thermo Elemental). The annual rings recorded concentration changes of trace elements, however, no significant changes in concentrations or lead isotope ratio with time were observed.

The use of annual rings as historical monitors has proved controversial, as it is unclear whether the relative concentration of trace elements accurately reflects relative changes in environment. Trees may

accumulate air pollutants by direct deposition on leaves and barks, or indirectly deposition on the soil and subsequent root uptake. Besides the main incorporate uptake process from the soil minerals and atmospherically deposited pollution, many other complex factors, such as solubility differences of the pollutants, migration discrepancies of heavy metals from the ground surface to the deep root layers etc., may strongly affect the reliability of dendrochemistry. Further studies are necessary to explore the reliable relation between changes of metal concentrations or lead isotope ratios caused by the atmospheric pollution with the growth of tree rings.

ACCU 采样和 PIXE 技术用于 PM_{10} 污染溯源的研究

张元勋 李德禄 李爱国 陆文忠 王荫淞 李 燕 张桂林 张元茂[1]

郑叶飞[1] 山祖慈[1] 韩 婷[2] 丁文斌[2]

关键词 PM_{10}，多通道采样仪，质子激发 X 荧光，元素浓度，源解析

为了建立一种全新的大气颗粒物污染溯源方法，使用多通道自动采样系统 (ACCU) 在上海吴淞工业区进行冬季 3 个月 8 个不同风向的 PM10 采样，同时使用质子激发 X 荧光发射方法 (PIXE) 测定颗粒物中 18 个无机元素浓度。结果发现 8 个风向的质量浓度分布取决于不同方位的大气质量状况。将大气颗粒物中的元素浓度作为环境污染指纹，8 个方位的无机元素浓度分布与采样点周围的居民住宅、道路交通和工矿企业的排放密切相关，表明该方法能准确地确定排放源的范围和污染来源。研究结果表明，ACCU 采样系统和 PIXE 分析技术的优化组合可为大气污染溯源、治理和改善环境空气质量提供一种快速和准确可靠的新方法。

1. 上海市环境监测中心

2. 上海市宝山区环境监测站

Source identification of PM_{10} aerosol samples by ACCU sampler and PIXE technique

ZHANG Yuanxun LI Delu LI Aiguo LU Wenzhong WANG Yinsong LI Yan

ZHANG Guilin ZHANG Yuanmao[1] ZHENG Yefei[1] SHAN Zuci[1] HAN Ting[2]

DING Wenbin[2]

Keywords PM_{10}, ACCU, PIXE, Elemental concentration, Source identification

The samples of PM_{10} inhalable particulate matter from eight wind directions had been collected at a representative site of Shanghai Wu Song industrial district in winter using Automated Cartridge Collection Unit (ACCU) in order to develop a new method of pollution source identification. The samples were analyzed to determine the average concentrations of up to eighteen elements by means of

the Proton Induced X-ray Emission (PIXE). The results show that the mass distribution of particulate matter from different directions depends on the air environmental quality. As the elemental fingerprint study of environmental pollution, spatial variation of elemental concentrations is closely related with the residential dense, the vehicle traffic, and the exhausts of refineries, chemicals and steel factories around the sampling site. It is demonstrated that the excellent combination of ACCU sampler and PIXE technique can provide a new and powerful means for environmental source apportionment.

1. Shanghai Environmental Monitoring Center
2. Shanghai Environmental Monitoring Station of Bao Shan District

同步辐射 X 荧光方法用于鼠脑锌元素功能的研究

张元勋　王荫淞　李德禄　李爱国　张桂林　龙建纲[1]　王福俤[1]　沈　慧[1]
黄宇营[2]　何　玮[2]

关键词　同步辐射 X 荧光，脑，锌元素，锌转运体，基因表达

为了探索 Zn 等金属元素在脑中的精细分布与 ZnT3 mRNA 表达之间的相互作用和功能，本项研究使用同步辐射 X 射线荧光技术 (SRXRF) 测定小鼠全脑和脑切片中 Zn 等金属元素分布，同时使用反转录多聚酶链式反应 (RT-PCR) 检测小鼠各组织中的 ZnT3 mRNA 的表达量。分析结果表明，脑中锌元素不是均匀分布的，主要分布在皮层、海马和齿状回部位，它们的锌浓度比最低部位高出 5~10 倍。与此结果相对应的是大脑皮层、海马和睾丸中的 ZnT3mRNA 有较高丰度，而其他组织中未检出 ZnT3mRNA。进一步的推断提示 ZnT3 能促进胞浆内的锌富集于囊泡中，通过介导胞浆锌的跨膜转运过程，从而构造囊泡的‘锌池’。

1. 第二军医大学军队卫生教研室
2. 中国科学院高能物理研究所

Study of zinc elemental function in mouse brain by SRXRF

ZHANG Yuanxun　WANG Yingsong　LI Delu　LI Aiguo　ZHANG Guilin
LONG Jiangang[1]　WANG Fudi[1]　SHEN Hui[1]　HUANG Yuying[2]　HE Wei[2]

Keywords　SRXRF, Brain, Zinc element, Zinc transporter, Gene expression

In order to explore the interaction and function between the ZnT3 mRNA expression and zinc distribution in brain slice of mouse, Zinc concentration and its distribution was determined by SRXRF and ZnT3 mRNA expression in tissue organization was examined by RT-PCR method. The analysis results show that the zinc element is not distributed evenly. The zinc content in cerebral cortex and hippocampus is nearly 5~10 times higher than that in other positions. A corresponding one is that ZnT3

mRNA in the cerebral cortex, hippocampus and testis has higher abundant degree, but have not examined out ZnT3mRNA in other tissues. Furthermore, the results promote that ZnT3 facilitates the accumulation of zinc in synaptic vesicles and may play important roles in structuring of vesicular zinc pool.

1 Department of Military Hygiene, Second Military Medical University
2 Institute of High Energy Physics, The Chinese Academy of Sciences

冬季上海吴淞地区大气颗粒物 PM_{10} 元素的主成份分析

李德禄　张元勋　李爱国　王荫淞　张桂林　李 燕

关键词　质子激发 X 射线荧光 (PIXE) 分析，PM_{10}，主成分分析；上海吴淞地区

从 2002 年 12 月到 2003 年 2 月，利用八通道采样器对上海吴淞地区进行三个月的大气气溶胶 PM10 (空气动力学直径小于 10μm 的颗粒) 的采样。使用 PIXE 分析方法进行了多元素质量浓度测定，然后对获取数据进行主成份分析，讨论了吴淞地区 8 个风向采集的 PM10 中含有的主要化学元素成分和可能的来源。结果表明，上海吴淞地区的钢铁尘污染普遍严重，尤其在南北两个方向更为突出，占总污染来源的 60%左右。

Principal component analysis of atmospheric aerosol PM_{10} in Wusong industrial district of Shanghai

LI Delu　ZHANG Yuanxun　LI Aiguo　WANG Yinsong　ZHANG Guilin　LI Yan

Keywords　PIXE analysis, PM_{10}, Principal component analysis, Wusong district of Shanghai

Atmospheric aerosol samples (PM_{10}) were collected using Automated Cartridge Collection Unit (ACCU) and TEOM1400 sampler in Wusong district of shanghai city during the period of December 2002 - February 2003. The elemental concentrations of PM10 were determined by Proton Induced X-ray Emission (PIXE) technique, and the results were analyzed by principal component analysis. The elemental component factors from eight directions and pollution sources are also presented and discussed in detail. The results show that there is heavy pollution by the steel dust in this area, especially from the southern and the northern directions, which almost occupy about 60% the particulate sources.

上海市大气气溶胶中铁的来源和化学种态研究

李爱国 张桂林 童永彭 李晓林 陆荣荣 朱节清 张元勋 李 燕

关键词 大气气溶胶，扫描质子微探针，穆斯堡尔光谱，铁元素

本文利用扫描质子微探针对上海市室内外大气气溶胶和排放源的单颗粒进行测量，用人工神经网络识别技术追踪了各种排放源对这些气溶胶中 Fe 的贡献。结果表明，对于上海的开放空间、半开放的公路隧道和室内环境，各种排放源的贡献并不相同。本文还利用穆斯堡尔光谱研究了室内外大气气溶胶中 Fe 的化学种态。实验发现，室内外气溶胶中 Fe 的种态不尽相同，在人民公园和高架桥开放空间中主要是铁的硫酸盐，在半开放的隧道中主要是 α-Fe_2O_3，在室内主要是 α-Fe_2O_3 (α-FeOOH)。Fe 种态的转变不仅和大气中 SO_2 有关，而且和空气中云雾等因素有关。

Source identification and speciation of iron in the aerosol particles of Shanghai city

LI Aiguo ZHANG Guilin TONG Yongpeng LI Xiaolin LU Rongrong ZHU Jieqing ZHANG Yuanxun LI Yan

Keywords Aerosol particles, SPM, Mössbauer spectroscopy, Iron

Individual outdoor, indoor aerosol particles and exhaust particles of different sources in Shanghai city were studied by SPM (scanning proton microprobe). The contributions of different sources to Fe in aerosol particles that collected from open space, semi-open tunnel, and indoor space, were analyzed by an artificial neural network. Also, Speciation of iron in aerosol particles was studied by Mössbauer spectroscopy. The results show that, in open space most of Fe is iron sulfate, in semi-open tunnel most is α-Fe_2O_3, and in indoor space most is α-Fe_2O_3 (α-FeOOH). The change of speciation is influenced by SO_2, clouds, fog, and so on.

电感耦合等离子体质谱法分析水泥样品中的铅同位素比值研究

陈建敏 谈明光 陆文伟[1] 李玉兰 张桂林 李 燕

关键词 铅同位素比，ICP-MS，污染源追踪

停用加铅汽油多年以来，目前上海市城市大气中仍然检测到高浓度的铅[1]。为了进一步控制和提高空气质量，准确的鉴别大气铅污染的来源是非常有意义的。王基庆[2]等人基于质子微探针研究的大气气溶胶单颗粒源解析识别了上海市大气中的含铅颗粒主要来源于水泥 (40%)、汽车尾气 (20%)、冶金尘 (16%)、燃油 (9%)、燃煤 (5%)等。考虑到水泥对上海市大气铅污染来源贡献的份额巨大，为有效控制水泥带来的铅污染水平，本研究工作利用电感耦合等离子体质谱仪 (ICP-MS) 对上海市市场上常见的 14 种不同品牌的水泥样品的铅含量和铅同位素比值特征进行

了分析， 研究和讨论了 ICP-MS 在进行铅的同位素比值测定过程中，影响测试结果的准确度和精密度的主要因素及其优化过程。在优化后的仪器分析条件下，测定了 14 个不同的水泥粉样品中的铅含量和铅同位素比值。

实验结果显示：14 种不同的水泥其 Pb 含量变化很大，Pb 的浓度范围为 20—318 μg/g，平均值为 104±72 μg/g，该值大大高于上海市的环境背景值。此外，14 种不同的水泥样品的铅同位素比值其 $^{207}Pb/^{206}Pb$ 的变化范围为 0.833～0.891，均值为 0.859±0.016，与上海市大气可吸入颗粒物的均值 0.8608±0.0018 非常接近，因此，结合大气单颗粒气溶胶研究，为了降低上海市大气气溶胶中的 Pb， 必须采取措施加强对建筑扬尘的控制。

参考文献

[1] Jian Zheng, Mingguang Tan, Yasuyuki Shibata, Atsushi Tanaka, Yan Li, Guilin Zhang, Yuanmao Zhang, Zuci Shan, Atmospheric environment, 2004, **38**:1191-1200

[2] Wang, J., Guo, P., Li, X., Zhu, J., Reinert, T., Heitmann, J., Spemann, D., Vogt, J., Flagmeyer, R.H., Butz, T Environ. Sci. Technol.2000, **34**(6): 1900-1905.

1 上海交通大学

Study on lead isotope ratio measurements of cement by inductively coupled plasma mass spectrometery

CHEN Jianmin TAN Mingguang LU Wenwei[1] LI Yulan ZHANG Guilin LI Yan

Keywords Lead isotoperatio, ICP-MS, Source appointment

It was reported that a high concentration of lead still remains in the air, despite the use of leaded-gasoline was phased out years ago in Shanghai[1]. To control and improve the atmospheric quality, the accurate identification of the possible atmospheric lead pollution sources is of great importance. Wang et al[2], using a nuclear microprobe for single aerosol analysis identified the sources of lead pollution in the atmosphere of Shanghai city were from the cement industry(40%), the automobile exhaust(20%), the metallurgic industry(16%), the oil combustion(9%), and as well as the coal combustion(5%). As far as the higher proportion of cement is concerned, efforts must be made to control this kind of lead pollution better. In this study, we applied Inductively Coupled Plasma Mass Spectrometery(ICP-MS) to the analysis of lead concentrations and isotope ratios of 14 cement samples collected in Shanghai market, and the major parameters affecting the accurate and precise measurement of lead isotope ratios by ICP-MS were also studied.

Measured with the optimized parameters, the results show that the concentration of lead in cement samples varied much, ranging from 20 to 318 μg/g, and the average value is 104±72 μg/g which is five fold higher than the environmental background. Besides, the lead isotope ratios in cement samples ranging from 0.833 to 0.891 for $^{207}Pb/^{206}Pb$, and the average value is 0.859±0.016 which is close to those obtained in PM_{10} in Shanghai(0.8608±0.0018). Therefore, in order to improve the air quality, strong measures must be made to reduce this kind of lead emission.

References

[1.] Jian Zheng, Mingguang Tan, Yasuyuki Shibata, Atsushi Tanaka, Yan Li, Guilin Zhang, Yuanmao Zhang, Zuci Shan, Atmospheric environment, 2004, 38:1191-1200

[2.] Wang, J., Guo, P., Li, X., Zhu, J., Reinert, T., Heitmann, J., Spemann, D., Vogt, J., Flagmeyer, R.H., Butz, T Environ. Sci. Technol.2000, 34(6): 1900-1905.

1 Shanghai Jiao Tong University

过渡金属化合物模拟大气颗粒物研究其对肺的毒效应

陈建敏 谈明光 童永彭 张桂林 李 燕

关键词 氧化铁颗粒，气管灌注，免疫炎症

大气颗粒物严重威胁人类健康。鉴于在上海市的大气颗粒物中过渡金属铁的含量非常丰富(铁的单元素的含量约占颗粒物总重的 1 %)，并且由于铁本身就具有氧化还原活性，能诱导催化化学反应，产生一系列的自由基，具有引起机体细胞膜脂质过氧化损伤、诱发或加重免疫及炎症反应的能力；因此，过渡金属铁在大气颗粒物的毒性中的作用正受到越来越多的关注。

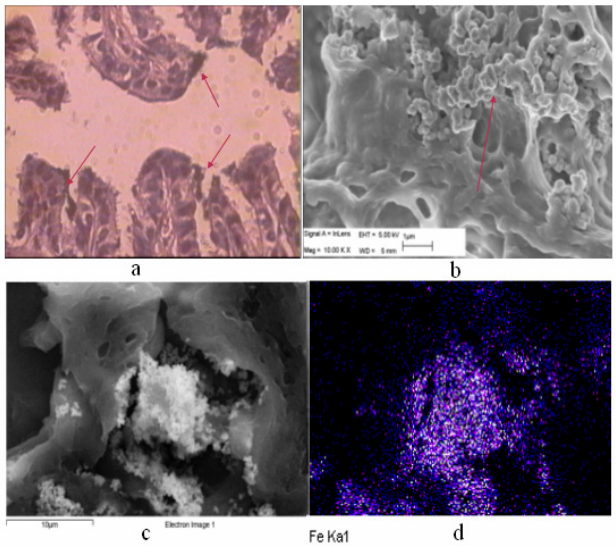

图 1. 利用不同手段观察大鼠肺组织中滞留颗粒物的形态与分布 (a.H&E 染色，光学显微镜观察，示支气管滞留的铁颗粒 b.扫描电镜观察，示滞留的颗粒物形貌 c.肺中滞留铁颗粒形貌的扫描电镜观察 d. 对应 c 图部位的 X 射线能谱分析，示元素铁分布)

Fig.1 The observation of iron particles in pulmonary tissues by different methods (a. Light micrograph (H&E stain) showing iron burden in the intratracheal, b. Scanning electron micrograph of the loaded iron particles, c. SEM image of particles loaded in the lung, d. The elemental mapping of iron)

考虑到钢铁工业尘的铁的排放主要以铁的氧化物形式存在，因此本研究工作使用粒径分别为 0.1～0.3 μm 和 0.6～0.9 μm 的简单不可溶过渡金属化合物 Fe_2O_3 模拟可吸入大气颗粒物，对成年雄性 SD 大鼠通过气管灌注染毒。动物分别于灌注后的 4 h、24 h 及 7d 处死，利用扫描电子显微镜等物理方法结合常规生化手段 (见图 1)，通过对大鼠肺的形态、功能、免疫及炎症反应等的观察比较，研究了铁颗粒物在大鼠肺内的分布与转移，探讨了不可溶颗粒物对肺的毒效应。初步的

结果表明：染毒后，显微镜下可见肺中有许多的巨噬细胞密集颗粒物质，经 SEM 形貌观察及 EDX 能谱分析显示颗粒物质为灌注入的 Fe_2O_3，并且颗粒物在肺中有明显的聚集现象。染毒后 4 h 及 24 h，氧化铁颗粒物由肺部支气管周围向整个肺组织弥漫性分布，伴随有肺组织急性炎症损伤；随着染毒时间延长，肺组织中滞留的较小的颗粒物明显减少，表明有进一步的清除发生，同时高剂量组的大鼠支气管组织周围可观察到纤维化现象。以上提示：颗粒物的毒效应可能与不可溶部分的免疫及炎症反应的刺激有关。

Study on the pulmonary toxicity induced by particulate matter using transition metal compounds as surrogate

CHEN Jianmin　TAN Mingguang　TONG Yongpeng　ZHANG Guilin　LI Yan

Keywords　Iron oxide, Intratracheal, Inflammtion

Human health is greatly affected by air pollution from particulate matter. Due to the high content of transition metals in particulate matter (for example, iron atomic weight is amount to 1 percent of total weight of the airborne particles in Shanghai), several recent animal studies have suggested that transition metals which have the ability to induce active oxygen species may be major determinants of its pulmonary toxicity.

As we know, anthropogenic iron is mainly from the metallurgic industry presented in the form of iron oxide. In the present study, we investigated the dependence of toxic effects on particulate matter by intratracheal instillation of Sprague-Dawley rats with insoluble iron oxide compounds having equivalent diameters as surrogate. Combined SEM image with commonly histopathological observation by normal microscopes (showed in Fig.1), the translocation of particulate matter in pulmonary tissues was studied, the possible role of transition metal components in the toxicity of airborne particulate matter was discussed. The result shows that the macrophage cells were loaded with many dusts after the instillation. SEM analysis identified these dusts as iron particles and found conglomeration occurred。 4 hrs and 24hrs after the treatment, the distribution of iron particles was found to translocate to lower airways in consistent with inflammation response. After 7days, the smaller particles showed the airway cleanup occurred and in high dose group some fibrosis were found. We concluded that this transition metal may involve in airway reactivity to insoluble particle challenge which could induce immune responses and inflammation reactions.

上海市大气总悬浮颗粒物中的铅污染状况研究

陈建敏　谈明光　李玉兰　张元茂[1]　张桂林　李 燕

关键词　铅污染，富集特征，ICP-MS

重金属铅对人体的神经系统和造血系统等有损伤作用，尤其儿童对铅的毒性特别敏感。因此，铅的研究一直是环境科学的研究热点之一；发达国家较早关注大气中铅污染的影响和危害。

近年来，随着经济的高速发展和产业结构的改变，上海大气污染状况正在发生变化，大气的

污染源也有明显改变，即便是大气总悬浮颗粒物 (TSP)污染在平稳下降，但是细小颗粒物污染却呈现出上升趋势。因此，为了进一步控制和提高空气质量，对上海市大气铅污染状况进行系统的研究是非常有必要的。本研究选择上海市环境监测中心的普陀区市级环境监测点为采样点，以 2002 年 1 月连续的 12 天 24 小时监测采样的大气总悬浮颗粒物 (TSP)采样滤膜为样品，使用稀硝酸超声浸取，经电感耦合等离子体质谱 (ICP-MS)进行铅含量测试。实验的测量误差小于 2%。分析结果见图 1。

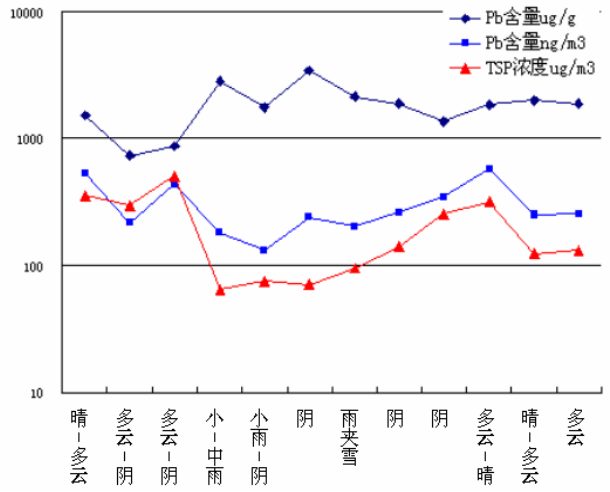

图 1. TSP 中的铅污染状况

Fig.1 The lead pollution status in TSP

从图中可以看出， TSP 中的污染状况与气象条件密切相关。TSP 浓度在有降水发生时，会明显降低；多云或阴天时 TSP 浓度相对升高，可能由于此时大气湍流活动较弱，不利污染物扩散；晴天 TSP 浓度介于两者之间。由于 TSP 浓度随气象条件的变化，因此，大气中的铅含量也受气象条件影响，以每单位体积计算时两者的变化趋势类似。但是，以每单位重量颗粒物计算时发现：铅含量的高值出现在降水发生及降水过后。考虑到降水的冲刷作用，此时较大的颗粒物较容易发生沉降，该结果与文献报道的铅主要富集在细颗粒物中的结论一致。此外，据文献数据欧美许多国家城市空气中铅含量已降至低于 100 ng/m^3 以下，而上海市 TSP 中铅含量均值为 307±114 ng/m^3，范围为 131—578 ng/m^3，表明停用加铅汽油多年以来，上海市大气中铅含量仍然处在较高的污染水平，因此，进一步开展准确鉴别大气铅污染来源的工作是非常有意义的。

1 上海市环境监测中心

Study on atmospheric lead pollution of Shanghai in total suspended particles

CHEN Jianmin TAN Mingguang LI Yulan ZHANG Yuanmao [1]

ZHANG Guilin LI Yan

Keywords Lead pollution, enrichment characteristic, ICP-MS, TSP

As lead, this heavy toxic metal trends to damage the nervous system, and particularly has a

detrimental effect on young children, atmospheric lead pollution has become a cause of major concern since as early as in 1970s in environmental research.

Due to the conversion of industrial framework and the achievement in technology, the air condition status in Shanghai has changed much in recent years. Although the average concentrations of TSP dropped down year by year, the proportion of fine particles kept uprising. To promote the sustainable development of economy, efforts must be made to better understand the pollution of airborne particles. In this study, TSP sampling site located in Putuo district was selected, and the sampling were normally carried out about 24 hours. Then continually 12 samples collected in winter in 2002 were treated with ultrasonic extraction by nitric acid, followed the analysis by ICP-MS. The result was showed in fig.1.

As was indicated in the figure, the concentration of TSP shows the feature of weather-dependent. In general, the concentrations of TSP dropped quite lower when raining occurred. In fine weather, the concentrations of TSP were moderate .The higher concentration was found in smog weather which made the diffusion of particles rather difficult. The lead content in the air was also affected by the weather, and the distribution pattern was similar with TSP when calculated by per cubic meter. The concentrations of lead content in TSP calculated by per gram were extremely high in rainy days. As coarse particles trend more easily to subside, our result show good consistent to document files which reported that lead was highly enriched in fine particles. Nowadays, in many western countries the lead concentrations in the air have dropped lower than 100 ng/m^3, but our study shows that the average lead concentrations of TSP in Shanghai was 307±114 ng/m^3,ranging from131 ng/$m^3$to 578 ng/m^3. To control and improve the air quality, the accurate identification of the possible atmospheric lead pollution sources is indispensable.

1 Shanghai Environment Monitoring Center

结构高度统一的多壁碳纳米管制备及其结构研究

王 森 俞国军 巩金龙 朱德彰 徐洪杰 陆荣荣 何绥霞 朱志远

关键词 碳纳米管，高温退火

碳纳米管是继石墨、金刚石、巴基球之后的又一种碳同素异形体。作为一种典型的一维纳米材料，碳纳米管表现出各种奇特的物理、化学性质，具有广阔的应用前景。但多数情况下得到的碳纳米管的形态各异、取向杂乱且互相缠绕难以分散。制约了人们对碳纳米管的物理、化学性质的认识及其应用研究。一种简单的制备结构高度统一的碳纳米管方法是模板法，用化学汽相沉积的方法可直接在氧化铝模板的孔内制备均匀的碳纳米管阵列，且这种碳纳米管具有均匀的管径和长度，但经研究表明其管壁微观结构是无定形碳和石墨纳米晶结构，因而它不具有理想多壁碳纳米管所具有的许多性质，严重限制了它的基础和应用研究。

本文用热化学汽相沉积 (CVD) 方法在多孔阳极氧化铝模板中合成了有序的碳纳米管阵列，后续高温退火处理提高了碳纳米管的晶化程度，得到了管径、长度高度统一的多壁碳纳米管。通过扫描电子显微镜 (SEM) 观察表明所得的碳纳米管的形貌和尺寸均受控于模板的结构。高分辨透射电子显微镜 (HRTEM) 和 X 射线粉末衍射 (XRD) 结果显示退火前碳纳米管管壁由无定型碳和石墨纳米晶组成，经 2000℃高温退火处理后管壁的晶化程度得到了明显改善。实验结果表明高温退火是得到高质量多壁碳纳米管的重要途径之一。

Synthesis and structural study of highly uniform multi-walled carbon nanotube

WANG Sen YU Guojun GONG Jinlong ZHU Dezhang XU Hongjie LU Rongrong
HE Suixia ZHU Zhiyuan

Keywords Carbon nanotube, High temperature annealing

Carbon nanotubes (CNTs) have attracted many scientists' interest because of their extraordinary mechanical and electronic properties. But in most cases, the CNTs produced are disordered in various shapes, they twist together and are difficult to disperse. This heavily restricts the research of their physical and chemical characteristics as well as their application. A simple route to uniform carbon nanotubes is using template with nanopores, such as porous anodic alumina membrane (PAAM). Carbon nanotube can be prepared by pyrolysis of carbonaceous gas in a thermal chemical vapor deposition (CVD) system, but it has been proved that the tube wall were made up of graphite nanocrystallite and amorphous carbon. The poor graphitization of the production is the deadly obstacle in their application.

In this work, uniform carbon nanotubes were synthesized by thermal CVD using PAAM as template, well graphitized multi-walled carbon nanotubes with uniform diameter and length were obtained by a following thermal annealing process. Scanning electron microscopy (SEM) images show the dimension and morphology of carbon nanotubes were completely controlled by the pore structure of template. The tube wall were made up of disorder graphite nanocrystallite and amorphous carbon as revealed by X-Ray diffraction (XRD) and high resolution transmission electron microscopy (HRTEM). The crystallization degree of tube wall has been improved after thermal annealing at 2000℃. It has been confirmed that thermal annealing is an effective way method to obtain high quality multi-wall carbon nanotubes.

扫描质子微探针装置性能研究

刘江峰 贾文红 岳伟生 万天敏 李晓林 王永其 裘惠源 张桂林 李 燕

关键词 SPM，扫描线圈，分辨率

上海应用物理所扫描质子微探针(SPM)系统建成于 1990 年，该系统聚焦透镜的光学平面距物孔约 8 m，距试样表面约 400 mm，物孔在 5—200 μm 范围内可调；靶室装有一 Au(Si)面垒探测器可用于 RBS 和 STIM 分析，另有一 Si(Li)探测器用于 X 射线荧光探测。10 多年来该 SPM 系统一直运行良好，科研人员在此线站上做了大量有意义的工作。但近来因设备老化等原因，出现了工作性能不稳定，影响实验正常进行的现象。为满足应用的需要对其进行了维护和性能测试。

针对该设备部分元器件老化损坏的情况我们更换了已经损坏的输出衰减芯片(x9c103p)；为扩大扫描范围，重新绕制了扫描线圈；更换了聚焦磁铁电源的输出电流调节电位器；对功放的部分元件进行替换；对真空系统进行了维护。

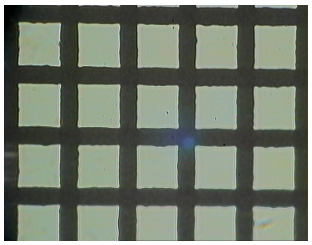

图 1. 1000 目 Ni 网的显微照片

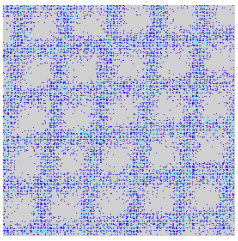

图 2. SPM 扫描所得的 1000 目 Ni 网图像

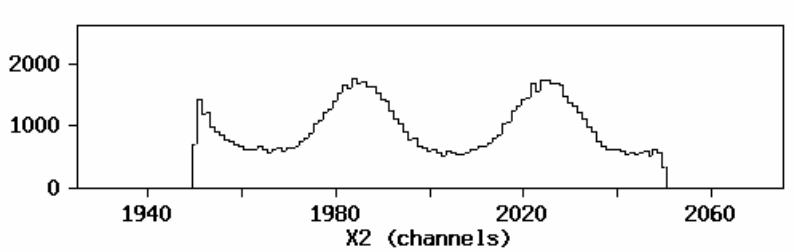

图 3. 1000 目 Ni 网网格线 x 方向线扫描荧光图谱

$f_R=\frac{2048}{A_s}\times f_s$（$f_R$ 为送到扫描线圈的实际扫描频率；f_s 为扫描控制计算机上设定的扫描频率；A_s 为扫描控制计算机上设定的扫描范围值）。

结论：测试结果表明上海应用物理研究所的 SPM 系统性能良好，扫描系统工作正常，完全可以满足对生物样品、大气颗粒物的元素分布分析，以及地矿和考古等方面的应用研究。

Scanning proton microprobe performance test

LIU Jiangfeng JIA Wenhong YUE Weisheng WAN Tianmin LI Xiaolin
WANG Yongqi QIU Huiyuan ZHANG Guilin LI Yan

Keywords SPM, Scan coil, Density distribution

The SPM system in Shanghai Institute of Applied Physics was built in 1990,the distance between the optical plane of the focusing lens in this system and the object slit is about 8m, the distance between the surface of samples and the optical plane is about 400mm. And the diameter of the object slit is adjustable in the range of 5μm —200μm. In the target room, there is an Au(si) detector which is for the use of RBS and STIM analysis and a Si(Li) detector for detecting X-ray fluorescence. The SPM system has run well for 13 years since its establishment and given great contribution to our research. However, for the reason of aging, it worked unstably sometimes. To satisfy the demand of application, we did

some work of examination and maintenance.

The work of maintenance included: replacing the spoiled output regulator chip(x9c103p) , rewinding the scanning winding, replacing the current output regulator of focused magnetic power supply, repairing the power magnifier and the vacuum system .

After maintenance we examined the system by scanning a Ni sample of 1000 mesh grid one inch. the micrograph of which is shown in Fig. 1. The X-ray fluorescence image is in Fig.2 and the energy spectrum of X direction of the meshwork is shown in Fig.3. With the analysis of the results, we could draw the following conclusions:

1) The space scanning resolution : $<2.5\mu m$
2) The scanning area : $800\mu m \times 800\mu m$
3) The scanning frequency :10Hz~1000Hz
4) The existence of the equation: $f_R = \frac{2048}{A_s} \times f_s$

f_R: the actual frequency of the scanning winding, f_s: the setting frequency in the controlling computer, A_s: the setting scan range in the controlling computer

Conclusion: the result shows that after the maintenance the SPM system run well and the scanning system is stable enough to obtain the element distributing of the biological samples and atmospheric particle. Also it can be applied in the area of geology and archeology.

超灵敏小型回旋加速器质谱计升级改造

刘永好 李德明 王胜利 陈国生 贾文红 徐建中 陈茂柏

关键词 小型回旋加速器，AMS，升级改造

超灵敏小型回旋加速器质谱计(SMCAMS)实验室经过几年坚持不懈的努力，于2005年胜利完成了中科院支持的升级改造项目。包括：成功地研制了一台24靶位气动垂直旋转型离子源多样品装置，实现连续、自动和快速的更换样品，具有0.02 mm的样品定位精度；建立了一套基于多点 RS-485 通信网络的分布式控制系统，实现了秒级的自动交替加速测量，更新了若干关键性电源和设备；并通过积极的实验探索，解决了长期困扰SMCAMS分析实际样品的X射线本底问题，使得 SMCAMS 在不需要磁铁预分析系统的情况下也可以正常开展实际样品的分析。经过升级改造的SMCAMS对来自国内4家AMS应用单位的包括考古、地质以及生物医学类的40多个 ^{14}C AMS样品进行了分析，结果达到国际同类水平,使得SMCAMS在生命科学、考古学、环境科学和地球科学等领域具有实际应用价值，可以为国内AMS应用单位提供更好的样品分析服务。目前，该装置运行良好，能正常开展无人参与的自动 ^{14}C AMS样品分析工作，并在2005年内升级改造完成前后，已经为国内几家AMS用户单位分析了多大近200只 ^{14}C AMS实际样品。

附：参加了2004年3月在韩国庆州举行的第三届亚洲粒子加速器会议，提交会议论文一篇，

“The Status of SMCAMS after Upgradings”，Liu Yonghao, Chen Maobai, Li Deming et al., the 3rd Asian Particle Accelerator Conference, Gyeongju, Korea, March 22~26, 2004.

Upgrades to Shanghai Mini Cyclotron Accelerator Mass Spectrometer (SMCAMS)

LIU Yonghao LI Deming WANG Shengli CHEN Guoshen JIA Wenhong
XU Jianzhong CHEN Maobai

Keywords Mini cyclotron, SMCAMS, Upgrades

After a few years of efforts, several upgrades to SMCAMS(Shanghai Mini Cyclotron Accelerator Mass Spectrometer) supported by CAS have been accomplished in 2004. A new pneumatic multi-cathode Cs sputter negative ion source with 24 sample positions was developed and has been employed in the routine measurements. This new device not only enables us to change samples continuously, automatically and faster than before, but also brings a 0.02 mm sample positioning precision. A new control system based on RS-485 multi-drop network was established to automatically control the sequential accelerations and measurements of different C isotopic ions and routine operations. Several critical power supplies have also been updated. X ray background problem has been eliminated by a totally novel way, which allows us to carry out routine sample measurements with no need to pre-analyze C^- beam with an extra magnet before beam injecting. The results from the measurements for more than 40 unknown ^{14}C AMS samples (attributes respectively to geology, archaeology and biomedicine et al) has demonstrated its competing performance with common tandem AMS widely used by the international AMS filed. The upgraded SMCAMS will play an active role in the AMS applications in biomedicine, archaeology, environment and geoscience et al. At present, the machine operates very well and routine measurement process could be carried out without intervention. Within a few months of operation after upgrading, as much as 200 ^{14}C AMS samples have been analyzed on SMCAMS.

附：参加了 2004 年 3 月在韩国庆州举行的第三届亚洲粒子加速器会议，提交会议论文一篇，

“The Status of SMCAMS after Upgradings”，Liu Yonghao, Chen Maobai, Li Deming et al., the 3rd Asian Particle Accelerator Conference, Gyeongju, Korea, March 22~26, 2004.

推行车用汽油无铅化过程后上海市大气总悬浮颗粒物中的铅污染来源变化

陈建敏 谈明光 李玉兰 张元茂[1] 陆文伟[2] 童永彭 张桂林 李 燕

关键词 铅同位素，ICP-MS，汽油，燃煤尘，冶金尘，TSP

为了研究在推行车用汽油无铅化过程中上海市大气中的铅污染来源变化，测量了中国上海 3 个市区国控环境监测点从 1995 年以来至 2003 年近 10 年来采集的大气总悬浮颗粒物样品中的稳定铅同位素比的组成和铅元素的浓度。实验发现：大气中的铅含量变化与采样点所处位置的功能分区有直接关系，最高的铅含量出现在传统的工业区杨浦；推行加铅汽油后，生活区黄浦和普陀的

大气铅含量有了一定的降低，但仍然大大高于国外同类城市水平。此外，铅同位素比数据进一步显示，生活区大气的 Pb 同位素比的组成也有了明显的改变，如：$^{207}Pb/^{206}Pb$ 的比值从 0.872±0.002 降至 0.861±0.002。通过使用二元混合方程，基于 $^{207}Pb/^{206}Pb$ 的比值进行源解析，结果表明：停用加铅汽油以前，加铅汽油对上海市大气中铅含量的贡献范围仍小于 30%。近 10 年来，上海市大气铅污染的主要来源都是由于能源结构上的煤炭的大量燃烧使用。

1. 上海市环境监测中心

2. 上海交通大学

A lead isotope record of Shanghai atmospheric lead emissions in total suspended particles during the period of phasing out of leaded gasoline

Chen Jianmin Tan Mingguang Li Yulan Zhang Yuanmao [1] Lu Wenwei [2]

Tong Yongpeng Zhang Guilin Li Yan

Keywords Lead isotope ratio, ICP-MS; gasoline, Coal combustion, metallurgic dust

The concentrations of lead as well as the stable lead isotope ratios were measured in the total suspended particles (TSP), collected at three monitoring sites in Shanghai, China, since 1995 ranging the period of phasing out of leaded gasoline. During all these years, the variation of lead concentrations in TSP showed the feature of site-dependent. In the traditionally industrial area of YangPu district, the concentrations were sometime extremely high and did not have temporal correlation. In the other residential areas, the concentrations dropped quite a lot, but were still highly above the average contents of other counterpart cities in the world. The analysis of stable lead isotope ratios showed that lead isotopic composition in YangPu district varied much and changed randomly with time, while in Huangpu and PuTuo districts, the value of $^{207}Pb/^{206}Pb$ dropped significantly from 0.872±0.002 to 0.861±0.002. Combined with the data of lead contents and isotopic compositions of source related samples, such as cements, coals, coal fly ashes, metallurgic dusts, oil combustion dusts, gasoline samples and soils, it was indicated that contribution from lead additives to airborne lead pollution in Shanghai was less than 30% in the time when leaded gasoline was used. However, stationary emission was always dominant source in Shanghai, and the primary component of lead was believed to contribute by the vast combustion of lead-containing coal emitted mainly as industrial activities through all these years.

1 Shanghai Environment Monitoring Center

2 Shanghai Jiao Tong University

放射性碘标记物气管灌注大鼠研究超细颗粒物在呼吸道内的转移与清除

陈建敏 谈明光 童永彭 吴元芳 李惠源 宋伟民[1]
张元茂[2] 张桂林 李 燕

关键词 空气污染，吸入，血液，转移，超细，放射性碘标记，聚苯乙烯，灌注

大气颗粒物严重威胁人类健康，流行病学结果显示：颗粒物浓度上升与心血管疾病的发病率、死亡率的关系更为密切。目前，大气颗粒物的毒理学机制研究正越来越细致和深入，但关于超细颗粒物是否能直接进入血液循环尚无定论。因此，本研究工作应用放射性碘标记手段利用 ^{125}I 标记的大气可吸入颗粒物 (PM_{10}) 和已知粒径及成分简单的聚苯乙烯微球对大鼠进行气管注入染毒，并作生理盐水的气管注入对照。分析检测了气管注入后不同时间间隔下 (0.5h、2 h、24 h 及 5 d) 大鼠的各主要脏器 (脑、血、肝、肾、脾、胃、肌肉、肠、睾丸及附睾和甲状腺) 的放射性剂量，实验结果表明：灌注入的聚苯乙烯微球主要沉积在肺中，清除的比例小。虽然极快就可检测到血液中的放射性，但剂量较低且清除的速度很快。其余脏器的情况类似于血液。此外，灌注初期不可溶颗粒物组数据与聚苯乙烯微球组类似，但随后其在肺中与血液及其其他脏器中的代谢都很快。以上结果中我们总结超细颗粒物在肺中的转移与清除需要考虑与其特定的物理化学性质，放射性碘标记模拟的超细颗粒物气管灌注实验动物是研究极小量的超细颗粒物肺外转移进入血液循环系统的有效研究手段。

1. 复旦大学公共卫生学院
2. 上海市环境监测中心

Translocation in small amounts of radioiodinated ultrafine particles to extrapulmonary tissues following the intratracheal instillation in rats

CHEN Jianmin TAN Mingguang TONG Yongpeng WU Yuanfang
LI Huiyuan SONG Weimin[1] ZHANG Yuanmao[2] ZHANG Guilin LI Yan

Keywords Air pollution, Inhalation, Blood, Translocation, Ultrafine, Radioiodinated, Polystyrene, Instillation.

Risk of death from cardiovascular disease in response to air pollution was much greater than that from lung disease. However, the current knowledge about the extrapulmonary translocation of ultrafine particles into blood circulation required more prudential thought. Therefore, the widely used radioiodinated technique was applied to radiolabel polystyrene particles with an average diameter of 58.8nm and the quantification of passage of these particles after intratracheal instillation was studied. Rats received a single instillation of 1.2 mg polystyrene particles labeled with 2.2×10^5Bq ^{125}I, and were

dissected after 0.5hr, 2hr, 24hr and 5d, respectively. The radioactivity was detected by a well type gamma counter. We found that most of the radioactivity was deposited in the lung and cleared slowly at this location. Although little amount of radioactivity was rapidly detected in blood, it decreased with time very quickly. Only low values of radioactivity were observed in secondary organs such as heart, liver, kidneys, spleen, stomach, muscle and testicles. In addition, the insoluble component of real-world particles with a diameter below 10μm was also studied in this way. The data confirmed the low content of the deposited particles into secondary organs. These findings showed that only a rather small fraction of intratracheal instilled ultrafine particles can passed rapidly into systemic circulation and the observed in vivo clearance of deposited particles needed carefully speculation of the specific physicochemical characteristics. We concluded that the application of radioiodinated technique to prove extrapulmonary translocation of small amounts of uftrafine particles is probably the ideal way.

1 School of Public health, Fudan University

2 Shanghai Environment Monitoring Center

上海市大气细颗粒物污染现状及其金属元素特征研究

陈建敏 谈明光 彭 岚 陆文忠 李玉兰 张元茂[1] 张桂林 李 燕

关键词 $PM_{2.5}$，铅同位素，ICP-MS，燃煤尘，冶金尘

鉴于颗粒物粒径越小对人体健康的危害就越大，大气细颗粒物 ($PM_{2.5}$) 污染正越来越受到人们的关注。我国目前对 $PM_{2.5}$ 的研究刚刚起步，上海市只有少数环境监测点有监测，尚不能对 $PM_{2.5}$ 的污染特征进行全面分析。本研究于 2004 年 1 月起在上海市的 4 个典型城市功能区内 (吴淞钢研所、人民广场、普陀环保局、应用物理所)，利用 4 台中流量采样仪就一年 12 个月每月同时采样，4 个采样点同步收集大气 $PM_{2.5}$ 样品，旨在对细颗粒物污染的研究及防治措施提供借鉴。

为期一年对上海市大气 4 个采样点大气中 $PM_{2.5}$ 的质量浓度和金属元素含量进行了分析。初步实验结果显示：上海市细颗粒物的污染比较严重，所选的 4 个采样点的大气细颗粒物质量浓度都大大高于国外同类城市水平。随着城市的发展，原来设置的对照区已有被污染的趋势。大气中的金属元素含量与采样点所处位置的功能分区明显相关，表明固定源的人为排放是上海市大气细颗粒物中金属元素污染的主要来源，如地处吴淞的钢研所的 $PM_{2.5}$ 的重金属污染十分明显。其中我们注意到：上海市的大气中的铅浓度仍然较高 ($>100ng/m^3$)，明显高于其它国际城市，并且各个采样点之间含量相关性强。结合 Pb 的同位素比值分析，实验结果进一步验证了上海市的大气铅污染来源受能源结构影响较大，工业上的燃煤尘是上海市目前大气铅污染的主要来源。

1 上海市环境监测中心

Ambient concentrations of fine particulate matters and their elemental composition in Shanghai for a one-year period

CHEN Jianmin TAN Mingguang PEN Lan LU Wenzhong LI Yulan

ZHANG Yuanmao [1] ZHANG Guilin LI Yan

Keywords $PM_{2.5}$, Lead isotope ratio, ICP-MS, Coal combustion, metallurgic dust

Air quality is an important issue in China and fine particulate matters($PM_{2.5}$) is a particularly primary concern due to its possible health hazards. China has a PM_{10} standard, but does not have one for $PM_{2.5}$. There are only a few data available concerning $PM_{2.5}$ concentrations and their metallic characteristics. In 2004, we initiated a $PM_{2.5}$ monitoring program in Shanghai that included the analysis of ambient concentrations and elemental compositions. $PM_{2.5}$ was collected monthly and simultaneously at four sampling sites with different pollution characteristics in Shanghai by four mid-volume air samplers for a one-year period.

Results from this study have showed that the values of annual average $PM_{2.5}$ concentrations in Shanghai are much higher than the reported data of the counterpart cities in western countries. The variation of elemental composition of fine particulate matters showed the feature of site-dependent which suggests that anthropogenic stationary emission was the major sources of metallic components in $PM_{2.5}$ in Shanghai. However, the concentration of lead which has generally good agreement between the four sites attracted us special attention since it is extremely higher than that of counterpart cities in other countries. By using a binary mixing equation, a source apportionment based on $^{207}Pb/^{206}Pb$ ratios, it was indicated that the continuously vast using of coal caused by the accelerating industrialization is believed to well interpret the higher lead burden in the air in Shanghai.

1 Shanghai Environment Monitoring Center, Shanghai 200030, China

Zn^{2+},Cu^{2+},Pb^{2+}对中国仓鼠肺成纤维细胞(CHL)的毒性作用研究

程 硕 王 伟 谈明光 张桂林 李 燕

关键词 大气颗粒物，$PM_{2.5}$，MTT

颗粒物 $PM_{2.5}$ 已成为国际上大气污染研究领域的热点和前沿。$PM_{2.5}$ 不是一种单一成分的空气污染物，而是由来自许多不同的人为或自然污染源的大量不同化学组分组成的一种复杂而可变的大气污染物。其中包含一些过渡金属和有毒元素，它们对细胞的毒性作用是目前颗粒物的细胞毒理研究的重点之一。

我们通过四唑盐(MTT)比色实验研究了 $PM_{2.5}$ 中含量比较高的几种金属离子 Zn^{2+},Cu^{2+},Pb^{2+} 对中国仓鼠肺成纤维细胞(CHL)的毒性。实验结果表明：在不同的浓度范围三种离子对细胞的毒

性作用不同。较低的浓度的 Zn^{2+}有利于细胞的生长，而 Zn^{2+}超过一定浓度，则对细胞的毒性成倍增强，并且 Zn^{2+}的毒性大于 Cu^{2+},Pb^{2+}其它两种离子。在一定的浓度范围内，Cu^{2+},Pb^{2+}对细胞的毒性损伤变化不大。证明 Zn^{2+}与细胞毒性之间的关系更加密切。

The study of the toxic effect of Zn^{2+},Cu^{2+},Pb^{2} on the Chinese hamster lung cell (CHL)

CHENG Shuo WANG Wei TAN Minggguang ZHANG Guilin Li Yan

Keywords aerosol, $PM_{2.5}$, MTT

Recently, environmental particulate matter $PM_{2.5}$ has arisen worldwide interest among scientists in the field of atmospheric pollution research. $PM_{2.5}$ is a complicated and changeable atmospheric pollution composed of various chemical components with their sources from anthropogenic or natural pollutants, including various transition metal ions and toxic elements.

Cytotoxities on the CHL of several metal ions of Zn^{2+}, Cu^{2+} and Pb^{2+}, which are major components of the $PM_{2.5}$,were studied by using the MTT colorimetric method. The results show that these metal ions have different cytotoxicities on CHL cells. Low level of Zn^{2+}may have a positive effect on cell growth, but have an adverse effect on the cell growth when the concentration increases. The cytotoxicity of Zn^{2+} is greater than that of Cu^{2+} and Pb^{2+}, indicating that Zn^{2+} may have an important effect on cell damages.

用扩展 X 射线吸收精细结构研究隧道颗粒物中铁和铅元素的种态变化

金 婵 陆文忠 王荫淞 张桂林 李 燕

关键词 二次效应，X 射线吸收精细结构，掠入射式的荧光探测方法

大气颗粒物中某些金属元素排放后，经过大气化学和物理作用后 (二次效应)，元素的种态也发生一系列变化，元素的可溶性、毒性也随之改变。因而研究颗粒物的变化过程具有重要意义。

对上海某隧道进行了样品采集，隧道总长度为 2720 m。设三个采样地点：第一点设在隧道中间，距离隧道口 1500 m 左右；第二点设在隧道口；第三点设在隧道外距离隧道口 600 m 处。隧道中间点是一个相对封闭的体系，直接收集排放的颗粒物，二次效应不显著；隧道外是一个开放的体系，直接暴露在自然环境下，有充分的二次效应；而隧道口是一个半封闭的体系，处于两种状态之间。

在北京同步辐射装置 (BSRF) 上的 XAFS 实验站进行实验，采用扩展 X 射线吸收精细结构 (EXAFS) 研究铁和铅的种态变化情况。由于样品中待测元素浓度较低 (ppm 量级)，实验中拟采用掠入射式的荧光探测方法来提高信噪比。此外还拟采用穆斯堡尔光谱测定样品中铁元素的种态变化，以及不同种态的百分含量变化情况。

Study on transformation of speciation on iron and lead element from tunnel by EXAFS

JIN Chan LU Wengzhong WANG Yinsong ZHANG Guilin LI Yan

Keywords EXAFS, Transformation, Tunnel

After atmospheric chemical and physic effect, the elemental speciation, the solubility and its toxicity of the element may have changed. So, study on transformation of element in the particulate is meanful.

There were three sampling sites: one was in the middle of the tunnel, about 1500m inside the entrance; the second was at the entrance of the tunnel; the third was out of the tunnel, about 600m outside the entrance.

The EXAFS spectra were collected on the XAFS station of Beijing Synchrotron Radiation Facility (BSRF). Study on transformation of iron and lead by EXAFS. Because the concentrations of elements in the samples was quite low (ppm level), a glancing incidence method in fluorescence mode was used to improve the signal-noise ratio. Besides also study on the transformation of iron speciation by Mössbauer spectroscopy, then to determine the content of different iron speciation.

吴淞地区空气中含铁悬浮颗粒物的穆斯堡尔研究

金 婵 李爱国 张桂林 李 燕

关键词 穆斯堡尔光谱，$PM_{2.5}$，大气气溶胶

大气颗粒物对环境和人体健康具有重要影响。而且对大气颗粒物中元素的种态进行研究，对大气毒性的评价，污染的形成和来源等都有重要的意义。在吴淞地区，铁是悬浮颗粒物中最主要的金属元素之一，研究表明在气相固相界面上，氧化铁化学吸附 SO_2 后，经氧化可转化为硫酸铁，从而转化为水溶性物质，而增强云雾的形成，对环境形成污染；并且在可吸入的小颗粒 PM2.5 中铁元素也是主要元素之一[1]。故而研究大气气溶胶铁的存在形式具有非常重要的意义。

采集上海市吴淞地区 PM2.5 (空气动力学粒径小于 2.5μ的颗粒物) 的样品，对该样品进行穆斯堡尔光谱测量，研究铁在含铁悬浮颗粒物中存在的种态，及各个种态的百分含量。实验分别在室温、80K 和 15K 三个温度条件下进行。结果表明：铁在吴淞地区 PM2.5 样品中,主要以 Fe_3O_4 的种态存在，占 42%左右；而 α–Fe_2O_3 在该 PM2.5 样品中含量也相对比较高，达到 20%左右；而两价铁在 PM2.5 样品中含量相对较低，仅为 2%左右。

参考文献

[1] Graedel T E , Weshler C J, Mandich M L. Influence of transition metal complexes on atmospheric droplet acidity[J]. Nature,1985.317:240-242.

Mössbauer studies on iron–containing atmospheric suspended particles of WuSong district

JIN Chan LI Aiguo ZHANG Guilin LI Yan

Keywords Mössbauer spectroscopy, Airborne particulate matter, $PM_{2.5}$

The element speciation of airborne particulate matter is important for evaluating the toxicology and the source of the pollution. In WuSong district, the iron is one of the most important elements of the airborne particulate. To study the iron-containing suspended particles is meaningful.

$PM_{2.5}$ was collected at WuSong district in Shanghai City, and measured by Mössbauer spectroscopy at room temperature, 80K, and 15K; studies on iron speciation and the content of the different species of iron was studies. The results show that the iron of the atmospheric aerosols in the WuSong district is mainly existing in the form of Fe_3O_4 with the percentage about 42%; and the α–Fe_2O_3 in this atmospheric aerosols is about 20%; and the Fe^{2+}in this atmospheric aerosols is lower compared to above two, only about 2%.

$PM_{2.5}$水溶成分的细胞毒性研究

程硕 王伟 谈明光 张桂林 李燕

关键词 $PM_{2.5}$，氧化损伤，细胞凋亡，锌

流行病学研究表明大气颗粒物 $PM_{2.5}$ 的长期暴露导致心肺疾病发病率、死亡率的增加。由于$PM_{2.5}$的长期暴露而导致健康危害的机制目前仍在积极研究，但仍然有一些不确定因素。一些研究表明，细颗粒 $PM_{2.5}$ 的长期暴露与心肺疾病发病率升高密切相关，尤其是呼吸系统疾病。$PM_{2.5}$ 中的一些过渡金属对体外培养的细胞具有很强的氧化能力，一些毒性元素对细胞有较强的毒性作用。

.本实验采集了上海吴淞地区细颗粒 $PM_{2.5}$，用水提取其可溶成分，通过 MTT、 Gimesa 染色、SOD、MDA、DNA Ladder 以及流式细胞仪等分析手段研究了 $PM_{2.5}$ 颗粒物的水溶成分对中国仓鼠肺成纤维细胞 (CHL) 的毒性作用。

结果显示：随着 $PM_{2.5}$ 的水溶成分染毒浓度 (300—1000 μg/mL) 的增加，细胞死亡率也在增加。同时 MDA 水平呈上升趋势，而 SOD 呈下降趋势，证明 $PM_{2.5}$ 的水溶成分对体外 CHL 细胞具有氧化损伤毒性。DNA Ladder 实验证明其能够导致细胞中 DNA 的断裂形成一定大小的片断，流式细胞仪实验证明其能够导致细胞凋亡。从而证明 $PM_{2.5}$ 水溶成分对肺细胞具有较强的毒性作用。

Cytotoxicity studies on the water soluble constituents of $PM_{2.5}$

CHENG Shuo WANG Wei TAN Minggguang ZHANG Guilin LI Yan

Keywords $PM_{2.5}$, Oxidative damage, Cell apoptosis, Zinc ion

Epidemiologists have linked airborne particulate matter (PM) exposure with increased

cardiopulmonary mortality and morbidity .The mechanisms by which PM exposure lead to health effects are under active investigation but still remain undefined. Recent studies show that the morbidity increase of these diseases is highly associated with long time exposure to $PM_{2.5}$, especially the respiratory system disease. Some transition metals have high oxidation ability to the cell cultured in vitro, and the toxic elements have impact cytotoxicities.

In our present studies, the cytotoxicity of $PM_{2.5}$ samples collected in Shanghai on the Chinese hamster lung cells has been studied by using MTT assay, Gimesa dyeing，SOD, MDA, DNA Ladder and Flow Cytometry techniques. The results show that the water soluble components of $PM_{2.5}$ have strong impact effects on the CHL cells.

SPM 扫描系统扫描线圈改进及分辨率测量

刘江峰 岳伟生 万天敏 李晓林 王永其 张桂林 李燕

关键词 SPM，扫描线圈，分辨率

扫描质子微探针系统可获得样品的元素微区分布图像。近年来因设备老化以及原系统固有的一些不足，上海应用物理研究所的 SPM 系统扫描分辨率一直达不到理想要求，为满足应用需求，我们对扫描线圈进行了改进，对束线相关的电源进行了检测和维护，并对扫描分辨率重新进行了测量和计算。

首先，分别对加速器聚焦四极透镜电源、加速器导向器电源、SPM 束线导向器电源以及 SPM 束线聚焦四极透镜电源进行了检测和维护。原来加速器导向器电源因内部接线原因，稳定性只有 19%，经维护后已达 0.1%；导向器电源稳定性由 0.1%提高到 0.05%；SPM 束线聚焦四极透镜电源稳定性由 0.2%提高到 0.07%。

其次，重新设计了扫描线圈，新线圈采用马鞍形，两端为半圆，中间为直线，分为水平和垂直两对。每对线圈都可有 40 匝、80 匝及 120 匝三种选用方案。线圈匝数的选择及线圈温度检测、报警、自动保护功能由我们专门设计的扫描线圈控制器来完成。操作人员通过遥控器实现对扫描线圈控制器的设定。

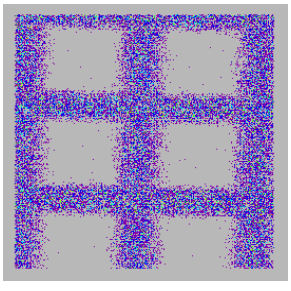

图1 1000目Ni网（物孔20μm，光阑0.5mm）

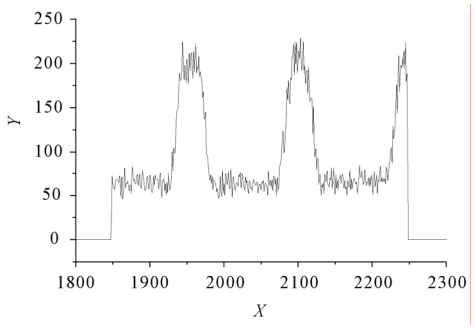

图 2 Ni 网 Y 方向线扫描数据

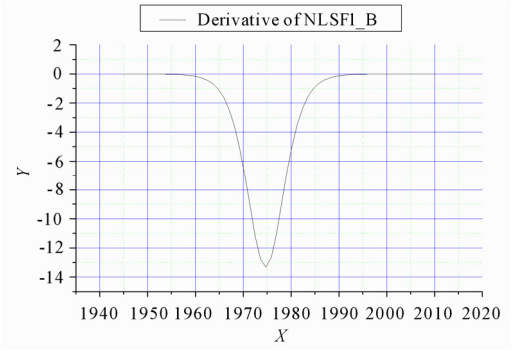

图 3 Ni 网网格线边沿计数曲线微分

最后，我们对 SPM 扫描分辨率进行了测量。测量用 1000 目 Ni 网作为标准样品，扫描得到清晰的 Ni 网图像。对 Ni 网网格边沿的扫描数据进行 S 拟合，然后对拟合所得曲线进行微分，从微分曲线的半高宽我们计算出了物孔为 20μm 时，束斑在 Y 方向的有效宽度为 1.48μm。同样的方法，计算出束斑在 X 方向的有效宽度为 1.25μm。这与 1μm 的理论值已经非常接近。考虑到 Ni 网边沿不是严格整齐，以及扫描图像的倾斜给计算带来的不利因素，实际束斑应比测量值更好。

The system maintenance and beam resolution test of the SPM

LIU Jiangfeng YUE Weisheng WAN Tianmin LI Xiaolin ZHANG Guilin LI Yan

Keywords SPM, Scan coil, Density distribution

Built In 1990, the scanning proton microprobe(SPM) in Shanghai Institute of Applied Physics provides the ability of multi-elemental mapping over the micro-area of the samples. In recent years, the spatial resolution of the SPM system could not reach the ideal level due to the inherent defects and the ageing problems. So the test and maintenance are carried out as follows:

Firstly, the power supplies in accelerator quadrupole lenses, accelerator oriented magnet, SPM quadrupole lenses and SPM oriented magnet are maintained. After the maintenance of the circuitry in this magnet power supplies, the fluctuation of the accelerator oriented magnet power supplies decreased form 19％ to 0.1%, and form 0.2% to 0.07% in SPM quadrupole lenses power supplies.

Secondly, the scanning windings are reshaped to be saddle-backed with a pair of semicircular windings at the end and a pair of linear ones in the medial vertical to each other and the number of each winding being 40,80 or 120 circles. The choice of the circles、 the measurement of winding temperature、alerting and the function of self-protect could be accomplished by the exclusive scanning winding controller designed on our own which could be set by a remote device.

Finally, the spatial resolution of the SPM system are tested. With a Ni mesh of 1000 grids one inch as the standard sample, a clear image of the Ni mesh are obtained. The results of the data processing show that when the object slits is 20μm, the estimated best spot size is 1.25—1.48 μm which has been very close to the theoretic value. The actual result could be better since the edge of mesh is not flat strictly and the obliqueness of the sample brings adverse effect to the data processing.

用同步辐射 X 荧光分析树木年轮元素含量的方法尝试

刘江峰 岳伟生 邓 彪 李晓林 谈明光 陈建敏 张元勋 张桂林 李 燕

关键词 同步辐射，年轮，ICP-MS

一般认为，树木的生长是和环境因素的影响分不开的。树木的年轮具有定年准确，连续性强的特点。有文献表明，树木的年轮记录了生长该年轮的年代的大气土壤信息，通过测定树木年轮中的元素浓度可以了解相应年代的环境污染情况。

本工作所用样品为上海嘉定的一棵约 40 年的樟树，从根部 1 米以上取横截面，然后沿断面直径方向切出约 2 cm 宽、2 cm 厚的一条，再用手术刀沿和横截面垂直方向切成约 200 微米厚的薄片。实验在北京同步辐射光源的荧光站上进行。实验条件如下：储存环电子能量为 2.2GeV，激发用 X 射线能量峰值在 10keV 左右，物孔狭逢为 100μm×100μm，加 1.07 mm 的铝吸收片，探测器距样品 6 cm。我们对数据谱用 Axil 软件进行本低扣除, 用氩峰进行归一，得到了 Ca、As、Zn 和 Fe 等元素与氩的计数比。做为一种实验方法的尝试，如下给出年轮中 Zn 元素的计数结果和 ICP-MS 所测数据的对照。由图可见，所得结果基本一致，说明该方法可行。若有合适的树木标准样品，该方法可用于定量分析。

A feasible method to measure the trace elements in the growth rings of tree by SRSRF

LIU jiangfeng YUE weisheng DENG biao LI xiaolin TAN mingguang

CHEN jianmin ZHANG yuanxun ZHANG guilin LI yan

Keywords X-ray, tree ring, ICP-MS, Synchrotron radiation

Generally, the growth of trees is inextricable with the environmental influence, therefore, the growth rings of trees (GRT) can be used for the definition of a year in an exact and successive way. And documents show that the GRT recorded the information of air and soil in the corresponding years and these information could be translated to the ambient pollution conditions through the measurement of element concentrations in the GRT.

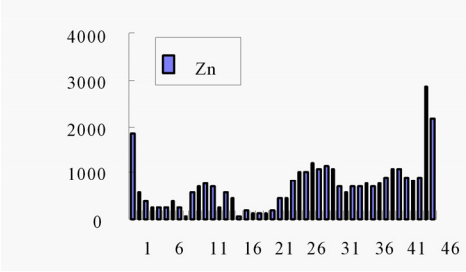

Fig 1 The count of Zn by SRXRF

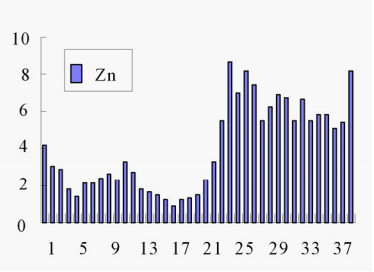

Fig 2 The Zn concentrations in rings detected by ICP-MS

In our experiment, a 40 year-old camphor was chosen for the measurement. A 2cm×2cm stick was cut from the cross section which is 1m high from the root of the tree, and 200μm thick slices were cut as the samples from the cross section vertically.

The element concentrations of Zn in the sample were measured by SRXRF in BSRF. And the feasibility of this method is shown by the consistency of its results with the data obtained by ICP-MS. This method can be improved for quantitative analysis with a standard sample of tree.

使用 HPLC-ICP-MS 联用技术研究环境样品中砷的形态

彭 岚 李玉兰 谈明光 陈建敏 张桂林 李 燕

关键词 形态分析，砷，HPLC-ICP-MS 联用

砷是在环境中可以以不同的化学形态普遍存在的有毒元素，常见的砷的化学形态有 As(III)、As(V)、MMA 和 DMA 等，而不同化学形态的砷的毒性差异很大，因此对环境样品中砷的化学形态作研究具有重要意义。

本工作采用高压液相色谱 (HPLC) 和电感耦合等离子体质谱 (ICP-MS) 联用技术进行砷的化学形态研究，该技术发挥了 HPLC 高效分离能力和 ICP-MS 高灵敏度的特点，利用新的碰撞池 (CCT) 技术较好地解决了 ArCl-离子对砷测定的干扰，保证了分析结果的准确性。本工作选用 Inertsil ODS-3 反相 C18 色谱柱对 As(III)、As(V)、MMA 和 DMA 进行了成功的分离，比较了采用水、甲醇、磷酸和磷酸二氢胺等体系对样品的萃取效果，对大气颗粒物、河流沉积物和土壤等环境样品中砷的化学形态作了研究。

Speciation of arsenic in environmental samples by using HPLC coupled to ICP-MS

PENG Lan LI Yulan TAN Mingguang CHEN Jianmin ZHANG Guilin LI Yan

Keywords Arsenic speciation, HPLC-ICP-MS

The toxicological impact of arsenic is directly related to its chemical species in environmental systems. It is essential to investigate the arsenic species in various environmental samples besides the total concentrations.

High-performance liquid chromatography (HPLC) coupled with ICP-MS has been applied to the speciation of arsenic in environmental samples. Four arsenic species, As(III)、As(V)、MMA and DMA, have been successfully separated by an Inertsil ODS-3 chromatographic column and detected by the ICP-MS. The arsenic speciation analysis of some environmental samples such as the airborne particulate matter, river sediment and soil has been carried out.

铂族元素中子活化分析的微型镍锍试金预富集方法研究

李晓林 M. Ebihara[1]

关键词 铂族元素，镍锍试金，中子活化分析

建立了适用于小样品 (≤1 克) 中铂族元素分离富集的微型镍锍试金流程。讨论了试金熔剂、捕集剂的用量和比例，以及熔炼条件。化学回收实验显示铂族元素全流程回收率 ≥ 90%，分析精度为 4.3%~7.7%。标准参考物质分析显示分析值与推荐值基本吻合，表明所建立的微型镍锍试金流程是可靠的。

1 Department of Chemistry, Graduate School of Science, Tokyo Metropolitan University, Tokyo 192-0397, Japan

Study of the microfire assay with nickel sulphide for determination of platinum-group elements by neutron activation analysis

LI Xiaolin M. Ebihara[1]

Keywords Platinum-group elements；nickel sulphide fire assay；neuron activation analysis

The procedure of microfire assay with nickel sulphide was developed for the determination of platinum-group elements (PGE) in small samples (≤ 1g). The amount and ratios of flux mixture and collector and fusion conditions were discussed. The recoveries of the PGE were measured, which shown that the recoveries were ≥ 90% and the precision was 4.3% ~ 7.7%. Analyses of standard reference materials (SRM) indicted that the results of this work well agreed with the certified values of these SRMs. This shows that the procedure of microfire assay with nickel sulphide is reliable.

基于扫描核探针技术的大气气溶胶单颗粒物源识别与解析方法研究与应用

李晓林 朱节清 郭盘林 王基庆 陆荣荣 裘惠源 李铭尧 姜 达 王永其 周 涛 李 燕 张桂林

关键词 气溶胶，大气颗粒物，扫描核探针，人工神经网络，PM_{10}

将高分辨、高灵敏的扫描核探针 (SNM) 技术与人工神经网络 (ANN) 模式识别方法相结合，以单个气溶胶颗粒物化学表征为基础，开展大气气溶胶源识别与解析的新方法研究。摸索出单颗粒气溶胶 SNM 靶样的制备方法。建立了 SNM 多站多参量分析模式的数据获取系统和分析条件。用 SNM 测定了单个大气气溶胶粒子的元素谱特征。基于标准的误差反向传输神经网络算法，建立 ANN 模式识别系统，直接对单个气溶胶粒子的 SNM 分析能谱模式进行识别，判别其来源，计

算源的贡献率。将建立的方法初步应用于上海市大气 PM_{10} 源识别与解析研究。结果表明该方法解析能力强，解析结果客观，具有查找未知污染源、解析低浓度污染源的特点。

The source identification and apportionment of aerosol particles in the atmosphere by analyzing single aerosol particles

Li Xiaolin Zhu Jieqing Guo Panlin Wang Jiqing Lu Rongrong Qiu Huiyuan
Li Minyao JIANG Da LI Yan ZHANG Guilin

Keywords Aerosol particle, Scanning nuclear microprobe, Artificial neural network, PM_{10}

A new method combining the scanning nuclear microprobe (SNM) with the pattern recognition of artificial neural network (ANN) was studied for the source identification and apportionment of aerosol particles. A method for the preparation of single aerosol particle sample was developed. A multi-station and multi-parameter data system for SNM was set up. An ANN program package was used for the source identification and apportionment of aerosol particles by the Micro-PIXE spectra. The new method was preliminarily applied for the source identification and apportionment of PM_{10} aerosol particles in the atmosphere of Shanghai City.

用扫描核探针研究上海市室内单颗粒气溶胶来源

李晓林 姜 达 仇志军 陆荣荣 李 燕 张桂林

关键词 室内空气污染，气溶胶，核探针

核探针用于上海市室内单颗粒气溶胶测定。每一个气溶胶颗粒物的 micro-PIXE 能谱可视为单颗粒物的指纹谱。模式识别技术用于单颗粒物的指纹谱识别。来自上海市 5 处有代表性的室内空气采样被分析，结果显示室内气溶胶颗粒物 22%来自土壤尘，36.9%来自水泥尘，13.6%来自机动车尾气，5.4%来自冶金工业尘，6.9%来自燃煤烟尘，4.6%来自燃油烟尘。

A study of the source of indoor aerosol particles in Shanghai by nuclear microprobe

LI Xiaolin JIANG Da QIU Zhijun LU Rongrong LI Yan ZHANG Guilin

Keyword Indoor air pollution, Aerosol, Nuclear microprobe

Nuclear microprobe was used to measure single aerosol particles (SAPs) indoors from Shanghai. Every particle is characterized with its micro-PIXE spectrum, which can be considered as the fingerprint of the SAPs. The pattern recognition technique (PR) was applied to trace the SAPs back to their source. Average results of five monitor homes at different locations in Shanghai show that the

major source contributions to the indoor air pollution are soil dusts (22.0%) and cement dusts (36.9%), and that the minor source contributions are the vehicle exhaust (13.6%), metallurgic industry (5.4%), coal combustion (6.9%) and oil combustion (4.6%).

上海市大气气溶胶中铅污染的综合研究

张桂林　谈明光　李晓林　张元勋　岳伟生　陈建敏　王荫淞　李爱国
李 燕　张元茂[1]　山祖慈[1]

关键词　大气气溶胶 PM_{10} 铅　同位素比 质子微探针 ICP-MS　EXAFS

本文介绍了用质子激发 X 荧光分析 (PIXE)、质子微探针 (SPM)、电感耦合等离子质谱 (ICP-MS) 和扩展 X-射线吸收精细结构谱 (EXAFS) 等分析手段研究上海市大气气溶胶 PM_{10} 中铅的浓度、化学种态和铅的源解析。研究发现 2002 年冬天和 2003 年上海地区大气气溶胶 PM_{10} 中铅的平均浓度分别为 369 ng/m^3 和 224 ng/m^3，铅的化学种态主要是 $PbCl_2$、$PbSO_4$ 和 PbO，燃煤烟尘、钢铁烟尘和汽车尾气是主要排放源，它们对气溶胶中铅的贡献率分别为 50%、35%和 15%。

1 上海市环境监测中心

A Comprehensive study of lead pollution in atmospheric aerosol of Shanghai

ZHANG Guilin　TAN Mingguang　LI Xiaolin　ZHANG Yuanxun　YUE　Weisheng
CHEN Jianmin　WANG Yinsong　LI Aiguo　LI yan　ZHANG Yuanmao[1]　ShanZhuci[1]

Keywords　Lead Pollution, Atmospheric Aerosol, PM_{10}, Isotope ratio, Proton microprobe, ICP-MS, EXAFS

The lead contamination, lead species and source assignment were studied by a combination of several analytical techniques such as Proton-induced X-ray emission analysis (PIXE), proton microprobe (μ-PIXE), inductively coupled plasma-mass spectrometry (ICP-MS) and Extended .X-ray absorption fine structure (EXAFS) techniques . The results indicate that the lead concentration in the air of Shanghai gradually decreased over the last years. The atmospheric lead concentration of PM_{10} in the winter of 2002 was 369 ng•m^{-3}, which had declined by 28% in 2001, and in the winter of 2003 it decreased further to 237 ng•m^{-3}. The main lead species in the samples collected in the winter of 2003 were probably $PbCl_2$, $PbSO_4$ and PbO. The source apportionment was calculated in terms of the combination of lead isotope ratios and lead mass balance method, assisted by single particle analysis with μ-PIXE and pattern recognition. The results suggested that the major contributors of atmospheric lead pollution in Shanghai were the coal combustion dust, the metallurgic dust and vehicle exhaust particles, with a contribution around 50 %, 35 % and 15 %, respectively.

1 Shanghai Environment Monitoring Center

基于 Micro-PIXE 能谱的大气单颗粒物污染源模式识别研究

万天敏 李晓林 岳伟生 李 燕 张桂林

关键词 模式识别，扫描质子探针，大气颗粒物

来自不同排放源的大气气溶胶， 其化学组成特别是微量元素组成具有各自的特征，在 Micro-PIXE 能谱上呈现不同的特征峰。因此单个气溶胶颗粒物的 Micro-PIXE 能谱特征可作为其指纹，查找污染源。本文提出了适应于 Micro-PIXE 谱的模式识别算法，并对这种以 Micro-PIXE 能谱特征溯源的方法进行了可靠性检验。结果表明以此种方法进行源解析具有较高的可信度。相应的模式识别算法具有准确，快速的特点。本文以单个大气颗粒物的 Micro-PIXE 能谱特征为基础，开展大气气溶胶源解析的模式识别方法研究，取得了以下认识：(1)单个气溶胶的 Micro-PIXE 能谱的特征峰可以作为气溶胶颗粒物的指纹，它反映了单个气溶胶的化学组成，而能谱中非特征峰部分则不具有这样的功能；(2)以 Micro-PIXE 能谱的特征峰相似程度作为识别的准则，用已知污染源 Micro-PIXE 能谱对特征峰模式识别方法进行检验，结果表明用特征峰相似程度作为识别准则是可靠的；(3)通过提取能谱特征进行模式识别，算法效率提高，可减少大量的人工劳动量。

Study of the pattern recognition method for source identification of aerosol particles by Micro-PIXE spectrum

WAN Tianmin LI Xiaolin YUE Weisheng LI Yan ZHANG Guiling

Keywords Pattern recognition, Scanning proton microprobe, Air particles

The Micro-PIXE spectra of aerosol particles from different emitter sources have different characteristic peaks, because these particles have different chemical components. Thus, the Micro-PIXE spectra are considered to be fingerprints of the aerosol particles. In order to identify the sources of aerosol particles, a pattern recognition method was developed. The method was examined. The result shows that the method is reliable and efficient.

以乙腈为碳源高效制备多壁碳纳米管

俞国军 巩金龙 朱德彰 何绥霞 曹建清 朱志远

关键词 乙腈，碳纳米管，分子筛

利用一种新型的镍/钼/分子筛催化剂，我们以乙腈为碳源非常高效的合成出了多壁碳纳米管(MWCNTs)。镍、钼以及稀土氧化物在分子筛中的协同作用被认为是催化剂之所以高度活性的原因。我们发现，当镍和钼的负载量在 0.1—4.5 %的范围时，MWCNTs 的产率随着金属负载量的提高而上升，在 2.5 h 内其不随生长时间的延长而下降。当镍和钼负载量各为 4.5%时，2 h 内就能制备出 0.9 g 的 MWCNTs，其质量大致相当于原始分子筛中镍催化剂的 60 倍。

值得一提的是，这些长出的 CNTs 都是以每一颗分子筛为中心的，其簇状形态貌似盛开的花朵。这种特殊的结构有可能作为一种新型的分子筛以作气体选择吸收和过滤之用。

Highly efficent growth of multi-walled carbon nanotubes from acetonitrile

YU Guojun GONG jinlong ZHU Dezhang HE Suixia

CAO Jianqing ZHU Zhiyuan.

Keywords Acetonitrile, Carbon nanotube, Zeolite

Here, we report a novel catalyst (Ni/Mo/zeolite), with which one can synthesize carbon nanotubes (CNT) with a very high yield using acetonitrile as a carbon source. The synergism of nickel, molybdenum and rare earth oxides (REO) in the zeolites, is considered the main reason for the high activity of the catalysts. We find that the yield ratio increases with the Ni and Mo wt% loading between 0.1-4.5 %, and does not decrease with the prolongation of CNTs growth within 2.5 h. With 4.5 % Ni and 4.5% Mo loading, 0.9 g CNT was produced in 2 h, at least 60 times the amounts of the Ni catalysts in zeolite supports.

In addition, it is very interesting that the as grown CNTs are around each zeolite in the form of clusters, and have a flower-like arrangement. This structure may be characterized as a new zeolite for gas selective absorption and filtration.

上海市吴淞地区大气 $PM_{2.5}$ 的细胞毒性研究

王 伟 程 硕 谈明光 陆文忠 童永彭 张桂林 李 燕

关键词 大气颗粒物，$PM_{2.5}$，细胞毒性

本文研究上海市吴淞地区大气细颗粒物 ($PM_{2.5}$) 的细胞毒性。采用滤膜法采集该地区大气中 $PM_{2.5}$，以中国仓鼠肺成纤维细胞 (CHL) 为靶细胞研究 $PM_{2.5}$ 有机及无机提取成分对细胞活力、代谢的影响及氧化损伤毒性，具体包括细胞形态、活力和细胞培养液中乳酸脱氢酶 (LDH)、乳酸 (LD)、丙二醛 (MDA) 及超氧化物歧化酶 (SOD) 水平的测定。大气 $PM_{2.5}$ 的两种提取成分分别以 10、50、100、200μg/mL 浓度染毒 CHL 细胞 10h，结果显示随着染毒剂量的增加细胞形态损伤加剧，细胞存活率、SOD 含量呈下降趋势，LD 和 MDA 则呈上升趋势，LDH 则呈现出先升后降趋势。在 200μg/mL 组的 LD 和 SOD 含量以及 100、200μg/mL 组的细胞存活率、LDH 和 MDA 的水平，与阴性对照组相比，均有显著性差异。有机和无机提取成分不同染毒浓度对 CHL 细胞的毒性呈现出了很好的一致性，但在某一浓度又存在一定差异，通常表现为低浓度时无机成分毒性高于有机成分毒性，而高浓度时相反的情况。上海市吴淞地区 $PM_{2.5}$ 的有机及无机提取成分可能均具有一定的细胞毒性，通常表现为低浓度 (10、50μg/mL) 无机成分毒性高于有机成分，高浓度 (100、200μg/mL) 则相反的情况。

Cytotoxicity of $PM_{2.5}$ collected at Wusong, Shanghai

WANG Wei CHENG Shuo TAN Mingguang LU Wenzhong TONG Yongpeng
ZHANG guilin LI Yan

Keywords Air particulate matter, $PM_{2.5}$, Cytotoxicity

This study was undertaken to determine the cytotoxicity of various concentrations of fine particulate matter smaller than 2.5 μm in aerodynamic diameter ($PM_{2.5}$) gathered at Wusong, Shanghai. $PM_{2.5}$ was collected onto Teflon filter by middle flux air sampler. Both organic and non-organic extracts of $PM_{2.5}$, varied from 10 to 200μg/ml, were incubated respectively in vitro with the cell line CHL 10h prior to testing their oxidation and metabolism, including cellular morphology, activity and the concentrations of LDH, LD, MDA, and SOD in cellular culture solution. In all experiments, CHL were sensitive to both parts of $PM_{2.5}$ exposure. Based on the results from the laboratory test $PM_{2.5}$ can metamorphose, oxidize and impair cell and cause cellular metabolic dysfunction. It may be concluded from our experiments that both extracts of $PM_{2.5}$ have some cytotoxicity.

碳纳米管/氧化锌纳米复合材料的生长机理及其形貌控制

吴小利 岳 涛 陆荣荣 朱德彰 朱志远

关键词 碳纳米管，氧化锌，复合材料

近年来，以碳纳米管为载体制备的纳米复合材料因其独特的应用潜力而受到广泛关注。纳米氧化锌是一种优良的半导体氧化物材料，在光电、化学方面表现出其它材料无可比拟的优越性能。

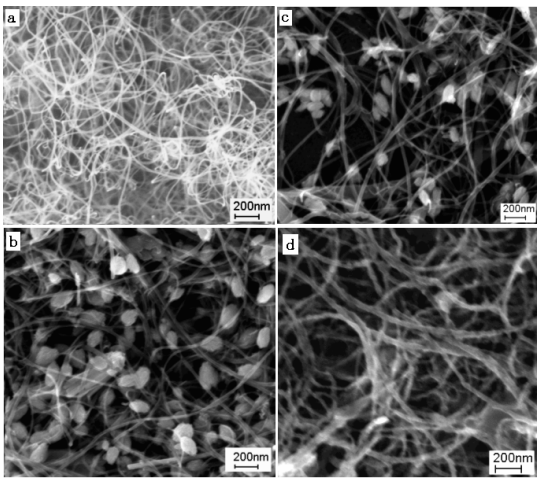

The SEM images of the CNT/ZnO nanocomposites produced under different reaction conditions:
(a) CNT, (b) pH=7, (c)pH=9, (d)pH=5

本文在水热条件下制备了碳纳米管/氧化锌纳米复合材料，纳米复合材料通过氢氧化锌在碳纳米管管壁上的沉积、溶解和结晶过程形成，氢氧化锌首先沉积在碳纳米管的管壁上，然后进一步

成核生长，最终形成具有均一形貌的碳纳米管/氧化锌纳米复合材料。

试验表明，这种纳米复合材料的形貌可以通过调节水热反应介质的 pH 值进行控制。在这种纳米复合材料中，碳纳米管作为氧化锌的载体有望降低氧化锌在光催化过程中电子空穴的复合率从而使氧化锌的光催化效率得以提高。

The study of preparation and morphology of the Carbon nanotubes/zinc oxide nanocomposite

WU Xiaoli　YUE Tao　LU Rongrong　ZHU Dezhang　ZHU Zhiyuan

Keywords　Carbon Nanotube, Zinc oxide, Composite

The potential of the ZnO powders in photocatalytic area has been studied extensively with its focus on the improvement of the photocatlytic efficiency of the ZnO powders. And the synthesis of various ZnO composites proves to be an effective way. Carbon multiwall nanotubes (MWNTs) could be considered as a good support for materials with photocatalytic properties due to their high mechanical and chemical stability and their mesoporous character. In this paper,Carbon nanotube/zinc oxide(CNT/ZnO) nanocomposites were prepared by the hydrothermal reaction in view of potential photocatalystic application for these nanocomposites. The study by SEM、TEM and XRD shows that homogeneous CNT/ZnO nanocomposites were synthesized successfully and the morphology of the composites is controllable by the adjustment of pH value during the hydrothermal reaction.

载能离子与碳纳米管相互作用的实验进展

夏汇浩

报道关于载能离子与碳纳米管相互作用的最新实验进展。研究了载能离子束在碳纳米管中的相干散射效应，并给出了载能离子在碳纳米管中沟道效应的实验结果。分别利用了直接测量方法和背散射测量方法测定了不同入射角度下载能离子传输过 AAO 和 CNTs/AAO 之后的束流强度。我们发现，在离子束入射角度大约 0.3 度的时候，能得到最强的背散射信号。本问还报道了我们得到的一些关于载能离子在碳纳米管中沟道效应的理论研究结果。

The experimental progress of channeling of charged particle along nanostructure

XIA Huihao

Recent research progress for the particle beam interaction with nanostructures in Shanghai Institute of Applied Physics (SINAP) is reported. The experimental results of channeling of charged particle along nanostructures at low energy are demonstrated. The coherent scattering effect of ion beam

transportation in carbon nanotubes (CNTs) is investigated. The direct measurement of beam intensity of angular distribution through AAO or CNTs/AAO sample, and the measurement of backscattering spectra of Au/Si pass AAO or CNTs/AAO sample are made. It is found that for incident angle in approx. 0.3° the maximum of Au/Si backscattering signal pass the sample can be detected. On the other hand, the simulation study for the channeling of charged particle along nanostructure is also investigated.

热化学气相沉积法低温大规模合成碳纳米管

俞国军 巩金龙 朱德彰 何绥霞 曹建清 朱志远

关键词 碳纳米管，热化学气相沉积，低温

自 1991 年首次被合成以来，碳纳米管 (CNTs) 以其独特的性质和广泛应用前景，已成为当前纳米科学研究的焦点之一。在众多合成 CNTs 的手段中，以催化化学气相沉积 (CCVD)，尤其是热化学气相沉积 (TCVD) 为首选。不过，尽管 CVD 法较电弧法制备 CNTs 所须温度低很多，450—1000°C 的温度范围还是必须的。因此，低温制备 CNTs 就成了人们所关心的问题。

Hofmann 等人利用等离子体化学气相沉积 (PECVD) 手段在 120°C 制备了所谓的 CNTs，但其实际结构为碳纳米锥。最近，水热法成为了低温制备 CNTs 的有效途径，但由于其反应是在反应釜内进行的，所须条件较普通的 CVD 法严格许多，并且 CNT 产量也很低。迄今为止，唯一的低温大规模制备 CNT 的报道是凭借微波辅助的 PECVD 手段，在 370°C 完成的。实际上，采用 TCVD 手段低温 (450°C 以下) 大规模制备 CNTs 还无人报道。我们发现稀土氧化物辅助的分子筛是低温分解乙炔及生长 CNTs 的理想催化剂。据此，以 TCVD 手段在低于 400°C 甚至在 280°C 条件下大规模合成了 CNT。据我们所知，这是迄今为止采用 TCVD 方法低温大规模制备 CNTs 的首次报道。

Low temperature and large scale synthesis of carbon nanotubes by thermal chemical vapour deposition

YU Guojun GONG jinlong ZHU Dezhang HE Suixia

CAO Jianqing ZHU Zhiyuan.

Keywords Carbon nanotube, thermal chemical vapour deposition, low temperature

Carbon nanotubes (CNTs) have become one of the research focuses in current nanoscience for their unique properties and wide applications, since their first synthesis in 1991. Of the variety of methods used to synthesize CNTs, the catalyzed chemical vapor deposition (CVD), particularly the thermal CVD, represents the current method of choice. However, although the previous catalyzed CVD methods offer the benefit of significantly lower deposition temperatures than arc-based techniques, the common temperature range of 450—1000°C is still necessary. Hence, there is much current interest in lowering the growth temperature of the CNTs.

In previously researches, Hofmann et al prepared so-called CNTs at 120°C by plasma enhanced chemical vapor deposition (PECVD), but the CNTs are actually carbon nanocorns. Recently, it has been reported that hydrothermal process is an alternative route for the synthesis of CNTs at very low

temperature. But the reaction conditions are much more rigorous than the common CVD methods, and the yields of the CNTs are very low due to using a supercritical reactor. Up to now, microwave assisted PECVD at 370 °C is the only accomplishment of low temperature and high yields growth of the CNTs. In fact, there is no report of large scale growth of the CNTs using thermal CVD below 450 °C. In this letter, we report a large-scale synthesis of the CNTs below 400 °C even at 330 °C by common thermal CVD. To our knowledge, it is the first report on low temperature and high yields growth of the CNTs using the common thermal CVD method. We find that rare earth oxides assisted zeolite is an ideal catalyst for acetylene decomposition and the CNTs growth at very low temperature.

碳纳米管的水热法切割和官能化

俞国军　巩金龙　朱德彰　何绥霞　曹建清　朱志远

关键词　碳纳米管，切割，官能化

碳纳米管 (CNT) 可能是现今纳米科学领域研究得最为广泛的材料。在过去十多年中，尽管研究人员在 CNT 的制备和纯化方面取得了不少进展，但一些大的挑战依然没有解决，比如对 CNT 进行化学操纵。

在以前的报道中，已有某些手段被用于对碳纳米管进行化学修饰。如利用液相或气相氧化使碳纳米管表面带上羟基、羰基或羧基。而这些表面官能团利用与某些物质如胺或乙醇等的反应又可使得 CNT 被进一步修饰。我们采用水热条件下的浓硫酸和浓硝酸的作用，使 CNT 表面化学官能化。通过控制水热反应条件，CNT 的官能化程度可很容易的被控制。

另外，我们发现这种水热法能很好的用于对 CNT 进行切割。以前也有用浓硫酸和浓硝酸的强氧化作用进行 CNT“缩短”的报道，但其过程相当耗时。而用水热法能快速的对 CNT 进行切割，同时保持对 CNT 的官能化。

Hydrothermal cutting and functionalization of carbon nanotubes

YU Guojun　GONG jinlong　ZHU Dezhang　HE Suixia　CAO Jianqing

ZHU Zhiyuan.

Keywords　Carbon nanotube, Cutting, Functionalization

Carbon nanotubes (CNTs) are probably the most popular material in current research on nanoscience. Although there have been many methods to synthesize and purify CNTs on a large scale in last decade, some big challenges are not broken through, such as chemical manipulation of the CNTs.

In previous reports, several routes to chemical modification have already been proposed. Liquid or gas phase oxidation has been employed to introduce hydroxyl, carbonyl, and carboacidic groups to the tube surface. These surface groups may be used for further modification, e.g., with amines or alcohols. We have reported on the chemical functionalization of the CNTs by hydrothermal treatment (HT) with concentrated sulfuric and nitric acids. By controlling the conditions of the HT, the degree of CNTs

functionalization can be easily controlled.

Another very interesting result is that the HT is an efficient method of cutting CNTs. Previous researches on chemically “shortening” the CNTs were also based on oxidation of the CNTs in a mixture of concentrated sulfuric and nitric acids. However, they were time-consuming processes. In our experiment, the CNTs can be rapidly cut and functionalized.

多壁碳纳米管的等离子体修饰及复合材料的合成

岳 涛 吴小利 朱德彰 何绥霞 朱志远

关键词 碳纳米管，等离子体，修饰，复合材料

近年来，随着对碳纳米管管壁表面进行修饰和功能化程度的进一步提高，碳纳米管在传感器及复合材料领域的应用领域更为广泛。等离子体技术是材料表面修饰与改性的一种手段，它可以对碳纳米管表面无定性化，改变电子传递的过程进行结构修饰，也可以在管壁表面化学功能化，增加它与聚合物的相容性，这些在文献中已有报道。

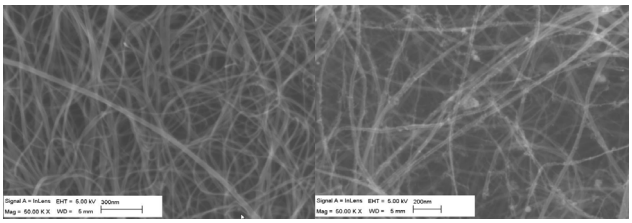

Fig.1 SEM images of (A)As-grown and (B)after plasma treatments

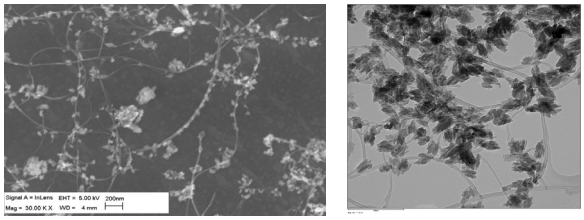

Fig.2 (A) SEM and (B) TEM image of the MWNTs/ZnO nanocomposites

我们利用氧的等离子体辐照多壁碳纳米管，在碳管表面制造微缺陷，增加化学反应的活性点，通过 SEM 和 Raman 进行了形貌和结构表征。在此基础上进行了等离子活化碳纳米管/氧化锌纳米复合材料的制备，用 TEM 和 XRD 对沉积在碳管管壁上晶体的结构和组成进行了分析。实验结果表明：经等离子体处理后的碳管管壁粗糙，缺陷增加 (如图 1)。在碳纳米管/氧化锌复合材料中，氧化锌晶种优先在碳纳米管缺陷位及曲率较大处沉积，水热条件下完成氧化锌纳米晶在管壁的生长 (图 2)。

The plasma activation and the synthesis of nanocomposite of multi-walled carbon nanotubes

YUE Tao WU Xiaoli ZHU Dezhang HE Suixia ZHU Zhiyuan

Keywords Carbon nanotube, Plasma, Modified, Composite

Recently, carbon nanotube has been proposed as promising materials for a variety of applications including in composite reinforcement, molecular electronical devices and sensors etc after it has been modified and functionalized successfully. Plasma treatment is an important role for etching the surface

of carbon nanotubes. In this paper, the oxygen (O_2) plasma irradiation of MWNTs was demonstrated as a simple modification method which increased any defects on the side-wall. The zinc oxide based plasma activation MWNTs nanocomposite was prepared by a hydrothermal treatment. The results indicated that the process yielded composite powder consisting of ZnO on the defect site of the MWNTs. Microstructural and characterizations were performed using different electron microscopy techniques.

碳纳米管/二氧化锡纳米复合材料的水热合成

岳 涛　何绥霞　朱德彰　朱志远

关键词　碳纳米管，二氧化锡，复合材料，水热合成

近年来，碳纳米管作为锂电池的负极材料引起人们的广泛注意。它不仅化学稳定性好、机械强度高、弹性模量大可吸收在充放电过程因体积变化而产生的应力，而且其特殊的微观结构使它具有优越的嵌锂性能。碳纳米管作为负极材料有利于提高锂离子电池的循环寿命，改善电池的动力学性能。金属氧化物是另一类负极材料，它具有低的嵌锂电压和高的比容量。因此，碳纳米管/金属氧化物纳米复合材料将成为一种新类型的锂离子电池负极材料。

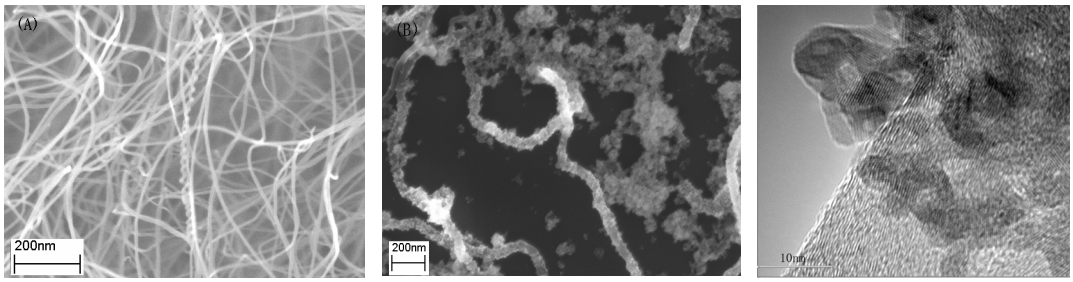

Fig.1　SEM images of (A) pristine MWNTs, (B) MWNTs /SnO_2 composite and (C) TEM of MWNTs /SnO_2 composite

我们通过溶胶凝胶和水热技术制备了碳纳米管/二氧化锡纳米复合材料: 多壁碳纳米管通过催化剂 CVD 技术在 700℃下得到。碳纳米管分散于 $SnCl_2$•H_2O 和乙醇形成的溶胶凝胶中，将此混合物置于反应釜中于 160℃条件下水热反应 6 h。产物通过 SEM，TEM 和 XRD 对其结构和形貌进行表征，如图。实验结果表明：在碳纳米管管壁上均匀地沉积了 SnO_2 的纳米晶，得到了碳纳米管/二氧化锡纳米复合材料。

The hydrothermal synthesis of multi-walled carbon nanotubes－SnO_2 nanocomposites

YUE Tao　ZHU Dezhang　ZHU Zhiyuan

Keywords　Carbon nanotube, Tin oxide, Composite, Hydrothermal synthesis

Multi-walled carbon nanotubes(MWNTs), due to their high mechanical, chemical stability, particular morphology and structure which favor the one-dimensional host for the intercalation of Li

and other alkali metals, is of great interest for many potential applications. In addition, various tin oxides (SnO and SnO_2) and composite oxides have been considered as the most promising negative-electrode materials for lithium-ion batteries for its low lithium insertion potential and their high volumetric and gravimetric capacity. So it is important to explore a feasible preparation technique of tin oxides materials deposition and growth on the MWNTs.

In this paper, we prepared a MWNTs-SnO_2 nanocomposite by coating SnO_2 on MWNTs using SOL-GEL and hydrothermal synthesis. The hydrothermal process employs high temperatures and high pressures for the crystallization of hydroxide into the oxide. The end product consisted of MWNTs coated with nano-sized SnO_2 particles. The morphology and microstructure of the nanocomposite have characterized by TEM, SEM, EDS and XRD.

用质子探针气溶胶单颗粒分析方法研究上海市工业区 PM_{10} 来源

岳伟生　李晓林　万天敏　刘江峰　张桂林　李 燕

关键词　PM_{10}，质子微探针，来源追踪

可吸入颗粒物又称为 PM_{10}(空气动力学直径≦10μm),它不仅可以造成一系列的环境问题，如城市烟雾、酸雨形成、臭氧层破坏、气候变化、空气能见度降低等，而且还是对人体产生危害的首要大气污染物。大气颗粒物的大小、形状及化学成分等与颗粒物的来源、在人体呼吸道的沉积部位及毒性等密切相关。对单个大气颗粒物的分析研究，有助于深入了解颗粒物对人体健康的影响以及更准确地研究颗粒物的来源，因此，单颗粒分析已经成为环境化学研究的一个新动向。单颗粒分析的方法在一定程度上弥补了总体分析方法的不足。某些微量元素，由于其含量可能低于总体分析的检测限，因而不能用总体分析的方法检测，而用单颗粒分析的方法就可以轻易地检测到这些元素。质子微探针有很高的空间分辨率 (μm 量级) 和 10^{-6} 水平的元素浓度检测能力，能够分析出颗粒物中 30 多种主、微量元素。另外，由于质子穿透能力强 (3 MeV 的质子在硅中的穿透深度约 60μm)，因而能探测到颗粒物的内部信息。质子微探针的这些特点使得它具有分析单颗粒中痕量元素的独特能力。

宝山是上海市的重工业区，也是我国重要的钢铁基地。宝山地区空气中颗粒物浓度远高于市中心颗粒物浓度，该地区的空气污染已经引起政府部门和环境工作者的重视。对宝山地区空大气颗粒物来源的研究，有助于更好地采取措施降低空气污染。本工作中的环境空气检测样品采集自上海市宝山地区的三个不同监测点，分别代表了工业区的中心区、工业区中心区与居民生活区的交界区以及居民生活区。单颗粒的测试工作在上海应用物理研究所扫描质子微探针装置完成。对 PM_{10} 来源追踪的基本做法是：首先，收集造成上海市大气污染的污染源，用 micro-PIXE 分析污染源样品单颗粒，获取颗粒物的 micro-PIXE 能谱，把单颗粒的 micro-PIXE 能谱作为污染源颗粒的“指纹”特征存入到计算机，建立污染源单颗粒指纹数据库；然后，用于分析污染源同样的实验条件分析环境空气监测样品，获取其单颗粒 micro-PIXE 能谱；最后，利用模式识别程序将环境空气监测样品颗粒物的能谱与数据库中污染源单颗粒指纹进行对比，从而识别出环境空气监测样品的来源。将单颗粒的 micro-PIXE 能谱与模式识别技术相结合，识别出上海市宝山工业区空气中 PM_{10} 主要来源于钢铁工业 (33%)、土壤 (14%)、无铅汽油汽车尾气 (18%)、燃煤 (14%) 和助动车尾气 (10%)。对未识别的颗粒物能谱用模糊聚类分析方法作了进一步的研究，将这些颗粒物分成了 7 类，为进一步的污染源解析提供了参考。

Origins of PM_{10} determined by the micro-PIXE spectrum of single aerosol particle

YUE Weisheng LI Xiaolin WAN Tianmin LIU Jiangfeng
ZHANG Guilin LI Yan

Keywords PM_{10}, Proton microprobe, Source identification

In urban area, PM_{10} (particulate matter with aerodynamic diameter≤10μm) is especially emphasized since it is considered to be a health hazard because it can reach the lower respiratory tract where they are phagocytized by alveolar macrophages. The advent of air quality standards for PM_{10} and for some elements created the need for identifying particle sources and their relative contribution so that effective control strategies could be planned.

Till now, by application of PIXE (proton induced X-ray emission) technique, a lot of studies about atmospheric particle analysis have been reported. Micro-beam PIXE, often called micro-PIXE, is a variation of PIXE. It is a combination of micro-beam technique and PIXE analysis, and has become a very important analytical tool in recent years. By the focused proton beam, a beam spot of μm size can be obtained. Therefore, it is possible to obtain the elemental information of single aerosol particles in several micrometers size. Micro-PIXE can analyze all the elements with atomic number $Z>11$ simultaneously. The relative detection limit of micro-PIXE is ppm (μg/g). In the atmospheric aerosol study, traditional methods of sample analysis are based on the analysis of total aerosol particles loaded on the filters (bulk analysis). These methods play an important role in the aerosol study. Single particle analysis methods have proven to be a valuable alternative for bulk analysis methods. The information concerning the origin, formation, transport, reactivity, transformation reactions and impact on the environment which can be obtained would be impossible to obtain from bulk analysis methods. In addition, some elements tend to be at relatively high concentration in a relatively small number of particles, in a bulk measurement these elements may be at concentrations below the detection limit, but these elements can be easily determined in a SAP method.

In this work, we study the sources of single aerosol particles by combining the micro-PIXE spectra of single aerosol particles with pattern recognition technique. A set of individual particles from 16 pollution sources were analyzed by proton microprobe, their micro-PIXE spectra were used to establish a fingerprint database for the pollution sources. Environment monitoring samples were collected from Baoshan district which is a heavy-industrial area of Shanghai. The single aerosol particles of Environment monitoring samples were analyzed by the same facility as that used for the analysis of pollution source particles.The results of this study show that the most of measured PM_{10} are derived from metallurgic industry (33%), vehicle exhaust (18%), coal combustion (14%), motorcycle exhaust (10%) and soil dust (14%). It should be noted that motorcycle exhaust is an important PM_{10} pollution source that should not be underestimated. The study also shows that proton microprobe is a useful tool for the analysis of SAPs.

基于 SPM 分析的大气气溶胶单颗粒源解析的取样量研究

岳伟生　李晓林　万天敏　刘江峰　张桂林　李 燕

关键词　单颗粒，取样量，源解析

用分析单颗粒的方法进行污染源解析，需要分析一定数量的颗粒物，然后用统计方法得到各个污染源对环境监测点颗粒物污染的贡献率。因此用这种方法解析污染源的一个基本的问题就是需要分析多少个颗粒物才能满足污染源解析误差要求。为了解决用 SPM 分析单颗粒解析污染来源所需要的颗粒数的问题，本工作研究不同的颗粒数与解析结果之间的关系，从而到污染源解析不同误差要求下需要的解析的颗粒数目。用 SPM 分析了采集于上海市工业区某个点的气溶胶单颗粒样品。首先从这些样品所组成的集合中随机抽取一定数目的单颗粒进行污染源解析，得到一次解析结果；然后将这一解析过程重复三次，以检验结果的可靠性。将三次的平均结果与所分析的最大颗粒数的解析结果进行比较，得到解析的误差。改变取样量，重复上述过程。通过对取样量和解析结果相对标准偏差的研究本工作初步得到了单颗粒取样量与源解析结果之间的关系，得到了针对某一污染源在一定解析偏差要求下判断最小取样量的数学模型。有以下结论：(1)单颗粒取样量越大，解析结果更为可靠；(2)源解析结果的相对标准偏差与取样量成指数衰减关系；(3)单颗粒分析的取样量大于 135 时，能满足污染源贡献率大于 10%的源解析结果要求。

How many particles should be analyzed for the source apportionment of atmospheric aerosol particles by analyzing single aerosol particles using SPM

YUE Weisheng　LI Xiaolin　WAN Tianmin　LIU Jiangfeng

ZHANG Guilin　LI Yan

Keywords　Single particle, Particle number, Source apportionment

It is important to study the relationship between the accuracy of the source apportionment result and the number of single particles analyzed for the source apportionment of airborne particles by analyzing single aerosol particles. In order to study the relationship between the result of source apportionment and the number of the particles, a total of 315 single aerosol particles were analyzed by scanning proton microprobe (SPM) for the source apportionment. The environmental monitoring sample was collected in the heavy-industrialized area of Shanghai. Single particles selected randomly by computer for the source apportionment. The results of source apportionment were analyzed by the statistical methods. The results of this study show that the relative standard deviation (RSD) of the result of source apportionment decreases exponentially with the increase of the particle number (N). The minimum number of the particles that should be analyzed under the condition of different relative standard deviation can be estimated according to the relationship between N and RSD.

RT-PCR 方法用于锌转运体基因表达模式的研究

张元勋 龙建纲[1] 王福俤[1] 王荫淞 李德禄 张桂林 沈 慧[1]

关键词 PCR，脑，锌转运体，基因表达

锌在脑组织中的转运过程是锌营养的重要研究内容，研究锌在脑组织中的转运过程对深入理解锌影响脑发育及功能机理具有重要意义。锌转运体 (Zinc Transporter, ZnT) 的发现使锌元素的研究有了突破性进展，为锌在细胞和分子水平的更深刻认识奠定了重要基础。随着研究的深入，锌元素与锌转运体之间的调节机制，锌转运体在锌内稳态中的功能作用以及锌转运体和锌的特异分布与相应细胞间相互作用的认识还有待深化。为了解 ZnT3 mRNA 在小鼠各组织中的表达状况，本项研究使用反转录聚合酶链式反应 (RT-PCR) 分子生物学新技术克隆 ZnT3 cDNA 片断，荧光标记的全自动测序法确定 ZnT3 cDNA 片断的碱基顺序，PT-PCR 法检测小鼠各组织中 ZnT3 mRNA 的表达和比较它们在组织中的表达量。RT-PCR 方法的实验结果获得单一条带的片断，其大小为 700bp，碱基顺序与文献报道的序列一致。在大脑皮层、海马和睾丸中检测到 ZnT3 mRNA 表达，其中睾丸中的表达量最高。大脑皮层和海马之间的表达量无显著性差异，心、肝、脾、肺、肾、小肠、嗅球和小脑等组织中未见 ZnT3 mRNA 表达。结果表明克隆到正确的 ZnT3 cDNA 片断，ZnT3 mRNA 主要表达于睾丸、大脑皮层和海马组织。实验结果进一步提示 ZnT3 可能在脑功能和生殖功能中具有重要作用。

1. 第二军医大学军队卫生教研室

Study of gene expression in zinc transporters using RT-PCR method

ZHANG Yuanxun LONG Jiangang[1] WANG Fudi[1] WANG Yingsong

LI Delu ZHANG Guilin SHEN Hui[1]

Keywords PCR, Brain, Zinc transporter, Gene expression

Zinc elemental transporting in the organism is an important research content of the zinc nutrition. Especially, the transporting course in the brain is a difficult topic for the zinc nutrition study. It is significant to understand thoroughly the zinc influences brain development and function mechanism. In order to determine the level of mouse zinc transporter3 (ZnT3) mRNA expression, the fragment is cloned by RT-PCR technique and is sequenced by dideoxynucleotide method. The expression of ZnT3 mRNA is also examined by RT-PCR method and is compared with β-actin that served as the control. As the result, a proper single fragment of 700bp is obtained with the sequence conformable to the corresponding fragment sequence of reported mouse ZnT3 cDNA. The ZnT3 mRNA is detected in cerebrum, hippocampus and in testis in that the highest expression is observed. However, the expression of ZnT3 mRNA is not detected in hart, liver, lung, spleen, kidney, intestine, olfactory bulb and cerebellum. The expression of ZnT3 mRNA in brain and testis suggests a physiologically functional

importance of ZnT3 in mental and reproductive activities of mouse.

1. Department of Military Hygiene, Second Military Medical University, Shanghai 200433

吴淞工业区道路扬尘的粒径分布研究

张元勋 徐明高[1] 李德禄 陆文忠 王荫淞 张桂林 李 燕 韩 婷[1] 丁文斌[1]

关键词 大气颗粒物，粒径分布，无机元素，PIXE

为了弄清道路扬尘对工业区污染的贡献量和研究采取的对策，我们使用日本 Dylec 公司的 LAN－120 型安德逊 9 级采样器对工业区内四个有代表性的采样点 (区环保局、区环境监测站、申杨家具厂和长江路)进行大气颗粒物的采集。使用称重法得到不同粒径颗粒物在四个典型监测点的质量浓度分布，同时使用 PIXE 技术获取不同粒径颗粒物样品中的 S、K、Ca、Ti、Cr、Mn、Fe、Ni、Cu、Zn、Br 和 Pb 等 12 种无机元素浓度。结果表明吴淞工业区大气可吸入颗粒物 (粒径 <10 μm) 的质量浓度分布曲线呈现为双峰型，峰值分别出现在 1.5 μm 和 5.5 μm 左右。在分析检测的无机元素中发现 S、K、Cr、Mn、Ni、Cu、Zn、Br 和 Pb 共 9 种元素的相对浓度峰值都出现在 <2.1 μm 粒径，这些元素绝大部分分布在细颗粒物中。而 Ca、Ti 和 Fe3 种元素在 4 个监测点的峰值和高浓度区域基本都在>2.1 μm 粒径，表明它们主要以粒径>2.1 μm 的粗颗粒物形态存在于大气中。吴淞工业区大气颗粒物的分布特征与这些颗粒物的污染来源特征十分相符。

1. 上海市宝山区环境监测站

Distribution of dust particulate size on the roads in Wusong industrial district

ZHANG Yuanxun XU Minggao[1] LI Delu LU Wenzhong

WANG Yinsong ZHANG Guilin LI Yan HAN Ting[1] DING Wenbin[1]

Keywords Particulate matter, Particle size distribution, Inorganic element, PIXE

In order to clarify the contribution amount of dust on the Wusong roads and study the countermeasure adopted, combined the environmental synthetic renovation of industrial district, we collected air particulate matters in four representative sampling sites of Wusong district using Anderson Model LAN-120 of nine grade's sampler imported from Dylec Company of Japan. The mass concentration distributions of the different particulate sizes in four typical sampling sites were obtained by weigh method. The inorganic elemental concentrations including S, K, Ca, Ti, Cr, Mn, Fe, Ni, Cu, Zn, Br and Pb in particulate matters were measured by PIXE technique. The results show that the mass concentration distribution of Wusong industrial district is bimodal with one peak at 1.5μm and another

peak at 5.5μm in diameter less than 10μm. We find that the relative concentration peak values of nine inorganic elements measured including S, K, Cr, Mn, Ni, Cu, Zn, Br and Pb are presented in less than 2.1μm. These elements are distributed mostly in the fine particulate matter. However, the peak values of elemental Ca, Ti and Fe are presented in large than 2.1μm. It means that these elements exist in the coarse particulate matters in the atmosphere. The distribution characteristic of the atmospheric particulate matter of Wusong industrial district conforms to the pollution source of these particulate matters.

纳米生物医药

Nano-biomedicine

可见光对 DNA 链的断裂作用

李 宾 胡 钧 汪 颖 吴世英 黄一波 李民乾

关键词 光裂解，单个 DNA 分子

人们在荧光显微镜下观察到了单个 YOYO 染色的 DNA 分子；用光镊的方法对 DNA 的弹性特征进行了研究；用改进的荧光显微镜实现了对 DNA 链的定位切割。本文报道了利用荧光显微镜研究可见光对 YOYO 染色 DNA 分子的断裂作用以及断裂过程中 DNA 分子的弹性回缩过程和水分子对断裂过程的影响。YOYO 是一种高效的 DNA 荧光染料，可引起 DNA 链断裂。人们认为是由于自由基的作用。

本文实验中结合这一特点对操纵拉直 DNA 分子在可见光作用下的断裂过程进行跟踪记录。实验中发现随着光照时间的增加所产生的断裂 DNA 分子数增加;单个 DNA 分子上的断裂点增加。同时，也观察到随着可见光亮度的增加 DNA 分子断裂的速度增加；所产生的结果也是断裂 DNA 分子数的增加和单个 DNA 分子上断裂点的增加。在拉直 DNA 分子断裂的过程中有明显的 DNA 分子弹性回缩现象。拉直的 DNA 分子可与衬底有多个黏附点，断裂点多发生在两个黏附点的中间。当 DNA 分子断裂的瞬间，断裂端迅速沿着 DNA 分子链的方向向断裂点的反方向移动，此弹性回缩过程多停止在 DNA 分子黏附在衬底上的黏附点为止。当 DNA 链的一端固定在衬底上而游离端断裂时，断裂端就会立即缩成一个小圆点随着布朗运动而运动到溶液中去。

我们发现，可见光对 YOYO 染色的 DNA 分子断裂作用与水溶液存在有关。相同实验条件下，在干燥的环境中我们没有观察到 DNA 分子的断裂；当 DNA 分子处在水环境下经 YOYO 染色的 DNA 分子发生了断裂；DNA 断裂的速度与 DNA 分子周围含水量的多少也有一定的关系，水溶液多的环境下 DNA 断裂的速度比水溶液少的环境下 DNA 断裂的速度要快。以上结果证明了可见光对 YOYO 染色 DNA 分子的断裂作用。此作用与 DNA 所处的环境有关如含水量的多少。DNA 分子的断裂过程也向我们展示了 DNA 分子的弹性特点。

Real time observation of photocleavage of a single DNA molecule

LI Bin HU Jun WANG Ying WU Shiying HUANG Yibong LI Minqian

Keywords Photocleavage, Single DNA molecule

YOYO-1 is one kind of high efficient DNA dyes. it was used to observe single DNA molecules in its different state like DNA stretching and relaxation at single molecular level. Meanwhile, it is one kind of photosensitive reagents; YOYO-1stained DNA may be photocleavaged at the exacting position under the light radiation. In this paper, the process of photocleavage process of single molecule DNA stained by YOYO-1 under radiation of blue light (450-490nm) and the factors that may influence on it were reported. A series of images were taken in real time by charge couple camera (CCD) coupled with fluorescent microscope (FM).These images showed us that at the first blue radiation a stretched DNA molecule presented a blue uninjured line. With time passed, some breakpoints at different position along DNA molecule could be observed. The more time of exposure for DNA molecule lasted, the more

breakpoints appeared in DNA molecule. At the ends of breakpoints there were visible big dots that were brighter and thicker than at its previous stretched states.The stretched single DNA molecule was fixed on the modified slide with several dots along its chain, and the break points usually occurred in the middle of fixed points. Once photocleavage took place, the two new free ends retracted immediately toward to its original fixed places and showed two bright dots. Sometimes the relaxation force of stretched DNA molecule was bigger than the adsorption force that fixed DNA molecule on modified slide, then the break fragments would shrink into bright dots and ran away into solution due to Brown movement. We noticed that the photocleavage speed of DNA stained with YOYO-1 under light radiation seemed to have the relation with the water around DNA molecules. Photocleavage speed of DNA molecules immersed in large amount of water was more quickly than that in a little water environment; photocleavage DNA was not observed when there was few water (water could not seen with our naked eyes under the microscope). This result hinted us there might be different degrees of light effects on DNA under different amount of water around DNA molecules. The results demonstrated that the effect of photocleavage of YOYO-1on DNA had the relation with environment around DNA molecules; and elastic property of DNA was revealed during the process of photocleavage.

动态组合模式蘸笔纳米刻蚀与单个 DNA 分子上的纳米阵列制造

李 宾　汪 颖　武海萍　张 益　张志祥　周星飞　李民乾　胡 钧[1]

关键词　蘸笔纳米刻蚀技术，纳米图形

“蘸笔”纳米刻蚀技术(DPN)是近几年来刚刚出现的，基于原子力显微镜(AFM)的纳米刻蚀新技术[1]。利用 DPN 技术可在金、硅等固相衬底上制作不同的纳米级图案 [2-7]。然而，在柔软的物体表面如生物大分子上直接制作纳米图形是尚需开拓的研究领域, 它可为研究 DNA 蛋白质超分子体系，人工组装 DNA 蛋白质复合物和分子马达等提供条件。

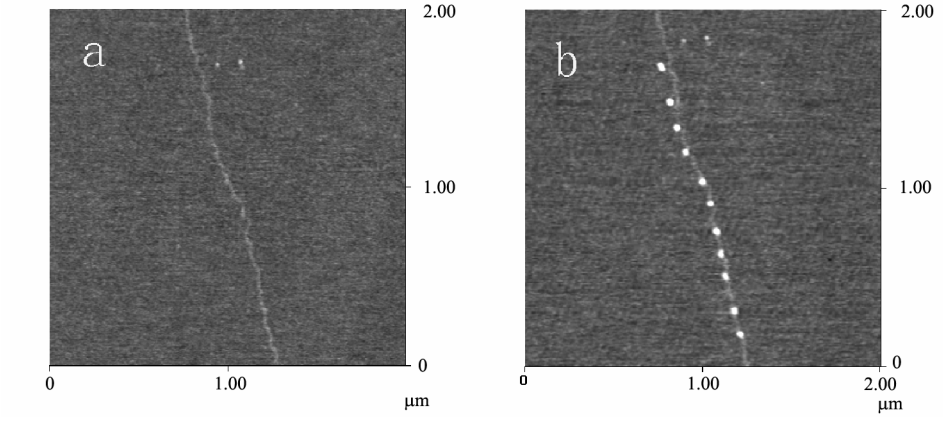

图 1　采用动态组合模式 DPN 在单个 λ DNA 分子上制作的纳米阵列
a 固定在云母表面上的单个 λ DNA 的表面形貌图
b 沿单个 λ DNA 分子的纳米阵列的表面形貌图
a The surface topography image of a single DNA molecule stretched on the modified mica
b The surface topography image of nanopattern along a single DNA molecule

本文报道中介绍一种新的，动态组合模式 DPN 方法——轻敲模式与接触模式的动态组合方法。 通过直接切换 AFM 的工作状态，即时转变轻敲模式与接触模式，实现了纳米图形的制作和成像检查在同一的位置上进行。对于表面吸附的柔软的生物分子，我们可以进行定点(扫描范围为零)接触沉积，这样就避免了对生物分子的破坏。动态组合模式 DPN 为我们在柔软的生物大分子上制作纳米图形提供了先决条件。我们成功地用动态组合模式 DPN 方法将蘸有蛋白质溶液的 AFM 针尖在单个 DNA 分子制造了纳米图形如图 1 中所示。图 1a 是纳米阵列制作之前，在轻敲模式下获得的单个拉直 DNA 分子图像。DNA 分子的右侧的两个小圆点为特定区域的标志；图 1b 是沿着 DNA 分子制作纳米阵列过程完成后用轻敲模式获得的图像。

1 上海交通大学, Bio-X 生命研究中心

Combined-dynamic mode “dip-pen” nanolithography and physical nanopattern along a single DNA molecule

LI Bin WANG Ying WU Haiping ZHANG Yi

ZHANG Zhixiang ZHOU Xinfei LI Minqian HU Jun[1]

Keywords DPN, Nanopattern

Dip-pen nanolithography (DPN) based on atomic force microscope (AFM) is an emerging approach for depositing nanostrucures on material surfaces [1]. It seems that many scientists have been becoming interesting in it and made a number of investigations on fabricating different nanopatterns incluing dots, lines, polygons and letters in different sizes with various ink solutions [2-7]. Unfortunately, they are all investigations on the surfaces which are relatively hard]. A novel method for nanofabrication on soft surfaces such as biomacromolecules will provide a powerful tool for studying DNA-protein supermolecular systems, assembling DNA-protein complexes and molecular motors.

Our new method termed combined dynamic mode DPN (CDDPN) combines advantages from both of contact mode with tapping mode of AFM without changing AFM tip, for example, a high resolution image for biomacromolecules with tapping mode and a good writing capability with contact mode. it allows us to deposit something on the biomacromolecules at the nanometer scale in real time and in situ. For a substrate like biomacromolecule which is adsorbed on the substrate loosely, zero scanning using contact modes is adopted to deposit ink to avoid destructions on them due to tip scanning. Using this method protein solution was used as ink to be deposited along a single stretched DNA molecule. As showed in Figure1, several nanospots are deposited on a single DNA molecule stretched on the mica substrate from top to bottom. For comparison, two AFM images are shown here, with one before and the other after nanopatterning procedures. Figure 1a is a surface topography image with only a single DNA molecule, whereas Figure1b is a surface topography image with a DNA molecule and subsequently deposited nanosports along the DNA strand also using tapping mode operation.

1 Shanghai Jiaotong University, Bio-X Science Research Centre

一种新的微米级多组分图形的制备方法
——连续收缩微纳米制备技术

李 海 武海萍 黄一波 欧阳振乾[1] 张晓东[1] 胡 钧[1]

关键词 多组分，微图形，连续收缩，制备方法

在固体表面快速、方便、廉价地制备高精度的二维和三维图形是当前的一个研究热点[1,2]。现在已经有许多方法可以用来在固体材料表面构建微米和纳米级的精细图形， 如光蚀刻技术[3,4]、微接触印刷法[5,6]、自组装技术[7]、DPN(Dip-pen Nanolithography)技术[8]等。但是这些方法每次只能在表面上用一种材料作图，不能同时用多种材料在同一表面上作图，当需要制备含有多种组分的图形时较为复杂而且耗时较长。然而，在一些微加工领域如生物芯片的制备[9]和光致发光显示器件[10]的制备方面，需要同时将多种材料排布在固体表面形成所需的图形。因此，发展一种可以同时在固体表面上用多组分材料制备微米或纳米级图形的快速、便捷的技术就成了当前亟待解决的一个问题。

为此，我们和合作者共同提出了一种多组分微米图形的制备方法——连续收缩微纳米制备(Serial shrinkage nano-manufacturing(SSN))技术。利用 SSN 方法我们将双组分彩色墨水组成的厘米或毫米级图形快速简便地缩小至微米级，同时仍保持了图形的忠实度和精度。利用一维 SSN 方法分别将线宽为 200 μm 和 500 μm 的平行线条缩小到约 1 μm 和 4 μm，并且制备了彩色微米级线条图形。用二维 SSN 方法制备了喷墨打印机彩色墨水的微米级点阵，将起始点大小为 700 μm 的墨水点缩小为 30 μm。

SSN 方法简便易行，所需材料廉价易得，在一般的实验室里都能做到，并且检测也很方便，它将会在多组分微米级图形的制备中发挥巨大的作用，而且随着研究的深入将来甚至可以应用于纳米级图形的制备。我们相信，随着研究的深入，SSN 方法将来一定会在材料研究、生物芯片制备、微电路印刷和制备衍射光栅等多个方面发挥巨大的作用。

---

1 上海交通大学, Bio-X 生命研究中心

参考文献

1 Devasish Chowdhury, Anumita Paul, Arun Chattopadhyay. Nano Lett, 2001, **1**(8): 409—412

2 Younan Xia, George M. Whitesides. Annu Rev Mater Sci, 1998, **28**: 153—84

3 Xing Cheng, L Jay Guo. Microelectronic Engineering 2004, **71**: 277—282

4 Kersten P, Bouwstra S, Petersen J W. Sensors and Actuators A 1995, **51**: 51—54.

5 Younan Xia, George M. Whitesides. J Am Chem Soc, 1995, **117**: 3274—3275

6 Hull R, Chraska T, Liu Y, *et al*. Materials Science and Engineering C, 2002, **19**: 383—392

7 Kim B J, Liebau M, Huskens J, *et al*. Microelectronic Engineering, 2001, 57—58, 755—760

8 Seunghun Hong, Chad A M. Science, **28**: 1808—1811

9 Inerowicz H D, Howell S, Regnier F E, *et al*. Langmuir, 2002, **18**: 5263—5268

10 Tatsuya Shimoda, Katsuyuki Morii, Shunichi Seki, *et al*. MRS Bulletin, 2003, **28**(11): 821—828

A novel microfabrication method for multi-component patterns—Serial shrinkage nano-manufacturing (SSN)

LI Hai WU Haiping HUANG Yibo OUYANG Zhenqian[1] ZHANG Xiaodong [1] Jun Hu[1]

Keywords Multi-components, Micropattern, Serial shrinkage, Microfabrication method

Patterning materials on solid surface in micrometer & nanometer scale is very important to the advance of micro- and nanotechnologies and the study of nanoscience. However, conventional microfabrication technologies, such as photolithography, microcontact printing，self assembly method and dip-pen nanolithography, just can generate single-component pattern each time and the operation is complex and time-consuming in terms of fabricating for multi-component patterns. However, multiple-material patterns are needed in terms of fabricating biochips and light-emitting polymer displays. So it is a challenge to develop an efficient technology to patterning multi-component materials simultaneously on solid surface.In order to get the multiple-components and shrinkable pattern at the same time, cooperators and we present an alternative contact lithography method—serial shrinkage nano-manufacturing (SSN). Colorful-ink parallel lines pattern was fabricated by SSN and the feature size as small as 4μm can be achieved from the initial 500μm line. Multi-color ink array, which is fabricated by ink-jet printer, can be miniaturized with the feature size was shrunk from 700μm to 350μm. The fidelity and the reproducibility of the pattern can be maintained well after several size-reduction operations.In comparison with other microfabrication technologies, SSN is cost-effective and straightforward and no expensive instrument and materials are needed in the fabrication process. The detection can be finished conventionally by microscope with a CCD. SSN is a powerful tool for fabricating multi-component patterns and even nanopatterns can be fabricated in the furture with the development of SSN. Potential applications of SSN are competitive, such as in the field of material research, biochip, integrated circuits and diffractive grating fabrication.

1 Shanghai Jiaotong University, Bio-X Science Research Centre

连续收缩微纳米制备技术制备 DNA 和蛋白质微阵列

李 海 张晓东[1] 欧阳振乾[1] 胡 钧[1]

关键词 连续收缩，DNA 微阵列，蛋白质微阵列，纳米制备技术

我们提出了一种新的制备多种芯片的方法——连续收缩微纳米制备技术，并且利用这种方法制备了 DNA 和蛋白质微阵列(芯片)。首先，用点样仪或机械手制备一个厘米级的阵列作为模板，每个点的大小约为 500 μm。然后，将这个模板阵列通过 SSN 方法缩小至所需的尺度。利用 SSN 方法，模板阵列的图形可以快速地缩小三十甚至几百倍，因此模板阵列的图形密度也相应地增加。由于目前用 SSN 方法制备的 DNA 或蛋白质微阵列密度可以达到 10^5 点/cm^2 或者更高，因此有望

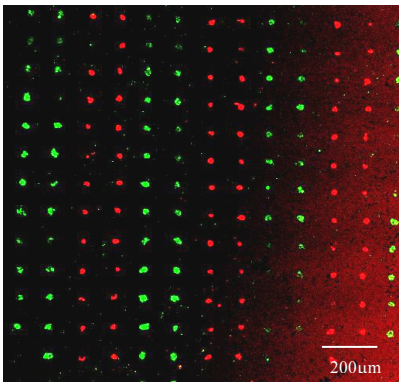

图 1 用 SSN 方法制备的寡核苷酸微阵列的双色杂交结果

Fig.1 An oligonucleotide microarray after hybridization with standard hybridization procedures

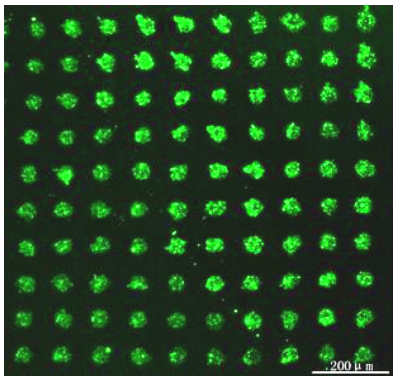

图 2 用 SSN 方法制备的蛋白质微阵列

Fig.2 A protein microarray fabricated by SSN technology

在将来对生命信息的高通量分析中得到应用。图 1 是用 SSN 方法制备的寡核苷酸微阵列杂交后的结果。首先将经过缩微的寡核苷酸微阵列固定在表面用环氧基试剂修饰过的载玻片上，然后分别用与其互补的 5’端带有 FAM(绿色)或 TAMRA(红色)荧光标记的探针在 28 °C 杂交。杂交后经过严格冲洗，结果用共聚焦激光显微镜(Zeiss LSM 510)扫描并记录。图中标尺：200 μm，阵列中点的平均尺寸为 25 μm。图 2 是用 SSN 制备的蛋白质微阵列结果。将用 SSN 方法缩微的人 IgG 微阵列固定在环氧基修饰的载玻片表面，冲洗载玻片并用封闭液封闭，然后加入 FITC 标记的羊抗人 IgG 抗体与之在 37 °C 孵育反应 30 min，结果用共聚焦激光显微镜(Zeiss LSM 510)扫描并记录。图中标尺：200 μm，阵列中点的平均尺寸为 50 μm。

1 上海交通大学, Bio-X 生命研究中心

DNA and protein microarrays generated by serial shrinkage nano-manufacturing

LI Hai ZHANG Xiaodong[1] OUYANG Zhenqian[1] HU Jun[1]

Key words SSN, DNA microarray, Protein microarray, Nanofabrication

We developed a novel technology for manufacturing various chips by serial shrinkage nano-manufacturing (SSN) technology. Here we reported the characteristics of DNA and protein microarray （or chip） generated by this technique. In the SSN technology, a master array in centimeter scale with feature size of 500μm was generated by an arrayer. Sequentially, the master array was miniaturized by SSN till approaching to the density and spots size what we expected. It rapidly microminiaturized the master array by a ratio of about thirty times or even hundreds times. The density of DNA or protein microarray generated by SSN technology could reach up to about 10^5 features/cm^2 or higher, so it can be

applied to high-throughout analysis of life information in the furture.

Fig.1 shows an oligonucleotide microarray after hybridization with standard hybridization procedures. In brief, the oligonucleotide samples in microarray were immobilized on the epoxy modified slides, the microminiaturized array was incubated at 28°C with complementary probes 5'-end labeled with fluorescence FAM (green) and TAMRA (red), respectively. The oligonucleotide microarray was washed and the hybridization result was recorded by Zeiss LSM 510 confocal laser microscope. Bar: 200μm, the average size of the spots: ~25μm.

Fig.2 shows a protein microarray fabricated by SSN technology. Human IgG microarray was immobilized on the epoxy modified slides by incubating overnight at 4°C. After washing the excess proteins and blocking, it was incubated with FITC labeled sheep anti-human IgG antibody at 37°C for 30min. The protein microarray was then washed and characterized by Zeiss LSM 510 confocal laser microscope. Bar: 200μm, the average size of the spots: ~50μm.

---

1 Shanghai Jiaotong University, Bio-X Science Research Centre

DNA 单分子的纳米定位切割与拾取研究

吕军鸿　王国华　雷晓玲 李民乾　胡 钧

关键词　原子力显微镜，DNA 单分子，定位切割，拾取，测序策略

报道了一种对 DNA 单分子进行精细的纳米定位切割和拾取的技术。首先用分子梳技术将 DNA 拉直固定在经 3-氨基丙基三乙氧基硅烷修饰的云母基底上，然后通过精细控制原子力显微镜针尖与 DNA 样品之间的作用力，实现了对 DNA 链的定位切割和拾取。这种方法不仅可制备应用于临床遗传诊断和致病基因的定位等多种的微小 DNA 探针，而且有望发展为一种基于纳米操纵技术的 DNA 有序化测序策略。

Positional nanodissection and picking-up of single DNA molecule

LÜ Junhong　WANG Guohua　LEI Xiaoling　LI Minqian　HU Jun

Keywords　Atomic force microscopy (AFM), Single DNA molecule, Positional dissection, Picking-up, Sequencing strategy

A technology for refined dissection and picking-up of single DNA molecule at nanometer level has been demonstrated. DNA molecules were firstly stretched by molecular combing technique and deposited on a 3-aminopropyl triethoxysilane-coated mica substrate, the nanodissection and picking-up of DNA strands at the desired position was realized by the fine control of the force between the atomic force microscopy (AFM) tip and DNA sample. This method could not only be used to prepare small

DNA probes which have great potential application both in clinic genetic diagnosis and positional cloning genes, but also to develop a new strategy for ordered DNA sequencing based on this nanomanipulation.

单分子 PCR 产物错误率分析

王国华　吕军鸿　雷晓玲　李民乾　方海平　胡 钧

关键词　单分子 PCR，错误率，忠实性，模板数

碱基错配致使 PCR 扩增产物中存在突变序列。大量模板 PCR 扩增时突变序列所占的比例较低，对随后进行的 PCR 产物分析影响不大，但当对微量甚至单个模板 DNA 扩增时，情况则完全不同。本文对单分子 PCR 产物的错误率进行了理论分析，结果表明：根据实验目的和条件，选择忠实性不同的聚合酶是十分关键的。

Error rate in single molecule PCR

WANG Guohua　LÜ Junhong　LEI Xiaoling　LI Minqian　FANG Haiping　HU Jun

Keywords　Single molecule PCR, Error rate, Fidelity, The number of template molecule

Mismatches during amplification result in some mutations in the PCR products. Our simulation indicates that the rate of mutation is quite low and has no influence on the consequent sequencing analysis when template DNA molecules are abundant, but it is not the case when the PCR amplification is performed with single or rare molecules as template. The error rate of single molecule PCR under different conditions shows that it is essential to select different polymerases according to different experimental purposes.

用分离并再放置单个纳米颗粒的方法构建纳米图形

汪 颖　张 益　胡 钧

关键词　原子力显微镜，纳米颗粒，操纵

运用不同的材料和方法制造纳米结构和纳米器件是一项快速发展的跨学科研究领域。金属纳米颗粒和半导体量子点等纳米级大小的颗粒被视为制造纳米结构和纳米器件的重要元件。精确而又可重复地逐个分离和放置这些单个颗粒能够极大地推动它们的直接运用。我们通过将原子力显微镜针尖进行化学或金属修饰，按常规方法利用原子力显微镜对固定在基底表面的纳米颗粒样品进行成像，然后选择所需进行纳米操纵的单个颗粒，并使该针尖与纳米颗粒接触从而实现单个纳米颗粒的拾取，接着控制原子力显微镜将该粘有颗粒的针尖定位到所预设的基底表面位置，将纳

米颗粒放置于该位置。从而能完成对纳米颗粒逐个进行拾取、转移、放置的一系列操纵，构建一定的纳米图案，为纳米水平的制造和控制提供一种新的有效手段。

Isolation of multi nanoparticles by a same afm tip

WANG Ying ZHANG Yi HU Jun

Keywords AFM, Nanoparticle, Isolation

An atomic force microscope (AFM) tip modified with chemicals or metal was used to capture one nanoparticle from a substrate by lowing down the tip from normal imaging position. Once the nanoparticle was capured by the tip, we changed the scan angle and moved the tip to a second nanoparticle. The similar operation to capture of the first nanoparticle was executed to the second nanoparticle. The second nanoparticle was then attached to another place of the tip. After a series of such operation, multi nanoparticles can be isolated by a same AFM tip.

用原子力显微镜针尖拾取多个纳米颗粒的方法

汪 颖 张 益 胡 钧

关键词 原子力显微镜，纳米颗粒，拾取

我们通过将原子力显微镜针尖进行化学或金属修饰，按常规方法利用原子力显微镜对固定在基底表面的纳米颗粒样品进行成像，然后选择所需分离的单个颗粒，并通过降低针尖的高度使该针尖与纳米颗粒接触从而实现一个纳米颗粒的拾取。 接着改变针尖的扫描角度，对下一个纳米颗粒进行同样的操作，完成第二个纳米颗粒的拾取。通过重复进行这一系列的操作，可实现用同一个针尖拾取多个数目确定的一种甚至是多种纳米颗粒。

Single particle dip-pen nanolithography

WANG Ying ZHANG Yi HU Jun

Keywords AFM, Nanoparticle, SP-DPN

A novel technique for site-specifically capturing and depositing nanoparticles in single particle-at-a-time fashion is presented. This technique, termed as single particle Dip-pen Nanolithography (SP-DPN), employs a chemical- or metal-modified atomic force microscope (AFM) tip as the “pen” and individual gold nanoparticles as the “ink”. The capturing and depositing process can be selectively executed by real-time monitoring the bi-directional transfer of an individual

nanoparticle between the tip and the substrate. The tip-modification procedure is found to be crucial to capture gold nanoparticles from the surface; otherwise the nanoparticles would be pushed around by the AFM tip and remain on the surface.

利用原子力显微镜和肽段切割研究α-synuclein 纤维在纳米尺度的自组装

张 峰 杜海宁[1] 吉丽娜[1] 林晓静[1] 汪剑霞[1] 唐 琳 何建华 胡 钧[2] 胡红雨[1]

关键词 α-synuclein，肽段切割，原子力显微镜

α-synuclein (α-Syn)是与 Parkinson 病相关的 Lewy 小体的主要成分，但是目前对α-Syn 如何积聚成为纤维的机理还不清楚。我们利用原子力显微镜和肽链截尾方法解释了α-Syn 纤维的自组装方式和积聚形貌。结果显示：蛋白酶 K 显著地把纤维从~ 6.6 nm 的高度切割到~ 4.7 nm， 而变性剂尿素则把纤维完全破碎成小颗粒。另外，我们发现α-Syn 纤维的粗细依赖于α-Syn 本身肽链的长度。一个九肽的 GAV 基序可以组装成很长(> 1 μm)且非常细的纤维(～2.2 nm)。我们提出了一个α-Syn 纤维自组装的模式图，其中α-Syn 肽链的中心区域是一个对于纤维组装必不可少的核心片段，而α-Syn 肽链的两端则自由的松散在纤维核心的外侧，且纤维的生长方向与β-sheets 结构的方向垂直。这项研究建立了一种在纳米尺度上联合使用生化技术与显微镜技术探测淀粉样纤维自组装的方法。本研究对于疾病相关的淀粉样变和相应的药物设计也提供了有用的信息。

1 中国科学院上海生命科学研究院生物化学与细胞生物学研究所

2 上海交通大学 Bio-X 研究中心

Nanoscale assembly of α-synuclein fibrils as revealed by peptide truncation and atomic force microscopy

ZHANG Feng DU Haining[1] JI Lina[1] LIN Xiaojing[1] WANG Jianxia[1] TANG Lin HE Jianhua HU Jun[2] HU Hongyu[1]

Keywords α-synuclein, Peptide truncation, Atomic force microscopy

α-synuclein (α-Syn) fibrils are the major component of Lewy bodies that are closely associated with the pathogenesis of Parkinson's disease, but the mechanism for the fibril assembly remains poorly understood. Here we report using a combination of peptide truncation and atomic force microscopy (AFM) to elucidate the assembly and morphology of α-Syn fibrils. The results show that protease K significantly slims the fibrils from ~ 6.6 nm to ~ 4.7 nm in height, whereas chaotropic denaturant urea completely breaks down the fibrils into small particles. Moreover, α-Syn fragments assemble into thinner filaments with the size depending on the peptide length. A nine-residue peptide corresponding to the homologous GAV-motif sequence can form very thin (~ 2.2 nm) but long filaments (> 1 μm). A

schematic model is proposed for the morphological assembly of α-Syn fibrils. In this model, the central sequence of α-Syn forms a fibrillar core by cross β-structure that is flanked by two flexible termini. The orientation of the fibril growth is perpendicular to the β-sheet structures. This study also establishes a method combining biochemical and microscopic techniques to explore the morphological assemblies of amyloid fibrils in nanoscale, which would provide information for understanding of the disease-related amyloidogenesis and design of anti-amyloid drugs.

利用原位原子力显微镜研究α-synuclein 纤维的结构证据

张 峰 吉丽娜[1] 唐 琳 胡 钧[2] 胡红雨[1] 徐洪杰 何建华

关键词 α-synuclein，原子力显微镜，GAV 肽

人类α-synuclein 蛋白是一种突触前的神经末端蛋白，现在被认为与多种神经退行性疾病如：帕金森病，路易小体病和阿尔茨海默病的路易小体突变症的发病机理有重要关系。α-synuclein 蛋白在体外经过 37℃摇动培养 6 d 形成了均匀的淀粉样纤维。利用原子力显微镜的轻敲模式和接触模式，原位研究了α-synuclein 蛋白纤维在溶液中的结构属性。结果发现：α-synuclein 蛋白纤维在接触模式下，迅速断裂成许多片断，而在轻敲模式下，α-synuclein 蛋白纤维在连续一个小时的原位扫描过程中一直保持原有的纤维形貌。另外在轻敲模式下，α-synuclein 蛋白纤维与盐酸胍(0.6 mol/L)共培养的原位实验也出现了与接触模式下相似的断裂现象。这些结果间接地提供了在纳米尺度 β 片层结构如何组成α-synuclein 蛋白纤维的结构信息。

1 中国科学院上海生命科学研究院生物化学与细胞生物学研究所

2 上海交通大学 Bio-X 研究中心

Structural evidence for α-synuclein fibrils using *in situ* atomic force microscopy

ZHANG Feng JI Lina[1] TANG Lin HU Jun[2] HU Hongyu[1] XU Hongjie HE Jianhua

Keywords α-synuclein, atomic force microscopy, tapping mode, contact mode, guanidine hydrochloride

Human α-synuclein is a presynaptic terminal protein and can form insoluble fibrils that are believed to play an important role in the pathogenesis of several neurodegenerative diseases such as Parkinson's disease, dementia with Lewy bodies and Lewy body variant of Alzheimer's disease. In this paper, *in situ* atomic force microscopy has been used to study the structural properties of α-synuclein fibrils in solution using two different atomic force microscopy imaging modes: tapping mode and contact mode. In the *in situ* contact mode atomic force microscopy experiments α-synuclein fibrils quickly broke into fragments, and a similar phenomenon was found using tapping mode atomic force microscopy in which α-synuclein fibrils were incubated with guanidine hydrochloride (0.6 mol/L). The

α-synuclein fibrils kept their original filamentous topography for over 1 h in the *in situ* tapping mode atomic force microscopy experiments. The present results provide indirect evidence on how β-sheets assemble into α-synuclein fibrils on a nanometer scale.

1 Key Laboratory of Proteomics, Institute of Biochemistry and Cell Biology, Shanghai Institutes for Biological Sciences, Chinese Academy of Sciences, Shanghai
2 Bio-X Research Center, Shanghai Jiaotong University, Shanghai

利用原子力显微镜探测 GAV 肽在不同衬底表面的自组装

张 峰 张 益 杜海宁[1] 张志祥 吉丽娜[1] 李洪涛[1]
胡红雨[1] 徐洪杰 胡 钧[2] 何建华

关键词 α-synuclein，原子力显微镜，GAV 肽

α-synuclein, amyloid β蛋白以及 prion 蛋白都是与一些神经性退行性疾病相关的蛋白。这 3 个蛋白包含一个共同的保守序列(GAV 基序)，这个 GAV 基序被认为与蛋白的纤维化和毒性有关。为了进一步了解 GAV 基序在蛋白纤维化过程中的作用，我们人工合成了 GAV 九肽(NH_2-VGGAVVAGV-$CONH_2$)，并且利用原位原子力显微镜直接观察 GAV 基序在不同衬底表面的自组装。结果显示 GAV 基序在不同衬底表面自组装成不同尺度和形态的纤维，而且自组装的动力学也显示出与不同衬底表面的物化特性有显著的相关性。在 APS 修饰的云母表面，GAV 基序形成了不规则的纤维状积聚；相反，在裸云母，高序石墨表面，GAV 基序自组装成为规则的长纤维，在高浓度的情况下，还可以形成β片层的单层膜。而且在裸云母，高序石墨表面形成的纤维都有很高的取向性，即纤维按照云母和石墨表面原子排列的 3 个方向互成 60° 夹角。我们这里提出了一个 GAV 基序在裸云母和高序石墨表面自组装的模式图。

1 中国科学院上海生命科学研究院生物化学与细胞生物学研究所
2 上海交通大学 Bio-X 研究中心

Probing self-assembly of GAV peptide on different dubstrates with *in situ* atomic force microscopy

ZHANG Feng ZHANG Yi Du Haining[1] ZHANG Zhixiang JI Lina[1]
LI Hongtao[1] HU Hongyu[1] XU Hongjie HU Jun[2] HE Jianhua

Key words α-synuclein, AFM, GVA peptide

α-synuclein, amyloid β-protein and prion protein are among the amyloidogenic proteins related to some neurodegenerative diseases. The three proteins contain a consensus sequence (GAV motif) that is proposed to be associated with the fibrillization and cytotoxicity. To further

understand the function of the GAV motif in fibril assembly, we chemically synthesized the GAV peptide, NH_2-VGGAVVAGV-$CONH_2$, and applied *in situ* atomic force microscopy to directly observe the self-assembly of GAV peptide on surfaces of different substrates. The results showed that the size and the shape of GAV peptide self-assembly, as well as the kinetics of their formation, exhibited pronounced dependence on the physicochemical nature of the substrates surface. On the surface of APS-coated mica, GAV peptide formed irregular fibriform aggregates. On contrast, on surfaces of bare mica and HOPG, GAV peptide formed uniform, elongated fibrils, which at higher GAV peptide concentration had the tendency to form monolayer of β-sheets. The fibrils formed on surfaces of bare mica, $NiNO_3$-coated mica and HOPG were oriented along three directions at 60^o to each other, resembling the crystallographic symmetry of surfaces of mica and HOPG. A schematic model for the self-assembly of GAV peptide on surfaces of bare mica and HOPG was presented.

1 Key Laboratory of Proteomics, Institute of Biochemistry and Cell Biology, Shanghai Institutes for Biological Sciences, Chinese Academy of Sciences, Shanghai
2 Bio-X Research Center, Shanghai Jiaotong University, Shanghai

纳米颗粒从在不同基底间转移的方法

汪 颖 张 益 胡 钧

关键词 原子力显微镜，纳米颗粒，转移

我们通过将原子力显微镜针尖进行化学或金属修饰，按常规方法利用原子力显微镜对固定在基底表面的纳米颗粒样品 1 进行成像，然后选择所需进行纳米操纵的单个颗粒，并使该针尖与纳米颗粒接触从而实现单个纳米颗粒的拾取。接着从原子力显微镜下取出吸附有纳米颗粒的样品 1，换上另外一个需要放置纳米颗粒的样品 2。用俘获了纳米颗粒的针尖对样品 2 进行正常的成像，找到需要放置该纳米颗粒的位置并记录下来，通过降低针尖的高度使吸附在针尖侧面的纳米颗粒与衬底接触从而将纳米颗粒放在该位置上。将针尖重新回到正常扫描模式，检测放置的结果并记录下来。操纵前后对纳米颗粒高度的测量结果是一致的，证明了纳米颗粒实现了从一个衬底转移到另一个衬底上。

Transportation of single nanoparticle from one substrate to another

WANG Ying ZHANG Yi HU Jun

Keywords atomic force microscope (AFM), Nanoparticle, Transportation

An atomic force microscope (AFM) tip modified with chemicals or metal was used to capture one nanoparticle from a substrate by lowing down the tip from normal imaging position. Once a

nanoparticle was capured by the tip, the substrate was replaced by another substrate, which needs a nanoparticle in a given region. After the region was found by normal AFM scanning, the tip with the captured nano- particle was lowed down enough to let the particle touch the region of interest. Then the nanoparticle attached to the AFM tip can be controllably released to the region of interest on another substrate.

利用原子力显微镜对人类 α-synuclein 蛋白及其两种缺失肽断的纤维形貌研究

张 峰 吉丽娜[1] 唐 琳 徐洪杰 胡 钧[2] 胡红雨[1] 何建华

关键词 α-synuclein，原子力显微镜，蛋白酶 K，α-synuclein$_{1-74}$，α-synuclein$_{61-140}$

α-synuclein 的纤维化和淀粉样积聚被认为与几种致死性的神经退行性疾病密切相关，如帕金森病，老年痴呆症。α-Synuclein$_{1-74}$和α-synuclein$_{61-140}$是α-synuclein蛋白的两个尾端缺失的肽断。这两个肽断同样也可以在体外积聚成淀粉样纤维。本文利用原子力显微镜观察到了α-synuclein$_{61-140}$肽断不同的纤维形貌，如细纤维，一端粗一端细的纤维，环状的纤维，以及成熟的粗纤维。我们也观察到了α-synuclein和α-synuclein$_{1-74}$积聚成的纤维经蛋白酶K切割前后其形貌的显著变化。在切割前，α-synuclein和α-synuclein$_{1-74}$的纤维都显示为典型的淀粉样纤维形貌，但是经蛋白酶K切割后，α-synuclein的纤维变成了很细的纤维和环状的纤维，α-synuclein$_{1-74}$的纤维变成了锯齿状的纤维形貌。这个结果对于在纳米尺度上理解一种可溶性的，天然不折叠的蛋白如何积聚成为高度有序折叠的淀粉样纤维提供了有用的实验证据。

1 中国科学院上海生命科学研究院生物化学与细胞生物学研究所

2 上海交通大学 Bio-X 研究中心

Fibril morphological study of wild type human α-synuclein and its two deletion mutants by atomic force microscopy

ZHANG Feng JI Lina[1] TANG Lin XU Hongjie HU Jun[2] HU Hongjie[1] HE Jianhua

Keywords Wild type α-synuclein, Atomic force microscopy, Proteinase K, α-synuclein$_{1-74}$, α-synuclein$_{61-140}$

Amyloid-like aggregation or fibrillization of α-synuclein is believed to be closely associated with several fatal neurodegenerative disorders, including Parkinson's disease and Alzheimer's disease. α-Synuclein$_{1-74}$ and α-synuclein$_{61-140}$ are two deletion mutants of α-synuclein protein. Both the two mutants also can self-assemble into amyloid fibrils in vitro. In this paper, atomic force microscopy was used to observe the distinctly different fibrils morphologies of α-synuclein$_{61-140}$ mutant such as thin fibrils, fibrils with one wide termini and the other thin termini, annular fibrils, and matured wide fibrils. We also obtained the different morphologies of wild type α-synuclein fibrils and α-synuclein$_{1-74}$ fibrils

before and after they were digested by proteinase K. Before digested, both of them showed typical amyloid fibrils morphologies, and after they were digested by proteinase K, wild type α-synuclein fibrils showed the thin and annular, and α-synuclein$_{1\text{-}74}$ fibrils showed dentate. The present results provide helpful evidence to understand how the natively unfolded protein self-assemble into highly orderly amyloid fibrils on a nanometer scale.

苯甲酸及其衍生物的 THz-TDS 研究

葛 敏 赵红卫 吉 特 余笑寒 王文锋

关键词 苯甲酸，太赫兹，时域光谱

太赫兹时域光谱分析(Terahertz time domain spectroscopy，THz-TDS)是国际上近年刚发展起来的研究技术，它利用物质对 THz 频带的不同特征吸收谱分析研究物质成分、结构及其相互作用关系。通常有机分子内化学键的振动吸收频率主要在普通红外波段，但对于分子之间弱的相互作用(如氢键)及大分子的骨架振动(构型弯曲)、偶极子的旋转和震动跃迁以及晶体中晶格的低频振动吸收频率则对应于 THz 波段范围，这些振动所反映的分子结构及相关环境信息都在 THz 波段内不同吸收位置及吸收强度上有明显的响应，有机分子的这些光谱特征使得利用 THz 时域光谱技术鉴别化合物结构、构型与环境状态成为可能。本文主要介绍了甲基、氨基及羧基等不同取代基的苯甲酸衍生物在 0.1—2.0 THz 波段的吸收谱图,并利用量化计算的方法对所得谱图进行理论拟合。实验结果表明取代基种类和位置的不同都会在样品的吸收谱图中得到明显的体现。利用不同化合物吸收谱图的差异，可以将这些化合物区分开来，这表明 THz-TDS 技术可以分辨化合物结构上的微小差异，可望应用于化合物分析鉴定、污染物检测、快速检测被信封或衣服等包藏起来的特殊物质(如毒品、爆炸物等)、以及用于生物医药中，研究药物分子与蛋白质等的结合状态。量子化学计算结果也与实验结果基本吻合，显示量子化学计算可以为 THz 时域光谱的解释提供参考。

Far-infrared vibrational spectra of benzoic acid and its derivates measured by THz time-domain spectroscopy

GE Min ZHAO Hongwei JI Te YU Xiaohan WANG Wenfeng

Keywords Benzoic acid, THz, Time-domain spectroscopy (THz-TDS)

Terahertz Time-Domain spectroscopy (THz-TDS) is a new technique based on femto-second laser technology. It has proven to be a versatile tool in physics and chemistry for spectroscopy on a wide variety of different samples in the FIR. In the article we present well-resolved absorption spectra of benzoic acid and its derivatives with one hydrogen replaced by a CH_3, an OH or a NH_2 group in the frequency region between 0.1 and 2.0THz at 293K using THz-TDS. Comparing the absorption spectra of different chemicals, we can distinguish the substances easily. From the results we can say that even minor changes in the molecular configuration lead to major differences in its FIR absorption. The

observed distinct differences between these molecules may be useful in drug tracing applications where the detection of small amounts of a substance is needed. An assignment of the different modes is dramatically complicated by the fact that benzoic acid and its derivatives form dimers which are arranged in a crystal structure in the solid phase. A thorough analysis and assignment of the individual FIR absorption bands of benzoic acid and its methyl derivatives was carried out using density functional theory.

常见五元糖的太赫兹时域光谱研究

葛 敏 赵红卫 吉 特 王文锋 余笑寒 李文新

关键词 五元糖，太赫兹，时域光谱

糖是人和动植物的主要能源物质也是生命必需的物质，许多重要的生物分子中含有糖单元，如核酸中的核糖、糖蛋白、糖脂中的糖链部分。以往认为，糖对代谢、生长、发育、胁迫和基因表达的调节是糖代谢的结果，然而近年的研究却表明其生理作用已远远超出了“生物体的能源物质及组织组成物质”的传统认识，它们在细胞的相互识别、细胞分化、免疫等方面起着极为重要的作用。很多学者利用傅立叶变换红外光谱、拉曼光谱等实验方法对糖类分子的振动、转动进行了系统的研究。但是，对于糖类分子远红外波段的信息仍然了解不多。本文利用近十几年来发展起来的太赫兹时域光谱技术 THz-TDS 对 D-木糖、D-核糖、D-阿拉伯糖、D-来苏糖及相关的五元糖的振动光谱进行了研究，得到了它们在 0.1－2.0THz 波段的 THz-TDS 吸收谱图。不同糖类化合物的吸收谱表现出明显的特征，表明 THz-TDS 技术可以分辨化合物结构上的微小差异，可以应用于物质检测与分析。同时还研究比较了不同旋光性五元糖的 THz-TDS 光谱。结果表明该技术可能无法对糖类分子的不同空间构型进行区分，但是却能够对单独的 D 或 L 构型与 DL 混合构型之间的区别作出反映。造成这种现象的原因还有待于我们的进一步研究。

Terahertz time-domain spectroscopy of some common pentose

GE Min ZHAO Hongwei JI Te WANG Wenfeng YU Xiaohan LI Wenxin

Keywords Sugar, Terahertz, Time-domain spectroscopy (THz-TDS)

Sugar plays a central role in animal and plant life. They not only are important energy sources and structural components but also act as central signaling molecules controlling gene expression, growth and development. And to some extent, sugars represent prototype systems for the investigation of H-bonded networks in crystalline, amorphous and dissolved forms. Though long-wavelength investigations (IR and Raman spectroscopy or neutron scattering) allow direct observation of the vibrational characteristics of the hydrogen bond linkage, there are few investigations on crystalline and amorphous saccharides in the far-IR below 200 cm^{-1}. In the article we present well-resolved absorption spectra of D-xylose, D-ribose, D-arabinose, D-lyxose and other related substances in the frequency region between 0.1 and 2.0 THz using Terahertz Time Domain Spectroscopy (THz-TDS) at room

temperature. Comparing the absorption spectra of different chemicals, we can distinguish the samples easily. Thus THz-TDS is demonstrated to be highly sensitive to the minor changes of the molecular structures, and can be applied to detect and analyze materials. Finally, we find that the difference between optical antipode may not been shown in this THz region. The reasons will be our next subject.

两种联苯酚类化合物的太赫兹时域光谱研究

葛 敏 赵红卫 张增艳 王文锋 余笑寒 李文新

关键词 联苯酚，太赫兹时域光谱技术，弱相互作用，量化计算

酚类化合物能够和许多物质形成分子间氢键，同时多酚化合物自身也可以形成分子内及分子间氢键。本文利用 THz-TDS 首次获得了 295K 时 2,2’-二羟基联苯(2,2’-Biphenol，2BP)和 4,4’-二羟基联苯(4,4’-Biphenol，4BP)在 0.1 至 1.6 THz 波段的光谱。并利用量子化学理论计算对这两种化合物的结构进行了分析，在此基础上对 THz 低频波段的运动模式进行了初步探讨。实验结果显示两种同分异构体在该太赫兹频率范围内的吸收谱有显著的差异。量子化学计算表明，2BP 和 4BP 分子中两个苯环的夹角分别为 53.637 和 40.704，其中 2BP 中的两个羟基间能够形成分子内氢键，它在 1.45THz 的运动模式初步判断为包含氢键在内的两个苯环间的低频摆动。

Far-infrared spectra of 2, 2’-biphenol and 4, 4’-biphenol measured by Terahertz time-domain spectroscopy

GE Min ZHAO Hongwei ZHANG Zengyan WANG Wenfeng

YU Xiaohan LI Wenxin

Keywords Biphenol, Terahertz time-domain spectroscopy (THz-TDS), Weak interaction, Quantum calculation

In the article we present firstly well-resolved far-infrared spectra of 2, 2’-biphenol and 4,4’-biphenol in the frequency range between 0.1 and 1.8THz at 295K with THz-TDS. We observed distinct differences between the two isomers. Quantum calculations by Gaussian 03 show that the angels between the phenyl rings are 53.637 in 2BP and 40.704 in 4BP and the hydroxyl groups in 2BP can form intramolecular hydrogen bond. Based on these results we infer that the absorption of 2BP at 1.6THz can be assigned to the low-frequency torsions of the two phenyl rings which contain the hydrogen bond.

太赫兹时域光谱——气体和自由基检测新方法

葛 敏 赵红卫 张兆霞 朱红平 王文锋 李文新

关键词 太赫兹，时域光谱，气体分子，自由基

对 THz-TDS 技术在气体和自由基检测中的应用及新进展进行了综述。通常气体分子的全部或部分转动光谱都位于远红外区，连续的 THz 波谱在气体光谱学研究中具有独到之处，能直接测定分子的转动光谱，宽带的 THz-TDS 脉冲检测可同时测定混合气体中不同成份的吸收、测定化学组成和浓度。这些应用对汽车和工厂排放的多组份气体以及附带颗粒物(如柴油机排放的烟灰等)的检测具有十分重要的意义，也预示着该技术在大气污染物监控和环境保护等方面的广阔应用前景。另外，由于许多气体反应中间体如 OH、CH、CO 等粒子在 THz 波段有较强的吸收特性，因此 THz-TDS 光谱技术还能够对自由基和反应活性分子进行有效的探测和分析。虽然与其他的光学技术相比 THz 光谱技术并不完善，但是它与众不同的频率范围给我们提供了一个新的机会，去对那些在一般光学范围内难以或无法测量吸收谱线的气体，自由基和反应活性分子进行有效的探测和分析。

Terahertz time-domain spectroscopy ——a new method for detection of gases and free radicals

GE Min ZHANG Hongwei ZHANG Zhaoxia ZHU Hongping

WANG Wenfeng LI Wenxin

Keywords Terahertz(THz), THz-TDS, Gas, Free radical

Terahertz Time-Domain spectroscopy (THz-TDS) is such a new technique based on femto-second laser technology. The purpose of this paper is to briefly introduce its applications in detecting and identifying gases and free radicals. THz-TDS has several advantages. Usually, the vibration of gases all or partly lies in the terahertz region. And many radicals and reactive molecules such as OH, CH, CO are spectroscopically active in the THz region. In term of expected detectivity, THz-TDS should not be better than the other optical techniques. However, the very different wavelength range gives the opportunity to study new radicals or molecules (such as NO_2 or CH_2) whose spectroscopic lines are difficult or impossible to observe in the optical domain.

单线态氧引起的蛋白质损伤研究

张兆霞 朱红平 葛 敏 赵红卫 王文锋

关键词 活性氧自由基，单线态氧，光敏剂

生物组织在光敏剂参与下，经特定波长光辐照后产生的损伤或死亡称为光敏反应或光动力反应。光敏剂的激发态与基态氧发生激发能转移或电子转移产生单线态氧($^1O_2$)和超氧阴离子自由基($O^{2\cdot-}$)。$^1O_2$ 是一种反应活性相当高的亲电瞬态中间体，能高效地氧化生物大分子，造成生物体的损伤。蛋白质分子是单线态氧氧化的主要靶分子之一。蛋白质中主要的发色基团有色氨酸、酪氨酸、苯丙氨酸、组氨酸、半胱氨酸、胱氨酸等，它们与单线态氧的反应受到普遍的关注。

研究表明单线态氧主要与蛋白质中的 Trp，Met, Cys，His, Tyr 等残基发生反应，形成短寿命的内生过氧化物或氢过氧化物。我们的研究从化学角度出发结合生物学意义，从微观、动态和分子反应的角度研究活性氧自由基对蛋白质、肽及氨基酸进行损伤的反应机理和动力学过程，探讨受活性氧自由基攻击而损伤的蛋白质、肽及氨基酸自由基的电荷转移或氢原子转移机制，为更好地理解退行性疾病中的自由基机理作用提供理论参考。

The damage of proteins caused by singlet oxygen

ZHANG Zhaoxia ZHU Hongping GE Min ZHAO Hongwei WANG Wenfeng

Keywords Reactive oxygen species (ROS), Singlet oxygen，Photo-sensitizer

Organisms produce ROS throughout their lives. ROS (including superoxide anions, hydroxyl radicals, hydrogen peroxide and singlet oxygen) are known to oxidize biological macromolecules, with proteins to be an important target. The accumulation of oxidized, or modified, extra-and intra-cellular proteins in vivo cause age-related diseases such as Parkinson’s disease, Cataract. So the research of the damage of proteins by photo-sensitizer is very promising. Singlet oxygen is a high reactive oxidant in biology systems, and that proteins are a major target for the damage initiated by this reactive species. Reaction with proteins occurs primarily at Trp, Met, Cys, His, and Tyr side-chains with this resulting in the formation of short-lived endo- or hydroperoxides on Trp, His, and Tyr residues. This paper is a brief introduction about the reactions of singlet oxygen with tyrosine and histidine.

对自由基引起的蛋白质损伤的保护和修复

朱红平 张兆霞 赵红卫 王文锋 姚思德

关键词 自由基，抗氧化剂，蛋白质

抗氧化剂能有效保护和修复 ROS 对蛋白质的损伤从而延缓疾病和衰老，对此的机理研究引起

广泛关注。由于体内环境的复杂性，很多问题如 ROS 在体内氧化蛋白质的准确位点，如何从结构和定量水平研究蛋白质的氧化，抗氧化剂在体内发挥作用的诸多影响因素等还有待进一步研究。

The protection and repair of the radical damage to protein

ZHU Hongping ZHANG Zhaoxia ZHAO Hongwei WANG Wenfeng YAO Side

Keywords Free radical, Antioxidant, Protein

Growing evidences show sufficient supplement of antioxidants can protect against free radical damage to protein by scavenging ROS or repair modified proteins and has beneficial effect in disease prevention. In order to better understanding of how to defense the protein oxidation and repair the oxidative protein, much interest has focused on mechanisms of ROS-mediated oxidation of proteins and their protection by antioxidants. However, the effect of protein conformation on the damage-site, the exact location of oxidative alteration and the reaction rate of the modification remain largely unclear. Identifying the protein oxidative on the structural and quantitative level, fully understanding the multitude factors which influence antioxidant's effect in vivo are needed for the anti-ageing therapies and delaying the age-related diseases.

皮秒级脉冲辐解装置在抗氧化剂研究中的应用

王文锋 姚思德 苗金玲 赵红卫 朱红平

关键词 脉冲辐解，抗氧化剂，动力学，自由基

生物体在呼吸和代谢过程都会产生活性氧自由基[ROS]，同时电离辐射、紫外线及致癌物质等也会通过直接或间接作用产生活性氧自由基。体内一定浓度的自由基是机体进行正常生命活动的必要条件之一。但过多的自由基会攻击生物膜的不饱和脂肪酸引起膜脂质过氧化反应；攻击蛋白质引起结构与构象的改变，造成肽链断裂、聚合与交联；可攻击 DNA，造成其永久性损伤。这些生物大分子结构与功能的改变，导致细胞功能的紊乱，导致细胞的衰老、畸变及死亡，是心脑血管疾病及癌症的祸首。随着人体年龄的增加，体内修复酶的活性不断下降，细胞中 DNA 氧化性损伤增多而修复能力下降，受损伤的 DNA 不断积累，使生物体患癌症的可能迅速上升，即癌症的发病率随年龄的 4 次方成正比。天然抗氧化剂是一类单电子氧化还原电位很低的活性物质，可清除活性氧自由基，又可通过电荷转移反应修复被氧化的 DNA 碱基及脂质过氧自由基等，因而是防止活性氧自由基对生物体损伤的有力措施。以往的研究表明，茶多酚、维生素 C 等天然抗氧化剂对心脑血管疾病等具有预防和保护作用。利用脉冲辐解装置在如下几个方面对抗氧化剂进行了大量的研究工作：1)研究抗氧化剂与各种氧化性自由基的研究。2)研究抗氧化剂对受损伤的 DNA 及其碱基的修复过程。该结果揭示了抗氧化剂不仅可以通过竞争反应清除体内有害自由基，而且可以对已受损伤的生物分子进行快速修复，减轻有害自由基对生物体的损伤。3)研究抗氧化剂对受损伤的蛋白质及其氨基酸自由基的修复过程。这些研究可以为更好地了解和解释抗氧化剂在生物体内的作用机理提供理论基础。

The studies of antioxidative properties by pulse radiolysis

WANG Wenfeng YAO Side MIAO Jinling ZHAO Hongwei ZHU Hongping

Keywords Pulse radiolysis, Antioxidant, Kinetics, Free radical

Reactive oxygen species (ROS) have been known for their deleterious action primarily due to their reactions with critical biological substrates, resulting in aging and various disorder such as autoimmune disorders, cancer, arthritis and cardiovascular diseases. They can be produced in many ways. In biological systems, they are generally derived from molecular oxygen by phagocytes during respiratory burst, oxidative stress and during catalysis of oxidases as well.

Physiological antioxidant protection is invoked as one of the major defense mechanisms fighting free radical induced, mediated and promoted disorder. The proper function of the immune system appears to depend on the level of dietary antioxidants. With increasing environmental challenges, efficient prevention of damage requires maintenance of highest possible level of chemical defense agents that include all available antioxidants, ranging from various nutrients, such as polyphenols, to metabolites, such as uric acid and 5-hydroxytryptophan. The importance of an individual antioxidant in averting a particular pathological condition would depend on its availability at a site of oxidative challenges and its reactivity with damaging free radical oxidants.

The paper brief introduce the system of ps pulse radiolysis and its application, especially in antioxidants. The acid-base equilibrium constant of antioxidants was calculated. Using photolysis and radiolysis techniques, the reactions of oxidants (OH, $N_3^{\bullet}$, $Br_2^{\bullet-}$, $^1O_2$ and $O_2^{\bullet-}$) and reductants (e_{aq}^- and $^{\bullet}H$) with antioxidants in aqueous media were studied. From the studies of electron transfer from standards to semi-oxidized antioxidants, the one electron reduction potential of antioxidants was determined.

Martynoside 的激光光解与脉冲辐解研究

王文锋 苗金玲 姚思德 Suppiah Navaratnam B.J. Parsons

关键词 激光光解，脉冲辐解，自由基，还原电位

利用激光光解与脉冲辐解装置对 Martynoside 的抗氧化特性进行了研究，它与 $N_3^{\bullet}$ 和 $Br_2^{\bullet-}$ 反应在 360 nm 处生成瞬态产物，其反应速率常数分别为：3.9×10^9 和 4.1×10^8 $dm^3\bullet mol^{-1}\bullet s^{-1}$，瞬态产物的二级衰变反应速率常数为 1.2×10^8 $dm^3\bullet mol^{-1}\bullet s^{-1}$。$O_2^{\bullet-}$ 和 O_2 与 martynoside 的反应速率常数分别为：8.5×10^4 和 3.3×10^6 $dm^3\bullet mol^{-1}\bullet s^{-1}$；以芦丁为参比物测得其还原电位($MH^{\bullet}$/ MH)为 0.66 V vs. NHE。它与还原性粒子 e_{aq}^- 和 H 的反应速率常数分别为：1.8×10^{10} 和 7.0×10^9 $dm^3\bullet mol^{-1}\bullet s^{-1}$。

Antioxidative properties of martynoside: pulse radiolysis and laser photolysis study

WANG Wenfeng MIAO Jinling YAO Side Suppiah Navaratnam Parsons B J

Keywords Martynoside, Pulse radiolysis, Antioxidant, Free radical, Redox potential

Martynoside, a phenylpropaniod glycoside derivative, was studied thoroughly in the aqueous solution by laser photolysis and pulse radiolysis techniques. The acid-base equilibrium of martynoside was detected from the pH dependent changes of the UV absorption at 330 nm and 384 nm, respectively, pKa = 8.8. Martynoside reacted with radicals, $N_3^{\bullet}$ and $Br_2^{\bullet-}$, to form main transient absorption band with ε_{max}= 360 nm and k =3.9×10^{9} and 4.1×10^{8} $dm^3\bullet mol^{-1}\bullet s^{-1}$, respectively, and the decay by second order, $2k = 1.2\times10^{8}$ $dm^3\bullet mol^{-1}\bullet s^{-1}$. The reaction of $O_2^{\bullet-}$ and $^1O_2$ with martynoside were studied with k = 8.5×10^{4} and k = 3.3×10^{6} $dm^3\bullet mol^{-1}\bullet s^{-1}$, respectively. Reduction potential of the martynoside couple ($MH^{\bullet}$/ MH), determined using rutin as reference compound, gave a value E = 0.66V vs. NHE. Martynoside react with reducing species, e_{aq}^- and H, were studied with k = 1.8×10^{10} and k = 7.0×10^{9} $dm^3\bullet mol^{-1}\bullet s^{-1}$ respectively. The rate constant and the extinction coefficients of the transients have been reported.

没食子酸的激光光解研究

朱红平 张兆霞 赵红卫 王文锋 姚思德

关键词 没食子酸，激光光解，三线态，光电离

用时间分辨激光光解技术研究了没食子酸的水溶液和乙腈溶液的光物理性质，研究发现：在溶液中没食子酸光解发生光电离同时产生激发三重态，^{3}GA*的吸收在 320nm 处，在 0.05mM 时其寿命约为 0.31 μs；分别测定了 ^{3}GA*在水溶液和乙腈溶液中的衰变速率常数；观察到了 ^{3}GA*和富马腈之间的能量转移；以 KI 溶液为参照，测得 GA 的光电离量子产额为 0.12。

Laser flash photolysis studies on gallic acid

ZHU Hongping ZHANG Zhaoxia ZHAO Hongwei WANG Wenfeng YAO Side

Keywords Gallic acid, Photolysis, Triplet state, Photoionization

The photophysical properties of gallic acid (GA) have been studied by nanosecond laser flash photolysis with 266 nm laser in aqueous solution and acetonitrile. GA undergoes photoionization testified by the concomitant of hydrated electrons with a characteristic absorption band at 500 - 700nm. The intermediate ($\tau \approx 0.31$ μs in aqueous solution) with absorption at 320nm is identified as a excited triplet state (^{3}GA*) corroborated by different methods whose decay rates are obtained in aqueous

solution and in acetonitrile respectively. The triplet energy transfer from GA to fumaronitrile is observed. The quantum yield of photoionization is determined to be 0.12 at room temperature with KI as a reference compound.

脉冲辐解技术研究偶氮染料甲基橙水相降解的微观机理

刘士恒　汪世龙　孙晓宇　王文锋　王 敏　姚思德

关键词　甲基橙，脉冲辐解，瞬态图谱，自由基，降解机理

采用纳秒级脉冲辐解技术研究了偶氮染料甲基橙在水溶液中与羟基、水合电子、氢原子的反应，对反应产生的瞬态图谱作了归属，提出了相应的反应机理，并通过准一级动力学模拟，首次求得了甲基橙与这三个瞬态粒子的反应速率常数 3 研究表明：羟基、水合电子、氢原子均能破坏甲基橙中的偶氮’苯环的共轭基团，导致其脱色，羟基主要加成到甲基橙的偶氮键和带甲氨基的苯环上，形成相应的加成物；水合电子则主要进攻与磺酸根相连的苯环，生成的阴离子自由基迅速质子化成偕腙肼自由基；氢原子进攻甲基橙形成含肼撑结构的自由基， 甲基橙与羟基、水合电子、氢原子的反应速率常数分别为 5.7×10^{9}，7.2×10^{9} 和 1.2×10^{10} $dm^{3}\cdot mol^{-1}\cdot s^{-1}$ 这些结果将有助于人们进一步了解偶氮染料降解的本质，从而为该类染料废水的降解处理提供理论基础。

Mechanism studies on the degrdation of azo dye-methyl orange in aqueous solution using pulse radiolysis

LIU Shiheng　WANG Shilong　SUN Xiaoyu　WANG Wenfeng　WANG Min　YAO Side

Keywords　Methyl orange, Pulse radiolysis, Free radical, Degradation mechanism

The kinetics and mechanism of the reaction of azo methyl orange with OH, e_{aq-}, H in dilute aqueous solution have been studied using pulse radiolysis. It is shown that the three radicals can all destroy the conjudative system made up of azo group and aryl ring, resulting in the decoloration of methyl orange. OH radical mainly attacks the azo group and the aryl ring bearing methylamino group, forming corresponding OH-adducts. Under the attack of e_{aq-} methyl orange undergoes H^{+} catalyzed reduction, leading to the formation of hydrazyl radicals. H radicals mainly induce the reductive addition to methyl orange, producing hydrazo type radicals. The rate constants for the reaction of methyl orange with OH, e_{aq-}, H are $5.7x10^{9}$, $7.2x10^{9}$ and $1.2x10^{10}$ $dm^{3}mol^{-1}s^{-1}$ respectively. These results shed light on the degradation mechanism of hydrosoluble azo-dyes in aqueous solution and hence provide the theoretical foundation for the treatment of the water contaminated with such kind of compounds.

富勒醇对贻贝棘尾虫的辐射防护机制*

赵群芬[1,2] 诸 颖[2] 李宇国 刘瑞丽 徐晶莹[2] 李晴暖 李文新

关键词 富勒醇，辐射防护，贻贝棘尾虫，自由基

为了进一步了解富勒醇对贻贝棘尾虫γ辐射防护的机制，在先前工作基础上测定了 0.10 mg·ml^{-1} 的富勒醇存在下，剂量为 100—2000Gy 范围内贻贝棘尾虫辐照后第 5 天的存活率, 并用光学和透射电子显微镜观察了辐照后贻贝棘尾虫形态和超微结构的变化，测定了与自由基相关的酶的活性(超氧化物歧化酶 SOD 和过氧化氢酶 CAT)和脂质过氧化产物(丙二醛 MDA 和脂褐素 LIP)。结果表明，当剂量为 100—1500Gy 时，富勒醇能明显提高贻贝棘尾虫γ辐照后的存活率，当剂量达到 2000 Gy 时，富勒醇对存活率无明显影响，表明富勒醇对贻贝棘尾虫γ辐射防护作用不仅和它浓度有关，而且与γ辐射剂量相关。显微镜观察结果在细胞和亚细胞层次揭示了贻贝棘尾虫辐射损伤的结构特征，并给出了富勒醇防护作用的附加证据。未加富勒醇辐照组中 SOD 和 CAT 的活性低于对照组(p<0.01)，加富勒醇辐照组中 SOD 和 CAT 的活性明显高于辐照和对照组(p<0.01, p <0.01)，而加富勒醇辐照组中 MDA 和 LIP 的含量却显著低于对照组(p <0.01， p<0.05,) 和辐照组(p <0.01)，由此推断富勒醇主要通过清除自由基，刺激 SOD 和 CAT 的活性，同时减少细胞膜上的脂质过氧化反应，达到对贻贝棘尾虫的辐射防护作用。

---

1 浙江宁波大学生命科学与生物工程学院

2 中国科学院研究生院

Study of radioprotection mechanism of fullerenol for the stylonychia mytilus

ZHAO Qunfen[1,2] ZHU Ying[2] LI Yuguo LIU Ruili XU Jingying[2]

LI Qingnuan LI Wenxin

Keywords Fullerenol，Radioprotection，*Stylonychia mytilus*，Free radical

To understand more better the radioprotection mechanism of the fullerenol for the *Stylonychia mytilus,* the surviving fraction was counted at 100Gy—2000Gy as the concentration of fullerenol was 0.10mgml^{-1} on the fifth day after irradiation. Morphologic and superstructure change observed by the optician microscope and transmission electricity microscope. Superoxide dismutase (SOD), catalase (CAT), malondialdehyde (MDA), and lipofusion (LIP) levels were also measured. The results showed that fullerenols could obviously enhance the surviving fractions except for the highest γ-ray dose (2000Gy) level. It indicated that the radioprotection was both fullerenols concentration – and γ-ray doses –dependent. The results of microscope showed the character of irradiated damage for the celluar and subcelluar structure of the *Stylonychia mytilus,* and also gave the additional evidence of the radioprotection of fullerenol. The activity of SOD and CAT of the γ-irradiation group (γ) were lower

than that of the control group (p<0.01). Fullerenol obviously increased the SOD and CAT activities of the γ-irradiation+fullerenols group (γ+F) compared to those of the γ group and the control group (p <0.01, p <0.01, respectively). The MDA and LIP levels in the γ+F group significantly lower than the control group (p <0.01, p <0.05,respectively) or the γ group (p <0.01). The findings of the study indicated fullerenols have a good protection for the *Stylonychia mytilus* exposed to γ-rays. The protective effect of the fullerenols on damage induced by γ-rays seems to be mediated through their antioxidantive and radical scavenger activities.

富勒醇对不同原生动物的毒性作用

赵群芬[1,2] 诸 颖[2] 冉铁成[2] 徐晶莹[2] 李晴暖 李文新

关键词 富勒醇，原生动物，毒性

研究富勒醇对贻贝棘尾虫和四膜虫生长的影响，结果显示随着富勒醇浓度的增加，两种生物体的存活率都呈下降趋势，贻贝棘尾虫的存活率随着时间的增加而减少，四膜虫的存活率随着时间的增加却有增加的趋势。荧光染料吡啶橙染色方法观察到富勒醇浓度为 0.25mg·ml^{-1} 时均能导致贻贝棘尾虫和四膜虫的大核受到不同程度的损伤。这可能是导致虫体存活率降低的原因之一。检测体内抗氧化酶和脂质过氧化产物的结果显示高浓度的富勒醇导致贻贝棘尾虫体内抗氧化酶的活性降低，脂质过氧化产物增加，推测这也是高浓度的富勒醇对细胞造成损伤的原因之一。

1 浙江宁波大学生命科学与生物工程学院， 2 中国科学院研究生院

Cytotoxicity of fullerols to different species of ciliated protozoan

ZHAO Qunfen[1,2] ZHU Ying[2] RAN Tiecheng[2] XU Jingying[2]

LI Qingnuan LI Wenxin

Keywords Fullerenol, Protozoan, Cytotoxicity

With increasing utility of fullerenes and its derivatives in many of fields, the toxicity and effects of fullerenes on human and environment have received a potent attention. In this work cytotoxicity of fullerol on two species ciliated protozoan *Tetrahymena pyriformis* and *Stylonychia mytilus* was studied. Cell growth inhibition was evaluated by the colorimetric MTT assay for *Tetrahymena pyriformis*. For the *Stylonychia mytilus*, all surviving cells were counted each day with an optical microscope after treatment and the surviving fractions were calculated. Morphologic and superstructure change were observed by the optician microscope and transmission electricity microscope (TEM). Agarose gel electrophoresis of DNA and comet assay were also used to measure the toxicity of the different

concentration of the fullerol. The result showed that high concentration of fullerol exhibited a dose-dependent inhibition to the cells, whereas low concentration of fullereol did not show the toxicity on the cells.

碳纳米管(CNTs)与贻贝棘尾虫的相互作用和毒性研究

诸 颖[2] 赵群芬[1,2] 蔡小青[2] 李宇国 李文新

关键词 贻贝棘尾虫, 碳纳米管(CNTs), 毒性， 存活率，大核

本工作用显微技术观察了贻贝棘尾虫对碳纳米管(CNTs)的摄取以及虫体分裂时 CNTs 在其体内的分布，代谢和再分布过程，测定了 0.1、0.5、1.0、5.0、10、50 和 200μgml^{-1} 7 个浓度的 CNTs 与贻贝棘尾虫存活率的响应曲线，发现加 CNTs 后第 5 天虫体的存活率分别为 111%、107%、75%、70%、53%、43%、38%左右，表明高浓度的 CNTs 对细胞的生长有浓度依赖的抑制作用，而当浓度降至足够低时，CNTs 对细胞的生长有促进作用，而用石墨做同样处理的细胞则显示正常；在此基础上用 PI 染色的方法初步探讨了高浓度 CNTs 对细胞生长产生抑制作用的原因，荧光显微镜观察结果显示 CNTs 损伤了贻贝棘尾虫大核和膜的正常生理功能。用电镜对细胞超微结构分析结果显示，高浓度的 CNTs 损伤了贻贝棘尾虫的大核，小核和线粒体。

1 浙江宁波大学生命科学与生物工程学院

2 中国科学院研究生院

The interaction of CNT with stylonychia mytilus and its toxicity

ZHU Ying[2] ZHAO Qunfen[1,2] CAI Xiaoqing[2] LI Yuguo LI Wenxin

Keywords *Stylonychia mytilus*, Carbon nanotubes(CNTs), Toxicity, Surviving fraction, Macronucleus

The uptake of CNTs by *stylonychia mytilus*，biodistribution, metabolism, and redistribution during dividing process of the cells were observed with optical microscope. The dose-effect relationship of surviving fraction of *stylonychia mytilus* was measured for the concentrations of the CNTs ranging from 0.1μgml^{-1} to 200μgml^{-1}. It was found that high concentration of CNTs exhibited a dose-dependent inhibition to the cells, whereas very low concentration of CNTs stimulated the growth of the cells, however, cells treated with graphite appeared normal. To undersdand the inhibition from the CNTs, cell morphology of control and performed was studied by using propidium iodide staining (PI). Fluorescent micrograph showed that the damage was occurred on the macronucleus and membrane of the cells. The superstructure change of cells obtained by electron microscope showed that high concentration of CNTs

destroyed the macronucleus，micronucleus and mitochondrion of *stylonychia mytilus*.

1 Cology of life science and bioengineering, Ningbo University

2 Chinese Academy of Science

富勒醇在由紫外光照射四膜虫诱导的氧化应急反应中的保护作用

赵群芬[1,2] 诸 颖[2] 冉铁成[2] 徐晶莹[2] 李晴暖 李文新

关键词 紫外光，四膜虫，氧化应急，富勒醇

细胞受到紫外光照射产生的活性氧(ROS)对细胞的结构造成损伤，而抗氧化剂可以抑制这种反应的发生。本实验主要运用 MTT 法检测和比较了在有富勒醇存在下，紫外辐照后四膜虫细胞的存活率，并测定了紫外辐照前后，富勒醇对细胞内丙二醛(MDA)，超氧化物歧化酶(SOD)，过氧化氢酶 (CAT) 谷胱甘肽(GSH)， 谷胱甘肽还原酶(GR)和 谷胱甘肽过氧化物酶(GSH-PX)的影响，结果显示，富勒醇能提高受紫外辐照后细胞的存活率，并且可能是通过刺激细胞内抗氧化酶的活性，减少脂质过氧化产物来减小紫外辐射对细胞的损伤。

1 浙江宁波大学生命科学与生物工程学院

2 中国科学院研究生院

The protective effect of fullerenol against ultraviolet induced oxidatives stress in *Tetrahymena pyriformis*

ZHAO Qunfen[1,2] ZHU Ying[2] RAN Tiecheng[2] XU Jingying[2]

LI Qingnuan LI Wenxin

Keywords Ultraviolet, *Tetrahymena pyriformis,* Oxidative stress, Fullerenol

Ultraviolet light exposed cells can induce the production of reactive oxygen species (ROS) which can damage the cellular elements. Antioxidants can interfere with the production of ROS. In this study, malondialdehyde(MDA), superoxide dismutase (SOD), catalase (CAT)reduced glutathione (GSH), Glutathione Reductase (GR) and glutathione peroxidase (GPx) levels were measured in the *Tetrahymena pyriformis* exposed to UV light at same dose. The effects of fullerenol as antioxidant were determined by those parameters. Cell growth inhibition was evaluated by the colorimetric MTT assay for *Tetrahymena pyriformis* after irradiation of 24 h and 48 h. *Tetrahymena pyriformis* were divided into

three groups as control, ultraviolet (UV) and ultraviolet+ fullerenol (UV+F). This study demonstrated that the exposure to UV led to oxidative stress as reflected by increased MDA levels and reduced enzymic antioxidant levels, fullerenol may be useful by reducing or preventing photobiologic damage.

1 Cology of life science and bioengineering, Ningbo University

2 Graduate school of the Chinese Academy of Sciences

三碘苯酚乙基纤维素微球的制备

刘瑞丽　李宇国　李晴暖　李文新

关键词　微球，造影剂

为提高造影剂的颗粒度，减少血池造影剂透过血管壁向组织间质渗出，影响血池造影剂的造影效果，采用液中干燥法(In-liquid drying method)制备了三碘苯酚乙基纤维素微球。具体制备及检测方法为：将不同比例的三碘苯酚和乙基纤维素(W/W 2:1，1:1，1:2)溶于适量二氯甲烷，加入到 3%的 PVA 水溶液中，12000 r/min 乳化 3 min，低速搅拌 20 h 使二氯甲烷挥发。放置 1—3d，使杂质沉降，同时有部分较大的颗粒也沉降在底部，弃去沉淀物，将乳白色悬浮液 12000 r/min 高速离心，得白色颗粒， 40℃真空干燥得到三碘苯酚乙基纤维素微球的白色粉末。

通过 SEM 检测了微球的形貌，发现药物与载体的比例为 1:2 和 1:1 时，所得微球的形貌较好，其中比例为 1:2 时，形成的微球形状较为规整，为圆球形，上有小的孔洞，比例为 1:1 时，所得微球中有部分形貌规整，为圆球形，上有小的孔洞，还有一部分微球上的孔洞较大而多，更有一些为不规则形状。比例为 2:1 时，所得微球形状极为不规则。用激光粒度仪检测了微球的粒径，发现随着 TIP:EC 比例的增加,所得微球的平均粒径逐渐增大，TIP:EC 比例越大，得到的较大粒径的微球所占比例越高，反之，TIP:EC 比例越小，得到的较小粒径的微球所占比例越高。总之，三碘苯酚与乙基纤维素的比例对微球成球性和粒径有一定的影响，两者的比例为 1:2 时成球性最好，所得微球为规整的球形，微球粒径最小，平均粒径 D50 为 3.68 μm。

Preparation of 2,4,6-triiodophenol microspheres with ethylcellulose

LIU Ruili　LI Yuguo　LI Qingnuan　LI Wenxin

Keywords　Microsphere, Contrast agent

In this paper, 2, 4, 6-triiodophenol-ethylcellulose-microsphere was developed by in-liquid drying method, in order to increase the granularity of the X-ray CT contrast agent and to prevent the blood vessel X-ray CT contrast agent from exuding through the vascular wall to the tissue. The influnces of

the composition ratio of 2, 4, 6-triiodophenol, ethylcellulose to the microspheres' shape and diameter, and the entrapment of 2, 4, 6-triiodophenol were studied. It was found that when the composition ratio was 1∶2, the microspheres' shape was round, the average diameter was only 3.68μm, and the entrapment of 2, 4, 6-triiodophenol was 41.4%.

固态多环芳香烃化合物的 THz 时域光谱研究

徐 慧 韩家广 余笑寒 吉 特 张增燕 李晴暖 李文新 朱志远

关键词 时域光谱，晶格振动，同分异构体

利用太赫兹(terahertz，THz)时域光谱室温下对芳香烃化合物萘、二联苯、蒽、α-萘酚和 β-萘酚在 0.1—2.2THz 频谱范围内进行了光谱测量。结果表明，多环芳香烃化合物在此波段有不同的吸收特征。对于不能形成氢键的三个化合物萘、二联苯和蒽在 2.0 THz 附近均有一吸收峰，这可能是由于分子之间的振动即晶格振动所引起的，对于能够形成氢键的化合物 α-萘酚和 β-萘酚，我们把他们的吸收峰归结于分子间氢键的相互作用所引起的集体振动模式。THz 时域光谱不仅能够鉴别分子结构存在微小差别的化合物而且还能鉴别同分异构体。

THz time-domain spectroscopy of polyring aromatic compounds in solid phase

XU Hui HAN Jiaguang YU Xiaohan JI Te ZHANG Zengyan

LI Qingnuan LI Wenxin ZHU Zhiyuan

Keywords Time-domain spectroscopy, Lattice vibrations, Isomer

We measured the absorption spectra of naphthalene, biphenyl, anthracene, α-naphthol and β-naphthol of aromatic compounds by terahertz time-domain spectroscopy over the frequency range from 0.1 to 2.2 THz at room temperature. We found different polyring aromatic compounds showed distinct characteristic spectra in the THz region. In crystals without hydrogen bonds the absorption may be assigned to lattice vibrations. In crystals with hydrogen bonds, there appears more absorption peaks between 1.1 THz and 1.6 THz. We contributed them to collective vibrational modes of hydrogen bonds networks. Terahertz time-domain spectroscopy can identify not only compounds with similar chemical constituents but also isomeric compounds.

基于生物识别调控供体-受体距离的生物传感器

武海萍　徐 慧　樊春海

关键词　生物传感器，供体–受体距离

生物分子识别为生物传感器研究提供了基础。我们提出了基于通过生物分子识别调控电子/能量转移来进行生物传感的新策略。电子/能量转移效率高度依赖于供体－受体距离。生物识别产生与之偶联的分子构象变化，这一距离相关过程为基于光电检测的生物传感器提供了一个可行思路。

Biosensors based on binding-modulated donor-acceptor distances

WU Haiping　XU Hui　FAN Chunhai

Keywords　Biosensor, Donor-acceptor distance

The promising recognition characteristics exhibited by biomolecules have motivated significant interest in biomolecule-based sensor strategies. Here we propose biosensor designs utilizing modulated electron or energy transfer to a bio-specific ligand as the signaling mechanism. The efficiencies of both electron transfer and energy transfer are strongly dependent on donor-acceptor distance. When coupled with the large conformational changes sometimes associated with biomolecular recognition, these distance-dependant processes provide a robust means of generating optical and electronic signals.

富勒醇对γ-射线辐照贻贝棘尾虫保护作用的研究

赵群芬[1]　李宇国　刘瑞丽　徐晶莹　李文新

关键词　贻贝棘尾虫，γ-射线，富勒醇，辐射防护，存活率

本工作测定了 ^{60}Co γ 射线 6 个辐照剂量(100Gy、300Gy、500Gy、800Gy、1200Gy、1500Gy)与贻贝棘尾虫存活率响应曲线，发现辐照后第 5 天虫体的存活率分别下降到 47%、18%、16%、8%、5%和 3%左右。在此基础上本文重点研究了在富勒醇存在下，^{60}Co γ 射线对贻贝棘尾虫的辐射损伤，结果表明在高、低剂量下富勒醇对虫体均产生保护作用，能明显提高贻贝棘尾虫受照射后的存活率，并且这种辐射防护作用与富勒醇浓度相关。富勒醇对贻贝棘尾虫的辐射防护可能基于其对自由基的清除反应，因而可能是一种潜在的辐射防护剂。

---

1 浙江宁波大学生命科学与生物工程学院

The radioprotection of fullerenols against the *Stylonychia mytilus* exposed to gamma-rays

ZHAO Qunfen[1] LI Yuguo LIU Ruili XU Jingying LI Wenxin

Keywords *Stylonychia mytilus,* Fullerenols, γ-rays, Radioprotection, Survival fraction

The dose-effect relationship between the gamma-ray and the surviving fraction of *Stylonychia mytilus* were studied. The Cells were exposed to ^{60}Co γ-rays at 6 doses of 100, 300, 500, 800, 1200 and 1500 Gy. The results showed that the surviving fraction of each doses decreased to about 47%、18%、16%、8%、5% and 3% with the increase of the dose on the fifth day after irradiation. Based on this, the radioprotection of fullerenols against the *Stylonychia mytilus* exposed to ^{60}Co γ-rays was also studied. The results showed that the surviving fraction increased significantly both at the high and low doses compared with the samples without fullerenols. The radioprotection was dependented on the concentration of fullerenols. The findings of the study indicated that fullerenols, as a potential radioprotection compound, could scavenge the free radical and reduce the damage of the cells from the γ-ray radiation.

1 Cology of life science and bioengineering, Ningbo University

共轭聚电解质层层组装膜的光谱学研究

武海萍 徐 慧 樊春海

关键词 共轭电解质，荧光膜

我们系统研究了荧光共轭聚电解质的层层组装膜的性质。研究表明，共轭聚电解质在层层组装过程中的荧光特性高度可调控，可以制备出具有高发光强度的组装膜，同时膜的荧光能被天然电子传递蛋白质细胞色素 c 通过电子传递过程有效猝灭。

Spectroscopic interrogation of layer-by-layer assembled films of conjugated polyelectrolytes

WU Haiping XU Hui FAN Chunhai

Keywords Conjugated polyelectrolyte, Luminescent film

We studied layer-by-layer fluorescent conjugated polyelectrolytes films. The photoluminescence of

conjugated polyelectrolytes was observed to be highly tunable during this film assembly process. We also observed efficient photoinduced electron transfer from thus prepared highly luminescent film to a natural electron-transfer protein cytochrome.

C60 吡咯烷苯氮芥的合成和放射性碘标记

冉铁成　刘瑞丽　尹娟娟　李晴暖　朱建华[1]　李文新

关键词　1，3 偶极环加成，C_{60} 吡咯烷苯氮芥，同位素标记，碘-125

利用 1，3 偶极环加成反应合成了带有抗癌活性药物基团的富勒烯衍生物 C_{60} 吡咯烷苯氮芥。用 ^{1}H NMR，UV，IR 进行了结构表征，在此基础上对其碘化后通过同位素交换的方法完成 C_{60} 吡咯烷苯氮芥的放射性 ^{125}I 标记，研究了标记率与反应时间和反应温度的关系，得到了对 C_{60} 吡咯烷苯氮芥进行碘标记的最佳条件，放射性碘标记率可达 94％。

1 复旦大学药学院

Synthesis and radioiodination of fullerene pyrrolidine benzoyl nitrogen mustard

RAN Tiecheng　LIU Ruili　YIN Juanjuan　LI Qingnuan　ZHU Jianhua[1]　LI Wenxin

Keywords　1,3 dipole[3+2] cycloaddition reaction, radioiodination, iodine-125, fullerene pyrrolidine benzoyl nitrogen mustard

The purpose of this article is to study the synthesis and radioiodination of the fullerene derivative including active antitumor groups. The fullerene pyrrolidine benzoyl nitrogen mustard was synthesized by the three-component reaction of fullerene, N-methylglycine and N,N-bis(2-chloroethyl)-4-aminobenzaldehyde through 1,3 dipole[3+2] cycloaddition reaction. Its chemical structure was characterized by the spectroscopic data. The compound synthesized, after connecting with the stable iodine, was radiolabeled with iodine-125 through isotope exchange. Dependence of the radiolabeling yields on the reaction temperature and exchange-time was examined. The results showed that the radiolabeling yield of fullerene pyrrolidine benzoyl nitrogen mustard was as high as 94 % after heating for 2 h at 130℃.

1 School of Pharmacy, Fudan University

放射性食管支架的制备

吴胜伟 李文新

关键词 食管癌，放射性支架，碳纳米管

中国局部地区食管癌发病率很高，患者食道狭窄，进食困难。在食管中植入支架能恢复患者的吞咽能力，但只能起到机械支撑作用，对病情改善没有作用。在支架上涂上放射性物质，能通过射线对癌细胞的杀伤作用起到抑制肿瘤组织的生长进而提高生存期的目的。实验中使用两种涂膜工艺，制备了 ^{32}P 支架和 ^{125}I 支架，并对支架在生理盐水中的泄漏情况进行了研究，同时对碳纳米管在支架材料中的应用进行了初步的探讨。支架的动物实验研究也在进行之中。

The preparation of radioactive esophageal stents

WU Shengwei LI Wenxin

Keywords Esophageal cancer, Radioactive stent, Cabon nanotube

Esophageal cancer is a serious disease in China. Excellent palliative relief from dysphagia has been obtained by using self-expandable stents. These devices can improve swallowing difficulty effectively but long-term survival cannot be expected because a cytoreduction effect cannot be achieved. When a self-expandable metallic stent is covered with a membrane and the membrane incorporates a potent radionuclide, relief from dysphagia can be achieved. In the experiments, ^{32}P stents and ^{125}I stents were prepared by two methods. The leak rate of the stents in saline water was also investigated. The application of carbon nanotubes in the stents was studied at the same time. The animal experiments were on going.

富勒醇对 ^{60}Co-γ 致小鼠损伤的防护作用

蔡小青 李宇国 刘瑞丽 吴胜伟 叶 波 冉铁成 郭金学 徐 慧 李文新

关键词 富勒醇，辐射保护作用

研究富勒醇对 $^{60}Co\ \gamma$ 损伤的防护和恢复治疗作用及机制。分别在辐照前和辐照后给小鼠腹腔注射富勒醇，$^{60}Co\ \gamma$ 射线全身均匀照射，吸收剂量 5.0 Gy，测定小鼠体重、脾指数、胸腺指数、血象和 SOD 含量的变化；取小鼠脾脏并制成脾细胞悬液，应用流式细胞仪(FCM)检测脾脏细胞的周期。辐照损伤后小鼠体重减轻、脾指数和胸腺指数降低、血象中各项指标下降、脾脏细胞周期中 S 期所占的比例升高。富勒醇可促进上述指标不同程度的恢复，并使脾脏细胞周期中 S 期恢复正常，加速了脾脏细胞的分裂增殖，从而使脾细胞能较快的得到修复。富勒醇对 $^{60}Co\ \gamma$ 辐照小鼠具有一定的防护和恢复治疗的作用。

Experimental studies of the radioprotective effect of fullerenol in ^{60}Co-γ radiation-injured mice

CAI Xiaoqing LI Yuguo LIU Ruili WU Shengwei YI Bo
RAN Tiecheng GUO Jinxue XU Hui LI Wenxin

Keywords Fullerenol, Radioprotective effect

To investigate the radioprotective effect of fullerenol, the ICR rats were given fullerenol intraperitoneally (i. p.) before and after whole-body ^{60}Co γ-ray irradiation with 5.0Gy. The change in body weight, index of spleen, index of thymus, peripheral blood counts and SOD activity were observed. Cell cycle of splenoeytes was detected with flow cytometry (FCM). fullerenol showed significant radioprective effect on irradiated mice including increasing the weight of mice, protecting normal immune function of spleen and thymus, curing the decreasing of white blood cell and platelet counts. Fullerenol also redused S phase ratio,promoted spleen cell division and proliferation. fullerenol had efficient capacity of radioprotection.The possible mechanism of the radioprotective effect of fullerenol were discussed in this paper.

固态氨基酸的 THz 时域光谱研究

徐 慧 余笑寒 张增燕 韩家广 李晴暖 李文新

关键词 THz 时域光谱，固态氨基酸

利用太赫兹(terahertz，THz)时域光谱室温下对手性对映体 D-酪氨酸、L-酪氨酸、外消旋化合物 DL-酪氨酸和 D-色氨酸、L-色氨酸、外消旋化合物 DL-色氨酸在 0.1-2.0THz 频谱范围内进行了光谱测量。结果表明，氨基酸在此波段有特征吸收峰，THz 时域光谱能够鉴别对映异构体和他们的外消旋化合物。

THz time-domain spectroscopy of solid amino acids

XU Hui YU Xiaohan ZHANG Zengyan HAN Jiaguang LI Qingnuan LI Wenxin

Keywords THz time-domain spectroscopy, Solid amino acid

We measured the absorption spectra of chiral compounds of D, L, DL-tyrosine and D, L DL-tryptophan by terahertz time-domain spectroscopy over the frequency range from 0.1 to 2.0 THz at room temperature. We found six amino acids showed distinct fingerprint spectra in the THz region. Our result also suggests that we can identify the enantiomers and their racemic compounds by measuring the absorption spectra in the THz region.

多壁碳纳米管γ辐照后的化学修饰

郭金学　李宇国　吴胜伟　李文新

关键词　多壁碳纳米管，γ辐照，化学修饰

经过γ辐照后的多壁纳米碳管经羧基化后利用癸胺进行化学修饰。每一步化学修饰后的产物都用FTIR and RAMAN进行表征。对最终可溶性碳管的元素和热重分析显示，由于γ光子对碳管表面的损伤效应，连接到碳管表面的官能团数量随着辐照剂量的增加而增加。而辐照后多壁碳管在甲苯和四氢呋喃的溶解度同未辐照的相比溶解度有显著的增加。这一结果为功能化修饰多壁碳管的应用提供了新的途径。

Effects of gamma-irradiation dose on chemical modification for multi-wall carbon nanotubes

GUO Jinxue　LI Yuguo　WU Shengwei　LI Wenxin

Keywords　MWNT, g-irradiation, Modification

Multi-walled carbon nanotubes (MWNTs), after irradiation with γ-rays, were subjected to chemical modification with thinychloride and decylamine. Products from each chemical treatment were characterized by FTIR and RAMAN spectra. Element and TGA analyses for the modified soluble MWNTs indicated that the concentration of functional groups bound in MWNTs increased with increasing radiation does, due to the increasing defects created on the MWNTs by γ-photons. The solubilities of gamma- irradiated MWNTs in acetone and DMF enhanced considerably compared with those unirradiated. The results provide a novel approach to various functionalized modification of carbon nanotubes.

新型含磷[60]富勒烯二聚体的合成，表征及性质研究

尹娟娟　李文新

关键词　富勒烯二聚体，AFM

利用过量的α-环烷氨基二膦酸酯在碱性条件下与C_{60}反应可方便快速的得到单碳桥的C_{60}二聚体。产物经过^{1}HNMR、^{31}PNMR、^{13}CNMR、FT-MALDI-MS、FT-IR、UV-Vis、DEPT、HMBC等光谱手段确定了它们的分子结构。通过AFM直接观测到了单个二聚体分子，并且其分子尺寸与理论值相一致。阻止实验证明该反应为自由基参与的亲核反应。

Synthesis and characterization of novel [60]fullerene dimer

YIN Juanjuan LI Wenxin

Keywords Fullerene dimer, AFM

Novel carbon bridged fullerene dimmers (HC_{60}-CR_2-$C_{60}H$ type) were obtained by the reaction of aminomethylenebispho-sphonate and [60]fullerene in high yield within three minutes at room temperature, and fully characterized by ^{31}P, ^{1}H, ^{13}C NMR, HMBC, DEPT, MALDI mass, UV-Vis, IR spectroscopy. They are stable in air in spite of steric effect. A single dimer molecule was observed clearly using AFM and the average molecular size of the dimer is very consistent with caculated molecular geometry. The reaction can be partly inhibited by hydroquinone which demonstrats a radical process is also involved.

新型含磷[70]富勒烯二聚体的合成，表征及性质研究

尹娟娟 李文新

关键词 富勒烯二聚体，电子相互作用

利用过量的α-环烷氨基二膦酸酯在碱性条件下与 C_{70} 反应可方便快速的得到单碳桥的 C_{70} 二聚体。产物经过 ^{1}HNMR、^{31}PNMR、^{13}CNMR、FT-MALDI-MS、FT-IR、UV-Vis、DEPT、HMBC 等光谱手段确定了它们的分子结构。其化学性质稳定。电化学研究表明在两分子的富勒烯分子存在电子的相互作用。

Synthesis and characterization of novel [70]fullerene dimer

YIN Juanjuan LI Wenxin

Keywords Fullerene dimmer, Electronic interaction

Novel carbon bridged fullerene dimers(HC_{70}-CR_2-$C_{70}H$ type) were obtained by the reaction of aminomethylenebispho-sphonate and [70]fullerene in high yield within three minutes at room temperature, and fully characterized by ^{31}P, ^{1}H, ^{13}C NMR, HMBC,DEPT, MALDI mass, UV-Vis, IR spectroscopy. They are stable in air in spite of steric effect. The reaction can be partly inhibited by hydroquinone which demonstrats a radical process is also involved. The cyclic voltammetry on the dimer indicated the presence of an electronic interaction between the two fullerene cages upon the electrochemical reduction.

碳纳米管-氧化铁复合材料的制备

吴胜伟　李文新

关键词　碳纳米管，均相沉淀，Fe_3O_4，Fe_2O_3

使用均相沉淀方法制备了碳纳米管-α-Fe_2O_3 复合材料，用共沉淀的方法制备了不同碳纳米管掺量的碳纳米管-四氧化三铁复合材料，分别用扫描电镜、透射电镜、X 射线衍射分析等方法对制备的材料进行了表征。发现 α-Fe_2O_3 颗粒均匀分布在碳纳米管上，而另一样品中碳纳米管上也有 Fe_3O_4 分布。用磁强计对碳纳米管-四氧化三铁复合材料的磁学性质进行了检测，结果表明，在四氧化三铁中掺加少量的碳纳米管能明显提高其磁学性质。

The preparation of carbon nanotubes based Fe_2O_3 and Fe_3O_4 materials

WU Shengwei　LI Wenxin

Keywords　Carbon nanotubes, Homogenous precipitation, Fe_3O_4, Fe_2O_3

Carbon nanotubes based Fe_2O_3 was prepared by homogenous precipitation method. The samples were characterized by SEM, TEM and XRD. It can been seen that α-Fe_2O_3 particles were distributed equably on the walls of carbon nanotubes. Carbon nanotubes based Fe_3O_4 materials with various content of carbon nanotubes were also prepared. The samples were characterized by SEM, TEM and XRD too and Fe_3O_4 particles can be found on the walls of carbon nanotubes. The magnetic properties of CNTs-Fe_3O_4 materials were tested by magnetometer. The results showed that the magnetic property of Fe_3O_4 could be improved when a small quantity of carbon nanotubes were added to it.

同位素示踪法在碳纳米管填充中的应用

吴胜伟　郭金学　李玉兰　李文新

关键词　放射性示踪法，纳米碳管，填充

应用放射性核素 $^{110}Ag^m$ 和 ^{125}I 示踪技术，对氧化开口后的碳纳米管(CNTs)分别用 $AgNO_3$ 和 NaI 溶液填充并洗涤，研究它们在水溶液中从碳纳米管中的释放情况；用高分辨透射电镜(HREM)、扫描电镜(SEM)、x 射线线衍射(XRD)、x 射线能量散射谱(EDS)对 CNTs 的填充情况进行了表征；根据放射分析测量结果计算了 CNTs 内部样品的填充量。结果表明，CNTs 腔内有材料填充，填充的 NaI 在水溶液中会缓慢释放出来而 $AgNO_3$ 则不会释放，放射性核素示踪技术能有效地应用于 CNTs 的填充、释放等行为的研究及材料填充量的定量测定。

Study of filling behaviors of carbon nanotubes by radioactive trace technique

WU Shengwei GUO JinXue LI Yulan LI Wenxin

Keywords Radioactive trace technique, CNTs , Filling

The behaviors of washing and elution, following soak of opened carbon nanotubes (CNTs) filled with radioactive (^{125}I) NaI and (^{110m}Ag) $AgNO_3$ solutions were investigated with radioactive trace technique. The observations with high-resolution electron microscopy (HREM) and X-ray energy dispersive spectroscopy (EDS) showed the validity of filling the soluble inorganic salts into the CNTs by the simple method. Great difference of release of (^{125}I) NaI and (^{110m}Ag)$AgNO_3$ from CNTs was found and discussed by chemical transformation which occurred in the cavity of the CNTs. The amount of filled materials could also be estimated by the trace technique.

富勒醇对不同细胞系的细胞毒性研究

徐晶莹 李晴暖 李宇国 李文新

关键词 富勒醇，胞吞作用，细胞毒性

通过中国仓鼠卵巢细胞系(CHO)和小鼠黑色素瘤细胞系(B16)，观测富勒醇的细胞毒性。在 96 孔板内，每孔接种 1000 个细胞，细胞融合度达到 75％时，梯度加入不同终浓度的富勒醇样品。在 5％CO_2,37℃培养 48h。使用 MTT 检测法，通过细胞毒性检测，计算出半数致死量(LD_{50})。结果表明，B16 细胞系比 CHO 细胞系对富勒醇更敏感。我们推测，这个现象很可能是由于细胞胞吞能力的不同造成。

The Cytotoxicity of fullerenol in different cells

XU Jingying LI Qingnuan LI Yuguo LI Wenxin

Keywords Fullerenol, Endocytosis, Cytotoxicity

To evaluate the cytotoxicity of fullerenol, a derivation of fullerene, two cells, Chinese hamster ovary cell (CHO) and murine melanoma cell (B16) were cultured. About 1000 cells were added into each well of a 96-well plate. Cells were grown to 75% confluency before the different concentration of fullerenol was added. The cells were incubated in 37℃/5% CO_2 for 48 h. The LD_{50} value was determined for evaluating cytotoxicity. The cytotoxity was measured using MTT assay. Taken together, the data demonstrate the B16 cell is more sensitive to fullerenol than CHO cell. We postulate that the induction of cytotoxity effect caused by the fullerenol is primarily depended upon their ability of endocytosis.

富勒醇在γ射线辐照下的细胞生物效应研究

李宇国 倪 瑾[1] 高建国[1] 韩 玲[1]

赵群芬 徐晶莹 李文新

关键词 富勒醇，γ 辐照，辐射保护

用 MTT 法测定了富勒醇对 K562 细胞的辐射防护作用以及乏氧条件下富勒醇对 K562 细胞的辐射防护作用。在实验中发现，富勒烯的水溶性衍生物富勒醇对细胞具有辐射防护作用，并且富勒醇对辐照细胞的保护作用与乏氧或有氧条件有密切的联系。

采用南京建成生物医学工程研究所的 MDA 试剂盒、SOD 试剂盒和活性氧试剂盒，测定了富勒醇对辐照细胞的 MDA、SOD 和活性氧的影响。实验结果显示，富勒醇显著提高 γ辐照后细胞的 SOD 活力，也即富勒醇作为辐射防护剂时能够提高细胞内的 SOD 活性，增强细胞的抗辐射能力。富勒醇对 γ辐照后细胞抑制活性氧的能力的影响并不显著，说明富勒醇对受辐照细胞的防护中并没有影响这些酶的活力。富勒醇降低了细胞 γ辐照后细胞的 MDA 含量，能够保护辐射产生的自由基对细胞膜的损伤。富勒醇有望作为辐射防护剂。

1 第二军医大学放射医学教研室

The effect of fullerols under γ on cell

LI Yuguo NI Jin[1] GAO Jianguo HAN Ling[1] ZHAO Qunfen

XU Jingying LI Wenxin

Keywords Fullerenols, γ radiation, Radioprotection

Using MTT method, three kinds of cells (L02 cells, K562 cells and murine thymocytes) were used to examine the γ radioprotective effects of fullerenols. The SOD, ROS (reactive oxygen species) and MDA were measured with chemistric colorimetry and cell cycles were also detected with flow cytometry (FCM). The results showed that fullerenols had certain protection to all three kinds of cells and the protective effects increased with the increase of radiosensitivity of cells, the ablities of fullerenols's protection were more distinct in hypoxic irradiation than in aerobic irradiation. Fullerenols also affected the cell cycles and the activities of SOD under γ irradiation. The radioprotective effects of fullerenols may be explained by fullerenols's character of scavenging $OH^{\bullet}$ and $O_2^{-\bullet}$.

1 Radiation Medicine Department, Second military Medical University

稀有三环核苷衍生物与羟基自由基快速反应动力学及理论计算

赵红卫 孔 玲 刘永彪 江致勤[1] 马允胜[2] 姚思德

关键词 稀有三环核苷衍生物，脉冲辐解，自由基，理论计算

运用脉冲辐解瞬态吸收光谱技术研究了稀有三环核苷衍生物 N-4-去甲基-wyosine(dYt)与•OH 自由基快速反应的动力学。结合 AM1 及 B3LYP/6-31G**方法对•OH 进攻 dYt 各位置形成的可能加成产物进行结构优化及热力学能量计算，阐述了反应的自由基机理，预测了可能的自由基加成产物。

1 同济大学化学系， 2 国家高性能计算中心

Fast reaction kinetics of •OH with the derivative of rare tricyclic nucleoside and theoretical calculation

ZHAO Hongwei KONG Ling LIU Yongbiao JIANG Zhiqin[1]
MA Yunsheng[2] YAO Side

Keywords Rare tricyclic nucleoside derivative, Pulse radiolysis, Radical, Theoretical calculation

Fast reaction kinetics of •OH with N-4-desmethylwyosine (dYt), a derivative of rare tricyclic nucleoside has been studied by using pulse radiolysis. The possible initial transient radicals of •OH adducts of dYt were studied by use of AM1 (with geometry optimization) and B3LYP/6-31G** (calculation of total energy). The radical reaction mechanism and the possible structure of OH-adducts were discussed and predicted.

核黄素与血清蛋白作用的光谱学研究

赵红卫 葛 敏 张兆霞 王文锋 吴国忠

关键词 核黄素，血清白蛋白，内源性荧光，荧光猝

用紫外吸收光谱和荧光发射光谱研究了核黄素与血清白蛋白水溶液的相互作用。核黄素能够有效地猝灭血清白蛋白 350nm 处内源性的荧光，猝灭机制包含静态猝灭和动态猝灭。获得了核黄素与血清白蛋白结合的数目和结合位点。其中结合位点靠近 BSA 的 214 位、HSA 的 212 位色氨酸。

Spectroscopic studies on the interaction of riboflavin and albumin

ZHAO Hongwei GE Min ZHANG Zhaoxia WANG Wenfeng WU Guozhong

Keywords Riboflavin, Albumin, Intrinsic fluorescence, Fluorescence quenching

The interactions between riboflavin (RF) and human and bovine serum albumin (HSA and BSA) were studied by using absorption and fluorescence spectroscopy method. Intrinsic fluorescence emission spectra of serum albumin in the presence of RF show that the endogenous photosensitizer acts as a quencher. The decrease of fluorescence intensity at about 350 nm is attributed to changes in the environment of the protein fluorophores caused by the ligand. The quenching mechanisms of albumin by RF were discussed. The binding constants and binding sites number were obtained at various temperatures. The distance between albumin and RF of their complexes suggests that the primary binding site for RF on albumin is close to tryptophan residues (Trp214) of HSA and Trp212 of BSA. The hydration process of albumin has been discussed.

稀有三环核苷衍生物单电子氧化反应的脉冲辐解研究

赵红卫 江致勤[1] 窦大营 吴铁一 王文锋 杜小行[1] 姚思德

关键词 稀有三环核苷衍生物，单电子氧化，脉冲辐解，自由基，瞬态吸收光谱

运用纳秒级脉冲辐解技术研究了稀有三环核苷衍生物 6-甲基三环鸟苷(dYt)与一些单电子氧化性自由基的反应，表征了反应过程中产生的阳离子自由基 $dYt^{\bullet+}$ 及其脱质子中性自由基 $dYt(-H)^{\bullet}$ 的瞬态吸收光谱及 pKa，并得到该化合物与$^{\bullet}OH$ 自由基及单电子氧化性自由基 $SO_4^{\bullet-}$、$CO_3^{\bullet-}$、$N_3^{\bullet}$ 反应的动力学速率常数，揭示了反应机理，为进一步了解该类化合物的氧化反应提供了的证据。

1 同济大学化学系

Pulse radiolysis of one-electron oxidation of rare tricyclic nucleoside derivative

ZHAO Hongwei JIANG Zhiqin[1] DOU Daying WU Tieyi
WANG Wenfeng DU Xiaoxing[1] YAO Side

Keywords Rare tricyclic nucleoside derivative, One-electron oxidation, Pulse radiolysis, Radical, Transient absorption spectra

One-electron oxidation of N-4-desmethylwyosine (dYt), a derivative of rare tricyclic nucleoside wyosine with several oxidative radicals, has been studied by using pulse radiolysis. The transient spectra of the radicals $dYt^{\bullet+}$ and $dYt(-H)^{\bullet}$ and the pK_a of the radical cation were measured. The rate constants of reactions of dYt with $SO_4^{\bullet-}$, $CO_3^{\bullet-}$, $N_3^{\bullet}$ and $^{\bullet}OH$ radicals have been determined and related reaction mechanisms were discussed.

1 Department of Chemistry, Tongji University

苯甲酸水溶液的双激光光解研究

赵红卫　付海英　王文锋　姚思德

关键词　苯甲酸，激发态，双激光光解

分步双激光技术为多光子化学特别是凝聚态光化学反应中间体、激发态和选键化学反应提供了有利的手段，开拓了光化学研究的视野。苯甲酸(BA)对远紫外光有强烈的吸收，可发生 n→π* 跃迁，在水溶液中 λ_{max}=230nm。本文首次采用 248nm 激光和 248－308nm 分步双激光技术对苯甲酸的光物理和光化学性质以及激发态反应活性进行了研究。在 248nm 激光作用下，BA 水溶液发生部分光电离并观察到激发三重态 $^3BA^*$的吸收。实验测得光电离水合电子的量子产额为 0.35，$^3BA^*$的寿命为 30μs，其特征吸收在 300nm 附近，并能被 O_2、Fumaronitrile、Mn^{2+}等有效地猝灭。在经过 1–2μs 时间延迟的第二束 308nm 激光激励下，$^3BA^*$能够被激发到高级激发态并可能产生新的自由基，这些中间体可以和鸟苷发生进一步的反应，更深入的研究还在进行中。

The studies on benzoic acid aqueous solution by two-steps laser flash photolysis

ZHAO Hongwei　FU Haiying　WANG Wenfeng　YAO Side

Keywords　Benzoic acid，Excited states, Two-steps laser flash photolysis

The photo-ionization and properties of excited state of benzoic acid aqueous have been studied by use of 248nm laser flash photolysis. The quantum yields of hydrated electron produced from photo-ionization, the characteristic absorption and life-time of excited triplet of benzoic acid have been determined as 0.35, 300nm and 30 μs respectively. The resonant excitation of triplet of benzoic acid has been explored by use of 248－308 nm two-steps laser flash photolysis firstly. The possible upper excited state and radical involved in the processes have been guessed. The transient intermediates produced from the two-steps laser photolysis would react with guanosine.

紫外光照射下富勒醇对细胞的防护作用

李宇国 倪 瑾[1] 韩 玲[1] 赵群芬[1] 高 福[1] 李晴暖 徐晶莹 李文新

关键词 富勒烯，紫外辐照，辐射保护

为了解紫外辐射下富勒烯衍生物富勒醇对细胞的生物效应，利用 MTT 法研究了富勒醇对紫外辐照细胞的存活率影响，紫外辐照细胞时富勒醇对细胞 SOD 和 MDA 的影响，同时比较了 C_{60}-PVP 对紫外辐照细胞的辐射生物效应。通过实验数据可知，富勒醇对细胞的紫外辐射防护作用并不是发生细胞内，而是在细胞外吸收紫外辐射产生的自由基，从而保护了细胞在紫外辐照后细胞膜不受损伤。研究结果表明，富勒醇能够有效的防护紫外辐射对细胞造成的损伤，其机理可能是富勒醇能够吸收紫外辐照产生的自由基，保护了细胞膜不被紫外辐照损伤。通过本研究，对于富勒烯衍生物的紫外防护作用机制有了进一步的了解，为富勒烯衍生物在生物医药方面的应用提供了一定的实验依据。

1 第二军医大学放射医学教研室

The effect of fullerols on cell under UV

LI Yuguo NI Jin[1] HAN Ling[1] ZHAO Qunfen[1] GAO FU[1]

LI Qingnuan XU Jingying LI Wenxin

Keywords Fullerene, Ultraviolet radiation, Radioprotection

The UV radioprotcetive effect of fullerols, which was compared with the effect of C_{60}-PVP, was studied using cultured L02 cells.The cell survivals were determined by MTT method, SOD and MDA also were studied with chemical colorimetry. The results showed that fullerols can effectively protect cells from damage induced by UV irradiation. The mechanism could be assosiated with the ability of fullerols to behave as an antioxidant compound, then fullerols protected cell membrane from damage by UV radiation.

多壁碳纳米管的超声切割初步研究

李宇国 郭金学 李晴暖 尹娟娟 吴胜伟 李文新

关键词 碳纳米管，超声切割，AEDP

利用强超声的方法，研究了多壁碳纳米管(MWCNT)在二磷酸(AEDP)溶液中的超声切割行为。超声产物可在水，乙醇，THF，氯仿中轻微超声几十秒即可分散，分散后的溶液放置 30 天不会发生沉降，但不能在苯，正己烷和丙酮中超声分散。通过 TEM，SEM，AFM，FTIR 的分析表明，

多壁碳纳米管在二磷酸溶液中被均匀的切割，其直径为 100nm 左右，并且发生了化学反应，在碳纳米管上形成了酰胺键。通过选择合适的超声条件和超声介质，可对多壁碳管进行提纯，切割，化学修饰和分散。该方法可以用于大量的切割和分散多壁碳管，并将碳管应用于材料研究等方面。

The study on the cutting of the carbon nanotube under the ultrasonic

LI Yuguo GUO Jinxue LI Qingnuan YIN Juanjuan

WU Shengwei LI Wenxin.

Keywords Carbon nanotube, Cutting, Ultrasonic, AEDP

The multiwall carbon nanotube (MWCNT)which in the solution of disphosphate (AEDP) were cut through strong ultrasonic. The behavior of the cutting MWCNT were analyzed by TEM，SEM，AFM，RAMAN，FTIR，TGA. The result showed that the MWCNT were equally cut by the strong ultrasonic in the solution of AEDP. The length of the cutting MWCNT were around 500nm, also the chemical reaction on the MWCNT was occurred. The cutting MWCNT can be dispersed in the water, ethanol, THF and acetone. The MWCNT may be purified, cut, chemical modified and dispersed by utilizing appropriate conditions of ultrasonic and medium. This way can be used to cut and dispers mass MWCNT, then the CNT may be better applied in the field of material.

太赫兹时域光谱技术在化学和生物学研究中的应用

赵红卫 葛 敏 王文锋 李晴暖 余笑寒

关键词 光谱测量，特征吸收，THz-TDS 技术

太赫兹时域光谱(Terahertz Time Domain Spectroscopy，THz-TDS)技术作为一种新的研究手段在凝聚态、气体以及生物分子研究中有着重要的作用。它利用物质在 THz 波段的不同特征吸收来研究物质的结构、组成及其相互作用等。本文主要介绍了 THz-TDS 技术在化学及生物学领域中的应用进展以及目前存在的问题，对其前景进行了展望。

Application of teraherz time domain spectroscopy in chemistry and biology

ZHAO Hongwei GE Min WANG Wenfeng LI Qingnuan YU Xiaohan

Keywords Spectroscopy measurement, Characteristic absorption, THz-TDS technique

As a new approach, Terahertz Time Domain Spectroscopy (THz-TDS) has shown important application in several research works, such as condensed matter, gas-phase, biochemistry and so on. The characteristic spectra of substances in THz range may provide important information of configuration, constitutes and the interactions of molecules. In this paper, a brief review is given to summarize the progress of THz-TDS technique in the field of chemistry and biology and problems to be solved.

稀有三环核苷衍生物的光谱学研究

赵红卫 窦大营 苗金玲 姚思德 江致勤[1] 赵春雷[1]

关键词 稀有三环核苷衍生物，单光子电离，自由基，激光光解，瞬态光谱

利用时间分辨激光光解技术对稀有三环核苷的前体化合物 N-4-desmethylwyosine(dYt)研究发现，该化合物能被 248nm 激光单光子电离，但未观察到明显的激发三线态。用氧化性自由基 $SO_4^{\bullet-}$ 引发其阳离子自由基，揭示了其光电离机理。以 KI 溶液为参照，测得该化合物中性条件下的光电离量子产额(Φ_e-)为 0.04。

1 同济大学化学系

Spectral studies of derivative of tricyclic modified nucleoside in aqueous solutions

ZHAO Hongwei DOU Daying MIAO Jinling YAO Side

JIANG Zhiqin[1] ZHAO Chunlei[1]

Keywords N-4-desmethylwyosine, Monophotonic ionization, Radical, Laser photolysis, Transient absorption spectrum

The absorption spectra of N-4-desmethylwyosine (dYt), a derivative of the tricyclic modified nucleoside wyosine, in aqueous solutions were studied by time-resolved laser photolysis. The oxidizing radical $SO_4^{\bullet-}$ was used to produce dYt radical cation. The mechanism of dYt monophotonic ionization

was suggested. Distinct triplet was not observed in this work. The quantum yield of formation of hydrated electrons (Φ_e-) was determined to be 0.04 at room temperature in neutral aqueous solution by using KI solution as a reference.

---

1 Department of Chemistry, Tongji University

应用加速器

Applied accelerator

应用加速器研究中心简介

应用加速器研究中心主要从事工业用低能加速器的研制。目前，主要致力于高压型电子辐照加速器的研究与开发。2003 年完成了 700 keV/300 mA 烟气脱硫用超大功率电子加速器试验样机的研制。2004 年电子束离子阱（EBIT）装置顺利出束。至 2004 年底研究中心为国内 14 家企业和单位提供了 2.5—3.0 MeV，20—30 mA 用于电线、电缆、热缩材料和其它高分子材料辐射改性的电子加速器。

研究中心现有各类人员 30 余人。其中研究员 3 人，副研究员级 10 人。研究中心目前正在研制烟气脱硫示范工程用的加速器实用样机和用于医疗卫生产品灭菌的 5 MeV 电子加速器。

上海电子束离子阱：设计和现状

朱希恺　蒋迪奎　郭盘林　盛树刚　闫和平　龚培荣　王纳秀
施卫国　陈永林　许祥义　冯淑卿　周团团

关键词　电子束离子阱

一台新的电子束离子阱（EBIT）正在上海建造，将安装在复旦大学。预期漂移管的对地电位为+30 kV，电子枪和收集器对地电位为-170 kV。电子枪（EGUN）和收集器中的所有电源均放在钢筒内，钢筒充 0.3 Mpa 的绝缘气体以提高耐压水平。我们用 EGUN 程序模拟了从电子枪到收集极的电子的轨迹。在电子束能量为 200 keV，束流为 200 mA 的条件下，在陷阱区的电子束半径为 32 μm。结果表明，电流密度约为 5000 A/cm^2。采用制冷机组的深冷系统来冷却超导磁铁线圈。用中性气体注入和金属蒸汽真空狐（MEVVA）离子源作为 EBIT 的离子注入系统。运行者通过控制系统可以方便地设定和监控全部的电源。

Shanghai EBIT: design and current status

ZHU Xikai　JIANG Dikui　GUO Panlin　SHENG Shugang　YAN Heping
GONG Peirong　WANG Naxiu　SHI Weiguo　CHEN Yonglin　XU Xiangyi
FENG Shuqing　ZHOU Tuantuan

Keyword　Electron beam ion trap

An electron beam ion trap (EBIT) is under construction in Shanghai. It will be installed in Fudan University. It is intended that the drift tubes will be floated at +30kV from earth, and the electron gun and the collector assembly will be floated at –170kV from earth. All the power supplies for the gun and collector assembly are put inside a metal tank filled with 0.3MPa SF_6 insulation gas in order to to achieve higher breakdown voltage. A computer simulation with the EGUN program was performed on the electron beam trajectories from the gun to the collector region. It shows that with a 200keV200mA beam, the electron beam radius in the trap region is around 32μm, hence a current density of about 5000A/cm^2. Therefore, a cryogenic system utilizing a cryorefrigerator is adopted to cool down the superconducting magnet coil. Neutral gas injection and a MEVVA ion source are used to supply EBIT with atoms and primary ions. A computer control system allows all the power supplies to be set and monitored by the user conveniently.

4–氯酚的γ射线辐射降解行为

王 敏 杨睿媛 沈忠群 王文锋

关键词 γ射线辐照，4-氯酚，降解，化学需氧量，脱氯

卤代酚类化合物是有机化工的重要原料，主要产生于精细化工、农药、造纸和医药工业，也被广泛地用作除草剂、木材的防腐剂、杀菌剂等释放到环境中，由于其具有致癌、致畸、致突变的潜在毒性，成为环境中的主要污染物之一。

本研究以 4－氯酚作为具体研究对象，^{60}Co 源产生的γ射线为辐照手段，通过分析测定在不同辐照条件下 4-氯酚溶液的化学需氧量（COD）、氯离子浓度和紫外可见吸收光谱，研究其在高能射线辐照下的活性自由基作用、氯离子的脱除和苯环分子结构的破坏并最终被降解为无机物的反应进行过程，并研究了辐照吸收剂量、过氧化氢浓度、不同 4-氯酚初始浓度和不同 pH 值对辐射降解反应的影响。

研究证明，4-氯酚的脱除效率随吸收剂量的增加而增加，不管是有机氯的脱除率还是 COD 去除率均可达到较好的效果，在吸收剂量为 14.9 kGy，H_2O_2 的浓度为 7.34 mmol/L 时，初始浓度为 1mmol·dm^{-3} 的 4-氯酚溶液的 COD 去除率可达 65.8％，有机氯脱除率可达 100％。有机氯的脱除率和 COD 去除率均与 4-氯酚溶液的初始浓度成反比，即 4-氯酚溶液的初始浓度越大，脱除率越低；而溶液的初始 pH 值对脱除率的影响不大。说明辐射降解 4-氯酚的适用 pH 值范围较大；过氧化氢的加入可以起到很好的促进降解的协同作用，可以较大幅度的提高有机氯的脱除率和 COD 去除率。本研究还对 4-氯酚的辐射降解机理进行了一定的实验和探讨，归纳总结了 4-氯酚的降解和脱氯途径。

γ-ray-induced degradation of 4-chlorophenol in aqueous solution

WANG Min YANG Ruiyuan SHEN Zhongqun WANG Wenfeng

Keywords γ-ray irradiation, 4-chlorophenol, Degradation, COD, Cl removal

Chlorophenols are a class of serious organic pollutants to the environment, especially in natural waters, as they are commonly used in industries of synthetic polymers, pigments and pesticides.

4-chlorophenol in aqueous solution was chosen for a chlorophenol γ-ray degradation study, in which UV-vis absorption, COD removal efficiency and inorganic Cl removal efficiency were measured. Different 4-chlorophenol concentrations and pH values, and amount of H_2O_2 added, were investigated with different irradiation doses.

The results showed that efficiencies of the COD removal and inorganic Cl removal increased with increasing dose, reaching 65.8% and 100% respectively at 14.9 kGy, whereas COD and Cl removal efficiencies decreased with increasing initial concentration of 4-chlorophenol. While pH value of the solutions had little influence on the decomposition, H_2O_2 played an important role in the degradation of 4-chlorophenol, enhancing dramatically removal efficiencies of COD and inorganic Cl.

辐射降解活性染料水溶液的研究

王 敏 杨睿媛 王文锋 沈忠群 边绍伟

关键词 电离辐射，染料水溶液，降解，脱色

辐射技术处理环境污染物显示了很大的应用前景，在燃煤烟气脱硫脱硝、挥发性有机化合物的净化、废污水的处理、污泥消毒和处置等方面正在逐步走向工业应用。本文介绍了我们利用电离辐射处理染料水溶液方面的相关研究。

1. 活性艳蓝（KNR）的γ射线辐照降解

利用 ^{60}Coγ射线辐照活性艳蓝 KNR 水溶液，以研究染料分子在γ射线辐射下的降解特性。从紫外可见光谱中可以看出，染料水溶液在可见光区和紫外区的特征吸收峰受到辐照后，随吸收剂量的增加，这些吸收峰渐渐下降，最后都接近为零。说明辐照降解反应既破坏了染料分子的发色基团，同时也破坏了染料的有机分子结构。

脱色率和化学需氧量（COD）去除率的分析表明：溶液的吸收剂量是影响脱色率和 COD 去除率的最主要因素，脱色率和 COD 去除率均随吸收剂量的增加而增加。溶液的初始 pH 值实验表明辐射技术处理印染废水的 pH 值适用范围很广。溶液的初始浓度越大，COD 去除和脱色效果越差。另外，不同气体饱和实验证明，氧的存在可以促进染料分子的降解。

2. 多种活性染料的电子束辐照降解

共选择了五种不同颜色的活性染料（活性红 m-3BE、活性艳红 KE-3B、活性蓝 XBR、活性橙 K-2RL 和活性黄 X-R），以研究活性染料溶液在电子束辐照下的降解特性。除了研究分析辐照前后溶液的紫外可见光谱、COD 去除率和脱色率以外，对辐照后溶液的 pH 值随吸收剂量的变化做了详细研究。在同样辐照条件下，染料的降解效果因染料分子的结构不同而略有不同。研究发现：染料溶液受到电子束辐照后，其 pH 值呈现下降趋势。表明染料分子能被降解成有机酸等中低分子的有机物，这与生化法中的厌氧酸化步骤有相似的效果。

3. 过氧化氢与辐射的协同作用

辐照前在染料溶液中加入了不同量的过氧化氢以考察其与辐射的协同作用，研究发现：在相同的吸收剂量下，脱色率和 COD 去除率均随过氧化氢的浓度增加而增加，当过氧化氢的浓度到一定量时，脱色率和 COD 去除率趋于饱和。电子束辐照时过氧化氢的作用比 γ 射线辐照时更明显。

4. 结论

研究表明，高能射线辐照都可以有效地降解染料水溶液。辐射技术和其它技术有很好的协同作用。与常规污染物处理技术相比，辐射技术一般在常温常压下进行，具有工艺简单，无二次污染等特性，尤其在处理难降解有机污染物上有其独到之处。

Radiation-induced degradation of reactive dyes in aqueous solution

WANG Min YANG Ruiyuan WANG Wenfeng SHEN Zhongqun BIAN Shaowei

Keywords Ionizing radiations, Reactive dyes, Decoloration and degradation, Hydrogen peroxide

Textile printing and dyeing industries produce large quantities of waste effluents containing toxic resistants that are difficult to be destructed by conventional treatment methods. Ionizing radiation technology, as an advanced oxidation process (AOP), has been recognized as a promising process for wastewater treatment against hazardous organics.

Decomposition and decoloration of reactive blue KNR by γ -ray irradiation

Aqueous solution of blue (KNR) reactive dye was irradiated by ^{60}Co γ-rays to 4.3 - 20.3 kGy and the irradiation degradation was investigated with decoloration measurement by UV-vis absorption spectra and COD removal measurement. There were several characteristic absorption bands in UV spectra of the dye solution and the peaks decreased with increasing dose, and peaks in visible area decreased faster than the UV peaks. It means that decoloration of the dye solution is much easier than their decomposion. Efficiency of the COD removal and degree of the decoloration can be 80% and 100%, respectively.

Degradation of reactive dyes in aqueous solution with EB irradiation

Electron beams were used to study radiation-induced degradation of five reactive dyes（red-3BE、bright red KE-3B、blue XBR、orainde K-2RL andyellow X-R）in water solution. UV-vis absorption spectra and pH values were measured before and after radiation, together with measurements of decoloration and COD removal efficiency. The results showed that the dye solutions could be decolored at relatively low doses, whereas higher doses would be needed to degrade the dye molecules into inorganic forms and to achieve satisfactory COD removal efficiency. It is recommended to use irradiation technology for treatment of dye wastewater with combination of other process.

Synergetic effect of H_2O_2

Hydrogen peroxide, as a strong oxidant, was used to enhance degradation of dye solutions. The radiation induced decoloration and COD removal increased with increasing H_2O_2 concentrations, as compared to sample solutions without H_2O_2 and irradiated to the same doses. However, when the H_2O_2 concentration increased to certain amounts, the COD removal efficiencies and decoloration of the dye solutions ceased to increase.

甲基橙溶液的辐射降解研究

杨睿媛 王 敏 沈忠群 王文锋

关键词 γ射线辐射，降解，化学需氧量，甲基橙

以 ^{60}Coγ射线为辐照源，对偶氮染料甲基橙进行了γ射线辐射降解研究，研究了偶氮染料的辐照降解特性。以脱色率和化学需氧量（COD）为降解指标，研究了辐照前后紫外可见吸收光谱和COD的变化。探讨了 H_2O_2 加入量、吸收剂量、初始浓度和溶液pH值对辐照降解结果的影响。结果表明，γ射线辐射能有效降解偶氮染料废水，吸收剂量为13.7 kGy，甲基橙的COD 去除率可达80％以上，脱色率可达100％；H_2O_2 加入量、吸收剂量、初始浓度均与甲基橙的降解效率有关，γ射线辐射过程中，吸收剂量在甲基橙的降解中起主要作用，但 H_2O_2 的存在能促进甲基橙的降解。溶液初始浓度对 COD 去除率有明显影响，而溶液的 pH 值对降解影响不大；γ 射线辐射与 H_2O_2 结合可以得到良好的处理效果。实验证实，利用γ射线辐射降解技术处理染料废水是一种可行的方案。

A study on degradation of methyl orange in aqueous solution by γ–irradiation

YANG Ruiyuan WANG Min SHEN Zhongqun WANG Wenfeng

Keywords γ–ray irradiation, Degradation, COD, Methyl orange

Methyl orange in aqueous solution was irradiated by ^{60}Co γ-rays under different irradiation conditions, and UV-vis absorption, COD, and degree of decoloration of the samples were studied. The results showed that the COD removal efficiency and the degree of decoloration reached 80% and 100% respectively at 13.7 kGy. It was found that H_2O_2 concentration, absorbed dose and methyl orange concentration were closely relevant to the degradation of the dye in water.

航向台天线杆强度分析

林 剑 王春玲[1] 靳 猛[1]

关键词 杆，拉索，风压，变形

在天线杆结构的设计中，为适应某些特殊要求，开始采用底部使用球支座结构、以拉索稳定的天线杆结构来满足特殊的使用要求。特殊环境下，其所受的外载荷（主要是风载）对结构的强度有很大影响。为提高天线杆结构的可靠性，应用力学基本原理与算法，对台风冲击条件下的杆结构受力与变形进行分析，提出一种结构强度和变形的简便计算方法，计算结果满足设计要求，符合工程实际。

1 哈尔滨工程大学

Strength analysis for body-mast

LIN Jian WANG Chunling[1] JIN Meng[1]

Keywords Mast, Cord, Wind pressure, Deformatio

The effect of external loads, especially the wind pressure of typhoon, on the structural strength of a body-mast is analyzed using the basic mechanics principle and algorithm with the strength and deformation calculated for the purpose of improving both the stability and reliability of a body-mast.

1 Harbin Engineering University

航向台天线杆稳定性分析

林 剑 王春玲[1] 靳 猛[1]

关键词 杆，拉索，温度，稳定性，安全系数

实际工程中大多数结构是处于变化较大的环境中，如：温度的变化等。由于环境的变化，将会导致结构的设计及计算发生相应的变化。为此以球支座结构、伞状分布的拉索稳固的天线杆为研究对象，在天线杆处于温度变化较大的环境中，应用力学基本原理与算法，给出了在温度变化影响下，该天线杆的稳定性及安全系数的计算方法。该计算方法符合工程实际，对同类或近似产品的分析具有一定的借鉴作用。

1 哈尔滨工程大学

Stability analysis for heading antenna mast

LIN Jian WANG Chunling[1] JIN Meng[1]

Keywords Mast, Cord, Temperature, Stabilization, Safety factor

An algorithm has been worked out using basic mechanics principles and algorithms for determination of stability and safety factor for an antenna mast secured with braces in an umbrella shape on a hemispheric base in an environment with significant temperature changes.

1 Harbin Engineering University

电子辐照加速器大功率工频高压电源

许祥义　赖伟全

关键词　加速器，桥式整流，纹波电压，电压脉动率

介绍了目前现有的两种用于烟气脱硫加速器的不同形式直流高压电源。一种是采用 1 台三相高压变压器，次级电压经整流形成 6 脉波后再用电容滤波；另一种采用 2 台三相高压变压器，借助不同的次级绕组接法进行整流实现 12 脉波的输出电压。分析了它们各自的原理和特点。指出了各自存在的不足之处：直流高压的脉动纹波依赖于变压器和电网的电压波形；初级绕组可能感应较高的来自加速器负载放电时的浪涌电压;特别是三相桥的 3 个绕组需耐受最高直流电压的峰值。针对以上不足，本文提出了一种全新的倍压型桥式整流线路，采用单台三相高压升压变压器供电，倍加线路采用上下对称的三相平衡式。这样能很好的解决前两种方案的不足，大大提高了高压电源的可靠性。本文对此线路进行了详细的理论推导，并列出了公式计算值和计算机模拟仿真值的比较。

High power line-frequency high-voltage source for an electron beam accelerator

XU Xiangyi　LAI Weiquan

Keywords　Accelerator, Bridge rectifier, Ripple voltage, Voltage pulsation rate

Low energy high power accelerators for electron beam purification of flue gases use transformer types of DC high voltage sources, which is either a single transformer with a six pulse wave rectifier circuit and smoothing capacitors, or a double transformer with a twelve-pulse wave rectifier circuit and by connecting the second windings differently to eliminate the smoothing capacitors. With these types of high voltage sourses, however, ripple voltage of the DC high voltage depends on waveform of the transformer and electric network, and the primary winding may induct high voltage from surge current from the accelerator operation. In addition, the second winding must withstand the peak value of the DC high voltage. Taking these limitations into consideration, a full-fresh voltage multiplying bridge rectifier circuit is designed, after theoretical analysis and computer simulations.

800kV 高压传输装置的电场数值计算

许祥义　赖伟全

关键词　电缆终端，电场强度，SF_6 绝缘气体，沿面电位梯度

本文介绍了 800kV 高压传输装置的组成和结构安排；该传输装置是由一根电缆和两个终端组成。其中，一个终端插入到变压器油环境中与高压发生器相连；另一终端插入到 SF_6 绝缘气体环境中与加速器的高压电极相连。这两个终端都要处理好 800kV 直流高压的顺利过渡问题。这在现成的电缆附件市场上是没有成熟产品的，只能在现有的电缆附件基础上加以修改试制。本文对在 SF_6 绝缘气体环境中的电缆终端进行了电场数值计算，并对计算结果进行了分析：由于加速器钢筒和电缆终端外钢筒之间充 6—7 个大气压的 SF_6 绝缘气体作为绝缘介质。这种 SF_6 气体的间隙电场强度可以达到 200kV/cm 左右，而经计算得到在整个电缆终端的解场区域中终端屏蔽罩端部的电场强度最高，为 130kV/cm，离允许的最大场强还有一定安全裕量，所以认为电缆终端的场强设计是可靠的。

Numerical computation of electric field for an 800kV voltage transmission system

XU Xiangyi　LAI weiquan

Keywords　Cable termination, Electric field strength, SF_6 insulating gas, Potential gradient on surface

Componants and structure of an 800kV voltage transmission system for a election beam accelerator are introduced. The system has a cable connecting the high voltage transformer with oil insulation and the accelerator electrode in SF_6 gas insulation. Problems must be solved for transitting the 800kV DC between the two terminals. However, as no ready-made cable product is available for such an application, we had to modify the terminals. Numerical computations were performed on the electric field of the cable termination in SF_6. The result showed that maximum electric field of the facility is 130kV/cm, which is far below the allowable value of 200kV/cm, as our experience in high voltage EB systems. Above all, it is concluded that electric field strength of the cable termination is reliable.

烟气脱硫用大功率电子加速器的研制

李民熙 赖伟全 朱希恺 徐洪杰 朱志远 斯厚智 邹志宜 张宇田
黄建鸣 施卫国 朱锦华 龚培荣 张 耀 冯淑卿 许祥义

关键词 烟气脱硫，加速器，高压发生器，电子枪，加速管，引出扫描

燃煤烟气是目前中国大气污染的主要来源，因此燃煤烟气的脱硫脱硝是当前大气环境保护的主要内容，电子束烟气脱硫脱硝工艺相对于其它烟气净化工艺具有很大的优越性，研制适用于燃煤烟气脱硫脱硝的大功率电子加速器是非常必要的，我们最近研制成功了电子束能量为 700 keV，电子束流强为 300 mA 的电子加速器。

1. 加速器的高压发生器

高压发生器采用 12 脉动整流线路。即将两台三相工频变压器的输出分别进行整流，然后串接起来，其总的输出电压为 12 脉动的直流电压 700 kV，其电压脉动系数小于 5%。

高压发生器和电子枪灯丝变压器均装在充满变压器油的大铁箱内。然后用两根电缆分别与两台电子束加速装置相连接，每台电子束加速装置可以引出电子束为 300 mA。采用这种高压发生器可以使电功率转换效率达到 90% 以上。

2. 加速装置

电子枪和加速管组成的加速装置在充满 SF_6 绝缘气体的钢筒内。电子枪阴极采用硼化镧(LaB_6)晶体。加速管由氧化铝陶瓷与钛电极经真空焊接而成。

3. 引出扫描装置

引出扫描采用双窗结构，电子束交替在两个箔窗上进行扫描，扫描窗的长度为 2200 mm。箔窗采用厚度为 0.04 mm 的钛箔，并用强风冷却。

Development of high power EB accelerator for purification of flue gases

LI Minxi LAI Weiquan ZHU Xikai XU hongjie ZHU Zhiyuan SI Houzhi
ZOU Zhiyi ZHANG Yutian HUANG Jianming SHI Weiguo ZHU Jinhua
GONG Peirong ZHANG Yao FENG Shuqing XU Xiangyi

Keywords Purification of glue gases, Electron accelerator, High voltage generator, Electron gun, Accelerating device, Extraction and scanning device

Nowadays the main source of atmosphere pollution is flue gases from coal burning power plants. It is an important task to protect the atmosphere environment from SO_2 and NO_x of flue gases. Electron beam purification of flue gases is advantageous in comparison with other technologies, and developing high power electron accelerator for purification of flue gases is of priority in China. A 700keV 300mA electron accelerator was developed in 2003 at SINAP.

High voltage generator

The high voltage generator uses 12- pulsating rectifier circuit. It contains two 3-phase transformers with 50Hz line frequency. The voltage outputs are rectified separately and connected in series to provide 700kV DC. The voltage pulsating coefficient is less than 5%.

The high voltage generator and the transformer for electron gun filament, are contained in a oil-insulating tank, from which two cables connect separately with two accelerators, each delivers 300mA beam current. With this kind of high voltage generator, power transfer efficiency can be up to more than 90%.

The accelerator

The accelerator consists of an electron gun and accelerating tubes, being contained in a tank with SF_6 gas insulation. Cathode of the electron gun is made of LaB_6 crystal. The accelerating tubes are made of aluminum dioxide ceramics and titanium electrodes welded in vacuum.

The beam extraction and scan

A double window structure is used for beam extraction and scan. The extracted electron beams are scanned alternatively through the two Ti windows of 2200mm in length. The Ti windows of 40μm in thickness are cooled by powerful air blast cooling.

辐射技术应用

Radiation technology application

辐射技术应用研究中心简介

辐射技术应用研究中心现有在职人员 14 名，硕士生、博士生、博士后共 19 名。主要研究方向为基于辐射技术的新型功能高分子材料制备与改性研究。近两年来，在利用辐射接枝技术提高多相聚合物之间或与无机材料之间的相容性、辐射聚合法制备纳米高分子、针对特殊需求的高分子材料辐射交联和辐射降解、以及特殊条件下的辐射化学行为研究等方面，取得了重要进展，在一些先进实验技术（如同步辐射、T-Ray、时间分辨等）的使用上也积累了宝贵经验。

聚乙烯薄膜辐射接枝丙烯酸羟丙酯诱导 $CaCO_3$ 晶体生长的研究

张凤英 侯铮迟 虞 鸣 谢雷东 李 晶

关键词 γ 射线辐照，异相成核，无机晶体，生物矿化，聚合物

采用了 γ 射线辐射接枝丙烯酸羟丙酯的聚乙烯薄膜作为模板，实现了在过饱和碳酸氢钙溶液中诱导碳酸钙晶体的异相成核和生长；对形成的碳酸钙晶体用扫描电子显微镜（SEM），傅立叶变换－红外光谱（FT−IR）和 X 射线衍射（XRD）进行了分析，发现生成碳酸钙晶体的晶型为方解石型。研究结果表明，除高分子薄膜的表面结构、晶体培养液选用的添加剂等影响因素之外，适当温度的波动也是导致碳酸钙晶体异相成核的关键因素。

Growth of $CaCO_3$ crystal on polyethylene films grafted with 2-hydroxypropyl acrylate by γ-irradiation

ZHANG Fengying HOU Zhengchi YU Ming XIE Leidong LI Jing

Keywords γ−radiation, Heterogeneous, Organic crystal, Biomineralization, Composite

Biomimetic heterogeneous nucleation and growth of calcium carbonate crystals took place in supersaturated calcium bicarbonate solution on PE films grafted with 2-hydroxypropyl acrylate by γ-irradiation, which served as a template. The specimens were characterized by FT-IR, SEM and XRD. The obtained crystals proved to be calcite. Lab results indicate that in addition to polymer surface structure and proper additives, temperature is a key factor for heterogeneous nucleation and growth of calcium carbonate crystals.

紫外光敏化对 PET 膜离子径迹结构的影响

朱智勇 前川康成[1] 刘 崎 吉田勝[1]

关键词 离子径迹结构，径迹蚀刻，紫外光敏化

无机晶体材料的离子径迹结构可以通过高分辨电子显微镜、扫描隧道显微镜以及原子力显微技术进行观测。对于聚合物类有机材料，由于材料本身对电离辐射很敏感，因而不利于使用这些技术研究离子径迹的结构。通过电导测量监测径迹膜化学蚀刻过程中径迹的穿孔过程为径迹结构的研究提供了新方法。已开展的工作显示，在聚合物中离子径迹呈径迹芯和径迹晕的结构，分析认为径迹芯与大分子的降解有关，而径迹晕则与分子键的交联相联系。

本工作中用高能 Xe 离子辐照了聚对苯二甲酸已二醇酯（PET）薄膜样品，并在膜的化学蚀刻过程中跟踪了孔的长大过程，由此研究了径迹的结构及其与紫外光敏化的关系。实验发现，电导平方根的时间微分随蚀刻时间呈现泾渭分明的结构：在开孔期间曲线呈尖峰状，之后有一小但很明显的平台，其可能与微孔中蚀刻液电导率的变化有关；在到达谷底后数值逐渐增加并最终趋于与材料体蚀刻速率相关的常数。蚀刻曲线的这些细微变化既与离子径迹的结构有关，也与蚀刻前样品在紫外光下敏化的时间有关。在假定径迹穿孔几率遵从高斯分布以及孔中蚀刻液的电导率随

蚀刻时间指数增加的情况下，对实验测量结果进行了数值分析，由此获得了径迹结构参数及其随紫外光敏化时间的变化关系。分析发现，随着紫外光敏化时间的增加，除蚀刻孔径分布变窄外，径迹芯的半径减小而径迹晕的半径增大并最终趋于常数。

1 日本原子能研究院高崎辐射化学研究所

Influence of UV light illumination on latent track structure in PET

ZHU Zhiyong Maekawa Y[1] LIU Qi Yoshida M[1]

Keywords Ion track structure, Track etching, UV illumination

Latent track structure of swift heavy ions in inorganic crystalline materials can be visualized through high-resolution electron microscope, scanning tunneling microscope and atomic force microscope. However, it is rather difficult to use these techniques to see latent tracts in polymeric materials because of the fact that polymeric materials are highly sensitive to radiolysis. Instead, conductance measurements in combination with chemical etching are suitable for studying samples of the kind. This technique was originally designed for studies of preferred etching of ion tracks, a key point at that time in ion registration with plastic detectors. It was later realized that the technique could be utilized to reveal track structures in polymeric materials and valuable information on track structures in polymers has been provided. It is now generally accepted that tracks in most polymers are of core and halo type. The track cores are formed as chain scission of the polymer molecules by strong energy deposition of heavy ions, whereas the track haloes are formed where cross-linking of the molecules is dominant over chain scission.

In this work Xe-ion irradiated PET films were chemically etched and pore growth process was monitored by the conductometric method. Track structure was evaluated from the measurements and studied with respect to UV light illumination time conducted before etching. It is found that the time differentiation of the conductance square root shows well-defined stages with respect to etching times. A sharp peak appears in the pore-opening period followed by a small but distinguishable step around 5000 s. The step is attributed to conductivity variation of etchant inside the pores. After reaching to a minimum, time differentiation of the conductance square root increased gradually and finally reached a constant value, corresponding to bulk-etching rate of the material. Detail of the whole process, however, changed significantly with the UV-light illumination time. By assuming that break-through probability of the pores is a Gaussian function of time and conductivity of the etchant inside pores increases exponentially with etching time after pore opening, the experimental measurements were numerically analyzed and information related to track structure and its variation with UV-light illumination were acquired. It is found for the first time that with increasing UV-light illumination time, in addition to a significant narrowing of pore size distribution, track core reduced in size whereas track halo increased in size.

1 Takasaki Radiation Chemistry Research Establishment, JAERI, Japan

辐射接枝 SBS 改性道路沥青应用研究

谢雷东　付海英　李林繁　虞 鸣　窦大营

姚思德　侯铮迟　张 艳　俞铁民

关键词　苯乙烯－丁二烯－苯乙烯辐射接枝，改性沥青，相容性，路用性能，流变性能

本工作利用辐射接枝技术，对苯乙烯－丁二烯－苯乙烯嵌段共聚物（SBS）进行改性，研究了辐射接枝共聚物 SBS-g-M/沥青共混体系的加工、使用性能和流变性能。研究表明：SBS-g-M 与沥青的相容性、分散稳定性明显提高，路用性能有所改善。中试加工的 SBS-g-M 改性道路沥青用于道路试验工程，工程检测结果显示：改性沥青低温延度为 65.7 cm、老化后延度为 34.9 cm，以及沥青混合料力学强度、抗剥落性能、低温抗开裂能力、抗车辙能力等路用性能指标均显著优于国家标准，并优于常规添加稳定剂方法制备的改性沥青。

A study on radiation grafted SBS --- a better binder for road asphalt

XIE Leidong　FU Haiying　LI Linfan　YU Ming

DOU Daying　YAO Side

HOU Zhengchi　ZHANG Yan　YU Tiemin

Keywords　SBS radiation grafting, Polymer modified asphalt, Pavement performance, Rheological properties, Compability

In our work styrene-butadiene-styrene (SBS) triblock copolymer was modified by γ-ray radiation grafting copolymerization, in order to improve binding property of SBS with road asphalt. Mechanical and rheological properties of mixtures of the modified SBS (SBS-g-M) and asphalt were investigated. Compatibility and stability of the SBS-g-M in asphalt increased obviously, and mechanical properties of the SBS-modified asphalt was improved. In trial tests, the results showed that ductility of the modified asphalt at 5°C was 65.7cm, and its ductility after aging of the asphalt was 34.9cm. The SBS-g-M modified asphalt is advantageous over conventional SBS-asphalts mixtures added with stabilizers, in terms of its properties of anti-strips formation, anti-tracks formation, and resistance to fractures at low temperatures, etc. The trial test results indicate that pavement performance of the SBS-g-M modified asphalt can be much better than what are required by national standards for China's polymer-modified asphalt industry.

γ 辐射接枝甲基丙烯酸改善聚醚砜膜亲水性的研究

李 晶 侯铮迟 谢雷东 张凤英 邓 波

关键词 辐射接枝，亲水性，聚醚砜，甲基丙烯酸

利用 γ 射线共辐照技术在聚醚砜（PES）膜上接枝了甲基丙烯酸。通过改变甲基丙烯酸单体浓度，获得了具有不同接枝率的改性 PES 膜。研究结果表明，在单体浓度<10%的范围内，接枝率与单体浓度成线性关系，提高接枝率有助于改善聚醚砜膜的亲水性。

Hydrophilicity improvement of polyethersulfone membranes by grafting methacrylic acid with γ-ray irradiation

LI Jing HOU Zhengchi XIE Leidong

ZHANG Fengying Deng Bo

Keywords Radiation grafting, Hydrophilicity, Poly(ether sulfone), Methyacrylic acid

The grafting of methyacrylic acid onto poly (ether sulfone) membranes was realized by means of simultaneous irradiation in liquids. And the modified membranes with different grafting ratioes were obtained by changing concentration of methyacrylic acid. It was shown that the grafting ratio increased linearly with monomer concentration when it was less than 10%, and hydrophilicity of the membranes improved with increasing grafting ratio.

高分子 PTC 材料的一种新理论模型

李荣群 李 威 苗金玲 王文锋 姚思德 彭 丽[1] 张志平[1]

关键词 高分子正温度系数材料，阻-温特性，正温度系数效应，应力模型

首次全面、系统讨论了高分子/无机导电性复合材料所具有的各种阻-温变化行为，并在前人有关高分子正温度系数（PTC）材料的实验和理论研究的基础上提出了一种新的物理模型——应力模型。应力理论能统一地解释不同类型高分子 PTC 材料在不同温度过程所表现出的复杂的阻-温特性，解决了目前理论与实验现象矛盾的问题。应力理论的提出可能为我们认识高分子 PTC 材料的本质和高分子 PTC 材料理论研究提供新的方向。

---

1 华东理工大学材料科学研究所

A new physical model for polymeric PTC materials

LI Rongqun LI Wei MIAO Jinling WANG Wenfeng YAO Side
PEN Li[1] ZHANG Zhiping[1]

Keywords Polymeric PTC materials, R-T behaviors, PTC effect, Stress mode

Previous studies on polymeric PTC materials were emphasized on PTC effect. However, the resistivity-temperatures behaviors in polymer composites are more complicated. In this paper, a new physical model, the stress model, was presented to better explain the R-T behaviors in polymeric PTC materials. It shows that this speculated model may provide a new direction to investigate essence of polymeric PTC materials for their applications.

1 East China University of Science and Technology, Materials Science Institute

ADE 光诱导原初过程的时间分辨研究：II. 生物分子复合物中的光化学

潘景喜 林维真 韩镇辉 苗金玲 王文锋 姚思德 林念芸 朱大元[1]

关键词 放线菌素 D，激光光解，脱氧核糖核酸，牛血清蛋白，电子转移

利用激光光解结合稳态吸收光谱技术，对放线菌素 D 的模型化合物 ADE 与脱氧核糖核酸（DNA）和牛血清蛋白（BSA）的相互作用进行了系统研究。结果发现，ADE 与单链 DNA（ssDNA）、双链 DNA(dsDNA)以及 BSA 都能发生非共价结合，并能发生光诱导的电子转移反应。结果表明，放线菌素类化合物有可能被用作 I 型的光敏治疗药物，并将为这类化合物的结构改造提供一些有益的启示。

1 中国科学院上海药物研究所

A time-resolved study on photodynamic primary process of ADE Part II: photochemistry in biomolecular complexes

PAN Jingxi LIN Weizhen HAN Zhenhui MIAO Jinling WANG Wenfeng
YAO Side LIN Nianyun ZHU Dayuan[1]

Keywords Actinomycin D, Laser flash photolysis, DNA, BSA, Electron transfer

By use of laser flash photolysis and steady state absorption techniques, a systematic study was carried out on interactions of ADE, which is a kind of model compound of actinomycin D, with DNA

and BSA. Non-covalent binding was found between ADE and ssDNA、dsDNA and BSA, and photoinduced electron transfer reaction was observed. These results indicate that actinomycines might be used as type I photodrugs in the future and will be helpful for structure modification of this kind of compound.

1 Shanghai Institute of Materia Medica, the Chinese Academy of Science

稀有三环核苷衍生物单电子氧化反应的脉冲辐解研究

赵红卫　江致勤[1]　窦大营　吴铁一

王文锋　杜小行[1]　姚思德

关键词　稀有三环核苷衍生物，单电子氧化，脉冲辐解，自由基，瞬间吸收光谱

运用纳秒级脉冲辐解技术研究了稀有三环核苷衍生物 6-甲基三环鸟苷(dYt)与一些单电子氧化性自由基的反应，表征了反应过程中产生的阳离子自由基 $dYt^{\bullet+}$ 及其脱质子中性自由基 $dYt(-H)^{\bullet}$ 的瞬间吸收光谱及 pK_a，并首次得到该化合物与 $^{\bullet}OH$ 自由基及单电子氧化性自由基 $SO_4^{\bullet-}$，$SO_3^{\bullet-}$，和 $N_3^{\bullet-}$ 反应的动力学速率常数，揭示了反应机理，为进一步了解该类化合物的氧化反应提供了一定的证据。

1 同济大学化学系

Pulse radiolysis of singlet-electron oxidation of rare tricyclic nucleoside derivative

ZHAO Hongwei　JIANG Zhiqin[1]　DOU Daying　WU Tieyi

WANG Wenfeng　DU Xiaoxing[1]　YAO Side

Keywords　Rare tricyclic nucleoside derivative, One-electron oxidation, Pulse radiolysis, Radical, transient absorption spectra

Singlet-electron oxidation of N-4-desmethylwyosine(dYt), a derivative of rare tricyclic nucleoside wyosine with several oxidative radicals, has been studied by using pulse radiolysis. The transient spectra of the radicals $dYt^{\cdot+}$ and $dYt(-H)^{\cdot}$ and the pK_a of the radical cations were measured. The rate constants of reactions of dYt with $SO_4^{\cdot-}$, $SO_3^{\cdot-}$, and $^{\cdot}OH$ radicals have been determined and related reaction mechanisms were discussed.

1 Department Chemistry, Tongji University

光聚合法对聚异丙基丙烯酰胺纳米凝胶粒径及形状的控制

乔向利　侯铮迟　盛康龙　姚思德

关键词　光聚合，聚异丙基丙烯酰胺纳米凝胶，窄分布粒径

纳米凝胶粒径和形貌的控制一直是纳米凝胶领域的研究热点。本研究利用光聚合的方法，无需其他有机添加剂，合成出 5—100 nm 范围的聚酰胺凝胶。其粒径分布范围可控制在 10 nm 以内。通过扫描电镜（SEM）对纳米凝胶形貌进行了表征。从结果看，可在纳米尺度上对凝胶的形状进行控制，并合成出树枝状、球状、核壳结构的纳米凝胶。这些结果未在文献中报道过。

Precise control of poly (N-isopropylacrylamide) nanogels by photopolymerization

QIAO Xiangli　HOU Zhengchi　SHENG Kanglong　YAO Side

Keywords　Photopolymerization, Poly N-isopropylacrylamide nanogel, Narrow size distribution

Poly (N-isopropylacrylamide) nanogels of different sizes (5—100nm) and morphologies were synthesized by photochemical method under different reaction conditions of monomer concentration, atmosphere, and photo-sensitizer. PCS and SEM characterizations revealed the photo-synthesized nanogels in desirable size within 10nm distributions and different shapes, depending on the reaction conditions. It has been found that UV light irradiation of low monomer concentrations would form branched and dendritic nanogels, whereas with higher monomer concentrations the products were archic and global nanogels. All the results showed that photo-polymerization mechanism is quite different from that of conventional polymerization, which needs to be explored.

激光光解研究焦脱镁叶绿酸-a 作为光活化农药的可能性

吴铁一　苗金玲　赵红卫　窦大营　王文锋　姚思德　陈志龙[1]

关键词　焦脱镁叶绿酸-a，光活化农药，激光光解

利用激光光解时间分辨吸收方法，对蚕砂叶绿素中提取的焦脱镁叶绿酸-a 的光化学性质进行了初步的研究。发现，该化合物在实验检测的波长范围内都有较强的吸收，且能产生较高量子产额的三重激发态。进而讨论它作为光化学农药的可能性。

---

1 中国人民解放军第二医科大学海军医学系

Laser flash photolysis of pyrophaeophorbide-a and its possible application as a photoactivated pesticide

WU Tieyi MIAO Jinling ZHAO Hongwei DOU Daying

WANG Wenfeng YAO Side CHEN Zhilong[1]

Keywords Pyrophaeophorbide-a, Photoactivated pesticide, Laser flash photolysis

By use of thime-resolved laser flash photolysis techniques, a preliminary study of the photochemical characters of pyrophaeophorbide-a derived from chlorophyll in silkworm excrement has been completed. It was found that these compounds had strong absorbance in all wavelength ranges under investigation, and produced excited triplet state with high quantum yields. Discussions were made on possible applications of the pyrophaeophorbide-a as photoactivated pesticide.

1 Faculty of Naval Medicine, No.2 Military Medical University

海藻酸钠的电离辐射降解研究

付海英 姚思德 吴国忠

关键词 海藻酸钠，激光光解，脉冲辐解，降解

采用 γ 射线辐照、激光光解和脉冲辐解技术，就海藻酸钠水溶液分子量与辐照剂量的关系，$SO_4^{\bullet -}$ 氧化切断海藻酸钠 C_1-O-C_4 键的机理开展研究。探索了海藻酸钠辐射降解规律，推导其在 γ 射线照射下的降解，主要由水辐解产物羟基自由基进攻其 C_1-O-C_4 键，导致链断裂引起的。

Radiation induced degradation of sodium alginate

FU Haiying YAO Side WU Guozhong

Keywords Sodium alginate, Pulse radiolysis, Laser photolysis, Radiation

Reaction rate constants of sodium alginate with both sulfate and carbonate anion radicals were determined by laser flesh photolysis and pulse radiolysis, respectively. The relationship between molecular weight of the sodium alginate and absorbed dose was discussed. Degradations of the sodium alginate were caused by $OH^{\cdot}$ radicals and other oxidative radicals, because the oxidation at the C-4 carbon resulted in the breakage of the glycosidic C_2-O-C_4 bond in the main chain of sodium alginate.

稀有三环核苷衍生物与羟基自由基快速反应动力学及理论计算

赵红卫 孔 玲 王文锋 刘永彪 江致勤[1] 马允胜[2] 姚思德

关键词 稀有三环核苷衍生物，脉冲辐解，自由基，理论计算

运用脉冲辐解瞬态吸收光谱技术研究了稀有三环核苷衍生物 N-4-去甲基-wyosine (dYt)与•OH 自由基快速反应的动力学。结合 AM1 及 B3LYP/6-31G 方法对•OH 进攻 dYt 各位置形成的可能加成产物进行结构优化及热力学能量计算，阐述反应的自由基机理，预测了可能的自由基加成产物。

1 同济大学化学系 2 国家高性能计算中心

Fast reaction kinetics of •OH with the derivative of rare tricyclic nucleoside and theoretical calculation

ZHAO Hongwei KONG Ling WANG Wenfeng LIU Yongbiao

JIANG Zhiqin[1] MA Yunsheng[2] Yao Side

Keywords Rare tricyclic nucleoside derivative, Pulse radiolysis, Radical, Theoretical calculation

Fast reaction kinetics of •OH with N-4-desmethylwyosine (dYt), a derivative of rare tricyclic nucleoside has been studied by pulse radiolysis. The possible initial transient radicals of •OH adducts of dYt were studied by AM1 (with geometry optimization) and B3LYP/6-31G (calculation of total energy). The radical reaction mechanism and the possible structure of OH-adducts were discussed and predicted.

1 Department of Chemistry, Tongji University

2 State High-Performance Computing Center

环境雌激素己烯雌酚的流动池脉冲辐解瞬间谱

窦大营 吴铁一 苗金玲 赵红卫 姚思德

关键词 己烯雌酚，瞬间光谱，脉冲辐解

己烯雌酚（DES）是一种活泼的环境雌激素。利用流动池脉冲辐解手段对其活性瞬间粒子的动力学特性作了初步研究，发现己烯雌酚自由基的苯环间双键可能是羟自由基优先进攻破坏的一个位点。该化合物对高能电子束非常敏感，通过自由基机理被降解。研究结果对 DES 环境降解机理和生物毒理，对探索解毒、环境修复等，具有一定的指导意义。

Radiolysis transient spectra of diethylstilbestrol in a flow-system

DOU Daying WU Tieyi MIAO Jinling ZHAO Hongwei YAO Side

Keywords Diethylstilbestrol, Transient spectrum, Pulse radiolysis

Diethylstilbestrol (DES) is one of the most active environment estrogens. In the paper pulse radiolysis was carried out to study dynamic characteristics of active transient species of DES. The double bond between the benzene rings was supposed to be one of sites attacked by hydroxyl radicals, DES was rather sensitive to high-energy electron beam and their radicals can be easily degraded easily. The works will be of help for us to study degrading mechanisms and biological effects of DES, and to explore environment-repairing ways against DES.

羊毛辐射接枝甲基丙烯酸缩水甘油脂研究

王会勇 刘瑞芹 谢雷东 盛康龙 陈亚力[1] 唐 欣[1]

关键词 羊毛，甲基丙烯酸缩水甘油脂，共辐射接枝

对甲醇溶液中甲基丙烯酸水甘油脂在羊毛纤维上的γ射线辐射接枝反应作了系统研究。考察了气氛、剂量、剂量率、单体浓度等实验条件对接枝反应的影响，发现气氛对接枝反应的影响很小，而接枝率随辐照剂量和单体浓度的增大而提高，接枝效率则随单体浓度的增大而减小。在剂量大于 11 kGy 后接枝率达到平稳状态。用红外吸收谱仪（IR）和扫描电镜（SEM）分析发现单体均匀地接枝在羊毛上。

1 上海二毛爱斯纺织实业有限公司

Radiation graft-copolymerization of wool with ethacrylic acid glycidyl ester

WANG Huiyong LIU Ruiqin XIE Leidong SHENG Kanglong

CHEN Yali[1] TANG Xin[1]

Keywords Wool, MAGE, Gamma ray radiation graft-copolymerization

A systematic study was done on radiation graft-copolymerization of wool samples irradiated by γ-rays with methanol solution of methacrylic acid glycidyl ester monomer. It was found that reaction atmosphere did not cause great effects to the graft-copolymerzation reaction. The graft rate increased with increasing dose, reaching a status of equilibrium at 11kGy. With increasing monomer concentrations, the graft rate increased, too, whereas the graft efficiency decreased. Results of IR and SEM characterizations of the grafted samples showed that monomer had been grafted uniformly onto the wool fibers.

丝绸的光引发丙烯酸羟丙酯接枝研究

刘瑞芹 王会勇 谢雷东 侯铮迟 李林繁 虞 鸣 姚思德 盛康龙

关键词 丝绸，光化学接枝，接枝共聚，丙烯酸羟丙酯

以丙烯酸羟丙酯为单体，就丝绸的紫外光光化学接枝改性进行了系统研究。用红外光谱（FT-IR）和差示扫描量热法（DSC）等对光接枝产物进行了表征。探索了光照时间、单体浓度、pH 值、温度、溶剂体系对接枝率的影响规律。研究表明，该方法较辐射接枝能获得更高的接枝率，且有无污染、设备简便、易于操作、均聚物较少等优点，不失为一种更有效的丝绸改性方法。

Graft copolymerization of 2-hydroxypropyl acrylate onto silk fabrics initiated by ultraviolet rays

LIU Ruiqin WANG Huiyong XIE Leidong HOU Zhengchi LI Linfan

YU Ming YAO Side SHENG Kanglong

Keywords Silk, Graft copolymerization, UV-irradiation, 2-hydroxypropylacrylate

Silk fabric samples were grafted with 2-hydroxypropyl acrylate monomer by ultraviolet rays, and a light-initiated graft copolymerization system without any additives or co-additives has been established. Experiments were performed to study the effects of monomer concentration, irradiation time, pH value, and reaction temperature on the grafting rate. FT-IR and DSC characterizations of the grafted silk samples were carried out to study the property changes in the silk fabrics. With advantages of fairly high graft rate, simpler equipment and operation, free of additives, and less homopolymer, the method can be an effective technique to improve the properties of silk fabrics.

聚 N-异丙基丙烯酰胺包覆 Fe_3O_4 磁导向纳米粒子的制备和表征

孙汉文 余家会 张春富 谢雷东 侯铮迟 徐冬梅 姚思德

关键词 辐照，聚 N−异丙基丙烯酰胺，四氧化三铁，磁性复合纳米粒子

选择 N−异丙基丙烯酰胺（N−isopropylacrylamide，NIPAM）为单体，N，N’−亚甲基双丙烯酰胺（Methylenebisacrylamide，MBA）为交联剂，用辐射化学方法合成了具有温敏的 PNIPAM 包覆 Fe_3O_4 磁导向纳米粒子。研究了 NIPAM 单体浓度、交联剂 MBA 用量、不同光照时间及温度对核壳结构磁性纳米粒子粒径的影响，发现在一定范围内随单体 NIPAM 浓度的增加、交联剂 MBA 浓度的减小、光照时间的增加，聚 NIPAM 包覆 Fe_3O_4 核壳结构纳米粒子的粒径增大。在 25—39 ℃温度范围内 PNIPAM 包覆 Fe_3O_4 核壳结构纳米粒子具有最低临界溶解温度特性（Lower critical solution temperature，LCST）。以 SEM 和动态激光光散射仪（PCS）对该核壳结构纳米粒子粒径进行测定，表明辐射化学方法合成的核壳结构纳米粒子比较均匀。

Preparation and characterization of Fe_3O_4 magnetic nano-particles modified with poly (N-isopropylacrylamide) by UV irradiation

SUN Hanwen YU Jiahui ZHANG Chunfu XIE Leidong

HOU Zhengchi XU Dongmei YAO Side

Keywords Radiation, Poly (N-isopropylacrylamide), Magnetite, Magnetic nanoparticles

Fe_3O_4 magnetic nanoparticles were modified with poly (N-isopropylacrylamide) under UVirradiation. It has been found that the diameter with narrow distribution of the modified Fe_3O_4 nanoparticles measured by PCS in aqueous solution can be controlled easily by changing concentration of monomer NIPAM and cross-linker MBA, temperature and time. It has been also shown that the modified Fe_3O_4 nanoparticles are featured by lower critical solution temperature (LCST) while the temperature varies from 25℃ to 39℃. This may suggest promising application of the nanopartucles in medicine.

白介素-6 对受全身分次照射荷瘤小鼠肿瘤细胞增殖与凋亡的影响

刘永彪 梅 开[1] 刘 颖[1] 赵 杰[1] 张先稳[1] 周 强[1] 郝兴芝[1] 姚思德

关键词 白介素-6，肿瘤，电离辐射，增殖，凋亡，p53，bcl-2

以受分次全身照射的三种荷瘤小鼠为研究对象，探讨白介素-6（IL-6）对不同肿瘤细胞增殖、凋亡及凋亡相关基因 p53、bcl-2 表达的影响。本实验采用流式细胞术检测 IL-6 对 S_{180} 肉瘤、H_{22} 肝癌、Lewis 肺癌三种荷瘤小鼠经 6 MV X 线分次全身照射后肿瘤细胞凋亡及增殖指数的影响；以免疫组织抗生蛋白链霉素−过氧化物酶−生物素（SP）法检测以上三种荷瘤小鼠肿瘤组织中 p53、bcl-2 的表达水平，及 IL-6 对经照射的三种荷瘤小鼠肿瘤组织 p53、bcl-2 表达水平的影响。结果表明：在接受全身分次照射的三种荷瘤小鼠中，Lewis 肺癌 IL-6 组 SPF 值及 PI 值均较对照组低，AI 值较对照组高（$p<0.05$），S_{180} 肉瘤荷瘤鼠结果相反（$p<0.01$）；而在 H_{22} 肝癌两组肿瘤细胞凋亡及增殖指数未见明显差异（$p<0.05$）。其机理可能与 IL-6 改变了肿瘤细胞所处周期时相的比例有关。IL-6 对凋亡相关基因 p53、bcl-2 的表达在不同肿瘤组织中具有不同影响，Lewis 肺癌荷瘤鼠 IL-6 组肿瘤细胞 p53 表达水平较对照组低；S_{180} 肉瘤荷瘤鼠 IL-6 组肿瘤细胞 bcl-2、p53 表达水平对照组高；而 H_{22} 肝癌荷瘤鼠两组肿瘤细胞 bcl-2、p53 表达水平无明显差异。其作用能与 IL-6 对不同肿瘤组织中凋亡相关基因 p53、bcl-2 的表达产生不同影响有关。

---

1 徐州医学院肿瘤研究所

Effects of IL-6 on tumor cell proliferation and apoptosis of tumorbearing mice

LIU Yongbiao MEI Kai[1] LIU Ying[1] ZHAO Jie[1] ZHANG Xianwen[1]
ZHOU Qiang[1] HAO Xingzhi[1] YAO Side

Keywords Interleukin-6, Tumor, Ionizing radiation, Proliferation, Apoptosis, p53, bcl-2

A study was carried out on effects of IL-6 on proliferation and apoptosis of tumor cells and expression of apoptosis relevant genes (p53, bcl-2) in tumor cells for three kinds of fractional total-body-irradiated tu-mor-bearing mice.The apoptotic index, proliferative index, S phase fraction of S180 sarcoma, H22 hepatocarcinoma and Lewis lung cancer cells were measured by flowcytometry (FCM) after total-body-irradiation and irradiation plusIL-6. The protein expression levels of p53, bcl-2 in three kinds of tumors were also determined by the immunohisto-chemical method (ultrasensitive S-P). The results showed that the S phase fraction and proliferation index in Lewislung cancer cells were lower in the irradiated plus IL-6 group than in the control, while apoptotic index was higher ($p< 0.05$). However, the experimental results for S180 sarcoma cells were opposite ($p < 0.01$). In addition, no significant effects were observed in H22 hepatocarcinoma. These results revealed that IL-6 promoted the apoptosis of irradiated Lewis lung cancer cells ($p < 0.05$) , while the apoptosis of S180 sarcoma ($p < 0.05$) was restrained, and there was no significant effects on the cellular cycle of H22 hepatocarcinoma ($p > 0.05$) . In Lewis lung cancer the expression level of p53 was lower in the IL-6 group and highter in S180 sarcoma ($p < 0.05$) , while unvaried in H22 hepatocarcinoma as compared to the control ($p > 0.05$) . It is considered that tumor cell's proportion in the cellular cycle is changed by IL-6 and the effects of IL-6 on the expression of p53, bcl-2 in different three kinds of tumors are different. IL-6 has radio-sensitive effects on some tumors and opposite effects on other tumors, it may be related to the expression of P53 and Bcl-2 in tumor cells.

SOD 对肿瘤细胞凋亡影响和抗氧化损伤的研究:
Ⅰ.SOD 与 DDP、ADM、VP16 合用对肿瘤细胞凋亡的影响

刘永彪 刘 颖[1] 赵 杰[1] 郝兴芝[1] 王 绪[1] 姚思德

关键词 超氧化物歧化酶，肿瘤化疗药物，细胞凋亡，宫颈癌 Hela 细胞

将顺铂（DDP）、阿霉素（ADM）和足叶乙甙（VP16）以不同时间作用于实验小鼠宫颈癌 Hela 细胞，测定细胞内活性氧（ROS）水平和细胞凋亡率，研究抗肿瘤药物诱导 Hela 细胞凋亡与细胞内 ROS 水平的关系。研究表明，在抗肿瘤药物作用前加入超氧化物歧化酶（SOD），会减少 Hela 细胞的凋亡，在抗肿瘤药物作用 24h 后加入 SOD，对 Hela 细胞的凋亡无影响，而且对 Hela 细胞 p53、c−fos 基因产物表达也无影响。荷瘤小鼠机体整体水平研究表明，在给予化疗药物 4h 后连续 5d 注入 SOD，与单纯化疗药物组相比，可显著减少荷瘤小鼠骨髓细胞，肝脏和脾脏组织

匀浆中 ROS 水平。表明后注入 SOD 可直接清除重要脏器细胞内因化疗药物产生的过量 ROS，还可提高其它抗氧化酶活性而协同清除化疗药物产生的过量 ROS，从而避免正常器官的氧化性损伤。本研究结果为肿瘤化疗中适时施用 SOD，减少化疗的毒副作用具有一定指导意义。

1 徐州医学院肿瘤研究所

Studies on tumor cell apoptosis with SOD and its anti-oxidation effect I The effect of SOD on apoptosis of tumor cell in DDP, ADM and VP16

LIU Yongbiao LIU Ying[1] ZHAO Jie[1] HAO Xingzhi[1] WANG Xu[1] YAO Side

Keywords Superoxide dismutase, Chemotherapic medicine, Apoptosis of tumor cell, Hela cell

By determination of ROS and apoptosis of Hela cells in mice at different hours after treatment with DDP, ADM or VP-16, the relations between apoptosis of Hela cell induced by chemotherapic Drug and concentration of ROS has been investigated. It has been found that there is no effect on apoptosis, and the P53 and c-fos expressions, of the Hela cells when SOD was applied 24 hours after the chemotherapy, whereas apoptosis of the Hela cells reduced when SOD was applied beforethe chemotherapy. Comparing with the control group, to which just ADM and DDP were given, ROS levels reduced markedly in bone marrow, liver and spleen of the tumor-bearing mice, which had been treated with SOD for five consecutive days 4 hours after the chemotherapy. It can be inferred that the oxidation damage of normal tissue can be avoided with scavenge of excessive ROS and increase of anti-oxidative enzymes by SOD in the chemotherapy. The results suggest that injecting SOD at suitable time in clinic chemotherapymay be useful for reducing the side effects.

SOD 对肿瘤细胞凋亡影响和抗氧化损伤的研究: Ⅱ.SOD 对荷瘤小鼠脾淋巴细胞的辐射防护效应

刘永彪 刘 颖[1] 赵 杰[1] 郝兴芝[1] 王 绪[1] 姚思德

关键词 超氧化物歧化酶，荷瘤小鼠，淋巴细胞亚群，辐射防护，脂质过氧化

以受照射荷瘤小鼠为实验对象，研究外源性超氧化物歧化酶（SOD）对荷瘤小鼠脾淋巴细胞分化、增殖、亚群间调节的影响，测定了抗氧化酶活性和氧化还原产物含量，观察了 SOD 对荷瘤小鼠脾脏超微结构的影响，同时检测 SOD 对射线杀伤肿瘤细胞效应的影响。结果显示，SOD 能够促进受全身照射的 H_{22} 肝癌荷瘤小鼠淋巴细胞分化、增殖及亚群间调节，同时增加脾脏组织中谷胱甘肽过氧化酶（GSH-Px）、血清超氧化物歧化酶总活力（T-SOD）活力和谷胱甘肽（GSH）

含量，降低氧化产物丙二醛（MDA）含量，并提高其免疫活性；SOD 可明显减轻电离辐射对荷瘤小鼠脾淋巴细胞超微结构的破坏，并通过延迟 S 期时相对改变其细胞周期。实验结果提示，SOD 通过清除自由基降低活性氧（ROS）浓度，减轻脾淋巴细胞脂质过氧化，延迟脾淋巴细胞 S 期时相而提高其辐射抗性，同时 SOD 可提高抗氧化物酶活性，并通过影响细胞凋亡信号转导途径，进而影响细胞凋亡基因的表达。

1 徐州医学院肿瘤研究所

Studies on tumor cell apoptosis with SOD and its anti-oxidation effect II. Radio-protective effect on spleen lymphocyte of tumor bearing mice with SOD

LIU Yongbiao LIU Ying[1] ZHAO Jie[1] HAO Xingzhi[1] WANG Xu[1] YAO Side

Keywords Superoxide dismutase, Tumor-bearing mice, Subpopulation of lymphocytes, Radiation-protection, Lipid peroxidation

In this paper the effects of exogenous SOD on differentiation, proliferation, regulation of subpopulation of spleen lymphocytes has been studied with irradiated tumor-bearing mice. The activity of antioxidant enzymes and the contents of redoxic products have also been determined. And the effect of SOD on ultra-structure of spleen of irradiated tumor-bearing mice has been investigated meanwhile the killed effect of spleen tumor under irradiation with addition of SOD has been observed. It has been found that SOD does emphasize the differentiation, proliferation, regulation of subpopulation of spleen lymphocytes cell with radiated tumor-bearing mice and increase the activities of GSH, GPX and total?vigor of SOD while MDA decreased in spleen. It has been also found that SOD injected before or after irradiation can reduce the injury of spleen obviously and makes the tissue have higher protection from irradiation while the tumor was killed as the same as no addition of SOD. It can be deduced that lighten of lipid peroxidation occurs from the scavenge of ROS by SOD, the high protection of sleep from irradiation is because of delay to S phase of lymphocytes and increase of activity of antioxidant enzymes. The concentration change of SOD and ROS may have some influence on signal transferring pathway and gene expression of cell apoptosis

SOD 对肿瘤细胞凋亡影响和抗氧化损伤的研究: Ⅲ.SOD 对受分次照射的荷瘤小鼠肿瘤细胞脂质过氧化影响及分子机制

刘永彪　赵 杰[1]　刘 颖[1]　郝兴芝[1]　王 绪[1]　姚思德

关键词　超氧化物歧化酶，荷瘤小鼠，辐射敏感性，原癌基因 c−jun，端粒酶

以荷瘤小鼠为动物模型，研究了全身照射下注射超氧化物歧化酶（SOD）对肿瘤细胞脂质过氧化、肿瘤组织端粒酶活性、肿瘤原癌基因 c−jun 蛋白表达的影响。研究发现，SOD 能增加 S_{180} 肉瘤及 Lewis 肺癌组氧化产物丙二醛（MDA）含量，降低 S_{180} 肉瘤谷胱甘肽（GSH）含量及血清超氧化物歧化酶总活力（T−SOD）、匀浆谷胱甘肽过氧化物酶（GPX−Px）活力；降低 Lewis 肺癌组 GPX−Px 及 T−SOD 活力，不影响 GSH 含量；降低 H_{22} 肝癌组 GPX−Px 的活力，不影响 MDA、GSH 含量及 T−SOD 活力。SOD 明显降低接受电离辐射的 S_{180} 肉瘤及 H_{22} 肝癌荷瘤小鼠肿瘤组织中端粒酶的阳性表达率，减少原癌基因 c−Jun 蛋白在 S_{180} 肉瘤、Lewis 肺癌荷瘤鼠中的表达。这一辐射增敏作用因肿瘤的种类而不同，可能与 SOD 在不同肿瘤中对癌基因 c−jun 蛋白表达和端粒酶活性影响及药物在不同器官的代谢差异有关。

1 徐州医学院肿瘤研究所

The studies of effect on tumor cell apoptosis with SOD and its anti−oxidation effect III. The effect of SOD on lipid peroxidation of tumor cell of tumor−bearing mice under fractional irradiation

LIU Yongbiao　ZHAO Jie[1]　LIU Ying[1]　HAO Xingzhi[1]　WANG Xu[1]　YAO Side

KEYWORDS　Superoxide dismutase, Tumor−bearing mice, Radiosensitivity, Rotooncogene c−jun, Telomerase

In this paper the effect of injury of SOD on lipid peroxidation of tumor cell, telomerase activities in tumor tissues, expression of protooncogene c−jun pretein were been studied with irradiated tumor−bearing mice. It has been found that content of MDA increased in S_{180} sarcom group and Lewis lung cancer group in situation of SOD injury while the content of GSH, GPX and activity of T−SOD decreased For former and with no change of GSH for later. It has also been found that SOD can reduce the telomerase activities in S_{180} and H_{22} and expression of protooncogene c−Jun in S_{180} sarcom, Lewis lung cancer tumor tissues. The radiosensitivity of SOD may have some relationship with the effect on expression of protooncogene c−Jun and telomerase activities, and metabolism of SOD in different kinds of tumor.

SOD 对肿瘤细胞凋亡影响和抗氧化损伤的研究: Ⅳ.SOD 对荷瘤小鼠正常组织氧化损伤的保护效应

刘永彪 刘 颖[1] 赵 杰[1] 郝兴芝[1] 王 绪[1] 姚思德

关键词 超氧化物歧化酶，电离辐射，抗肿瘤药物，荷瘤小鼠，活性氧，丙二醛，胱苷肽过氧化物酶，过氧化氢酶

探讨超氧化物歧化酶（SOD）对电离辐射和肿瘤化疗药物对荷瘤机体正常组织损伤的保护效应及机制，测定荷瘤鼠肝脏、脾脏、肾脏、心脏、肺、脑和骨髓组织的活性氧（ROS）、氧化产物丙二醛(MDA)水平和谷胱苷肽过氧化物酶（GSH−Px）、过氧化氢酶（CAT）活性，并观察 SOD 对荷瘤小鼠肝脏超微结构的影响。结果表明，荷瘤小鼠受照射和化疗药物后其骨髓、肝脏、肾脏、脾脏、组织匀浆中 ROS、MDA 含量明显升高，而 GSH−Px 和 CAT 活性明显降低，其机制是电离辐射和化疗药物造成抗氧化酶的损伤及机体内 ROS 含量上升。加入 SOD 与对照组相比，显著降低荷瘤小鼠骨髓、肝脏、脾脏组织匀浆中 ROS、MDA 含量，略微升高 GSH−Px 和 CAT 活性，而对肾脏组织匀浆中 ROS、MDA 含量和 GSH−Px 和 CAT 活性无明显影响，同时 SOD 可明显减轻电离辐射对荷瘤小鼠肝细胞超微结构破坏，SOD 通过直接清除自由基和保护抗氧化酶的损伤起辐射保护作用。

1 徐州医学院肿瘤研究所

The studies of effect on tumor cell apoptosis of SOD and its anti-oxidation effect Ⅳ.The protection effects of SOD on oxidized damage of normal tissue with tumorbearing mice with SOD

LIU Yongbiao LIU Ying[1] ZHAO Jie[1] HAO Xingzhi[1] WANG Xum[1] YAO Side

Keywords Superoxide dismutase, Ionizing radiation, Antitumor drugs, Tumor-bearing mice, Reactive oxygen species, Malondialdehyde, Glutathione peroxidaes, Catalase

In order to investigate protection effects of SOD on the oxidized damage of normal tissues induced in chemotherapeutic drug and irradiated tumor-bearing mice, the contents of ROS and MDA, the activation of GSH-Px and CAT in liver, kidney, spleen and bone marrow have been determined. The effect of SOD on the ultra-structure of liver cell has been evaluated. It has been found that chemotherapeutic drug and irradiation can increase the contents of ROS and MDA and decrease activation of GSH-Px and CAT. And SOD can decrease contents of ROS and MDA and increase the activation of GSH-Px and CAT slightly for liver, spleen, marrow, but for kidney there is no significant change while SOD can reduce the damage of ultra-structure of liver. It can be inferred that SOD have some protec- tion effects on the normal tissue of tumor-bearing mice via scavenging free radicals and activate anti-oxidative en-zymes after TBI and drugs injection

放射性药物

Radiopharmaceuticals

3-(4-氟苄基)-8-羟基-1，2，3，4-四氢苯并吡喃[3，4-c]吡啶-5-酮的合成

李谷才　尹端沘　夏姣云　程登峰　汪勇先

关键词　苯并吡喃[3，4-c]吡啶-5-酮，合成，表征

以间苯二酚和 4-酮-3-甲酸甲酯哌啶盐酸盐为原料，通过两步反应，合成了 8-羟基-3-(4-氟苄基)-1，2，3，4-四氢苯并吡喃[3，4-c]吡啶-5-酮，并对其进行了表征。

Synthesis of 3-(4-fluorobenzyl)-8-hydroxy-1, 2, 3, 4-tetrahydrochromeno[3, 4-c]pyridin-5-one

LI Gucai　YIN Duanzhi　XIA Jiaoyun　CHENG Dengfeng　WANG Yongxian

Keywords　Chromeno[3,4-c]pyridin-5-one, Synthesis, Characterization

3-(4-Fluorobenzyl)-8-hydroxy-1,2,3,4-tetrahydrochromeno[3,4-c]pyridin–5-one was prepared from resorcinol and methyl-4-oxo-3-piperidine carboxylate hydrochloride through two reactions and their structures were confirmed by elemental analysis, IR, ^{1}H NMR and ESI-MS spectra.

7-氮杂吲哚衍生物——一种新多巴胺 D_4 受体显像剂的合成

田海滨　尹端沘　张春富　张 岚李俊玲　王丽华　周 伟　汪勇先　郭子丽

关键词　7-氮杂吲哚类似物，多巴胺 D_4 受体，合成

7-氮杂吲哚的衍生物 L-750667 是一个新的、高亲和性(Ki = 0.51 nmol/L)的 D_4 受体选择性配体，采用还原的胺烷基化反应合成了 L-750667 的类似物:3-[4-(4-氟苯甲基)哌嗪-1-基]-甲基-1H-吡咯并[2，3-b]吡啶。同时制备出[^{18}F]标记前体 4-三甲基铵苯甲醛-三氟甲基磺酸盐，及用于放化合成目标化合物的中间体 3-(哌嗪-1-基)-甲基-1*H*-吡咯[2，3-b]吡啶，为放射化学合成 3-[4-(4-[^{18}F]氟苯甲基)哌嗪-1-基]-甲基-1*H*-吡咯并[2，3-b]吡啶提供了可靠的技术。

7-Azaindole derivative syntheses of a potential dopamine D_4 receptor imaging agent

TIAN Haibin　YIN Duanzhi　ZHANG Chunfu　ZHANG Lan　LI Junling

WANG Lihua　ZHOU Wei　WANG Yongxian　GUO Zili

Keywords　7-azaindole analog, Dopamine D_4 receptor, Synthesis

The 7-azaindole derivative 3-{[4-(4-iodophenyl) piperazin-1-yl]-methyl}-1H-pyrrolo[2, 3-b] pyridine (L-750667) is a novel, high-affinity (Ki = 0.51 nmol/L) and selective D_4 R ligand. L-750, 667 analogue 3-[4-(4-fluorobenzyl)] piperazin-1-yl} methyl-1*H*-pyrrolo [2, 3-b] pyridine was synthesized, and the trimethylammonium-benzaldehyde triflate which can be radiolabeled with fluorine-18($t_{1/2}$ 110 min) was also prepared. These techniques will provide potentiality to synthesize a labeled compound 3-[4- (4-[^{18}F]fluorobenzyl)] piperazin-1-yl}methyl-1*H*-pyrrolo[2, 3-b]pyridine.

N-琥珀酰亚胺 4-[^{18}F](氟甲基)苯甲酸酯标记蛋白的应用

李俊玲　汪勇先　张秀利　周 伟　田海滨　尹端泓

关键词　N-琥珀酰亚胺 4-[^{18}F](氟甲基)苯甲酸酯，IgG，标记，体积排阻色谱

合成了 N-琥珀酰亚胺 4-[^{18}F](氟甲基)苯甲酸酯(S^{18}FMB)，耗时 30 min，放化产率 57%(EOB)。探讨了影响 S^{18}FMB 与 IgG 反应的因素:反应 pH、IgG 与 S^{18}FMB 用量、反应时间、反应温度及所用溶剂乙腈的干燥度。得出最佳标记条件:以无水已腈为溶剂，0.2 mg/mL IgG，pH=7.8—8.5，25 ℃，反应 15 min，标记率可达 80%以上。S^{18}FMB 与 IgG 反应物用体积排阻色谱分离。

Application of N-succinimidyl 4-[^{18}F](fluoromethyl) benzoate to protein labeling

LI Junling　WANG Yongxian　ZHANG Xiuli　ZHOU Wei

TIAN Haibin　YIN Duanzhi

Keywords　S^{18}FMB, IgG, Protein labeling, Size exclusion chromatography.

N-succinimidyl 4-[^{18}F](fluoromethyl) benzoate for protein labeling was prepared (57%, EOB) in about 30min. Reaction conditions of S^{18}FMB with IgG including pH of solutions, protein concentration, reaction temperature and time were studied. The optimal labeling conditions were: 0.2 mg/mL IgG, pH=7.8—8.5, 25℃, reaction time 5min, yield was about 80%. The ^{18}F-labeled protein was purified by size exclusion chromatography.

^{18}F 标记氨基酸的研究进展

李俊玲　田海滨　张 岚　汪勇先

关键词　^{18}F-氨基酸，合成，亲电氟化，亲核氟化

介绍了用于脑肿瘤显像的氨基酸的选择标准；对 ^{18}F 标记氨基酸的 3 种方法:Balz-Schiemann 反应、亲电取代和亲核取代反应的优缺点进行了对比，得出了亲核取代法为较佳选择方法的结论。

Advances in fluorine-18 labelling amino acids

LI Junling WANG Yongxian TIAN Haibin ZHANG Lan

Keywords ^{18}F- amino acid, Synthesis, Electrophilic fluorination, Nucleophilic fluorination

The selecting criteria of amino acids suitable for evaluation of brain tumors were introduced. Three methods for ^{18}F labeling amino acids , namely Balz-Schiemann reaction、electrophilic fluorination and nucleophilic fluorination, were compared. It was concluded that nucleophilic substitution was the best method among those.

Fac-[M(CO)$_3$]$^+$(M=$^{188/186}$Re，^{99}Tc^m)化合物生物标记及应用

夏姣云 汪勇先 于俊峰 尹端沚

关键词 fac-[M(CO)$_3$]$^+$，$^{188/186}$Re，^{99}Tc^m，生物小分子，蛋白，多肽

Fac-[M(CO)$_3$L$_3$]$^+$(M=$^{188/186}$Re ，^{99}Tc^m，L＝H$_2$O)具有良好的放射生物学特性，是一种很有发展前途的标记前体。本文综述了 fac-[M(CO)$_3$]$^+$(M=$^{188/186}$Re，^{99}Tc^m)核标记生物小分子(生物素、雌激素……)、大分子蛋白及多肽的研究进展，并探讨了其今后发展的方向。

Biolabeling and application of the fac-[M(CO)$_3$]$^+$ （M=$^{188/186}$Re, ^{99}Tc^m）compounds

XIA Jiaoyun WANG Yongxian YU Junfeng YIN Duanzhi

Keywords Fac-[M(CO)$_3$]$^+$, ^{99}Tc^m , $^{188/186}$Re, Small biomolecule, Protein, Peptide

fac-[M(CO)$_3$L$_3$]$^+$（M=$^{188/186}$Re, ^{99}Tc^m, L=H$_2$O）is a promising radiolabeling precursor due to its favorable radiobiological characteristics. The progress of small biomolecules, proteins, and peptides labeled with the fac-[M(CO)$_3$]$^+$（M=^{99}Tc^m ,$^{188/186}$Re）core is summarized, and its development in future is also discussed.

三羰基铼[^{188}Re]的放射化学合成

夏姣云 汪勇先 于俊峰 张春富 周 伟 李谷才 王明伟 程登峰 尹端沚

关键词 三羰基铼，^{188}Re，放射化学合成

合成了化合物 [N(Et)$_4$Br]$_2$[Re(CO)$_3$Br$_3$]，并用 IR、ICP-MS、元素分析等方法对化合物进行了

表征。分析了此化合物溶于水后，阴离子部分的 3 个 Br^-可定量地被 3 个 H_2O 分子取代，得到前体化合物 fac-$[Re(CO)_3(H_2O)_3]^+$。同时合成了放射性前体化合物 fac-$[^{188}Re(CO)_3(H_2O)_3]^+$，放化产率约为 80%， Sep-Pak 分离后，放化纯度大于 95%。通过 HPLC 分析比较了这两个前体，确定了放化前体 fac-$[^{188}Re(CO)_3(H_2O)_3]^+$的结构。

Radiosynthesis of tricarbonal rhenium[^{188}Re]

XIA Jiaoyun WANG Yongxian YU Junfeng ZHANG Chunfu ZHOU Wei

LI Gucai WANG Mingwei CHENG Dengfeng YIN Duanzhi

Keywords Tricarbonyl rhenium, ^{188}Re, Radiosynthesis

The complex of $[N(Et)_4Br]_2[Re(CO)_3Br_3]$ was prepared and characterized by IR, ICP-MS, elemental analysis. When the complex was dissolved in water, the three Br^- ligands were quantitatively exchanged with three water molecules and the precursor of fac-$[Re(H_2O)_3(CO)_3]^+$ could be obtained. The complex of fac-$[^{188}Re(H_2O)_3(CO)_3]^+$ was synthesized with an overall radiochemical yield of 80%, and with more than 95% radiochemical purity after Sep-Pak seperation. Taken the complex of fac-$[Re(H_2O)_3(CO)_3]^+$ as a standard sample, the structure of the precursor, fac-$[^{188}Re(H_2O)_3(CO)_3]^+$, was comfirmed by HPLC.

N-琥珀酰亚胺-4-氟[^{18}F]苯甲酸酯的合成

程登峰 尹端沚 周 伟 王明伟 夏姣云 李谷才 汪勇先

关键词 氟-18，N-琥珀酰亚胺-4-氟[^{18}F]苯甲酸酯($S^{18}FB$)，合成

生物小分子凭借其好的亲和性、特异性、选择性、体内稳定性和较小的体积，已显示出其作为一种核医学显像试剂的潜力。借助这些小分子的标记化合物，较高的靶/背景比以及快速的血液清除性很容易实现。同时，通过高分辨率的正电子发射断层显像仪(PET)，较小的靶组织的显像更加容易成功。短寿命的发射正电子核素氟-18 由于具有优良的物理和化学特性(0.635 MeV 的正电子能量、高分辨率和灵敏度、110 min 的半衰期)也吸引了放射性药物学家们积极地将其应用于 PET 显像试剂。但是氟-18 标记生物小分子只有借助于标记前体才能实现。N-琥珀酰亚胺-4-氟[^{18}F]苯甲酸酯由于能和生物分子达到较高的标记率以及较好的体内稳定性，成为一种最适宜的氟-18 标记试剂。

首先合成标记前体乙基-4-三甲胺苯甲酸酯-三氟磺酸盐，将等物质的量比的 4-二甲胺苯甲酸乙酯与甲基三氟甲基磺酸盐以乙腈为溶剂在室温下反应过夜，然后蒸发溶剂，粗产物经二氯甲烷/正己烷重结晶即可得纯的标记前体，经核磁检测与文献报道一致。接下来经三步放射性合成，通过 Sep-PakC18 柱分离可得 $S^{18}FB$。合成时间约 1 h；放化产率约 50%(衰变校正)；经 TLC 分析(流动相 $V_{乙酸乙酯}$:$V_{正己烷}$=1:4)，R_f=0.86，以及 HPLC 分析(VydacC18 柱，$V_{乙腈}/V_{0.1\%乙酸水溶液}$＝50:50，流速为 1 mL/min)，R_t＝4.26 min，放化纯度大于 95%。

Synthesis of N-succinimidyl-4[^{18}F]fluorobenzoate

CHENG Dengfeng YIN Duanzhi ZHOU Wei WANG Mingwei

XIA Jiaoyun LI Gucai WANG Yongxian

Keywords Fluorine-18, N-succinimidyl-4[^{18}F]fluorobenzoate($S^{18}FB$), Synthesis

Small biomolecules have shown their potential as imaging agents for nuclear medicine with respect to their affinity, specificity, selectivity, in vivo stability and smaller size. With the smaller size of the labeled compounds, both of higher target-to-background ratio and faster blood clearance are often obtained, in addition, the higher resolution with positron emission tomography (PET) allows the detection of smaller targets. Short-lived PET isotope Fluorine-18 attracs many radiopharmacists to apply it as PET imaging agents due to its good physical and chemical character(low positron energy of 0.635MeV, high resolution and sensitivity, the half-life of 110min).However,^{18}F-labeled small biomolecules can only be executed with labeling prosthetic groups. N-Succinimidyl-4[^{18}F]fluorobenzoate seems to be the most suitable ^{18}F-labelling agent due to its higher conjugation efficiency with biomolecules and stability in vivo.

At first, triflate salt of ethyl p-trimethylammonium benzoate was synthesized with equivalent molar ration of methyl triflate and ethyl 4-(dimethylamino) benzoate reacting in CH_2Cl_2 at room temperature over night, then evaporating solvent, pure product was obtained recrystallizing from CH_2Cl_2/hexone. $S^{18}FB$ was obtained by three steps radiosynthesis and separated by Sep-PakC18 cartridge. The decay-corrected radiochemical yields was about 50% with radiochemical purity>95% within 60 min. The results of TLC and HPLC were ethyl acetate:CH_2Cl_2=1:4(V/V), Rf=0.86, HPLC-analysis: acetonitrile/0.1%acetic acid (50/50, V/V), t_R＝4.26 min.

N-琥珀酰亚胺-4-氟[^{18}F]甲基苯甲酸酯合成方法的改进及其应用

程登峰 尹端沘 周 伟 李俊玲 汪勇先

关键词 氟-18，N-琥珀酰亚胺-4-氟[^{18}F]甲基苯甲酸酯($S^{18}FMB$)，合成

正电子核素标记的生物活性分子的应用已经成为核医学中一个有用的和令人感兴趣的领域。由于氟-18 具有良好的物理和化学性质，因此它成为那些 PET 核素中的首选。但是，氟-18 标记生物活性分子的过程繁琐且耗时，$S^{18}FMB$ 相比较而言一种非常有用的标记生物活性分子的酰基化试剂。 $S^{18}FMB$ 由 **N-**琥珀酰亚胺-4-[(4-硝基苯磺酰基)氧甲基]苯甲酸酯(SNOB)与 $^{18}F^-$经一步反应可得。SNOB 可以由 4-硝基苯磺酸银与 N-琥珀酰亚胺-4-溴甲基苯甲酸酯在室温下反应 6 d 而得。通过优化反应参数，$S^{18}FMB$ 的放化产率可达 57%(衰变校正)，另外，用简单的 Sep-Pak 硅胶柱可以代替繁琐的 HPLC 来实现产物的分离。为了给 $S^{18}FMB$ 标记其他生物分子提供方法学研究，我们成功的进行了 $S^{18}FMB$ 标记 IgG。在最佳标记条件下(0.2 g/L 的 IgG，PH＝7.8—8.5，25℃，反应 15 min)，标记率达到 80%。在 $S^{18}FMB$ 标记奥曲肽的基础上，我们还实现了 $S^{18}FMB$ 标记 VIP，$S^{18}FMB$-VIP 是一种很有潜力的 PET 显像剂，可用于许多肿瘤的诊断。

An improved radiochemical synthesis of N-succinimidyl 4-^{18}F-(fluoromethyl)benzoate and its application

CHENG Dengfeng YIN Duanzhi ZHOU Wei LI Junling WANG Yongxian

Keywords Fluorine-18, N-Succinimidyl-4[^{18}F] Fluoromethylbenzoate(S^{18}FMB), Synthesis

The application of biologically active peptides labeled with position-emitting nuclides has emerged as a useful and interesting field in nuclear medicine. Among a number of PET nuclides, fluorine-18 appears to be the best candidate for labelling by virtue of its favorable physical and chemical characteristics. However, the process of bioactive molecule labeling with ^{18}F is laborious and time-consuming. N-succinimidyl 4-(^{18}F) (fluoromethyl)-benzoate (S^{18}FMB) was found to be a very useful acylation agent in labeling biologically active molecule.

S^{18}FMB was synthesized by one step reaction of N-succinimidyl-4-[(4-Nitro benzensulfonyl) oxymethyl] benzoate(SNOB) with ^{18}F$^-$. SNOB could be obtained with the yield of 75% by the reaction of silver 4-nitrobenzene sulfonate and N-succinimidyl 4-(bromomethyl) benzoate at room temperature for 6 days. After optimizing the radiosyntheses parameters, the radiochemical yield of S^{18}FMB is up to 57% (corrected for decay), in addition, a simple separation method on small Sep-Pak silica column was used to replace the complicated HPLC method and high radiochemical purity could be obtained. In order to provide methodology research for labeling other biological molecules, we labeled IgG with S^{18}FMB successfully. By using the optimal labeling condition (0.2 g/L of IgG, pH =7.8—8.5, 25 ℃,and reaction time 15 min), the yield of S^{18}FMB labeling IgG was above 80%. To peptide, on the basis of the conjugation of octreotide with S^{18}FMB, we realize that the S^{18}FMB labeling VIP is a useful PET imaging agent in diagnosing many kinds of tumor.

磁性颗粒固相分离剂的制备及其在放射免疫分析中的应用

董 墨 张春富 曹金全 尹端沚

关键词 磁性颗粒，固相，二抗，放射免疫

研制了一种用于放射免疫测试的磁颗粒固相分离试剂。将粗二抗溶液纯化，采用氨基硅烷化修饰的磁性颗粒选择不同的酸度经戊二醛活化后，在不同的酸度下与纯化的二抗交联。同时进行了未活化磁性颗粒对二抗的吸附实验。经放射免疫药盒测试:未活化磁性颗粒固相二抗结合率低且极不稳定；活化后磁性颗粒固相二抗结合率高且稳定性好，提高了放免药盒的灵敏度，标准曲线的相关性系数达 0.9950。在液相分离法与磁性颗粒固相分离法的放射免疫测试比较中，其测得样品浓度的相关性也达到了 0.9895。因此该磁性颗粒固相二抗是一个可用于放射免疫测试的通用分离试剂。

Preparation and application of solid-phase magnetic particle second antibody for RIA

DONG Mo ZHANG Chunfu CAO Jinquan YIN Duanzhi

Keywords Magnetic particle, Solid-phase, Second antibody, RIA

A separation reagent of solid-phase magnetic particle for RIA has been studied. Amine silane modified magnetic particle was activated using glutaraldehyde and coupled with purified second antibody at different value of pH. And the experiment on adsorption of purified second antibody by non-activated magnetic particle at pH 8 was carried out simultaneously. The RIA test demonstrated that the binding percentage of non-activated solid-phase magnetic particle was lower and its stability was less than that of the activated solid-phase magnetic particle. The sensitivity was increased and the correlation coefficient of standard cure was 0.9950 for the activated solid-phase magnetic particle second antibody for CEA RIA. The correlation coefficient of testing in RIA between separations with liquid-phase and solid-phase was 0.9895. Therefore, it is possible for the solid-phase magnetic particle to be used as a general separation reagent for RIA.

SARS 病毒抗原蛋白的碘-125 标记及其免疫活性的研究

董 墨 张春富 汪勇先

关键词 SARS，碘-125，免疫活性

严重急性呼吸道综合征(Severe acute respiratory syndrome，SARS)是发病急、传播快、严重威胁患者生命的急性传染病，也称非典型性肺炎。其病原体是冠状病毒的一个变种，该病毒的早期检测是防止 SARS 病毒传播及治疗的关键。进行了 BSA-多肽抗原碘-125 放射性标记，对标记物进行免疫活性的检测，并初步进行了 BSA-多肽抗原标记物在小动物体内的分布实验和康复病人血清的检测。通过对 N-蛋白抗原的多次标记实验，经免疫活性测试，与抗体的最大结合率(Bo)从 21%到 43%再增加到 65%(抗体稀释度为 1:1250)，非特异性结合率(NSB)从大于 10%下降到 5%左右，说明经 I-125 标记后 N 蛋白抗原还保持着免疫活性，基本符合放射免疫分析对标记品的要求。

Study of SARS virus antigen protein labeled with iodine-125 and its immunoactivity

DONG Mo ZHANG Chunfu WANG Yongxian

Keywords SARS, I-125, Immunoactivity

The Severe Acute Respiratory Syndrome is an acute disease and can spread quickly. The original in disease is a mutation of the coronal virus. The earlier period detection for the virus becomes the key of cure and preventing the virus of SARS from spreading. The antigen of BSA-peptide of SARS virus was

labeled with iodine-125 and was examined by immunoactivity. The labeled compound was experimented the biodistribution in vivo with small animals. The serum of convalescent patient was detected using the labeled compound. The antigen of N-protein of SARS virus was labeled with iodine-125 for many times. The rate of binding was from 21 percent up to 65 percent by detection of immunoactivity with its antibodies and the rate of non-specific binding was from 10 percent down to 5 percent. The results displayed that the labeled compound kept the immunoactivity and accorded with the demand for RIA.

重组人肿瘤坏死因子受体 Fc 融合蛋白与配体(rhTNF-α)平衡解离常数测试

董 墨 吴 芳 汪勇先

关键词 重组人肿瘤坏死因子，碘-125，标记，受体融合蛋白，平衡解离常数

通过放射性配体饱和曲线方法，分别测定了重组人肿瘤坏死因子受体 Fc 融合蛋白产品和国外上市受体产品与该配体的平衡解离常数(Kd)，并进行了二个受体产品 Kd 值的比较。用 Iodogen 法对配体进行了碘-125 标记，Sephadex G-25 柱分离，配体的放化纯度大于 95%。用固定化了的受体的单克隆抗体作为分离试剂，进行了放射性配体饱和曲线实验，作出 Scatchard 图并计算出配体与受体的 Kd 值。实验得出的国内和国外受体与配体的平衡解离常数分别为 0.92 nmol/L、0.95nmol/L。

The detection of equilibrium dissociation constant (Kd) of rhTNF-α receptor Fc fusion protein and rhTNF-α

DONG Mo WU Fang WANG Yongxian

Keywords rhTNF-α, Receptor fusion protein, Iodine-125, Labeled，Equilibrium dissociation constant (Kd)

The equilibrium dissociation constant (Kd) were tested two rhTNF-α receptor Fc fusion proteins both domestic and alien using the method of radio-ligand saturated curve respectively and compared with each other. The ligand (rhTNF-α) was labeled with iodine-125 and separated by Sephadex G-25. Its radiochemical purity was over 95 percent. The immobilized monoclonal antibody of receptor was used for separation reagent. Figure of Scatchard was drawn through experiment of radio-ligand saturated curve and the equilibrium dissociation constant (Kd) was calculated. The equilibrium dissociation constant (Kd) both domestic and alien receptors were 0.92 nmol/L, 0.95nmol/L, respectively.

3-(4-羟基苄基)-8-甲氧基-1，2，3，4-四氢苯并吡喃[3，4-c]吡啶-5-酮的合成

李谷才　尹端沚　汪勇先

关键词　苯并吡喃[3，4-c]吡啶-5-酮，合成，表征

精神分裂症是一种非常复杂的慢性神经疾病，成年人中约有 0.7%的人患有该病。多巴胺功能亢进可能是引起精神分离症的主要原因之一。多巴胺是一种内源性儿茶酚胺类神经递质，它对脑、心血管、肾、肾上腺等重要器官机能具有调节作用。多巴胺主要通过多巴胺受体发挥作用。多巴胺 D_4 受体在精神分裂症病因发展中起着重要作用，编码 D_4 受体的基因与精神分裂症之间可能存在着重要联系。以 3-甲氧基苯酚和 4-酮-3-甲酸甲酯哌啶盐酸盐为原料，通过分子间环加成反应和 N-烷基化反应，合成了一种潜在的多巴胺 D_4 受体配基 3-(4-羟基苄基)-8-甲氧基-1，2，3，4-四氢苯并吡喃[3，4-c]吡啶-5-酮，并用 ^{1}H NMR、IR、ESI-MS 对其进行了表征。

Synthesis of 3-(4-Hydrobenzyl)-8-methoxy-1,2,3,4 -tetrahydrochromeno[3,4-c]pyridin-5-one

LI Gucai　YIN Duanzhi　WANG Yongxian

Keywords　Chromeno[3,4-c]pyridin-5-one, Synthesis, Characterization

3-(4-Hydrobenzyl)-8-methoxy-1,2,3,4-tetrahydrochromeno[3,4-c] pyridine-5-one was prepared as a potential dopamine D_4 receptor ligand from 3-methoxyphenol and methyl-4-oxo-3-piperidine carboxylate hydrochloride through two-step reactions and their structures were confirmed by IR, ^{1}H NMR and ESI-MS spectra.

3-(4-[^{18}F]氟苄基)-8-羟基-1,2,3,4-四氢苯并吡喃[3,4-c]吡啶-5-酮的放射化学合成

李谷才　尹端沚　程登峰　王明伟　郑明强　汪勇先

关键词　苯并吡喃[3,4-c]吡啶-5-酮，氟-18，放射化学合成，多巴胺 D_4 受体

基于受体-配体特异性结合关系，通过核医学显像仪器，利用发射正电子的放射性核素标记的配基进行活体脑内的受体示踪，可从分子水平确定受体在活体脑内的分布、密度和功能等，进而对一些与受体有关的疾病进行早期诊断和研究。D_4 受体属于 G 蛋白偶联的受体族，由 387 个氨基酸组成。D_4 受体可能与精神分裂症、帕金森病、老年痴呆症、情绪障碍性疾病、药物滥用等有关。多巴胺 D_4 受体在精神分裂症病因发展中起着重要作用，编码 D_4 受体的基因与精神分裂症之间可能存在着重要联系。用三氟甲基磺酸-4-三甲基铵苯甲醛作标记前体，采用“一锅法”制备了一种潜在的多巴胺 D_4 受体 PET 显像剂 3-(4-[^{18}F]氟苄基)-8-羟基-1,2,3,4-四氢苯并吡喃[3,4-c]吡啶-5-酮。其总的合成时间为 105min，放射化学产率为 19.7%，比活度为 120GBq/μmol。

Radiochemical Synthesis of 3-(4-[^{18}F]Fluorobenzyl) -8-hydroxy-1,2,3,4-tetrahydrochromeno[3,4-c]pyridin-5-one: a putative dopamine D_4 receptor PET imaging agent

LI Gucai YIN Duanzhi CHENG Dengfeng WANG Mingwei WANG Yongxian

Keywords Fluorine-18, Chromeno[3,4-c]pyridin-5-one, Dopamine D_4 receptor, PET

The dopamine D_4 receptor has lately received increasing interest since it has been hypothesized to be involved in the pathology and pharmacotherapy of schizophrenia. While this receptor is expressed in lower density in various extrastriatal brain regions and its distribution is still unclear due to lack of suitable imaging agent and its change in schizophrenia is controversial. Herein, based on the structure-activity analysis of chromeno[3,4-c]pyridin-5-ones as potential dopamine D_4 receptor ligands, a putative D_4 receptor positron emission tomography (PET) radioligand, 3-(4-[^{18}F]fluorobenzyl)-8-hydroxy-1,2,3,4-tetrahydrochromeno[3,4-c]pyridin-5-one ([^{18}F]FHTP), was designed and synthesized. The radiochemical synthesis of [^{18}F]FHTP took around 105 min from EOS with an overall radiochemical yield 19.5% (decay-corrected) and its radiochemical purity was more than 95%.

^{18}F 标记多肽药物的研究进展

李俊玲 汪勇先 张秀利 周 伟 林英武 尹端沘

关键词 正电子核素，生物活性多肽，^{18}F 标记试剂，放射性氟化技术，药物动力学

正电子核素标记的生物活性多肽已成为目前核医学领域的研究热点。在大量发射正电子的核素中，^{18}F 因为具有良好的物理与核性质，成为标记生物活性多肽的优选核素。小的生物活性多肽在显像方面优于蛋白与单抗。^{18}F 标记的多肽药物有望成为核医学领域极有应用前景的显像试剂。本文综述了 ^{18}F 标记的小生物活性多肽的研究进展。另外，对不同的 ^{18}F 标记试剂、放射性氟化技术及 ^{18}F 标记多肽的药物动力学特征也进行了叙述。

Recent progress in ^{18}F-labelled peptide radiopharmaceticals

LI Junling WANG Yongxian ZHANG Xiuli ZHOU Wei

LIN Yingwu YIN Duanzhi

Keywords Positron-emitting nuclides, Bioactive peptides, ^{18}F labeling reagents, Radiofluorination techniques, Pharmacokinetics

The application of biologically active peptides labeled with positron-emitting nuclides has emerged

as a useful and interesting field in nuclear medicine. Among a number of positron-emitting nuclides, fluorine-18 appears to be the best candidate for labeling peptides by virtue of its favourable physical and nuclear characteristics. Small peptides are currently the preferred reagents over proteins and antibodies for diagnostic imaging. The ^{18}F-labelled peptides hold enormous clinical potenial. This review presents the recent progress in ^{18}F-labelled small active peptides. In addition, the different ^{18}F labeling reagents, radiofluorination techniques and pharmacokinetics of ^{18}F-labelled bioactive peptides are addressed.

^{18}F 标记甘氨酸-苯丙氨酸盐(HGP)的研究

李俊玲 汪勇先 张秀利 周 伟 田海滨 尹端泍

关键词 ^{18}F，S^{18}FMB，HGP，HOBT，标记率

本文利用间接标记的方法对甘氨酸-苯丙氨酸的乙酸盐(HGP)进行了 ^{18}F 标记。研究了 pH、反应时间、HGP 的浓度及催化剂 1-羟基苯并三唑(HOBT)用量等对标记率的影响。结果表明，在标记条件为:pH＝9.2，1 mg/mL HGP，室温反应 5 min 时，标记率可达 90%。

The study of labeling acetate GLY-Phe with fluorine-18

LI Junling WANG Yongxian ZHANG Xiuli ZHOU Wei

TIAN Haibin YIN Duanzhi

Keywords S^{18}FMB, HGP, HOBT, Labeling yield

Acetate Gly-Phe (HGP) was indirectly labeled with ^{18}F. The effects of pH, reaction time, HGP concentration and the amount of catalysis HOBT on labeling yields were studied. The optimum conditions were: pH=9.2, 1 mg/mL HGP, 5 min at room temperature, the labeling yield was 90%.

N-琥珀酰亚胺 4-^{18}F(氟甲基)苯甲酸酯(S^{18}FMB)的合成

李俊玲 汪勇先 张秀利 田海滨 周 伟 林英武 尹端泍

关键词 放化合成，N-琥珀酰亚胺-4-^{18}F(氟甲基)苯甲酸酯，IgG

本文合成了 ^{18}F 标记蛋白常用中间体 N-琥珀酰亚胺 4-^{18}F(氟甲基)苯甲酸酯 (S^{18}FMB)，用操作简单的 Sep-Pak 硅胶柱代替了繁琐耗时的 HPLC 分离。并探讨了反应溶剂、温度、K/222 与 K_2CO_3 物质的量比及反应时间等诸因素对 S^{18}FMB 放化合成的影响。得出较佳标记条件:以无水乙腈为溶剂、K/222 与 K_2CO_3 物质的量比 1:1、80 ℃下反应 5 min，可得 57%的标记率，较文献提高了 3 倍以上。并对 IgG 进行了标记，室温反应 15 min，可达 88%的标记率。

The radiochemical synthesis of n-succinimidyl 4-^{18}F-(fluoromethyl)benzoate

LI Junling WANG Yongxian ZHANG Xiuli TIAN Haibin ZHOU Wei
LIN Yingwu YIN Duanzhi

Keywords Synthesis, N-succinimidyl 4-^{18}F-(fluoromethyl)benzoate, Radiochemical yield, IgG

N-succinimidyl 4-^{18}F-(fluoromethyl) benzoate (S^{18}FMB) of labeling proteins has been synthesized. Laborious and time-consuming HPLC is substituted by simple Sep-pak silica during the process of isolation. Many factors affecting the radiochemical synthesis of S^{18}FMB including reaction solvents, temperature, the mole ratio of K/222 to K_2CO_3 and reaction time are studied. The better labeling conditions are as follows: dry acetonitrile as solvent, the mole ratio of K/222 to K_2CO_3 is 1:1, reaction time is 5min at 80℃, the radiochemical yield is about 57% (EOS) and about 3 times than published in papers. IgG is indirectly labeled by S^{18}FMB and the labeled yields are about 88% at room temperature.

有潜力的 PET 脑肿瘤显像剂——^{18}F 标记的氨基酸药物

李俊玲 汪勇先 张 岚 张秀利

关键词 ^{18}F，PET，氨基酸

本文综述了 ^{18}F 的核素性质、常用标记方法及 ^{18}F 标记的多种氨基酸药物的合成、应用前景与以后的发展趋势。

A Potential fluorine-18 radiopharmaceutical ——^{18}F labeled amino acid

LI Junling WANG Yongxian ZHANG Lan ZHANG Xiuli

Keywords ^{18}F, PET, Amino acids

The nuclear and chemical properties of ^{18}F are excellent. ^{18}F, which can be produced in Ci-quantities, is an ideal positron-emitting radionuclide. Its low positron energy of only 0.64MeV results in low radiation doses and short ranges in tissues. Its half-life of 110min permits syntheses and scanning procedures extending over hours, thus facilitating kinetic studies. The nuclear properties , labeling methods and labeled amino acids of fluorine-18 are described in detail here. Fluorine-18 labeled amino acids are useful and greatly potential tracers for detecting brain cancers.

N-琥珀酰亚胺 3-[^{125}I]碘苯甲酸酯($S^{125}IB$)的放射化学合成

李俊玲　汪勇先　王丽华　张 岚　田海滨

关键词　Iodogen 法，N-琥珀酰亚胺 3-(三正丁基锡)苯甲酸酯，N-琥珀酰亚胺 3-[^{125}I]碘苯甲酸酯 放射性碘标

利用 Iodogen 法成功地对 N-琥珀酰亚胺 3-(三正丁基锡)苯甲酸酯(ATE)进行了放射性碘-125 标记，利用 SEP-PAK 硅胶柱实现了干扰蛋白标记的 ATE 及 Iodogen 与 $S^{125}IB$ 的分离，得到了放射性碘间标蛋白质有用的中间体 $S^{125}IB$，标记率 93%以上。并研究了影响标记的因素，得出较佳的标记条件为: ATE 与 $Na^{125}I$ 物质的量比 6:1、氧化剂 Iodogen 用量 7μg、室温反应 5 min。

Synthesis of radioiodinated N-succinimidyl 3-[^{125}I]iodobenzoate

LI Junling　WANG Yongxian　WANG Lihua　ZhANG Lan　TIAN Haibin

Keywords　Iodogen, N-Succinimidyl 3-[^{125}I]Iodobenzoate, N-Succinimidyl 3-(tri-n-butylstannyl) benzoate, Radioiodination

N-Succinimidyl 3-(tri-n-butylstannyl) benzoate (ATE) was radioiodinated using Iodogen as oxidant and useful conjugate $S^{125}IB$ of labeling proteins was obtained. ATE and Iodogen affecting labeling proteins were successfully isolated from $S^{125}IB$ by sep-pak silica. The labeling efficiency was more than 93%. Several factors affecting labeling such as labeling time、the amount of Iodogen and the mole ratio of ATE and $Na^{125}I$ were studied. The better labeling conditions were obtained as follows: mole ratio of ATE to $Na^{125}I$ = 6:1、Iodogen=7μg、labeling time = 5min in room temperature.

^{188}Re-硫化锑纳米胶粒的制备及其被兔淋巴结摄取的实验研究

林英武　尹端沚　魏海鹏　张秀利　李俊玲　邱 实　汪勇先

关键词　^{188}Re-Sb_2S_3，纳米胶粒，淋巴结，γ 探针

制备了两种不同粒径的硫化锑纳米胶粒，研究了 ^{188}Re 标记两种胶粒的条件以及标记物被兔腘窝淋巴结和腹股沟淋巴结的摄取情况。实验结果表明:两种硫化锑纳米胶粒的平均粒径分别为 10.2 nm 和 44.7 nm。当 $SnCl_2{\cdot}2H_2O$ 的浓度为 4 mg/mL，抗坏血酸的浓度为 6 mg/mL 时，加入适量的 $^{188}ReO_4^-$淋洗液，60℃水浴加热 60 min，标记率均大于 95 %，而且有较好的体外稳定性。从正常的新西兰大白兔双足趾蹼皮下分别注射两种标记物，γ 探针探测的结果表明:腘窝淋巴结对 10.2 nm 和 44.7 nm 胶粒的摄取在注射后 1.5—2 h 之间达到最大值，分别占各自注入量的 17.4 % 和 19.4 %；腹股沟淋巴结对 10.2 nm 和 44.7 nm 胶粒的摄取在注射后 2 h 左右达到最大值，分别占各自注入量的 4.7 % 和 4.2 %。

Synthesis and Uptake of ^{188}Re-Antimony Sulfide Nanocolloids by Rabbits Lymph node

LIN Yingwu YIN Duanzhi WEI Haipeng ZHANG Xiuli LI Junling
QIU Shi WANG Yongxian

Keywords ^{188}Re-Sb_2S_3, Nanocolloids, Lymph node, Gamma detecting probe

Two different particle sizes of antimony sulfide nanocolloids were prepared and labeled with ^{188}Re. The uptake of them by rabbit's popliteal lymph node and inguinal lymph node was also studied. Results showed that the mean diameters of the two kinds particles were 10.2nm and 44.7nm respectively. The labeling condition was optimized. When 4mg/mL $SnCl_2 \cdot 2H_2O$, 6mg/mL Vit C and 1 mL nanocolloids were reacted in 60℃ water bath for 60 min, the labeling yield were both greater than 95% and excellent in vitro stability were also observed. White New Zealand rabbits were injected subcutaneously on the dorsum of the hind foot with two kinds of ^{188}Re-Sb_2S_3. The uptake by popliteal lymph node and inguinal lymph node were measured quantitatively by using a gamma detecting probe. Results showed that the highest uptake of 10.2nm and 44.7nm nanocolloids by popliteal lymph node reached 17.4% and 19.4% of the total after 1.5 to 2 hr post injection, respectively; the highest uptake by inguinal lymph node reached 4.7 % and 4.2% of the total about 2 hr post injection, respectively.

药用载体——硫化亚锑纳米胶粒的制备及表征

林英武 尹端沚 曹金全 汪勇先

关键词 硫化亚锑，纳米胶粒，药用载体

采用两种不同的硫源，制备了两种不同粒径分布的药用载体——硫化亚锑纳米胶粒。透射电镜(TEM)和原子力显微镜(AFM)表征显示，两者的平均粒径分别为 10 nm 和 40 nm，且均为球形颗粒。同时讨论了硫源和分散剂对纳米胶粒粒径的影响。

Preparation and characterization of antimonous sulfide nanocolloids for pharmaceutical carrier

LIN Yingwu YIN Duanzhi CAO Jinquan WANG Yongxian

Keywords Antimonous sulfide, Nanocolloids, Pharmaceutical carrier

Two different particle sizes of antimonous sulfide nanocolloids for pharmaceutical carrier were prepared by using two different sources of sulfide. Particle size and morphology were detected using Transmission Electron Microscope (TEM) and Atomic Force Microscope (AFM). The average

diameters of the prepared two different spheric nanocolloids were 10 nm and 40nm respectively. At the same time, the factors such as source of sulfide and dispersant, affecting the size of antimonous sulfide nanocolloids, were discussed.

3-正丁基锡-N-琥珀酰亚胺苯甲酸酯的合成及其碘标记

刘振锋　汪勇先　周 伟　王丽华　夏姣云　尹端沚

关键词　化学合成，3-正丁基锡-N-琥珀酰亚胺苯甲酸酯(ATE)，N-琥珀酰亚胺3-碘苯甲酸酯($SI^{125}B$)

为了解决碘标记蛋白质，多肽，和单克隆抗体体内脱碘的问题。合成了标记前体 3-正丁基锡-N-琥珀酰亚胺苯甲酸酯(ATE)，以及非放碘标物 N-琥珀酰亚胺 3-碘苯甲酸酯(SIB)，其产率分别 45.4%，71.42%，用核磁、质谱、红外等对它们进行了表征 。并对 ATE 进行了碘标记，得到 N-琥珀酰亚胺 3-碘苯甲酸酯($S^{125}IB$)， 标记率可达 93%，放化纯度>98%。本方法为放射性药物碘的间接标记提供了一个平台。

Synthesis and Radioiodination of N-Succinimidyl 3-（tri-n-butylstannyl）benzoate (ATE)

LIU Zhenfeng　WANG Yongxian　ZHOU Wei　WANG Lihua

XIA Jiaoyun　YIN Duanzhi

Keywords　Chemical synthesis, N-Succinimidyl 3-(tri-n-butylstannyl)benzoate (ATE)N-Succinimidyl 3-iodobenzoate ($S^{125}IB$)

Problems of deiodination in vivo when using them as radioiodinated monoclonal antibodies were studied. Radioiodination precursor N-Succinimidyl-3-(tri-n-butylstannyl) benzoate (ATE) and cold radioiodination N-Succinimidyl-3-iodobenzoate (SIB) was synthesized. The structures of ATE and N-Succinimidyl-3-iodobenzoate (SIB) were confirmed with ^{1}H NMR, MS and IR spectra. The yields of ATE and SIB were 45.4% and 71.4%, respectively. ATE was labeled with iodine-125. The radiolabel rate was 93% and radiochemical purity was over 98%. The synthesis of ATE and the labeling of SIB can be used as a platform for indirect radioiodination of radiopharmaceuticals.

放射性碘间接标记人 IgG

刘振锋　汪勇先　董 墨　周 伟　夏姣云　王丽华 尹端沚

关键词　碘标，人 IgG，N-琥珀酰亚胺 3-(三正丁基锡)苯甲酸酯(ATE)

研究能有效降低体内脱碘的抗体的标记方法。碘标记 N-琥珀酰亚胺 3-(三正丁基锡)苯甲酸酯(ATE)前体，得到 N-琥珀酰亚胺 3-碘苯甲酸酯($S^{125}IB$)，与人 IgG 进行联结，探索标记最佳条件以及测定标记物的稳定性和生物活性。ATE 通过 N-氯代琥珀酰亚胺酯(NCS)法得到的标记率>98%，SIB 标记人 IgG 的标记率达到 90%，稳定性、生物活性良好。以 ATE 为前体对人 IgG 进行放射性碘标记，解决了直接标记稳定性差，体内脱碘严重的问题，反映出碘间接标记单克隆抗体，蛋白质及多肽有良好的临床应用前景。

The indirect radioiodination of human IgG

LIU Zhenfeng Wang Yongxian Dong Mo Zhou Wei

XIA Jiaoyun WANG Lihua YIN Duanzhi

Keywords radioiodination, Human IgG, ATE

To seek an effective way to acquire radiolabeled antibody with excellent in vivo stability, N-Succinimidyl 3-iodobenzoate ($S^{125}IB$) was obtained from radioiodination of N-Succinimidyl 3-(tri-n-butylstannyl) benzoate (ATE). And then $S^{125}IB$ was conjugated to human IgG. The optimized radioiodinated condition was optimized and the stability and biological activity in vitro of ^{125}IBA-IgG were evaluated. The labeling ratio of radioiodination of ATE by N-chlorosuccinimide(NCS) was over 98%.and the conjugation efficiency of $S^{125}IB$ and human IgG was up to 90%. The stability and biological activity was well. The indirect radiolabeling procedure with ATE was an excellent and efficient way of radiohalogenation of Human IgG and even for other proteins and peptides, the most important is the excellent in vitro stability plus biological activity of ^{125}IBA-IgG, which makes better f prospect of the clinical application practicable

肿瘤 PET 显像剂 O-(2-[^{18}F]氟乙基)-L-酪氨酸的放射化学合成

王明伟 尹端沚 汪勇先 李俊玲 张 岚 周 伟

关键词 氨基酸，酪氨酸，氟烷基化，FET，PET，脑肿瘤

放射性核素标记的氨基酸近年来已成为放射性药物领域的研究热点。O-(2-[^{18}F]氟乙基)-L-酪氨酸([^{18}F]FET)从问世以来一直备受关注，是一种很有希望的脑肿瘤 PET 显像剂。本文选择“两步法”合成了[^{18}F]FET: 第一步，通过 1，2-二对甲苯磺酸基乙烷的[^{18}F]氟化制备标记中间体，即烷基化试剂 2-[^{18}F]氟乙基对甲苯磺酸酯；第二步，L-酪氨酸的[^{18}F]氟乙基化合成了目标化合物[^{18}F]FET。总合成时间约为 50 min，放射化学产率为 20%—30%(未经衰变校正)，放射化学纯度大于 98%。

Radiochemical Synthesis of O-（2-[^{18}F]fluoroethyl）-L-tyrosine as PET imaging agent for tumor diagnosis

WANG Mingwei YIN Duanzhi WANG Yongxian

LI Junling ZHANG Lan ZHOU Wei

Keywords Amino acids, L-tyrosine, Fluoroalkylation, FET, PET, Brain Tumor

Radiolabelled amino acids have become the interesting field of radiopharmaceuticals for several years, of which O-(2-[^{18}F]fluoroethyl)-L-tyrosine is very promising as PET imaging agent for tumor diagnosis. [^{18}F]FET was synthesized via a two-step reaction consisting of [^{18}F]fluorination of 1,2-bis (tosyloxy) ethane for preparing the alkylating agent 2-[^{18}F]fluoroethyltosylate and [^{18}F]fluoroethylation of L-tyrosine for obtaining the objective [^{18}F]FET. The synthesis was typically finished in less than 50 min with overall radiochemical yields of 20%—30% （non-decay corrected） and radiochemical purity more than 98%.

比较性优化研究 O-(2-[^{18}F]氟乙基)-L-酪氨酸的放射化学合成

王明伟 尹端沚 汪勇先 程登峰 李谷才 周 伟

关键词 ^{18}F，L-酪氨酸，比较，优化，放射化学合成

O-(2-[^{18}F]氟乙基)-L-酪氨酸(O-(2-[^{18}F]fluoroethyl)-L-Tyrosine，[^{18}F]FET)是一种比较有希望应用于临床诊断的脑肿瘤 PET 显像剂。本文针对[^{18}F]FET 的“两步法”合成路线，从反应组分、加热方式与反应方式等 3 个方面进行了比较性优化研究。

Comparative and optimized studies on radiosynthesis of O-(2-[^{18}F]fluoroethyl)-L-Tyrosine

WANG Mingwei YIN Duanzhi WANG Yongxian

CHENG Dengfeng LI Gucai ZHOU wei

Keywords ^{18}F, L-tyrosine, Comparison, Optimization, Radiosynthesis

O-(2-[^{18}F]fluoroethyl)-L-Tyrosine, one of radiolabelled amino acids, is a very promising brain tumor PET imaging agent and holds clinical potential. A comparative and optimized study was carried out on radiosynthesis of O-(2-[^{18}F]fluoroethyl)-L-Tyrosine. Three aspects of its two-step method of synthesis, including reaction components, heating methods and reaction models, were studied.

适用于[^{18}F]FET 的常规生产的半自动化合成装置

王明伟　尹端沚　汪勇先　周 伟　柏卫民[1]

关键词　^{18}F，L-酪氨酸，放化合成，半自动化

放射性标记的氨基酸 O-(2-[^{18}F]氟乙基)-L-酪氨酸是一种很有希望应用于临床的脑肿瘤 PET 显像剂。为了满足其常规生产的需要，研制了一台便于远距离控制操作的半自动化合成系统。该系统具有如下若干优点: 1)系统中所有管路的直径最小化，放射性活度的吸附损失减少到最低程度；2)远距离控制操作，使得工作人员受到的辐射照射降到最小水平；3)对系统的运行稍作修改，还可以应用于其它小分子标记中间体在线合成有关的放射性药物。

1 安盛科兴药业公司

Semi-automated radiosynthesis device suitable for routine production of O-(2-[^{18}F]fluoroethyl)-L-tyrosine

WANG Mingwei　YIN Duanzhi　WANG Yongxian　ZHOU Wei　BAI Weimin[1]

Keywords　^{18}F, L-tyrosine, Radiosynthesis, Semi-automation

A convenient remotely controlled semi-automated synthesis system of *O*-(2-[^{18}F] fluoroethyl)-L-Tyrosine, a brain tumor PET imaging agent, was developed to meet the need of its routine production. The system has several potential advantages: a) decrease the radioactivity loss in the line to a low level due to being designed to minimize the inner volume of the synthesis line; b) reduce the radiation exposure to operator to a low level because of the remote-controlled operation; c) modified to allow the labeling of other small molecule labeled intermediate.

1 Amersham Kexing Pharmaceuticals Co. Ltd.

一个潜在的多巴胺 D_4 受体显像剂:3-[4-(4-[^{18}F]氟苯甲基)哌嗪-1-基]-甲基-1H-吡咯并[2，3-b]吡啶的放化合成

田海滨　尹端沚　张 岚　张春富　李俊玲　周伟　汪勇先

关键词　^{18}F，7-氮杂吲哚类似物，多巴胺 D_4 受体，PET，放化合成

7-氮杂吲哚的衍生物 L-750，667 是一个新的、高亲和性(Ki = 0.51 nmol/ L)的 D_4 受体选择性配体，采用一锅法用氟[^{18}F]化物放化合成了 L-750，667 的类似物: 3-[4-(4-[^{18}F]氟苯甲基)哌嗪-1-基]-甲基-1H-吡咯并[2，3-b]吡啶。4-氟[^{18}F]苯甲醛是由无载体的 [^{18}F]F^-与标记前体 4-三甲基铵苯甲醛-三氟甲基磺酸盐在 DMSO 中反应获得。在同一容器中，4-氟[^{18}F]苯甲醛和 3-(哌嗪-1-基)甲基

-1H-吡咯并[2，3-b]吡啶的胺烷基化反应使用氰基硼氢化钠为还原剂、在甲醇、乙酸中完成。产物的纯化使用 HPLC，产物保留时间 t_R=9.4 min。在同一条件下，确定产物的放化纯度。放化产率为 12.0%，放化纯度大于 98%，比活度高于 1000 Ci/mmol，全部合成时间(包括高效液相分离)为 73min，产物的放化合成在短的时间内完成，并有高的产率和高的比活度。制备的产物可作为潜在的多巴胺 D_4 受体正电子显像示踪剂。

A potential dopamine D4 receptor imaging agent : radiosyntheses of 3-[4-(4-[^{18}F]fluorobenzyl)]piperazin-1-yl} methyl-1*H*-pyrrolo[2,3-b]pyridine

TIAN Haibin YIN Duanzhi ZHANG Lan ZHANG Chunfu

LI Junling ZHOU Wei WANG Yongxian

Keywords **F**luorine-18, 7-azaindole analog , Dopamine D_4 receptor, PET, Radiosyntheses

The 7-azaindole derivative 3-{[4-(4-iodophenyl)piperazin-1-yl]-methyl}-1H-pyrrolo [2,3-b] pyridine (L-750667) is a novel, high-affinity (Ki = 0.51 nmol/L) and selective D_4 receptor ligand. We radiolabeled L-750667 analogue 3-[4-(4-[^{18}F]fluorobenzyl)]piperazin-1-yl} methyl-1*H*-pyrrolo [2,3-b]pyridine with Fluorine-18, it was prepared by reacting 3-(piperazin-1-yl)-methyl-1H-pyrrolo[2,3-b]pyridine with 4-[^{18}F]fluorobenzaldehyde. The 4-[^{18}F]fluorobenzaldehyde was prepared by nucleophilic substitution using the no carrier added [^{18}F]fluoride from trimethylammonium- benzaldehyde triflate in DMSO. The radiochemical yield of 3-[4-(4-[^{18}F]fluorobenzyl)]piperazin-1-yl} methyl-1H- pyrrolo[2,3-b] pyridine was 12.0% (decay –corrected) with a radiochemical purity better than 98% and a specific activity greater than 1000Ci/mmol, and the time of synthesis including HPLC purification was 73min.**.** Our studies have demonstrated that reductive alkylation of amine with 4-[^{18}F]Fluorobenzaldehyde using sodium cyanoborohydride in DMSO was found to be a good method for the preparation of N-benzyl group compounds. This labeled compound may be a useful PET tracer for dopamine D_4 receptors.

多巴胺 D_4 受体显像剂的研究进展

田海滨 尹端沚 张 岚 张春富 李俊玲

关键词 多巴胺 D_4 受体，受体显像剂，正电子发射断层显像，单光子发射断层显像

多巴胺受体可分为 5 种受体亚型，D_4 受体亚型是其中一种。多巴胺 D_4 受体的表达及功能与精神分裂症等疾病的病理相关联，其显像剂的研究具有重要的意义。至今尚无理想的核素标记的 D_4 受体配体可作为 D_4 受体的显像剂，用于研究其在活体中的分布及其代谢行为。本文综述了近年来多巴胺 D_4 受体显像剂的研究进展，对于 ^{11}C，^{18}F，^{123}I 核素标记的 D_4 受体的配基、激动剂或拮抗剂及其类似物作为 D_4 受体 PET 或 SPECT 显像剂，着重分析了其在动物体内实验中结合 D_4 受体的亲和力及选择性，并给予评价。

Progress of study on the dopamine d_4 receptor imaging agent

TIAN Haibin YIN Duanzhi ZHANG Lan ZHANG Chunfu LI Junling

Keywords Dopamine D_4 receptor, Imaging Agent, PET, SPECT

Dopamine receptors were originally classified into five subtype receptors, the dopamine D_4 receptor was one of those. Schizophrenic pathophysiology may be associated with expression and function of the dopamine D4 receptor, it is of great importance to study the imaging agent of dopamine D4 receptor. The study on radioactivity distribution and metabolize of radioligand remains hampered by the lack radioligand for the D_4 receptor which can be labeled using suitable nuclein. This paper reviews the progress of study on the dopamine D_4 receptor imaging agent, with particular emphasis vary nuclein, for example ^{11}C, ^{18}F, ^{123}I, labeled D_4 receptor ligands, antagonists and analogs as PET or SPECT imaging agents. We estimated affinity and selectivity of radioligands for the dopamine D4 receptor in laboratory animal tests

芳环有机锡化合物的放射性碘标记

王丽华 汪勇先 尹端沚 李俊玲

关键词 放射性标记，芳基锡化合物，IQNB，SIB

研究了两种芳基锡化合物——三正丁基锡-3-奎宁环基苯甲酸酯 TQNB 和琥珀酰亚胺-3-(三正丁基锡)苯甲酸酯 STB 的放射性碘标记。STB 用 Iodogen 法可以有效标记得到琥珀酰亚胺-3-碘苯甲酸酯 $S^{125}IB$。TQNB 用氯胺 T 法标记得到放射性碘-3-奎宁环基苯甲酸酯 $^{125}IQNB$。$S^{125}IB$ 和 $^{125}IQNB$ 在室温条件下避光保存时可稳定存在。

Radioiodination of aromatic organostannates

WANG Lianhua WANG Yongxian YIN Duanzhi LI Junling

Keywords Radioiodination, Aromatic organostammates, IQNB SIB

Radioiodination of tri-n-butylstannyl-3-quinuclidinyl benzilate (TQNB) and N-succinimidyl-3-(tri-n-butylstannyl) benzoate (STB) was studied. STB was radiolabeled efficiently using Iodogen to prepare radioactive N-succinimidyl-3- iodobenzoate ($S^{125}IB$). TQNB was radioiodinated using chloramine-T to obtain radioactive iodo-3-quinuclidinyl benzilate ($^{125}IQNB$). Both $S^{125}IB$ and $^{125}IQNB$ showed good stability at room temperature in the dark.

用于多巴胺 D4 受体体内研究的 3-[4-(4-[^{18}F]氟苯甲基)哌嗪-1-基]-甲基-1H-吡咯并[2，3-b]吡啶的合成及生物学评价

田海滨　尹端沚　张春富　张 岚

王丽华　李俊玲 周 伟　汪勇先　吴春英 [1]

关键词　^{18}F，7-氮杂吲哚类似物，多巴胺 D_4 受体，组织分布，代谢物

7-氮杂吲哚的衍生物 L-745，870 是一个新的、高亲和性(Ki = 0.43 nmol/L)的多巴胺 D_4 受体选择性配体，我们放化合成了其类似结构的新化合物 3-[4-(4-[^{18}F]氟苯甲基)哌嗪-1-基]-甲基-1H-吡咯并[2，3-b]吡啶([^{18}F]3)，并作了大鼠体内生物学评价。 ([^{18}F]3)的放化合成是通过 3-(哌嗪-1-基)甲基-1H-吡咯并[2，3-b]吡啶和 4-氟[^{18}F]苯甲醛的胺烷基化反应完成，放化产率为 9.0%—12.0%，放化纯度大于 98%，比活度高于 37 GBq/μmol。大鼠体内的组织分布和代谢物研究表明: [^{18}F]3 在大鼠脑组织区域有特异性分布，提示其可能作为适合的显像剂用于多巴胺 D_4 受体的体内研究。

1 复旦大学附属华山医院核医学科

Synthesis and biological evaluation of 3-{[4-(4-[^{18}F] fluorophenyl)methyl] piperazin-1-yl}-methyl-1H-pyrrolo [2,3-b]pyridine for *in Vivo* studies of dopamine D_4 receptor

TIAN Haibin　YIN Duanzhi　ZHANG Lan　WANG Lihua　ZHANG Chunfu

LI Junling　WANG Yongxian　ZHOU Wei　WU Chunying[1]

Keywords　Fluorine-18, Dopamine D_4 receptor, 7-azaindole analog, Tissue Distribution,metabolism

We synthesized and evaluated 3-{[4-(4-[^{18}F]fluorophenyl)methyl]piperazin-1-yl}-methyl-1H-pyrrolo [2,3-b]pyridine ([^{18}F]3), which is an analog of L-745,870 binding D_4 receptor in vitro . The [^{18}F]3 was prepared by reductive alkylation of 3-(piperazin-1-yl)-methyl-1H-pyrrolo [2,3-b]pyridine with 4-[^{18} F] fluorobenzaldehyde in radiochemical yield (decay-corrected, 9.0–12.0%) and with high specific activity (37 GBq/μmol). Tissue distribution studies in rats demonstrated specific distribution of the [^{18}F]3 in brain regions, suggesting that it may be a suitable agent for in vivo studies of dopamine D_4 receptor.

1 Depatment of Nuclear Medicine, Hua-shang Hospital , University of Fudan

Iodogen 法制备 N-琥珀酰亚胺-3-[125]碘代苯甲酸酯

王丽华 汪勇先 尹端沚 李俊玲

关键词 有机锡化合物，放射性碘标记，稳定性，Iodogen

有机锡化合物是放射性碘标记的非常重要的前体化合物。琥珀酰亚胺-3-(三正丁基锡)苯甲酸酯 STB 用 Iodogen 法标记得到琥珀酰亚胺-3-碘苯甲酸酯 $S^{125}IB$，放化产率达到 96%。放化纯度用 HPLC 来给出。$S^{125}IB$ 在室温避光保存时非常稳定。同时合成冷 SIB 作为标准，产物用 IR 和 NMR 表征。

Preparation of N-succinimidyl-3-[^{125}I]iodobenzoate using Iodogen

WANG Lihua WANG Yongxian YIN Duanzhi LI Junling

Keywords Organostannanes, Radioiodination, Stability, Iodogen

Organostannanes were important precursors which were easy to radioiodinate. N-Succinimidyl-3-(tri-n-butylstannyl) benzoate (STB) was radiolabeled using Iodogen to get radioactive N-Succinimidyl-3-iodobenzoate ($S^{125}IB$) with 96% of high radiochemical yield. The radiochemical purity was given by high performance liquid chromatograph (HPLC). $S^{125}IB$ was very stable at room temperature in dark. Using cold SIB as a standard and IR and NMR were given in this article.

铼[^{188}Re]羰基化合物标记新双功能螯合剂的研究

夏姣云 汪勇先 李世强 于俊峰 唐 林 尹端沚

关键词 铼-188，羰基化合物，双功能螯合剂

合成了 3 种新的三齿配体 L^1NH_2、L^2H 和 L^3NH_2，用于设计合成新的以 fac-$[^{188}Re(CO)_3]^+$为核心的放射性药物。标记条件实验证明，3 种配体在低浓度(10^{-5} mol/L)的条件下，反应时间为 60 min 内，配体标记率可达 92%以上，放射化学纯度大于 95%。同时合成了冷羰基铼配合物 fac-$[Re(CO)_3L^1NH_2]^+$、fac-$[Re(CO)_3L^2H]$和 fac-$[Re(CO)_3L^3NH_2]$作为参照标准品。稳定性实验也说明三种标记物均具有很高的体外稳定性，标记后 24 h 内基本不发生分解；组氨酸和半胱氨酸体外竞争实验证实 fac-$[^{188}Re(CO)_3L^1NH_2]^+$和 fac-$[^{188}Re(CO)_3L^2H]$比 fac-$[^{188}Re(CO)_3L^3NH_2]$稳定，不易被组氨酸和半胱氨酸取代，可能羧基上的-OH 与 fac-$[^{188}Re(CO)_3]^+$的配位能力比吡啶环上的 N 稍低，也可说明 3 种配体均是较理想的标记 fac-$[^{188}Re\ (CO)_3(H_2O)_3]^+$的双功能螯合剂。

Research of novel bifunctional chelating agents for the ^{188}Re-tricarbonyl complexes labeling

XIA Jiaoyun WANG Yongxian YU Junfeng TANG Lin YIN Duanzhi

Keywords Rhenium-188, Tricarbonyl complexes, Bifunctional chelating agents

The organometallic precursor fac-[^{188}Re $(CO)_3(H_2O)_3$]$^+$ is reacted with three novel tridentate ligands (L^1NH_2, L^2H , L^3NH_2) and the properties of their ^{188}Re complexes in vivo have been evaluated. The results of labeling condition experiments show that a radiochemical purity higher than 95% can be obtained within 60 min by the reaction of fac-[^{188}Re $(CO)_3$]$^+$ core in a condition (pH=7.4) with a very small amount (10^{-5} mol/L) of these three new ligands. At the same time, three Re-tricarbonyl complexes of three ligands were also synthesized as reference samples, which were used to confirm the structures of ^{188} Re-tricarbonyl complexes of three ligands by HPLC. The stability experiments in vitro demonstrate that fac-[^{188}Re$(CO)_3L^1NH_2$]$^+$, fac-[^{188}Re$(CO)_3L^2H$] and fac-[^{188}Re$(CO)_3L^3NH_2$] do not decompose within 24 h (37 ℃, new born small calf serum). Histidine and cysteine challenge experiments (37 ℃, PBS, pH =7.4) show that fac-[^{188}Re$(CO)_3L^1NH_2$]$^+$ and fac-[^{188}Re$(CO)_3L^2H$] have higher stabilities than fac-[^{188}Re$(CO)_3L^3NH_2$], which indicate that combination ability of –OH of –COOH with fac-[^{188}Re$(CO)_3L^2H$] core is higher than that of –N of pyridine. But also indicate three novel tridentate ligands (L^1NH_2, L^2H, L^3NH_2) are better bifunctional chelating agents for the labeling by the precursor fac-[^{188}Re $(CO)_3(H_2O)_3$]$^+$.

VIP 及其受体的分子生物学基础与显像研究

王丽华 汪勇先 尹端泍

关键词 血管活性肠肽，受体显像，肿瘤，核医学

血管活性肠肽(VIP)是一个具有 28 个氨基酸的多肽，具有广泛的生理作用，能通过受体调节正常及肿瘤细胞的增殖和分化。VIP 受体(VIPR)广泛存在于各种正常组织和肿瘤组织中，其中在多种恶性肿瘤中都有过度表达，这成为 VIPR 受体显像的病理学基础。本文综述了 VIP 及其受体的相关知识，介绍了 VIP 在核医学中的应用和前景。

The molecular biology basis of vasoactive intestinal peptide and its receptor and receptor imaging study.

WANG Lihua WANG Yongxian YIN Duanzhi.

Keywords Vasoactive intestinal peptide, Rreceptor imaging, Tumor, Nuclear medicine

Vasoactive intestinal peptide (VIP) is a naturely occurring 28-amino acid peptide with a wide range of biological activities. It can regular the cellular proliferation and differentiation through its receptors. VIP receptor (VIPR) is greatly distributed in normal and tumor cells, especially overexpressed in most malignancy tumors, which become the pathology basis of VIPR imaging in clinical application. This report reviewed VIP and VIPR knowledges and introduced application of VIP in nuclear medicine.

生长抑素及其类似物的标记技术的发展

王丽华 汪勇先 尹端沚

关键词 生长抑素及其类似物，奥曲肽，放射性标记，生物分布，受体显像剂

生长抑素受体显像剂是临床上用的最多的放射性多肽类受体显像剂。用多种放射性同位素 ^{111}In，^{90}Y，^{67}Ga，^{68}Ga，^{64}Cu 或是用 ^{99m}Tc，^{188}Re 以及卤族同位素 ^{123}I，^{18}F 等对奥曲肽及其类似物进行标记得到的放射性多肽药物，已广泛用于临床显像。文章详细介绍了生长抑素类似物及标记技术的发展，对目前临床上比较成熟的生长抑素类显像剂做了综述和比较。同时介绍了目前在 SST 类似物开发领域及生物行为研究领域中的最新发展动态。

The application of somatostatin and their analogues in nuclear medcine

WANG Lihua WANG Yongxian YIN Duanzhi

Keywords Somatostatin，Octreotide，Radiolabel，Biodistribution，Receptor imaging agent

Receptor targeting with radiolabeled peptides has become very important in nuclear oncology in the past few years. The most frequently used peptides in the clinic are analogs of somatostatin, e.g. octreoscan, which contain chelators of ^{111}In, ^{90}Y, ^{67}Ga, ^{68}Ga, ^{64}Cu, ^{99m}Tc and ^{188}Re, or labeled with the halogens of ^{123}I and ^{18}F. Somatostatin analogs and their radiolabeling are introduced in this article, and the most frequently used somatostatin analog imaging agents are reviewed. In addition, the important new development in this area and biological action study are presented too.

含吡啶基的乙酸衍生物的合成及表征

夏姣云 汪勇先 于俊峰 李谷才 唐 林 刘振峰 尹端沚

关键词 吡啶基，乙酸衍生物，合成，表征

分别以吡啶-2-甲醛和二吡啶甲基胺为原料，合成了两种含有吡啶环的新型乙酸衍生物——[(6-胺基-N-叔丁氧基羰基-己基)-吡啶-2-甲基氨基]-乙酸和[二(2-吡啶甲基)-氨基]-乙酸。并通过 IR、MS(ESI)、^{1}HNMR 和(或)元素分析对两个化合物进行了表征。

Synthesis and characterization of two novel acetic acid derivatives containing pyridyl

XIA Jiaoyun WANG Yongxian YU Junfeng

LI Gucai TANG Lin 刘振峰 YIN Duanzhi

Keywords Pyridyl, Acetic acid derivatives, Synthesis, Characterization

Two novel acetic acid derivatives containing pyridyl, [(6-amino-hexyl)-pyridyl-2-methyl-amino]-acetic acid and (Bis(2-pyridylmethyl)-amino)-acetic acid, were synthesized from pyridine carbaldehyde and bispicolylamine respectively. Both were characterized by IR, ^{1}HNMR, MR (ESI) and (or) elemental analysis.

叶酸在放射性金属标记应用中的研究进展

夏姣云 汪勇先 唐 林 于俊峰 尹端沚

关键词 叶酸，放射性标记，肿瘤

叶酸在人体内起重要的生理功能作用，它能特异性结合过渡表达于许多肿瘤细胞膜表面(卵巢癌、乳腺癌、直肠癌等)的叶酸受体。在肿瘤靶向药物输运体系中，其中包括输运放射性标记的叶酸螯合物显像剂，叶酸受体是一种潜在的分子靶。近年来，研究放射性标记的叶酸螯合物显像剂的文章越来越多。本文着重介绍了放射性核素 ^{111}In、^{67}Ga 和 ^{99m}Tc(Re)标记叶酸的螯合物显像剂以及它们在肿瘤诊断方面的临床应用。这些资料表明，^{99m}Tc 标记叶酸的螯合物是一种比较有发展前途的显像剂。

Recent progress in application of folate in radio-metals labeling

XIA Jiaoyun WANG Yongxian TAN Lin YU Junfeng YIN Duanzhi

Keywords Folate, Radiolabeling, Tumor

The folate receptor is known to be overexpressed by a variety of neoplastic tissues, including ovrian, breast, colorectal and other human tumors. It is a potential molecular target for tumor-selective drug delivery, including delivery of radiolabeled folate-chelate conjugates for diagnostic imaging. Recently, papers on tumor imaging with radionuclide agents targeted to the folate receptor are growing, this review mainly summarizes the clinical application of ^{111}In、^{67}Ga and ^{99m}Tc（Re）labeling folate-chelate conjugates in tumor diagnostic imaging . However, these existing data shows that the ^{99m}Tc（Re）labeling folate-chelate conjugate is a better folate receptor imaging agent.

^{188}Re——一个有希望的治疗用放射性核素

尹端沚 于俊峰 汪勇先

关键词 铼-188，钨-188，治疗，发生器

综述了 ^{188}Re-高铼酸钠的物理化学性质、核性质和体内生物学行为; ^{188}W-^{188}Re 发生器的制备; ^{188}Re 标记化学及目前 ^{188}Re 及其标记化合物在肿瘤治疗，关节滑膜切除和防止冠状动脉血管术后再狭窄等方面的临床应用最新进展。

^{188}Re: a promising radioisotope for therapy

YIN Duanzhi Yu Junfeng Wang Yongxian

Keywords Rhenium-188, Tungsten-188, Therapy, Generator

Rhenium-188(β_{max} =2.11MeV; γ=155keV; $T_{1/2}$ =16.9hrs) is an attractive therapeutic radionuclide which is produced from decay of the reactor-produced tungsten-188 parent ($T_{1/2}$ =69hrs) and thus conveniently obtained on demand by elution from the tungsten-188/rhenium-188 generator system, so that it is very useful for the remote places far from the reactor. This paper describes in detail the physical and chemical properties, nuclear characters as well as the biological behavier in vivo and vitra of the rhenium-188; preparation of the tungsten-188/rhenium-188 generator and labeling chemistry of ^{188}Re. The recent progress of the rhenium-188 and its labeled compounds applied in the clinical studies of cancer therapy, synovectomy and intravascular radiation therapy were also exampled. It is convinced that the application of tungsten-188/rhenium-188 generator in the clinic therapy should be expanded as the ^{99}Mo/^{99m}Tc generator in the clinic diagnosis.

用于多巴胺 D_4 受体显像的[^{18}F]FMTP 的放射化学合成

田海滨　尹端沚　张 岚　张春富　王丽华　李俊玲　张勇平　汪勇先

关键词　^{18}F，苯并吡喃类似物，多巴胺 D_4 受体，PET，放化合成

8-甲氧基-3-(4-氟苄基)-1，2，3，4-四氢苯并吡喃[3，4-*c*]吡啶-5-酮作为选择性多巴胺 D_4 受体拮抗剂显示出高的亲和性和选择性(与 D_4 受体的结合常数 K_i = 4.3 nmol/L，与 D_2 受体的结合常数 K_i >5800 nmol/L)。文章采用三氟甲基磺酸 4-三甲基铵苯甲醛为前体完成了[^{18}F]氟标记的亲核取代反应，用[^{18}F]氟标记的中间体同 8-甲氧基-1，2，3，4-四氢苯并吡喃[3，4-c]吡啶-5-酮完成胺烷基化反应得到目标产物:8-甲氧基-3-(4-[^{18}F]氟苄基)-1，2，3，4-四氢苯并吡喃[3，4-*c*]吡啶-5-酮([^{18}F] FMTP)。产物的放射化学合成全部时间(包括高效液相纯化)为 110 min，放化产率为 19.5%，放化纯度大于 98%，比活度高于 37 GBq/μmol。[^{18}F] FMTP 可用于活体脑内多巴胺 D_4 受体显像剂。

Radiosyntheses of [^{18}F]FMTP for of dopamine D_4 receptor

TIAN Haibin　YIN Duanzhi　ZHANG Lan　ZHANG Chunfu　WANG Lihua

LI Junling　ZHANG Yongping　WANG Yongxian

Keywords　Fluorine-18, Chromene analog, Dopamine D_4 receptor, PET, Radiosyntheses

3-(4-fluorobenzyl)-8-methoxy-1, 2, 3, 4-tetrahydrochromeno [3,4-c]pyridin-5-one (FMTP), a selective D_4 receptor antagonist , has exhibited nanomolar affinity and high selectivity. [^{18}F]FMTP is synthesized in a multistep reaction in which fluorine-18 is introduced by nucleophilic halogen displacement on a quaternary ammonium group precursor. The fluorine-18 labeled intermediate is subsequently reductively aminated with 8-methoxy-1, 2, 3, 4-tetrahydrochromeno [3,4-c]pyridin-5-one to give the final products. The radiosynthesis of [^{18}F] FMTP needs approximatively 110 min with an overall radiochemical yield of 19.5% (decay-corrected) and with high effective specific activities (>37 GBq/μmol). [^{18}F]FMTP may be a useful positron emission tomography (PET) tracer that can be applied to map brain dopamine D_4 receptor.

放射性关节滑膜切除最新研究进展

于延豹　于俊峰　尹端沚　汪勇先

关键词　放射性，关节滑膜，切除，进展，^{188}Re

类风湿性关节炎(Rheumatoid arthritis，RA)是一种系统的多关节炎症，通常会侵犯动关节(Diarthrodial joint)如指、膝、足等。除了会导致滑膜发炎外，还会引起关节翳增生并侵犯关节软骨和其它骨组织。放射性关节滑膜切除是一种有效的治疗滑膜增生的方法。它采用直接关节内注射放射性药物，相对于其它疗法，其操作简单，病人痛苦小，恢复期短。经过临床实验证明，疗

效明显，并能大大改善病人的生活质量。本文从设计药物制剂的几个方案，如核素、载体、剂量、颗粒度、疗效等方面，综述放射性关节滑膜切除的研究现状及进展。

Recent advances in radiation synovectomy

YU Yanbao YU Junfeng YIN Duanzhi WANG Yongxian

Keywords Radiation, Synovectomy, Rheumatoid arthrosis, Joints

Radiation synovectomy is an attractive alternative to surgical or chemical synovectomy for the rheumatoid arthritis. The procedure only requires an intra-articular injection of a radiopharmaceutical with the appropriate nuclear to counteract and control synovial inflammation.In this article the clinical results obtained with radiation synovectomy from1990s are summarized and reviewed. The paper has also attempted to provide a perspective of radiosynovisis, their radionuclide characteristics, kinds of carriers, evaluation of dosimetry and methods for control of colloids diameter so as to diminish the leakage from the cavity are thoroughly described. It is assumed that new approaches to the preparation of radiolabeled particles for use in radiation synovectomy promise to minimize the extra-articular leakage and thus allow the full potential of this important radiotherapy to be realized.

不同颗粒度硫化铼[^{188}Re]混悬液的制备及其稳定性研究

于延豹 汪勇先 董 墨 于俊峰 胡伟青[1] 周 伟 杨学忠[1] 尹端泓

关键词 铼，混悬液，分布，颗粒度，沉降

本文介绍了两种分散方法制备不同粒径分布的硫化铼[^{188}Re]混悬液，以筛选适合关节腔注射的药物颗粒。实验采用涡旋法制备大颗粒的混悬液，大于 5 μm 颗粒有 55%，其中大于 10 μm 占 19%；超声法所得混悬液小于 5 μm 颗粒占 93%，大于 10 μm 只有 0.3%。两种方法所得粒径分布有显著差异(p<0.01)。稳定性测试结果表明涡旋法所得混悬液在 6 min 内稳定可靠，超声法所得混悬液在 15 min 内能均匀分散，此后取药需重新分散，且药物仍然均匀可用，颗粒度和放化纯度无明显变化。实验采用涡旋分散装置制备大颗粒混悬液，操作简便，验结果重现性良好，并同时避免涡旋分散过程中因手动操作对人体造成的辐射损伤，减少人为因素对颗粒度的影响。

---

1 安盛科兴药业有限公司

The study of preparation and stability of [^{188}Re] rhenium sulfide suspension with different particle size distribution

YU Yanbao WANG Yongxian DONG Mo YU Junfeng HU Weiqing[1] ZHOU Wei YANG Xue-zhong[1] YIN Duanzhi

Keywords ^{188}Re, Suspension, Particle size

Two different dispersing methods were studied in order that rhenium[^{188}Re] sulfide suspension, which is an attractive synovectomy agent, with obviously different particle-size distribution can easily be obtained. Swirling device, which is not only advantageous to self-defence, offers us large-sized particles, 55% of which are larger than 5μm and 19% are larger than 10μm. However, ultrasonic dispersion can only produce suspension with large quantities of smaller particles, only 0.3% of which are larger than 10μm and almost 93% are within 5μm. Consequently, the first suspension made by swirling device appears deposition within 6 minutes, and the second suspension is not uniform after 15 minutes. Radiochemistry purity and particle-size distribution does not change distinctively within 24 hours. The conclusion is that both of the suspension should be regarded as radiopharmaceuticals for testing the optimal particle-size ranges for intra-articular injection.

1. Amersham Kexing Pharmaceutical Co. Ltd

高浓度、无载体的 ^{188}Re-MAG$_3$ 的合成

张秀利 汪勇先 李俊玲 张春富 尹端沚

关键词 ^{188}Re-MAG$_3$，合成，标记，无载体，放射免疫治疗

^{188}Re 与 MAG$_3$ 的螯合会降低对病人的辐射剂量，螯合物将很快排出体外。高浓度的 ^{188}Re 标记的放射性药物可以缩短对病人照射时间。为了合成高浓度，无载体的 ^{188}Re-MAG$_3$，合成了 S-Bz-MAG$_3$，并用无载体的 ^{188}Re 标记。S-Bz-MAG$_3$ 的总产率高于文献报道的数值。对影响标记的条件，如还原剂的浓度，pH 值，反应时间等因素进行了优化，得到了最佳标记条件。用 C18 Sep-Pak 柱浓缩得到了高浓度的 ^{188}Re-MAG$_3$。^{188}Re-MAG$_3$ 的标记率高于 98%。放射化学纯度在 24 h 内高于 24%。

The synthesis of highly concentrated, carrier free ^{188}Re-mercaptoacetyltriglycine

ZHANG Xiuli WANG Yongxian LI Junling ZHANG Chunfu YIN Duanzhi

Keywords ^{188}Re-MAG$_3$, Synthesis, Labeling, Carrier free, RIT

Chelation of ^{188}Re to compounds such as MAG_3 will further reduce the radiation dose to the patient in case of balloon rupture by the rapid excretion from the body. Highly concentrated ^{188}Re-labelled radiopharmaceuticals may shorten irradiation time for patients with prerequisite concentration of solutions. In order to prepare highly concentrated, carrier free ^{188}Re-MAG_3, S-benzoyl mercaptocaetyltriglycine (S-Bz-MAG_3) was synthesized, labeled with carrier free ^{188}Re. The overall yield of S-Bz-MAG_3 is higher than those published in the literature. Dependence of the labeling yield of ^{188}Re-MAG_3 upon concentrations of reducing agent,pH,reaction time, *et al* was examined and optimum conditions were confirmed. The concentration procedure was succeeded with C18 Sep-Pak to obtain highly concentrated ^{188}Re-MAG_3. In the case of optimun conditions,the labeling yield of ^{188}Re-MAG_3 was more than 98%. Radiochemical purity of ^{188}Re-MAG_3 was more than 92% in 24 h.

无载体 ^{188}Re 间接标记 IgG 的研究

张秀利　汪勇先　李俊玲　尹端泚

关键词　无载体 ^{188}Re，IgG，S-Bz-MAG_3，放射免疫治疗，双功能螯合剂，间接标记

在放射免疫治疗中，^{188}Re 标记单克隆抗体具有一定的潜在性。S-Bz-MAG_3 作为双功能螯合剂，用于无载体的 ^{188}Re 标记 IgG。采用先标记螯合方法标记。优化了结合条件，在室温下反应 2 h，pH＝6。^{188}Re-MAG_3-IgG 的体外稳定性很高。结果表明，^{188}Re 间接标记 IgG 的研究对放射免疫治疗非常有用。

The study on indirect radiolabeling of IgG with carrier free ^{188}Re

ZHANG Xiuli　WANG Yongxian　LI Junling　YIN Duanzhi

Keywords　Carrier free ^{188}Re, IgG, S-Bz-MAG_3, Radioimmunotherapy, Bifunctional Chelating agent, Indirect radiolabeling

^{188}Re labeled monoclonal antibodies are potential candidates for use in radioimmunotherapy. S-Bz-MAG_3 as a bifunctional chelating agent was used for labeling of IgG with carrier free ^{188}Re by pre-radiolabeling of chelate approach. The conjugation conditions were optimized. The reaction was 2 hours at room temperature, pH was 6. The stability of ^{188}Re-MAG_3-IgG *in vitro* was high. The results may be useful to the studies of ^{188}Re labeled MAbs for radioimmunotherapy.

无载体 ^{188}Re 标记氟哌酸的研究

张秀利　汪勇先　张春富 李俊玲 尹端沚

关键词　无载体 ^{188}Re，氟哌酸，合成

用 ^{188}W/^{188}Re 发生器得到的 ^{188}Re 研制了具有潜在临床应用价值的 ^{188}Re 标记的氟哌酸(^{188}Re-Norfloxacin)。研究了在无载体的条件下，pH 值，温度，时间，氯化亚锡含量对标记率的影响，确定了最佳标记条件。实验结果表明:用无载体 ^{188}Re 标记的 ^{188}Re-Norfloxacin 的标记率为 92%以上，标记后调 pH 为 4，24 h 后，放化纯度基本不变。

A study on carrier-free ^{188}Re labeled Norfloxacin

ZHANG Xiuli　WANG Yongxian　ZHANG Chunfu　LI Jun-ling　YIN Duanzhi

Keywords　Carrier free ^{188}Re, Norfloxacin, Synthesis

The synthesis of a carrier free ^{188}Re-norfloxacin was investigated using ^{188}Re eluted from the ^{188}W/^{188}Re generator. Stannous chloride was used as the reducing agent for the reduction of the carrier free ^{188}Re. Influences of upon concentrations of reducing agent, pH, temperature, reaction time on the labeling yield of ^{188}Re-norfloxacin were examined and optimum conditions were obtained. In case of optimum conditions, the labeling yield of ^{188}Re-norfloxacin was more than 92%. The stability of ^{188}Re-norfloxacin at pH=4 was studied. Radiochemical purity of ^{188}Re-norfloxacin was nearly constant in 24h.

分子极化效应指数与脂肪族醛酮的沸点

张秀利　汪勇先　林英武　李俊玲

关键词　分子极化效应指数，醛酮，沸点，QSPR 研究

利用分子的极化效应指数，建立了三参数方法计算脂肪族醛酮沸点的关系式: $\ln(820.5-T_b)=6.38330-1.37357\times10^{-1}N_c+5.39350\Delta PEI+8.02603\times10^{-2}N$。式中 N_c 为脂肪族醛酮中烷基部分的有效碳链长度；ΔPEI 为具有相同碳原子数目的支链烷基与直链烷基的极化效应指数的差值，它表示羟基对醛酮沸点的影响；N 为碳原子数。

Molecular polarizability effect index and boiling point of aliphatic aldehydes and alkanones

ZHANG Xiuli WANG Yongxian LIN Yingwu LI Junling

Keywords Molecular polarizability effect index, Aliphatic aldehydes and alkanones, Boiling point, QSPR study

Based on the molecular polarizability effect index, a formula of $\ln(820.5\text{-}T_b)=6.38330-1.37357\times10^{-1}N_c+5.39350\Delta PEI+8.02603\times10^{-2}N$ by using three parameters was proposed to calculate the boiling point of aliphatic aldehydes and alkanones. Where the *N*c is the effective length of carbon chain of alkyl group in the aliphatic aldehydes and alkanones. The ΔPEI is the polarizability effect index difference between the corresponding branched and normal alkyl isomer containing the same carbon atom number, which expressed the effect of carbonyl group on the boiling point of aliphatic aldehydes and alkanones. *N* is the carbon numbers of aliphatic aldehydes and alkanones.

诱导效应指数与脂肪族胺、醇、醚的气相碱性

张秀利 汪勇先 李俊玲

关键词 气相碱性，诱导效应指数，元素电负性

用烷基诱导效应指数 *I* 和 RX 分子中质子亲合原子 X 所带电荷 q_x 及元素电负性 X_N 与脂肪胺、醇、醚的气相质子亲合能 *PA* 进行关联。结果表明，脂肪胺、醇、醚的气相碱性可以用下式定量描述: $PA(\text{kJ}\cdot\text{mol}^{-1})= 2732.0333- 2457.1510\Sigma I - 1492.2351q_x - 732.6277X_N$。利用上式对 64 种化合物的气相碱性进行预测，平均相对误差为 0.34%，预测值和实验值的偏差均在实验误差范围内。

Inductive effect index and gas phase basicity for aliphatic amine, alcohol, ether

ZHANG Xiuli WANG Yongxian LI Junling

Keywords Gas phase basicity, Inductive effect index, Electronegativity of element

The relationship was studied between gas phase proton affinity (*PA*) of aliphatic amines, alcohols, ethers and inductive effect index (*I*) of alkyl group, atomic charge (q_x), electronegativity of element (X_N) of affinity atom in RX molecules. The results indicate that *PA* of aliphatic amines, alcohols, ethers can quantitatively be described as follows: $PA(\text{kJ}\cdot\text{mol}^{-1}) = 2732.0333 - 2457.1510\Sigma I - 1492.2351q_x - 732.6277X_N$ Based on the relation, the gas phase basicities of 64 aliphatic amines, alcohols, ethers are predicted with average relative error≤0.34%.

MAG_3 在放射性金属标记应用中的最新研究进展

张秀利 汪勇先 尹端泔 李俊玲 曹金全

关键词 MAG_3(巯乙酰基三甘氨酸)，生物分子，$^{186/188}Re$，^{99m}Tc

MAG_3(巯乙酰基三甘氨酸)是一种有效的双功能螯合剂， 已被用于多克隆免疫球蛋白(HIG)，抗体，多肽，DNA 寡核苷酸及肽核酸(PNA)等的 ^{186}Re，^{188}Re，^{99m}Tc 的标记中。本文综述了利用 MAG_3 标记的多肽的生物学特性。 ^{99m}Tc 标记物的标记率和比放射性高，体内稳定性好，与血清蛋白的非特异性结合低；$^{186/188}Re$ 标记物也具有良好的体内外稳定性。因此 $^{186/188}Re$，^{99m}Tc 标记的生物分子为核医学提供了具有广阔应用前景的放射性诊断和放射性治疗的药物。

The recent progress in application of mag3 labeling radio-metals

ZHANG Xiuli WANG Yongxian YIN Duanzhi LI Junling CAO Jinquan

Keywords MAG_3, Biomolecules, $^{186/188}Re$, ^{99m}Tc

Mercaptoacetyltriglycine, an effective bifunctional chelating agent, has been applied in $^{186/188}Re$, ^{99m}Tc labeling HIG, monoclonal antibodies, peptides, antisense oligodeoxynuclides and peptide nucleic acid (PNA). The biological behaviors of the labeling conjugates with MAG_3 were summarized. The ^{99m}Tc labeling conjugates show high labeling efficiencies and high specific activities and hold desirable stability in vitro and in vivo. The binding of the labeling conjugates with plasma protein is low; The $^{186/188}Re$ labeling compounds also hold desirable stability in vitro and in vivo. So many potentially useful biomolecules labeled by ^{99m}Tc, $^{186/188}Re$ for diagnosis and therapy may be produced via MAG_3.

氮杂大环化合物在放射性金属标记中的应用研究进展

张秀利 汪勇先 李俊玲 尹端泔

关键词 氮杂大环化合物，放射性金属，标记，双功能螯合剂

氮杂大环化合物作为双功能螯合剂进行标记生物分子(一般为小肽，蛋白质或单克隆抗体等)。这些放射性金属标记的生物分子为核医学提供了具有广阔应用前景的放射性诊断和放射性治疗的药物。综述了氮杂大环化合物在放射性金属标记中的应用研究最新进展，介绍了用于标记的氮杂大环化合物，用于标记的放射性核素；介绍了标记物的生物学特性。并指出了氮杂大环化合物在不同核素标记中的优缺点。

The recent progress in application of polyazamacrocyclic compounds labeling radio-metals

ZHANG Xiuli WANG Yongxian LI Junling YIN Duanzhi

Keywords Polyazamacrocyclic compounds, radio-metals, Labeling, Bifunctional Chelating Agent

Polyazamacrocyclic compounds, the effective bifunctional chelating agents, have been applied in radio-metals labeling peptides, protein and monoclonal antibodies. Those biomolecules labeled radio-metals provide raiopharmaceuticals for radiodiagnosis and radiotherapy in nuclear medicine. The recent progresses in application of polyazamacrocyclic compounds labeling radio-metals are summarized. This paper introduces polyazamacrocyclic compounds labeled radio-metals, radionuclides and biological characters of labeling conjugates. It points out the advantages and disadvantages of polyazamacrocyclic compounds labeling radio-metals.

放射性金属核素标记反义寡核苷酸的研究进展

张秀利 汪勇先 周 伟 李俊玲 尹端泓

关键词 反义显像，放射性核素反义治疗，反义寡核苷酸，放射性金属核素

随着分子核医学的发展，反义显像技术和放射性核素治疗技术已经受到人们的重视。阐述了在反义显像技术和放射性核素反义治疗技术中对反义寡核苷酸的要求；介绍了放射性金属核素 ^{111}In、^{99m}Tc、^{90}Y 标记的不同反义寡核苷酸的生物学特性。脂质体、受体介导的反义寡核苷酸的转移，反义寡核苷酸的修饰以及标记方法的改进将大大加快其临床应用。

The progress in labeling of antisense oligonucleotide with radio-metal nuclides

ZHANG Xiuli WANG Yongxian ZHOU Wei LI Junling YIN Duanzhi

Keywods Antisense imaging, Radionuclide antisense therapy, Antisense oligonucleotide, Radio-metal nuclide

With the rapid development of molecular nuclear medicine, antisense imaging and radionuclide antisense therapy technology was taken into account. The demands for antisense oligonucleotide in antisense imaging and radionuclide antisense therapy technology were expounded, the biological behaviors of the labeling of antisense oligonucleotide with radionuclides, such as ^{111}In、^{99m}Tc、^{90}Y were introduced. The progression in antisense imaging and radionuclide antisense therapy, such as the transfer of antisense RNA mediated by liposomes or receptors, chemical modification of antisense oligonucleotide and the improvement of labeling, will improve the clinical application of antisense imaging and radionuclide antisense therapy.

Radiolabeling of magnetic targeted carriers (MTC) with indium-111

Urs O. Häfeli[1] YU Junfeng Farhad Farudi[2] LI Yuhua [3] Gilles Tapolsky[3]

Keywords Magnetic targeting, Microspheres, Radiolabeling, Indium-111, Yttrium-90, Imaging

Magnetic targeted carriers (MTC) are magnetically susceptible microparticles that can be physically targeted to a specific site. MTC were radiolabeled with ^{111}In using three different methods. Reaction parameters were investigated in order to optimize the final properties of the labeled MTC. The reaction parameters studied were chelation agent, chelation time, temperature, radiolabeling time, solvent, and molar ratios. A (97.7±0.9)% binding efficiency and plasma stability of (92.6±0.1)% over 7 days were achieved when 2-p-aminobenzyl-1,4,7,10-tetraazacyclododecane-1,4,7,10-tetra-acetic acid (ABz-DOTA) was used as the chelating agent. A preliminary animal biodistribution study confirmed the binding stability. The labeling of the MTC with the diagnostic isotope ^{111}In was undertaken to allow for quantitative imagingand dosimetry prior to therapy with ^{90}Y radiolabeled MTC.

1 Cleveland Clinic Foundation, Department of Radiation Oncology, 9500 Euclid Ave T28, Cleveland, OH, 44195, USA

2 Cleveland Clinic Foundation, Department of Cardiology, 9500 Euclid Ave F25, Cleveland, OH 44195, USA

3 FeRx Inc., 12635 E. Montview Blvd.-Suite 300, Aurora, CO 80010, USA

Radiolabeling of poly(histidine)-derivatized biodegradable microspheres with rhenium-188 tricarbonyl complex $[^{188}Re(CO)_3(H_2O)_3]^+$

YU Junfeng Urs O. Häfeli[1] XIA Jiaoyun LI Shiqiang DONG Mo

YIN Duanzhi WANG Yongxian

Keywords Microsphere, Radiolabeling, Rhenium-188, Tricarbonyl, Histidine, Radiation synovectomy

Many radiopharmaceuticals have been studied as radiation synovectomy agents. In this paper, we developed a new potential agent for radiation synovectomy: poly lactic acid-histidine (= PLA-his) microspheres radiolabeled with $[^{188}Re\ (CO)_3\ (H_2O)_3]^+$. The reaction conditions for the chelation of $[^{188}Re(CO)_3(H_2O)_3]^+$ and the radiolabeling of PLA-microspheres were optimized and the stabilities for both steps tested *in vitro*. The chelation efficiency of $[^{188}Re\ (CO)_3\ (H_2O)_3]^+$ reached (93.12±1.82)% with >95% radiochemical purity once the colloidal and free ^{188}Re was removed by a small Sep-Pak column (Plus QMA). More than 90% of radioactivity stayed in $[^{188}Re\ (CO)_3\ (H_2O)_3]^+$ form over 5hours. The radiolabeling efficiency of PLA-his microspheres with $[^{188}Re\ (CO)_3\ (H_2O)_3]^+$ was above 92%. After 3 days of incubation at 37℃ in calf serum, more than 80% of the radioactivity was still microsphere-

bound. Conclusion such microspheres are potentially useful as a radiation synovectomy agent for the treatment of chronically inflamed arthritic joints. Furthermore, they might be valuable in cancer brachytherapy.

1 The University of British Columbia, Faculty of Pharmaceutical Sciences, Vancouver, B.C., V6T 1Z3, Canada

^{90}Y-oxine-Ethiodol, a potential radiopharmaceutical for the treatment of liver cancer

YU Junfeng Urs O. Häfeli[1] Mark Sands[1] Yonghua Dong[1]

Keywords ^{90}Y, Oxine, Lipiodol, Radiolabeling, ^{111}In, Liver cancer

Ethiodol (or Lipiodol) is selectively retained in hepatocellular carcinoma and is used as a vehicle to deliver radioactive agents following intraarterial hepatic infusion. We prepared the lipophilic complex ^{90}Y-oxine with a chelation efficiency of (97.6±1.1)%. After extraction into Ethiodol, a stability test in serum at 37℃ showed that 87.8% of the ^{90}Y remained Ethiodol-bound for 7days. Bremsstrahlung imaging of a rabbit for 48 hours confirmed that radiolabeled Ethiodol stayed in the targeted liver lobe.

1 Cleveland Clinic Foundation, 9500 Euclid Ave., Cleveland, OH 44195

先进探测仪器

Advanced detectors and instruments

先进探测仪器研究中心简介

我研究中心目前编制 27 人, 其中有百人计划 2 名, 拥有博士学位者 2 名，硕士学位者 4 名。现担负培养博士研究生 2 名，硕士研究生 6 名。

按照我所的发展战略，结合我中心的具体情况，坚持我中心实验方法学研究和仪器设备研制的特色, 紧跟所的布局方向，与大科学装置紧密结合，发挥自身优势。

主要研究方向有：

（1）探测方法和成像技术研究。其中包含爆炸物毒品检测、X 荧光谱仪的研制、微区 XRF 成像技术研究、小动物 microSPET 装置和成像技术以及 CdZnTe 化合物半导体探测器的制备工艺研究。

（2）生物特征检测。其中包含图像采集系统、算法研究、指纹识别和基于指纹识别技术和智能卡技术的研究。

（3）自动控制系统和电子学电源研制。其中包含加速器和钴源辐照装置的控制系统设计制造, 基于 ARM 和 DSP 的嵌入式仪器的研究, 核信息测量仪器和特种高压电源和开关电源的研究与开发。

毒品、爆炸物品在线检测技术的前期研究
——离子迁移率方法在毒品、爆炸物品检测中的研究与应用

蒋大真　魏永波　赵国璧　成 诚

关键词　毒品，爆炸物品，在线检测，离子迁移率，交变梯度电场聚焦

毒品和爆炸物品危害社会稳定、国家安全，很多国家投入大量资金来研究在线毒品、爆炸物品检测方法，开发先进的检测仪器，打击日益猖獗的毒品走私活动和危害严重的恐怖犯罪活动。为加强国家安全和社会稳定，我国众多机场、港口、码头、海关、边防哨所以及即将举办国际赛事的体育场馆及相关设施、即将举办的国际展览等人群高密度聚集的场所，迫切需要此类检测设备。离子迁移率 (Ion mobility spectrometer，简称 IMS)方法以其工作原理简单、仪器灵敏度高、分析迅速、工作状况稳定，并且由于结构简单无机械动作的优点而适于小型化做现场分析。中国科学院上海应用物理研究所在国内最先采用 IMS 方法，首次引入离子约束机制和直线加速交变梯度电场聚焦技术，实现了在实验室条件下在 1—2 min 内完成若干种物质的鉴别，仪器对物质单峰分辨率小于 0.2 ms，显示出其在毒品、爆炸物品检测方向上广阔的发展前景。

IMS 技术研究及在空间物质探测中的应用

魏永波　蒋大真

关键词　离子迁移率探测器，火星探测器，离子约束，交变梯度电场聚焦，嫦娥工程

IMS 原理简单、灵敏度高、分析迅速、工作状况稳定。其在非真空条件下，对一些物质分子进行直接分析的特点，适用于行李检测等应用目的：其体积小、灵敏度高的特点，则可在航天工程中用于探测星际物质。中国嫦娥工程项目的科研目标之一：探测地月空间环境，可以用简单易行的 IMS 技术来实现。

IMS technique for detecting interspatial substances

WEI Yongbo　JIANG Dazheng

Keywords　Ion mobility detector, Mars detector, Ion bondage, Electric field focusing, The Lady in the Moon Project

Ion mobility spectrometry (IMS) has many advantages such as simple principles involved, high sensitivity and stability, and fast speed of analysis. It can be used for baggage checking because of its excellent capability of detecting and analyzing trace molecular substance in non–vacuum conditions. And its high sensitivity and compact volume suggests its application of detecting interspatial substances for a space project, such as detection of molecular substances between the Earth and the Moon, an important research subject of the Chinese space project of the Lady in the Moon (the Chang’e Project).

IMS 电场优化设计的研究

魏永波　蒋大真

关键词　离子迁移率，毒品，爆炸物品，离子约束

IMS（Ion mobility spectrometer）在大气环境条件下，可以直接对一些物质分子进行分析，尤其是爆炸物品和毒品的在线分析检测上，显示出广泛的应用前景。IMS 电场设计是 IMS 物质分辨率的重要影响因素，通过对 IMS 电场模拟分析和实际测量结果的对照，得到了优化的电场结构。

The study of optimization of IMS electric field

WEI Yongbo　JIANG Dazheng

Keywords　Ion mobility, Drugs, Explode, Ion bondage

Ion mobility spectrometry (IMS) has been known recently as an analytical technique for detecting and charactering of vapors in atmospheric pressure, especially for the ability of detecting hiding explosives and drugs. Design of the electric field is critical for resolution and performance of an IMS system. By electric field simulation and optimization, a better IMS spectrum was obtained.

基于多探测器的便携 X 荧光能谱仪的研究

成 诚　魏永波　徐慧超　蒋大真

关键词　多探测器，SI-PIN 探测器，CdZnTe 探测器，便携能谱仪

本文分析了 SI-PIN 探测器与 CdZnTe 探测器的特点，提出了一种基于多探测器便携能谱仪的结构，利用不同的探测器测量不同能量范围内的元素特征 X 射线来提高测量精度，展宽便携能谱仪可测量的能量范围，拓展便携能谱仪的应用范围。

Research of multi-detector based portable X-rays analyzer

CHENG Cheng　WEI Yongbo　XU Huichao　JIANG Dazhen

Keywords　Multi-detector, SI-PIN detector, CdZnTe detector, Portable energy-dispersive analyzer

In this paper, two room temperature detectors: SI-PIN detector and CdZnTe detector are demonstrated, and a multi-detector based portable X-ray analyzer architecture is proposed. The main idea of this architecture is to measure characteristic X-rays in different energy ranges with different

detectors. In this way,,a portable X-ray analyzer equipped with multi-detectors extends its energy range of the measurement and areas of applications as well.

基于样本自校正的 X 荧光无源能量刻度

成 诚　魏永波　蒋大真

关键词　能量刻度，校正因子，自校正

由于放射源使用的特殊性，近年来发展了许多用于便携 X 荧光分析仪的能量刻度方法。本文介绍了一种基于样本校正的无源能量刻度方法。该法首先存贮大量样本数据作为仪器的历史信息，建立样本库；测量标样来检验仪器当前状态是否正常；将历史信息和当前状态信息分别乘以校正因子作为当前测量的能量刻度。这种能量刻度的方法同固定能量刻度法相比有着较高的精度和稳定性。

Use of sampling based correction for non-radioactivity X-ray energy calibration

CHENG Cheng　WEI Yongbo　JIANG Dazhen

Keywords　Energy calibration, Correction index, Self-correction

As requirements of nonradioactivity measurement increased in recent years, various energy calibration methods applied to portable X-ray fluorescence spectrometers have been developed. In this paper, a sampling based correction energy calibration has been discussed. With this method, which uses history information and current state of the instrument as energy calibration, one is able to obtain relatively high precision and reliability in calibrating a portable X-ray fluorescence spectrometers.

便携能谱仪放大电路的集成化研究

成 诚　魏永波　蒋大真

关键词　前置放大器，成形放大器，集成化

性能优良的前置放大器和成形电路往往电路系统较为复杂，庞大而不适用于便携能谱仪中。本文介绍了一种基于前放芯片 CR-110 及成形芯片 CR-200 的能谱仪电子学系统，在减少体积的同时保证了良好的性能，适用于各种便携能谱型仪器。

Development of integration of amplifier circuits used in portable spectrometers

CHENG Cheng WEI Yongbo JIANG Dazhen

Keywords Preamplifier, Shaping amplifier, Integration

Preamplifiers and shaping amplifiers with excellent performance can hardly be adapted to portable spectrometers because of their complex structures and installment volume. This paper mainly introduce a kind of mini electronics system used in portable energy spectrometers based on CR-110 & CR-200 chips. The system, having a much smaller volume at the expense of losing a tiny performance, could be widely used in various spectrometers.

基于碲锌镉的便携 X 荧光能谱仪的研究

成 诚 魏永波 蒋大真

关键词 CdZnTe 探测器，X 荧光，便携能谱仪

CdZnTe 探测器是近年来发展迅速的常温探测器，在室温下通过电致冷最佳能量分辨率可达 200 eV。本文采用 N 型碲锌镉材料研制的探测器，结合最近开发的集成化谱仪放大电路，用于便携 X 荧光能谱仪中，室温下在 59.54 keV 的能峰处获得了 2.37%（FWHM）的相对分辨率，体积减小至普通探测器的二十分之一。采用电致冷可进一步降低热噪声，降低检测下限，提高分辨率，非常适用于中高能区的 X 特征荧光的检测。

A CdZnTe detector based portable X-ray analyzer

CHENG Cheng WEI Yongbo JIANG Dazhen

Keywords CdZnTe detector, X-ray fluorescence, Portable energy-dispersive spectrometer

CdZnTe detectors work at room temperatures and have been studied intensively in recent years. And it was reported that by electric cooling an energy resolution of 200 eV can be achieved at room temperatures. Detectors made of N-type CdZnTe materials and an integrated amplifiers circuits were developed recently for portable energy-dispersive X-ray analyzers, which has a relative energy resolution of 2.37 % (FWHM) at 59.54 keV at room temperatures, and the volume of which is reduced to one twentieth of a conventional X-ray analyzer. Thermal noise can be minimized through electric cooling. With improved lower detection limit and energy resolution, it is suitable for measuring of X-ray fluorescence in medium or high energy regions.

N 型碲锌镉探测器的制备和性能

张金洲 徐慧超 沈浩元 张光明

关键词 碲锌镉，探测器，制备，能量分辨率，稳定性，极化效应

碲锌镉（CZT）晶体由于原子序数高、禁带宽、密度大，制成低能 γ 射线和 χ 射线探测器不需液氮冷却就能得到很好的能量分辨率，且有相当高的探测效率。因此近年来发展迅速。我们实验室已制成 Φ8×1.7mm^3 灵敏体积的 CZT 探测器,室温 22℃下对 ^{241}Am 放射源、59.54keV 能量的 γ 射线能量分辨率可以达到 2.06keV(FWHM)（未使用准直器）,连续测量没有极化效应,并且具有很好的长期稳定性。

Fabrication and performances of N type CdZnTe detector

ZHANG Jinzhou XU Huichao SHEN Haoyuan ZHANG Guangming

Keywords CZT, Detector, Process, Energy resolving power, Stability, Polarization

Cadmium zinc telluride (CZT) crystal is an ideal material for fabrication of X-ray and low energy gamma-ray detectors. Thanks to relatively high atomic numbers, high density and wide band-gap, CZT detectors have sharp energy resolution and high detection efficiency without cryogenic cooling. A prototype planar CZT detector with sensitive volume of Φ8×1.7mm^3 was fabricated. Energy resolution of the 59.54keV gamma-ray from ^{241}Am was 2.06keV (FWHM) at room temperatures. No polarization has been observed in long term measurement, and the stability has been very satisfactory.

高频高压电子加速器 PLC 控制的改进

刘 平 龚培荣

关键词 辐照，PLC，加速器

上海应用物理研究所生产的 3 MeV、30 mA 高频高压电子加速器，应用于热缩材料生产、电线电缆辐照等工业领域。以前采用的是继电器手动控制方式，我们进行了升级换代，采用西门子的 300 型 PLC 控制。PLC（Programmable Logic Controller）即可编程控制器，是将微机技术与继电器常规控制方式相融合，以微处理器为核心，专为工业环境下应用而设计的一种数字运算操作的电子学系统。已有 6 台采用 PLC 控制的加速器安装于曲阜、佛山、吴江、苏州、深圳等地。

根据现场调试情况，我们进行了改进完善，针对高压放电打火现象，增加开关量和模拟量的输入输出光电隔离模块，有效的保护了元器件；针对能量稳定度要求，优化了能量控制板的闭环负反馈电路，现在的能量稳定度为±1%；针对束流稳定度要求，编写了新的 PID 算法程序，使束流稳定度为±3%。我们也重新设计了计算机人机界面，使其画面美观，操作方便。

The improvement of PLC controller of E-beam accelerator

LIU Ping GONG Peirong

Keywords Radiation, PLC, Accelerator

Electron beam accelerators are widely used for radiation processing of heat-shrinkable material, cable and wires, or other products. Control system of the high voltage E-beam accelerators developed at SINAP was remoduled with Siemens 300 type PLC，programmable logic controller, which is an electronic system using microprocessor for industry environment applications. So far, six E-beam irradiators with the PLC controller have been installed in Qufu, Fushan, Wujiang, Suzhou and Shenzhen.

Several measures were taken to improve the control system according to problems found in testing the accelerators. To reduce discharge sparking while building up the high voltage, the isolation modules of digital I/O and analog I/O were increased in number, and this protects the chips effectively from the sparking. To achieve ± 1% of the beam energy stability, the close loop reactive circuit of control energy was optimized. And a new PID code was designed to meet requirements on beam current stability of ± 3%. In addition, the human interface was redesigned, improving greatly the screen appearance and operation convenience.

基于 WINDOWS 的多道脉冲幅度分析器的软件开发

刘 平 阮裕泉 浦世节

关键词 多道脉冲幅度分析器，虚拟设备驱动程序，程序设计，动态连接库

多道脉冲幅度分析器是核能谱测量中的必备仪器。以前的分析软件多是 DOS 平台的，需要升级到 WINDOWS 平台。该软件的开发解决了中断方式数据采集问题，提供了友好的 WINDOWS 操作界面，大大方便了使用 WINDOWS 操作系统的用户。

Software uograding of multi-channel pulse amplitude analyzer

LIU Ping RUAN Yuquan PU Shijie

Keywords Multi_channel pulse amplitude analyzer, Virtual device driver, Program design, Dynamic link library

Multi-channel pulse amplitude analyzers made at SINAP are widely used for nuclear spectrum measurement. The traditional operation environment was many based on DOS. This paper presents an MS Windows based operation environment which settles the problem of data acquiring by interrupt mode and with a friendly user interface.

3 kW 大功率高压电源的研制

阮裕泉

关键词 大功率，功率因子

该高压电源的最大输出电压和电流为-60 kV 和 50 mA。在低压（400V）供电电源的设计中，采用了功率因子补偿线路，获得了在-220 V 条件下可以达到 400 V 8 A 的输出功率。在高压部分的设计中，采用 PWM 方式，倍压部分用油箱散热，从而获得大功率的输出。

The 3kW high voltage power supply

RUAN Yuquan

Keywords Power supply, Power factor

Maximum voltage output and current of the high voltage power supply are –60kV and 50mA.In designing low voltage part (400V) of the power supply, a circuit of power factor compensation is adopted, and power output of 400V 8mA can be achieved under -200V. A PWM mode and an oil box for heat dispersion were used in the designing the high voltage part, with which a 3000W output power can be obtained.

-200 kV 高稳定高压电源的研制

阮裕泉

关键词 高压电源，纹波，电子束离子阱

本文叙述了用于电子离子阱装置的高稳定-200 kV 高压电源的研制，在输出电压为-130 kV、空气环境条件下，每小时稳定性优于 100×10^{-6}。当输出电压为-180 kV，负载为 400MΩ 时，高压输出纹波小于 50×10^{-6}。

The –200kV high voltage power supply with high stability

RUAN Yuquan

Keywords High voltage power supply, Ripple, EBIT

A –200kV 1mA high voltage power supply with high stability was designed for an electron beam ion trap (EBIT). When the output voltage is –130kV under ambient conditions, the stability is less than 100ppm per hour. And when the output voltage is –180kV and load is 400Meg, the ripple of the output voltage is less than 50ppm.

基于 USB 通信的多道分析器接口设计

黄跃峰　阮裕泉

关键词　通用串行总线，多道分析器，固件，设备驱动程序

完成了一种新型多道分析器的接口电路设计，它采用 USB 技术与计算机进行通信，使多道分析器具有了通用性强、即插即用的优点。结合 EZ—USB FX（CY7C64613）的结构及工作原理，介绍了基于 USB 通信的多道分析器接口的电路设计和软件设计。

The interface for the USB-based multi-channel analyzer

HUANG Yuefeng　RUAN Yuquan

Keywords　Universal serial bus, Multi-channel analyzer, Firmware, Device driver

A new style interface circuit was designed for a multi-channel analyzer, which communicates with a computer via universal serial bus (USB). This favors users with increased universality and convenience of “plug and play”. According to structure and principles of the chip EZ-USB FX, the design of the interface of the USB-based multi-channel analyzer is described.

指纹防盗锁通用技术条件

牟晓生　李勇平　戎 玲　王永强　陈伟元

关键词　指纹特征，指纹登录，指纹匹配，匹配时间，认假率，拒真率

指纹防盗锁是近几年发展和应用最快的新一代生物特征识别技术产品，为适应市场发展需求，统一产品规范，公安部科技局成立“指纹防盗锁标准起草小组”，研究制订相应的技术标准，编号 TC100/SC1。该标准规定了指纹防盗的通用技术要求和测试方法，适用于主要以指纹图像作为输入信号，识别、处理其相关信息，以控制机械锁定结构启、闭的锁。该标准亦适用于指纹锁及保险箱使用的独立式指纹识别模块。

General specifications of theft prevention fingerprint locks

MOU Xiaosheng　LI Yongping　RONG Ling　WANG Yongqiang　CHEN Weiyuan

Keywords　Fingerprint template, Enrollment, Fingerprint matching, Match time, False accept rate (FAR), False Rejection Rate (FRR)

As a new generation of biometrics products, theft prevention fingerprint locks have been in fast development and applications in recent years.　In order to standardize product specifications in China

where the fingerprint locks are of high demands, a sub-committee of TC100/SC1 has been setup by the Ministry of Public Security to study and formulate the specification standard. Technique requirements and testing schemes are defined in the standard for a theft prevention lock that activates its opening or closing mechanisms on completing fingerprint image processing and correlated information identification. This standard is also suitable for general fingerprint locks and the strong-boxes that use the standalone fingerprint verification modules.

三角波束流扫描电源的改进

李纪明　龚培荣

关键词　扫描，三角波

电子束辐照装置的束流扫描为 X-Y 扫描，（其中 Y 扫描为提高剂量均匀度而设，行程较小）。在原有电源的基础上，新的开关型扫描电源采用了全新的驱动电路，并对原电源的一些电路参数进行了修改，选用了更合适的元器件。改进后的扫描电源，X 扫描电源为桥式输出电路，Y 扫描电源采用半桥式输出电路。

IGBT 功率管驱动电路采用美国 IR 公司生产的 IR2110 驱动器。IR2110 的内部结构和特点决定了它是一种性能优良的驱动集成电路，它兼有光电隔离和电磁隔离的优点，是中小功率变换装置中驱动器件的首选品种，在应用中扩展的附加硬件成本也不高，空间增加不大，使整个电路更加紧凑。与其他驱动集成电路相比，保护功能略显不足，我们增加了额外的保护措施加以弥补。为防止功率器件误导通，我们在应用中采用了栅极负偏置驱动。

为确保钛窗安全，电子束应始终处于扫描状态。因此，一旦该 X 扫描出现故障，应立即将其切换到市电供电。我们调整了电路参数，使切换时间缩短到约 11 ms，更利于对钛窗的保护。Y 扫描电源不需故障输出联锁，但有故障报警指示。在波形显示方面，增加了三角波中心线的上下调节功能，有利于调整扫描对称度。

新扫描电源在加速器调试过程中经受住了大量高压打火的冲击和电压锻炼，使用过程中性能更加稳定，运行更加可靠。

An improved power supply for beam scanning magnet of an EB irradiator

LI Jiming　GONG Peirong

Keywords　EB irradiator, Scanning, Triangular waveform

The irradiator has X and Y beam scans to ensure uniform dose distribution in irradiated products. The switching type power supply for the beam scan magnet was improved with a new drive circuits, and the circuit parameters were optimized with suitable electronic components. The X beam scan power supply is of a bridge type output circuit, whereas the Y scan power is of a half bridge type.

The IGBT is driver by an IR2110 driver (IR Corp., USA), an integrated circuit driver which is

advantageous with features of both optical and electromagnetic insulations, compact size and reasonable cost for median power drivers. However, the IR2110 should be additionally protected so as to avoid misleading the transient, and we adopted a negative bias control circuit for the grid of IGBT.

The electron beam should be scanned continuously to safeguard the Ti window when the accelerator is in operation. Therefore, an emergent switching to AC line has to be performed whenever a failure should occur to the power supply of the beam's X scan. For better protection of the Ti window, parameters of the power switching circuit were improved to reduce the switching time to about 11 ms. It is not necessary to do this for the Y scan power supply, but an alarm would work with a Y scan failure. In addition, baseline of the triangle waveform can be adjusted for scanning the beams symmetrically.

The beam scan power supply withstood the accelerator tests, when considerable sparks occurred to the accelerator tube during the conditioning, and operations of the EB irradiator show that the beam scan power supply is more reliable than before.

上海 EBIT 装置电源和控制系统的研制

龚培荣　李纪明　刘 平　肖龙笙　季 萍

关键词　EBIT，电源，控制，联锁

上海 EBIT 装置是一台用于研究高电荷态离子物理特性的实验设备。其电源的性能直接影响着电子束流品质，共有 36 台不同输出电压和电流的电源分布在 7 个不同的电压平台上，其中有 10 台高压电源（输出电压>8 kV）、11 台低压电源（输出电压<3 kV）、12 台稳流电源（最大输出 140 A/30 V）和一台超导磁场电源，以及 2 台离子源脉冲电源。电源的输出稳定性好于 0.05%，输出电压纹波系数小于 0.1%。

除超导电源外，所有电源均采用 PWM 专用芯片进行设计，根据其输出电流（功率）的不同分别选用推挽式输出、半桥式电路或桥式输出电路，经过高频（升压）变压器耦合，（倍压）整流滤波，产生所需的输出电压或电流。所有电源均可工作在“本地”或“遥控”两种模式下，计算机遥控遥测，使用方便，电源机箱一律采用 19”标准化机箱。

上海 EBIT 装置的控制由基于 GROUP3 公司的光纤环路控制模块组成分布式控制系统，共有三个光纤环路、14 个控制站点，控制和调节除超导电源外的所有电源的开关和输出大小，以及实施 EBIT 装置的部分安全联锁功能。总共有 109 路模拟控制信号和 169 个开关控制信号。

上海 EBIT 装置的控制系统分为静态控制和动态控制。静态控制包括各电源输出参数的设置、回读及保存，安全联锁信号的控制，真空及油流量的采集。EBIT 的静态控制由 GROUP3 模块实现，逻辑控制仪完成装置的联锁操作，对来自 EBIT 各子系统的安全联锁信号进行采集，并执行相应的保护动作，完成人身安全保护、设备运行安全防护等功能，真空及油流量的采集通过 485 总线由计算机完成。动态控制是为电子束能量扫描而设，使离子的注入、引出以及束缚电离过程协调动作，由时序发生器主导工作，对 DT3、DT2 以及离子源触发极电源进行调控，实现离子的“注入引出”过程。整个控制系统的程序编制采用 LabVIEW 语言实现。

The power supply and control system for Shanghai EBIT

GONG Peirong LI Jiming LIU Ping XIAO Longsheng JI Ping

Keywords EBIT, Power supply, Control, Interlock

Shanghai Electron Beam Ion Trap (EBIT) is built for spectroscopic studies and collision cross sections of highly charged ions. Its 36 power supplies working at 7 voltage levels include 10 high voltage (> 8kV) power supplies, 11 low voltage (< 3kV) power supplies, 12 constant current output power supplies, one superconductor power supply and two ion pulse power supplies. Stability requirement of the power supplies is 0.05% maximum and the voltage ripples shall be less than 0.1%.

Except for the superconductor power supply, all the power supplies are of the PWM chip type, and generate required voltage or current via circuits of push-pull output, half bridge output or bridge type output (according to different current or power requirements) with high frequency transformer coupling and rectifier filtering. Every power supply is in a 19” standard case and works at Local model or Remote Control model to facilitate the measurements.

Design of the control system is based on GROUP3 fiber optical control module DI (device interface), with three Fiber loops (14 DI) to switch on and off the power supplies (except the superconductor power supply), preset the output volt or current, and perform interlock functions of the EBIT, which has 109 analogue singles and 169 digital singles.Group3 Control is a fiber optically linked distributed control system. The control system operates safely and reliably. The control programming of Shanghai EBIT is written by LabVIEW.

双极性对称输出扫描电源的研制

龚培荣 李纪明 刘 平 邹宇斌[1] 郭之虞[1]

关键词 双极性，扫描，对称，三角波

双极性对称输出扫描电源是为北京大学重离子物理研究所测试强流离子束发射度而专门设计的。该电源能同时输出连续可调且正负对称的扫描电压，最大扫描电压幅度为±1200 V，最高扫描频率（外输入控制）可达 4 Hz。扫描电压的幅度可由计算机外控调节，输出监测电压与输出电压成严格的线性比例且具有较好的准确度。

此扫描电源的设计思想是建立在两个正负稳压电源对称输出的基础上，通过快速开关的切换来实现输出电压的极性转换，保证输出正负电压的连续可调。电源输出电压变化速率好于 9 V/1 ms，且电源的响应速率与输出纹波间是矛盾的，较快的响应速率，其输出纹波不能小；减小了输出纹波，其响应速率必然降低。

1 北京大学重离子物理研究所

A bi-poles symmetry output scanning power supply

GONG Peirong LI Jiming LIU Ping ZHOU Yubin[1] GUO Zhiyu[1]

Keywords Double poles, Scan, Symmetry, Triangular waveform

The power supply is designed specially to measure emitance of large current ion beams for Institute of Heavy Ion Physics of Peking University. The power supply provides simultaneously positive and negative voltages adjustable continuously for symmetry scanning. The maximum voltage is ± 1200V and maximum scanning frequency is 4Hz. The voltage is controlled by a remote computer, and monitoring voltage readings track strictly the output voltage.

The power supply establishes on two steady voltage power supplies, one for positive, and the other for negative. Conversion of output parity is realized by fast switch, output voltage is continuous adjustable. The power supply output speed is better than 9 Vs/ms.

1 Institute of heavy icon physics University of Peking

新 技 术

Noval technology

新技术中心简介

中国科学院上海应用物理研究所新技术中心是主要从事分离膜科学和水处理的科研单位之一，科学研究包括先进环保与水资源化技术、膜科学与技术、膜的应用技术、膜生物反应器等诸多方面，尤其以超滤膜的研制和水处理研究见长，在苦咸水处理用纳滤膜等方面也具有一定的研究特色，在国内具有一定的影响。多年来一直承担国家、上海市及中科院的重要科研任务。不仅为国家培养了科研人才，也取得了大批重要的科研成果，为国家的分离膜科学和工业发展作出了重要贡献。已初步形成科学研究和技术开发相结合的分离膜科学人才培养和科学研究的重要基地。2003 年我们引进了二名博士，招收博士研究生一名、硕士研究生一名，使中心拥有了一支研究领域广泛、中青年相结合、勇于创新的研究团队。

超滤膜的改性研究及应用

陆晓峰　卞晓锴

关键词　超滤膜，表面改性

随着超滤膜技术的发展，人们对超滤膜提出了各种各样的特性要求，其中解决膜表面的污染问题变得越来越紧迫。超滤膜改性，尤其是在膜表面引入亲水性基团是解决问题的关键。本文从这点出发,结合自身的工作，总结了近年高分子超滤膜改性方面的研究进展，包括表面活性剂在膜表面的吸附改性、等离子体改性、辐照改性、高分子合金和表面化学反应等几种改性方法。

Surface modification of ultrafiltration membrane and its application

LU Xiaofeng　BIAN Xiaokai

Keywords　Ultrafiltration membrane, Surface modification

With the development of membrane technology, people have a variety of requirements for UF membranes, amomg them is to solve fouling problem of membrane surface. Especially, surface modification to introduce hydrophilic groups onto membrane surface is an effective way. In this paper, a review is given on progresses in membrane surface modification with methods of surface surfactant adsorption, plasma treatment, radiation modification, polymer alloy and surface reaction etc.

聚丙烯酸钠复合超滤膜研制初探（Ⅰ）UPANA - 1 复合膜的制备

樊文玲　陆晓峰

关键词　聚丙烯酸钠，复合超滤膜，制备

以聚丙烯酸钠为复合膜分离层材料，多孔的聚醚砜（PES）超滤膜为基膜，研制出具有超薄分离层的聚丙烯酸钠复合超滤膜（UPANA – 1）。用浓度为 0.005 g / L、分子量为 1000 的聚乙二醇水溶液作为介质溶液，在室温和 0.6 MPa 压力下进行膜性能测试。UPANA - 1 膜的截留率大于 90 %，水通量为 32.6 L / (m^2·h)。着重研究了基膜的选择、超薄分离层膜液的组成等制膜条件对复合膜性能的影响。

Preliminary study on preparation of polyacrylic sodium composite ultrafiltration membrane: Part I, Preparation of UPANA-1 composite membrane

FAN Wenling LU Xiaofeng

Keywords Polyacrylic sodium, Composite ultrafiltration membrane, Preparation

Polyacrylic sodium composite ultrafiltration membrane (UPANA-1) was prepared by coating an asymmetric PES substrate ultrafiltration membrane (MWCO = 70 000) with polyacrylic sodium solution.UPANA-1 membranes were tested at room temperatures under 0.6 MPa. With a PEG (Mw =1 000) solution in mass concentration of 0.005g/L, a water flux of 32.6 L/ m^2h and a rejection of 92.2% could be achieved. Studies were carried out on effects of membrane preparation conditions, such as concentration of polyacrylic sodium, glycerol, mass radio of glycerol and HCl, mass radio of acetic acid and methanol, substrate membrane and clearance of stroll scraper on the membrane property. The following results were obtained: (1) Materials of substrate affected composite membrane performance, PES-700 ultrafiltration membrane with MWCO 70 000 was the best choice. (2) Concentration of polyacrylic sodium in casting solution was an important parameter to affect membrane properties. The separation performance of the membrane was the best when 0.19 g polyacrylic sodium was added into the coating solution,. (3) Adding glycerol was of much more help in improving selectivity of composite membrane in comparison with glycerol and PEG-400. (4) The composite membrane performed perfectly when mass radio of glycerol and HCl was 3:2. (5) Adding 3 mL acetic acid and 2 mL methanol was favorable to enhance flux of the composite membrane. (6) With a clearance of 40 μm between the scraper and the surface of substrate , the thickness of skin layer was the most suitable.

原子力显微镜在聚合物膜研究中的应用

樊文玲 陆晓峰

关键词 原子力显微镜, 聚合物膜

原子力显微镜（AFM）已被用来研究膜的孔径和孔径分布、膜孔的结构、表面粗糙度、表面接点结构、膜的表面整体形态、膜污染机制和膜材料的选择等 7 个方面。原子力显微镜作为一种崭新的、有效的物理观测工具，在聚合物膜研究方面仍具有应用潜力。

A review on AFM studies of polymeric membranes

FAN Wenling LU Xiaofeng

Keywords Atomic force microscopy, Polymeric membranes

Atomic force microscopy (AFM) has been used to study such characteristics of membranes as pore size, pore size distribution, pore structure, surface roughness, nodules on the membrane surface, surface general morphology, mechanism of membrane fouling and the choice of membrane material. AFM, as a novel and effective physical method, still has potential on the examination of polymeric membranes.

聚乙烯醇复合膜的制备

卞晓锴 施柳青 梁国明 陆晓峰

关键词 聚乙烯醇，涂敷法，复合纳滤膜，膜制备

以亲水性的聚乙烯醇为原料,采用机械涂敷法制备复合纳滤膜。考查了基膜、聚乙烯醇的浓度、交联剂的浓度及配比、涂层厚度、交联时间以及热处理等对膜分离性能的影响，确定了最终制备条件。在一定的温度和湿度条件下，在截留相对分子质量为 100 000 的基膜上，通过 5 %的聚乙烯醇溶液与 1 %的戊二醛的交联反应，研制了截留相对分子质量为 600 的 PVA 复合纳滤膜.

Preparation of PVA composite nanofiltration membranes

BIAN Xiaokai SHI Liuqing LIAN Guoming LU Xiaofeng

Keywords Polyvinyl alcohol, Coating method, Composite nanofiltration membrane, Membrane preparation

Composite nanofiltration membranes were prepared by coating hydrophilic polyvinyl alcohol on substrate membrane. Performance of the membrane was studied with substrate membrane of different properties, different concentrations of PVA and crosslinking solution, and different thicknesses of the surface layer etc. The results showed that PVA composite membrane could be formed by coating 5% PVA solution and 1% glutaraldehyde solution on the base membrane with cut-off molecular weight of 100 000.

直接甲醇燃料电池用磺化聚醚醚酮膜

李 磊 张 军 王宇新

关键词 聚醚醚酮（PEEK），质子电导率，甲醇透过性，直接甲醇燃料电池（DMFC）

制备了不同磺化度的磺化聚醚醚酮（SPEEK）膜。研究了 SPEEK 膜的质子电导率和甲醇透过性能与温度的关系。结果表明：温度高于 80 °C 时，SPEEK 膜的质子电导率超过 10−2 S/cm, 接近同等条件下的 Nafion® 115 膜。甲醇透过性能则比 Nafion® 115 膜低一个数量级。80 °C 时，SPEEK 膜的直接甲醇燃料电池性能优于 Nafion® 115 膜。

Sulfonated poly (ether ether ketone) membranes for direct methanol fuel cell

LI Lei ZHANG Jun WANG Yuxin

Keywords Poly(ether ether ketone) (PEEK), Proton conductivity, Methanol permeability, Direct methanol fuel cell (DMFC)

Sulfonated pol (ether ether ketone) (SPEEK) membranes with various degrees of sulfonation (DS) were prepared. Their proton conductivity and methanol permeability as a function of temperature were investigated. It was found that the proton conductivity of SPEEK membranes exceeded 10−2S/cm above 80℃, which is close to that of Nafion® 115 membrane under the same condition. The methanol permeability of SPEEK membranes was about an order of magnitude lower than that of Nafion® 115 membrane. The direct methanol fuel cell (DMFC) performance of the SPEEK membranes was better than that of Nafion® 115 membrane at 80℃.

高浓度酸性硅溶胶的制备技术

许念强 顾建祥 罗 康 郑松保

关键词 酸性硅溶胶, 稳定性, 研制

提供了一种制备高浓度、低黏度酸性硅溶胶的工艺方法, 研究了二氧化硅粒径大小对酸性硅溶胶的稳定性及黏度的影响作用, 得出要制备高浓度、低黏度酸性硅溶胶应先提高硅溶胶粒径的结论。

Preparation of acidic silicasol of high concentration

XU Nianqiang GU Jianxiang LUO Kang ZHENG Songbao

Keywords Acidic silica sol, Stability, Preparation

This study provides a method for preparing high concentration and low viscosity acidic silicasol. It was found that silicon particle size is very important for stability and viscosity of the acidic silicasol, and high concentration and low viscosity acidic silicasol should be prepared with silicasol of larger particle sizes.

二氧化硅粒径对酸性硅溶胶稳定性的影响

许念强 顾建祥 罗 康 郑松保

关键词 酸性硅溶胶，粒径，稳定性，二氧化硅

研究了不同条件下纳米二氧化硅粒径对酸性硅溶胶稳定性、粘度的影响。结果表明，随着二氧化硅粒径的增加，酸性硅溶胶的稳定性及粘度均得到较好的改善，提高纳米二氧化硅的粒径控制对制备高浓度、低粘度的酸性硅溶胶有十分重要的作用。

Effects of SiO_2 particle size on stability of acidic silicasol

XU Nianqiang GU Jianxiang LUO Kang ZHENG Songbao

Keywords Acidic silica sol, Grain diameter; Stability, Silicon dioxide

Relationships between stability and viscosity of acidic silicasol and particle size of nano SiO_2 was studies in different conditions. It was found that stability and viscosity of the silicasol improved with increasing size of the particles. And it is crucial to control the SiO_2 particle size in preparation of high concentration and low viscosity acidic silicasol.

大粒径纳米二氧化硅的制备技术

许念强 顾建祥 罗 康 郑松保

关键词 硅溶胶，纳米二氧化硅，大粒径，制备

介绍了一种制备大粒径、高浓度硅溶胶的工艺方法，研究了硅溶胶生产中影响纳米二氧化硅粒径的增长因素。结果表明，纳米二氧化硅粒径的平均大小、粒度分布受 pH 值、温度、杂质离子浓度等诸多因素的影响，控制条件处于最佳状态有利于二氧化硅粒径均匀提高。

Preparation of nano SiO_2 of large particle size

XU Nianqiang GU Jianxiang LUO Kang ZHENG Songbao

Keywords Silica sol, Nanon silicon dioxide, Large particle size, Preparation

Methods for preparing high concentration silicasol of large particle sizes was studied. Growth factors of nano SiO_2 particle size in preparation of silicasol were investigated. The results showed that particle's size and size distribution of the nano SiO_2 were affected by conditions of the pH value, temperature and salt concentration, which should be under optimum control for uniform growth of the SiO_2 size.

核技术开发和产业化

Industrial development in nuclear techniques at SINAP

上海应用物理研究所核技术产业化

上海应用物理研究所依托自身的学科和技术优势，积极发展以科技成果开发为基础的高技术产业。近两年来，在优化科技产业发展框架、加强与国内外知名企业合作、争取并推进国家发改委民用非动力核技术产业化专项、健全对企业经营者的激励约束机制等方面均取得了较大进展。

一、科技产业基本状况

截至 2004 年底，我所直接投资的科技企业共有 6 家：日环科技投资公司、日环仪器厂、日环光电仪器公司、辐射技术基地、实验工厂、特种变压器公司。另有日环科技投资公司控股（或参股）的企业 3 家：世龙科技公司、奥瑞恩诊断试剂公司、安盛科兴药业公司。企业的组织形式大多为有限责任公司，其中 2 家为中外合资（合作）企业。上述企业 2004 年底的总资产共约 1.7 亿元，净资产共约 1.3 亿元，，其中按股权比例属我所的净资产共约 6000 万元；从业人员共约 550 人，其中尚属我所事业编制的职工 181 人。9 家企业近两年实现年销售收入均近亿元，年利税总额 1000 余万元；主要产业方向为应用核仪器仪表、辐射改性高分子新材料和辐照装置及放射性药物等。

二、优化科技产业发展框架

近两年，我所为适应我国市场经济环境及大科学工程派生技术转化和知识创新成果的产业孵化，以业已形成的三个产业方向为主线，通过对有关企业的资产重组，调整和优化了科技产业的组织架构和布局，以提升我所科技企业的核心竞争力和技术创新能力。其中，完成的重要工作之一是于 2004 年 4 月将原上海核技术开发公司改制设立为上海日环科技投资有限公司，旨在为科技企业的进一步发展构建一个良好的资本运作平台，并使其重新发挥产业孵化器的作用。

三、加强与国内外知名企业合作

加强与国内外知名企业的合作，更多地利用社会资源（包括资金、先进的经营理念、管理人才和经验等），是进一步发展我所科技产业的有效途径。2003 年 12 月我们完成了将上海科兴药业公司部分股权转让并改制设立为中外合资安盛科兴药业有限公司的工作，为企业发展创造了良好条件。日环科技投资公司、世龙科技公司等也已经并将继续与多家知名企业洽谈合作事宜。

四、争取并推进国家发改委民用非动力核技术产业化专项项目

2004 年初，国家发展与改革委员会发布了《关于实施民用非动力核技术高技术产业化专项的公告》。我所积极组织世龙公司和日环科技投资公司，通过中科院分别申报了“辐射改性功能型高分子新材料产业化示范工程”和“辐射加工用新型电子加速器系列产业化示范工程”两个专项项目，均已被国家发改委作为专项的 2004 年第一批和第二批项目批准立项，并将分别获得国家相当的安排资金或资助额度。该两项目的实施，将大幅度提高我所辐射技术产业的整体创新水平和竞争力。

五、规范管理与完善激励机制

企业经营者积极进取与否是企业经营成败最关键、最重要的因素，因此，必须通过一定的制度安排，对经营者进行激励和约束。我所在初步建立对企业考核办法的基础上，2003 年又出台了《企业经营者年度薪酬管理指导意见》，在考核指标的选取、年度经营指标的确定、年薪的组成和水平、短期激励与长期激励的兼顾等方面逐步予以规范，通过激励机制的完善，促进经营者的积极性。同时通过企业自查、内部审计与社会审计结合、专项审计与年度审计结合、一年两次的经济分析等手段，找出企业经营及发展中存在的问题，监督和约束企业经营者的经营行为，努力构建规范经营的企业诚信体系，推进管理上台阶。

磺酸型阳离子交换膜的性能研究

俎建华[1] 吴明红[1] 邱士龙 姚思德 叶 寅

关键词 磺酸型阳离子交换膜，化学稳定性，热稳定性

通过辐照接枝法在高密度聚乙烯（HDPE）上引入磺酸基团，从而制备了一种强酸性阳离子交换膜。就所制备离子交换膜的热稳定及化学稳定性能进行了详细考察。结果表明，接枝膜上引入磺酸基团后抗氧化性能较仅含羧酸基团的离子交换膜有所提高，接枝膜的热稳定性较之接枝前稍差，热重分析表明，接枝后样品的成碳量较接枝前有相当大的提高，原因归结于表面接枝层对成碳过程有促进作用。由于接枝膜中 HDPE 组份的“结晶破坏”及接枝链对晶区的“稀释作用”综合影响，结晶度随着接枝率的升高而降低。

1 上海大学射线应用研究所

聚乙烯辐照接枝体系中添加金属盐对接技率的影响

俎建华[1] 吴明红[1] 叶 寅 姚思德 邱士龙

关键词 辐照接枝，添加剂，pH 效应，同离子效应

采用辐照接枝的方法, 在高密度聚乙烯（HDPE）上接枝丙烯酸（AA）和对苯乙烯磺酸钠（SSS）, 从而制备出了一种含羧酸基团和磺酸基团的阳离子交换膜。详细研究了接枝体系中引入添加剂醋酸钠或氯化钠对接枝率的变化规律。实验表明, 在预辐照接枝和共辐照接枝中, 当 AA 接技 PE 或 AA 与 SSS 共同接枝 PE 时, 强碱弱酸盐醋酸钠通过 pH 效应同离子效应对接枝率呈现复杂的影响, 而中性盐氯化钠经离子对效应显著提高接枝率。

1 上海大学射线应用研究所

Properties of cation-exchange membranes containing sulfonate groups

ZU Jianhua[1] WU Minghong[1] QIU Shilong YAO Side YE Yin

Keywords Cation-exchange membranes, Thermal stability, Chemical stability

Strong acid cation-exchange membranes were obtained by radiation grafting of acrylic acid (AA) and sodium styrene sulfonate (SSS) onto high-density polyethylene (HDPE). Thermal and chemical stability of the cation-exchange membranes was investigated. The effectiveness of sulfonate-containing films was conformed in inducing high resistance to oxidative degradation. Thermal stability of the

grafted HDPE was weaker than HDPE as detected by TGA . Char residue by TGA of the grafted HDPE is greater than that of HDPE. It shows that the branch chains including –SO_3Na and –COOH was grafted onto the backbone of HDPE, and thus give a catalytical impetus to the charring. Crystallinity of the grafted membranes decreased with increasing grafting yield of the membrane samples. Is is supposed that the decreased crystallinity is due to collective effects of the inherent crystallinity dilution by the amorphous grafted chains and disruption of spherulitic crystallites of the HDPE component.

1 Institute of Radiation Applications, Shanghai University

固相亲合素技术在游离甲状腺素免疫分析中的应用

宋世平　唐国忠　杨建忠

关键词　固相亲合素，游离甲状腺素，免疫分析

以亲和素-生物素分离技术为基础，尝试通过固化抗原（标记抗体）和固化抗体（标记抗原衍生物）两种免疫分析构型实现具有代表性的游离激素—游离甲状腺素（FT_4）的固相免疫分析测定。应用牛血清白蛋白-亲和素联接物制备固相亲和素，依次为基础制备固相生物素化甲状腺素衍生物和固相生物素化抗甲状腺素抗体，并分别用于标记抗体法和标记抗原衍生物法的 FT_4 免疫分析。考察方法的主要技术指标，得到了较为满意的结果：标准曲线的四参数非线性拟合度良好；标记抗体法测定的灵敏度为 0.42 pmol/L，批内批间的 CV.% 均小于 7%；标记衍生物法的灵敏度为 0.36 pmol/L，批内批间的 CV.%均小于 7%；两种方法相关性良好（r=0.9734，p<0.01）。通过应用固相亲和素固化抗原和固化抗体两种方式，进一步肯定了固相亲和素作为通用固相分离技术在免疫分析中的应用价值，为游离甲状腺素测定提供了一定实验依据，对游离激素检测进一步实现免疫分析自动化提供了一定的参考依据。

免疫微阵列同步多元分析系统的建立及其初步应用

宋世平　李 宾　王惠琼　胡 钧　李民乾

关键词　免疫微阵列，同步多元分析，肿瘤蛋白标志物

本研究建立了一种基于抗体微阵列芯片的用于多个生物样品同步检测的分析方法。通过制备条件实验，确定了抗体在微阵列芯片基片表面的多项固化条件；通过鉴定及应用条件实验，确定了抗体微阵列分析系统用于三种肿瘤标志蛋白检测的方法学技术指标。本分析系统体现了微阵列检测的高通量性、夹心免疫分析的高特异性和亲合素–生物素系统的高灵敏度。实验及结果分析表明，该系统具有较强的应用价值及开发潜力。

Radiation grafting of AA or SSS onto FEP films

WANG Hengdong YE Yin ZHANG Xuebing QIU Shilong

Keywords Poly (tetrafluoroethylene-co-hexafluoropropylene), Radiation grafting, Sodium styrene sulfonate

Poly (tetrafluoroethylene-co-hexafluoropropylene) (FEP) films were immersed in aqueous solution of acrylic acid (AA) or sodium styrene sulfonate (SSS), and were irradiated by ^{60}Co γ rays at 25℃. The effects of reaction time, irradiation dose, inhibitor and monomer concentration on the grafting yield were studied. Either grafting yield of AA or SSS onto FEP increased with irradiation dose, but showed some saturation at high doses and high monomer concentration. The grafting yields increased with reaction time at first but decreased with longer reaction times. Grafting SSS onto FEP was more difficult than AA. The grafted films were characterized by DSC and FT-IR.

Effects of metal salt additives on radiation grafting yield of high density polyethylene films

ZU Jianhua[1] WU Minghong[1] YE Yin YAO Side QIU Shilong

Keywords Radiation grafting, Additives, pH effect, The same ion effect

Acrylic acid (AA) and sodium styrene sulfonate (SSS) were grafted on to high density polyethylene films by 60Co γ-rays. In this way, ion exchange membranes with strong and weak acid groups were prepared. Effects of metal salt additives of sodium acetate and sodium chloride on grafting yield was studied. It was found that in either preirradiation method or simultaneous irradiation method sodium acetate, a salt with strong base and weak acid, has complex effects on grafting yield by pH effect and the same ion effect, whereas the addition of sodium chloride, which is neutral salt, helped increasing the grafting yield by ion pair effect.

1 Institute of Radiation Applications, Shanghai University

Simultaneous multianalysis for tumor markers by antibody fragments microarray system

SONG Shiping LI Bin HU Jun LI Minqian

Keywords Simultaneous multianalysis, Tumor marker, Antibody fragment, Microarray

It is often necessary to measure a spectrum of tumor markers in oncology. We have developed a simultaneous multiplexing immunoassay method to determine six tumor markers: α-fetoprotein (AFP),

carcinoma embryonic antigen (CEA), human chorionic gonadotropin beta (β-HCG), carbohydrate antigen 125 (CA 125), carbohydrate antigen 19—9 (CA 19—9), carbohydrate antigen 15—3 (CA 15—3). $F(ab')_2$ fragments of six capture antibodies were prepared and printed as microarrays on silylated slides to perform sandwich immunoassays with the use of an avidin-biotin system for amplified fluorescence signals. Each antigen with different concentrations was detected to assemble its calibration curve, and combinations of different markers were determined to examine the specificity of simultaneous detection based on the $F(ab')_2$ microarrays. Some clinical samples were analyzed to compare with results obtained with the use of Immunoradiometric assay (IRMA) method. Wide range calibration curve and its R value were obtained for each analyte. Calibration curves concentrations were 0—640μg/L for CEA, AFP and β-HCG, and were 0—1280kU/L for CA 125, CA 19—9 and CA15—3. The antibody fragments microarray system bears comparison with conventional immunoassays and may find feasible application in measurement of series markers in oncology and other areas of medicine.

附录 1

2003－2004 年科研人员赴港台及国外活动情况

1. 朱希恺，2003 年 2 月 16 日至 2003 年 2 月 23 日，赴日本（日本电通大学激光），参加合作研究（高电荷离子的产生和物理的研究）。
2. 蒋迪奎，2003 年 2 月 16 日至 2003 年 2 月 23 日，赴日本（日本电通大学激光），参加合作研究（高电荷离子的产生和物理的研究）。
3. 李亚虹，2003 年 2 月 16 日至 2003 年 2 月 23 日，赴日本（日本电通大学激光），参加合作研究（高电荷离子的产生和物理的研究）。
4. 郭盘林，2003 年 2 月 16 日至 2003 年 2 月 23 日，赴日本（日本电通大学激光），参加合作研究（高电荷离子的产生和物理的研究）。
5. 张桂林，2003 年 2 月 25 日至 3 月 19 日，赴韩国（Pohang 科技大学），参加合作研究（相反衬成像实验）。
6. 童永彭，2003 年 2 月 25 日至 3 月 19 日，赴韩国（Pohang 科技大学），参加合作研究（相反衬成像实验）。
7. 夏绍建，2003 年 3 月 1 日至 2003 年 3 月 24 日，赴日本（日本高能加速器研究所），参加合作研究（光学镜面精密测量技术研究）。
8. 戴志敏，2003 年 3 月 9 日至 3 月 15 日，赴日本（日本高能加速器研究），参加会议（加速器运行研讨会）。
9. 汪勇先，2003 年 3 月 15 日至 3 月 23 日，赴马来西亚（马来西亚核技术），参加合作研究（加速器放射性同位素生产合作研究）。
10. 夏绍建，2003 年 3 月 15 日至 4 月 7 日，赴日本（日本高能加速器研究），参加合作研究（光学镜精密测量技术研究）。
11. 张桂林，2003 年 3 月 24 日至 3 月 28 日，赴埃及（AI-Azhar 大学理学院），参加会议（第五次国际科学大会）。
12. 蔡翔舟，2003 年 3 月 30 日至 2003 年 6 月 30 日，赴美国（美国 Brookhaven 国家），参加合作研究（RHIC-STAR 国际合作项目研究）。
13. 肖体乔，2003 年 5 月 5 日至 5 月 4 日，赴意大利（意大利底里亚斯特），参加合作研究（硬 X 射线相衬成像的医学应用研究）
14. 沈文庆，2003 年 6 月 4 日至 6 月 11 日，赴美国（美国 Duke 大学），参加会议（第 17 届少体物理国际会议（FB17)）。
15. 沈文庆，2003 年 6 月 16 日至 6 月 22 日，赴俄罗斯（俄罗斯核研究联合），参加会议（第八届国际核-核碰撞会议）。
16. 张虎勇，2003 年 6 月 16 日至 6 月 22 日，赴俄罗斯（俄罗斯核研究联合），参加会议（第八届国际核-核碰撞会议）。
17. 尹端芷，2003 年 8 月 9 日至 8 月 15 日，赴澳大利亚（澳大利亚悉尼 ISRC 组织）。
18. 肖体乔，2003 年 9 月 7 日至 9 月 8 日，赴意大利（意大利底里亚斯特），参加合研（硬 X 射线相衬成像的医学应用研究）。
19. 赵振堂，2003 年 9 月 7 日至 9 月 13 日，赴日本（日本原子能研究所），参加会议（第 25 届自由电子激光国际会议及第 10 届自由电子激光用户）。

20. 戴志敏，2003 年 9 月 7 日至 9 月 13 日，赴日本（日本原子能研究所），参加会议（第 25 届自由电子激光国际会议及第 11 届自由电子激光用户）。
21. 韩家广，2003 年 9 月 23 日至 9 月 27 日，赴日本（东京大学电通研究所），参加会议（第 11 届 IEEE 太赫兹国际会议）。
22. 徐洪杰，2003 年 9 月 26 日至 10 月 3 日，赴韩国（浦项科技大学），考察（讨论双方合作事宜）。
23. 朱志远，2003 年 9 月 26 日至 10 月 3 日，赴韩国（浦项科技大学），考察（讨论双方合作事宜）。
24. 赵振堂，2003 年 9 月 26 日至 10 月 3 日，赴韩国（浦项科技大学），考察（讨论双方合作事宜）。
25. 李亚虹，2003 年 9 月 26 日至 10 月 3 日，赴韩国（浦项科技大学），考察（讨论双方合作事宜）。
26. 朱志远，2003 年 10 月 7 日至 10 月 19 日，赴德国（来比锡大学 Leipsion），访问（访问和商谈合作事宜）。
27. 徐洪杰，2003 年 10 月 7 日至 10 月 19 日，赴德国（来比锡大学 Leipsion），访问（访问和商谈合作事宜）。
28. 李　燕，2003 年 10 月 7 日至 10 月 19 日，赴德国（来比锡大学 Leipsion），访问（访问和商谈合作事宜）。
29. 巩金龙，2003 年 10 月 7 日至 10 月 19 日，赴德国（来比锡大学 Leipsion），访问（访问和商谈合作事宜）。
30. 郑丽芳，2003 年 10 月 12 日至 10 月 18 日，赴韩国（韩国 Pohang 加速器），参加会议（2003 国际加速器控制系统年会）。
31. 周　伟，2003 年 10 月 12 日至 10 月 18 日，赴奥地利（国际原子能结构），参加合作研究（用于诊断和治疗的放射性同位素的加速器生产的标准高束流）。
32. 周巧根，2003 年 10 月 19 日至 10 月 25 日，赴日本（日本高能加速器），参加会议（第 18 届国际磁铁技术会议）。
33. 蒋迪奎，2003 年 10 月 28 日至 11 月 12 日，赴日本（日本高能加速器研究），参加合作研究（SSRF 加速器和光束线的机器元件的研发）
34. 王志山，2003 年 10 月 28 日至 11 月 12 日，赴日本（日本高能加速器研究），参加合作研究（SSRF 加速器和光束线的机器元件的研发）。
35. 吴国忠，2003 年 11 月 8 日至 11 月 14 日，赴日本（日本明古屋大学），参加会议（第二届有关超临界流体在能源和环境方面的应用的国际会议）。
36. 李　燕，2003 年 11 月 11 日至 11 月 26 日，赴日本（日本高能加速器），参加合作研究（SSRF 加速器和光束线的机器元件的研发）。
37. 马余刚，2003 年 11 月 23 日至 12 月 4 日，赴日本（日本理化研究所），参加会议。
38. 叶恺容，2003 年 11 月 23 日至 12 月 8 日，赴日本（高能加速器研究机构），参加合作研究（SSRF 加速器和光束线的机器元件的研发）。
39. 谈明光，2003 年 11 月 27 日至 12 月 12 日，赴英国（美国热电公司在英国），参加会议（美国热电公司在英国举办的仪器技术研讨会）。
40. 丁建国，2003 年 12 月 4 日至 12 月 19 日，赴日本（日本高能加速器），参加合作研究（SSRF 加速器和光束线的机器元件的研发）。

41. 徐洪杰，2003 年 12 月 14 日至 12 月 27 日，赴日本（日本同步辐射研究所），考察（管理和同步辐射应用的合作）。
42. 陆晓峰，2003 年 12 月 14 日至 12 月 27 日，赴日本（日本同步辐射研究所），考察（管理和同步辐射应用的合作）。
43. 曹珊珊，2003 年 12 月 14 日至 12 月 27 日，赴日本（日本同步辐射研究所），考察（管理和同步辐射应用的合作）。
44. 周福根，2003 年 12 月 14 日至 12 月 27 日，赴日本（日本同步辐射研究所），考察（管理和同步辐射应用的合作）。
45. 何建华，2003 年 12 月 14 日至 12 月 27 日，赴日本（日本同步辐射研究所），考察（管理和同步辐射应用的合作）。
46. 贺战军，2003 年 12 月 14 日至 12 月 27 日，赴日本（日本同步辐射研究所），考察（管理和同步辐射应用的合作）。
47. 严培明，2003 年 12 月 14 日至 12 月 27 日，赴日本（日本同步辐射研究所），考察（管理和同步辐射应用的合作）。
48. 朱彬华，2003 年 12 月 14 日至 12 月 27 日，赴日本（日本同步辐射研究所），考察（管理和同步辐射应用的合作）。
49. 王 芳，2003 年 12 月 14 日至 12 月 27 日，赴日本（日本同步辐射研究所），考察（管理和同步辐射应用的合作）。
50. 张 岚，2004 年 1 月 1 日至 12 月 31 日，赴美国（美国斯坦福大学），参加合作研究（与放射性治疗分子影像相关的正电子发射放射性示踪剂）。
51. 吴国忠，2004 年 1 月 7 日至 1 月 13 日，赴印度（印度孟买 Bhabha），参加会议（第 7 届辐射化学与光化学会议）
52. 朱志远，2004 年 1 月 10 日至 1 月 17 日，赴美国（美国加州劳伦斯），参加会议（第 17 届超相对论性核-核碰撞-夸克物质 2004 国际会议）。
53. 沈文庆，2004 年 1 月 10 日至 1 月 17 日，赴美国（美国加州劳伦斯），参加会议（第 17 届超相对论性核-核碰撞-夸克物质 2005 国际会议）。
54. 马余刚，2004 年 1 月 10 日至 1 月 17 日，赴美国（美国加州劳伦斯），参加会议（第 17 届超相对论性核-核碰撞-夸克物质 2006 国际会议）。
55. 殷立新，2004 年 1 月 10 日至 1 月 17 日，赴日本（日本高能加速器），参加合作研究（SSRF 加速器和光束线的机器元件的研发）。
56. 蔡翔舟，2004 年 1 月 10 日至 1 月 17 日，赴美国（劳伦斯伯克莱国家），参加会议（第 17 届超相对论核-核碰撞（夸克物质 2004））。
57. 方海平，2004 年 2 月 1 日至 2 月 15 日，赴韩国（韩国浦项），参加会议（生物高分子和生物膜研讨会）。
58. 程卫星，2004 年 2 月 2 日至 3 月 12 日，赴日本（日本高能加速器），参加合作研究（SSRF 加速器和光束线的机器元件的研发）。
59. 陈 敏，2004 年 2 月 2 日至 3 月 8 日，赴日本（日本高能加速器），参加合作研究（SSRF 加速器和光束线的机器元件的研发）。
60. 张桂林，2004 年 2 月 8 日至 3 月 5 日，赴韩国（韩国浦项科技大学），参加合作研究（同步辐射实验）
61. 李 燕，2004 年 2 月 8 日至 3 月 5 日，赴韩国（韩国浦项科技大学），参加合作研究（参加同步辐射实验）。

62. 童永彭，2004 年 2 月 8 日至 3 月 5 日，赴韩国（韩国浦项科技大学），参加合作研究（参加同步辐射实验）。
63. 马国亮，2004 年 2 月 15 日至 5 月 15 日，赴美国（美国布鲁克海文国家），参加合作研究（REIC-STAR 有关飞行时间谱仪的电子学设计的实验）。
64. 方德清，2004 年 2 月 19 日至 4 月 21 日，赴日本（日本理化研究所），参加合作研究。
65. 朱志远，2004 年 3 月 6 日至 3 月 11 日，赴日本（日本九州大学），参加国际会议。
66. 沈文庆，2004 年 3 月 6 日至 3 月 11 日，赴日本（日本九州大学），参加国际会议。
67. 马余刚，2004 年 3 月 6 日至 3 月 11 日，赴日本（日本九州大学），参加国际会议。
68. 宋宏秋，2004 年 3 月 6 日至 3 月 11 日，赴日本（日本九州大学），参加国际会议。
69. 马余刚，2004 年 3 月 10 日至 4 月 21 日，赴日本（日本理化研究所），参加合作研究。
70. 沈文庆，2004 年 3 月 10 日至 4 月 21 日，赴日本（日本理化研究所），参加合作研究。
71. 蔡翔舟，2004 年 3 月 10 日至 4 月 21 日，赴日本（日本理化研究所），参加合作研究。
72. 徐洪杰，2004 年 3 月 15 日至 3 月 19 日，赴日本（The Saga Prefectural Government），参加国际会议。
73. 赵振堂，2004 年 3 月 15 日至 3 月 19 日，赴日本（The Saga Prefectural Government），参加国际会议。
74. 吴国忠，2004 年 3 月 15 日至 3 月 19 日，赴日本（The Saga Prefectural Government），参加国际会议。
75. 徐洪杰，2004 年 3 月 21 日至 3 月 27 日，赴韩国（韩国浦项大学，浦项加速器实验室）参加国际会议。
76. 赵振堂，2004 年 3 月 21 日至 3 月 27 日，赴韩国（韩国浦项大学，浦项加速器实验室）参加国际会议。
77. 李民熙， 2004 年 3 月 21 日至 3 月 27 日，赴韩国（韩国浦项大学，浦项加速器实验室）参加国际会议。
78. 张宇田，2004 年 3 月 21 日至 3 月 27 日，赴韩国（韩国浦项大学，浦项加速器实验室）参加国际会议。
79. 巢树煊，2004 年 3 月 21 日至 3 月 27 日，赴韩国（韩国浦项大学，浦项加速器实验室）参加国际会议。
80. 刘永好，2004 年 3 月 21 日至 3 月 27 日，赴韩国（韩国浦项大学，浦项加速器实验室）参加国际会议。
81. 刘桂民，2004 年 3 月 21 日至 3 月 27 日，赴韩国（韩国浦项大学，浦项加速器实验室）参加国际会议。
82. 周巧根，2004 年 3 月 21 日至 3 月 27 日，赴韩国（韩国浦项大学，浦项加速器实验室）参加国际会议。
83. 谷 鸣，2004 年 3 月 21 日至 3 月 27 日，赴韩国（韩国浦项大学，浦项加速器实验室）参加国际会议。
84. 李德明，2004 年 3 月 21 日至 3 月 27 日，赴韩国（韩国浦项大学，浦项加速器实验室）参加国际会议。
85. 顾 强，2004 年 3 月 21 日至 3 月 27 日，赴韩国（韩国浦项大学，浦项加速器实验室）参加国际会议。
86. 朱希恺，2004 年 3 月 22 日至 3 月 27 日，赴日本（日本电通大学），参加合作研究。

87 巩金龙，2004 年 4 月 1 日至 2005 年 3 月 31 日，赴日本（日本国家材料科学研究所，纳米实验室），参加合作研究。

88. 侯仁昌，2004 年 4 月 10 日至 4 月 25 日，赴德国，分院组织考察。

89. 蒋迪奎，2004 年 4 月 12 日至 4 月 20 日，赴日本，（日本电通大学）参加国际会议。

90. 郭盘林，2004 年 4 月 12 日至 4 月 20 日，赴日本，（日本电通大学）参加国际会议。

91. 骆玉宇，2004 年 4 月 18 日至 5 月 22 日，赴意大利（意大利国际物理中心），参加合作研究。

92. 宋宏秋，2004 年 5 月 1 日至 5 月 8 日，赴台湾（台湾中央研究院物理所），参加两岸会议。

93. 韩家广，2004 年 5 月 10 日至 8 月 5 日，赴日本（日本 KEK 物质结构研究所），参加合作研究。

94. 张春富，2004 年 5 月 18 日至 5 月 23 日，赴法国（法国 Ecole Normale Superieur de Lyon），参加国际会议。

95. 汪勇先，2004 年 5 月 18 日至 5 月 23 日，赴法国（法国 Ecole Normale Superieur de Lyon），参加国际会议。

96. 尹端沚，2004 年 5 月 18 日至 5 月 23 日，赴法国（法国 Ecole Normale Superieur de Lyon），参加国际会议。

97. 殷立新，2004 年 5 月 22 日至 5 月 28 日，赴法国（欧洲同步辐射装置（ESRF）），参加国际会议。

98. 王 晓，2004 年 5 月 22 日至 5 月 28 日，赴法国（欧洲同步辐射装置（ESRF）），参加国际会议。

99. 张元勋，2004 年 6 月 2 日至 6 月 9 日，赴斯洛文尼亚（Jezef Stefan Institute,Ljubljana, Slovenia），参加国际会议。

100. 魏 逊，2004 年 6 月 18 日至 6 月 17 日，赴日本（日本高能加速器研究机构（KEK）），参加合作研究。

101. 沈文庆，2004 年 6 月 26 日至 7 月 3 日，赴瑞典（瑞典哥德堡大学），参加国际会议。

102. 朱德彰，2004 年 6 月 27 日至 7 月 3 日，赴芬兰（赫尔辛基大学加速器实验室），参加国际会议。

103. 沈文庆，2004 年 7 月 3 日至 7 月 10 日，赴德国（德国 GSI），参加合作研究。

104. 徐洪杰，2004 年 7 月 4 日至 7 月 19 日，赴瑞士、法国（瑞士的 PSI 及法国的 SOLEIL）参加国际会议/访问。

105. 赵振堂，2004 年 7 月 4 日至 7 月 19 日，赴瑞士、法国（瑞士的 PSI 及法国的 SOLEIL）参加国际会议/访问。

106. 童永彭，2004 年 7 月 5 日至 2005 年 7 月 5 日，赴德国（德国 Leipzig 大学），参加合作研究。

107. 邰仁忠，2004 年 7 月 9 日至 7 月 14 日，赴日本（东京学芸大学（Tokyo Gakugei Uiversity）），参加合作研究。

108. 殷立新，2004 年 7 月 12 日至 7 月 25 日，赴日本（日本高能加速器研究机构（KEK））参加合作研究。

109. 陈 楚，2004 年 7 月 12 日至 7 月 26 日，赴日本（日本高能加速器研究机构（KEK））参加合作研究。

110. 杨 珩，2004 年 7 月 12 日至 7 月 27 日，赴日本（日本高能加速器研究机构（KEK））参加合作研究。
111. 孙 森，2004 年 7 月 12 日至 7 月 28 日，赴日本（日本高能加速器研究机构（KEK））参加合作研究。
112. 朱志远，2004 年 8 月 1 日至 8 月 9 日，赴日本（日本高能加速器研究机构（KEK））参加合作研究。
113. 钟 晨，2004 年 8 月 16 日至 8 月 22 日，赴日本（日本东京大学），参加科学研究生院核研究中心 国际会议。
114. 魏义彬，2004 年 8 月 16 日至 8 月 22 日，赴日本（日本东京大学），参加科学研究生院核研究中心 国际会议。
115. 李勇平，2004 年 8 月 21 日至 9 月 4 日，赴英国（英国机器视觉协会（BMVA）），参加国际会议。
116. 马余刚，2004 年 8 月 22 日至 8 月 30 日，赴捷克（第 18 届欧洲物理学会的国际核物理会议），参加国际会议。
117. 徐洪杰，2004 年 8 月 22 日至 8 月 31 日，赴日本（日本 Spring-8, KEK），参加束线研讨会。
118. 何建华，2004 年 8 月 22 日至 8 月 31 日，赴日本（日本 Spring-9, KEK），参加束线研讨会。
119. 肖体乔，2004 年 8 月 22 日至 8 月 31 日，赴日本（日本 Spring-10, KEK），参加束线研讨会。
120. 夏绍建，2004 年 8 月 22 日至 8 月 31 日，赴日本（日本 Spring-11, KEK），参加束线研讨会。
121. 余笑寒，2004 年 8 月 22 日至 8 月 31 日，赴日本（日本 Spring-12, KEK），参加束线研讨会。
122. 郜仁忠，2004 年 8 月 22 日至 8 月 31 日，赴日本（日本 Spring-13, KEK），参加束线研讨会。
123. 朱卫华，2004 年 8 月 22 日至 8 月 31 日，赴日本（日本 Spring-14, KEK），参加束线研讨会。
124. 王纳秀，2004 年 8 月 22 日至 8 月 31 日，赴日本（日本 Spring-15, KEK），参加束线研讨会。
125. 柳 义，2004 年 8 月 22 日至 8 月 31 日，赴日本（日本 Spring-16, KEK），参加束线研讨会。
126. 陈 陶，2004 年 8 月 22 日至 8 月 31 日，赴日本（日本 Spring-17, KEK），参加束线研讨会。
127. 李民熙，2004 年 8 月 25 日至 9 月 3 日，赴日本（日本日新高压株式会社（NHV Corporation）），考察访问。
128. 张海荣，2004 年 8 月 25 日至 9 月 3 日，赴日本（日本日新高压株式会社（NHV Corporation）），考察访问。
129. 盛康龙，2000 年 8 月 25 日至 9 月 3 日，赴日本（日本日新高压株式会社（NHV Corporation）），考察访问。
130. 张宇田，2004 年 8 月 25 日至 9 月 3 日，赴日本（日本日新高压株式会社（NHV Corporation）），考察访问。

131. 尹端沚，2004 年 9 月 9 日至 9 月 20 日，赴加拿大（第五届放射性卤素国际研讨会（加拿大 TRIUMF)），参加国际会议。
132. 周 伟，2004 年 9 月 9 日至 9 月 20 日，赴加拿大（第五届放射性卤素国际研讨会（加拿大 TRIUMF)），参加国际会议。
133. 孙立涛，2004 年 9 月 10 日至 9 月 18 日，赴意大利（Riva dek Garda, Trentino, Italy），参加国际会议。
134. 马余刚，2004 年 9 月 13 日至 9 月 22 日，赴南非（第届“夸克物质中的奇异性”国际会议），参加国际会议。
135. 田文栋，2004 年 9 月 20 日至 12 月 19 日，赴意大利（意大利南方国家实验室），参加合作研究。
136. 郜仁忠，2004 年 9 月 21 日至 9 月 26 日，赴意大利（意大利的 Trieste），参加国际会议。
137. 朱智勇，2004 年 9 月 24 日至 10 月 1 日，赴比利时（第 6 届电离辐射与聚合物国际会议），参加国际会议。
138. 顾 强，2004 年 9 月 25 日至 10 月 17 日，赴日本（日本高能加速器研究机构（KEK)），参加合作研究。
139. 陆晓峰，2004 年 9 月 29 日至 10 月 10 日，赴荷兰（X-Flow Corporation），考察。
140. 梁国明，2004 年 9 月 29 日至 10 月 10 日，赴荷兰（X-Flow Corporation），考察。
141. 张春富，2004 年 10 月 2 日至 10 月 31 日，赴德国（德国 Forschungszentrum Rossendorf），参加合作研究。
142. 于成浩，2004 年 10 月 2 日至 10 月 8 日，赴瑞士（瑞士 CERN 第 8 届加速器准直测量国际会议），参加国际会议。
143. 殷重先，2004 年 10 月 12 日至 11 月 15 日，赴日本（日本高能加速器研究机构（KEK)），参加合作研究。
144. 夏汇浩，2004 年 11 月 1 日至 11 月 7 日，赴意大利（意大利 Frascati (Rome)国家实验室），参加国际会议。
145. 殷立新，2004 年 11 月 13 日至 11 月 28 日，赴加拿大（Canadian Light Source Inc.），参加合作研究。
146. 戴志敏，2004 年 11 月 13 日至 11 月 28 日，赴加拿大（Canadian Light Source Inc.），参加合作研究。
147. 王 芳，2004 年 11 月 13 日至 11 月 28 日，赴加拿大（Canadian Light Source Inc.），参加合作研究。
148. 许皆平，2004 年 11 月 13 日至 11 月 28 日，赴加拿大（Canadian Light Source Inc.），参加合作研究。
149. 唐 琳，2004 年 11 月 14 日至 2005 年 2 月 15 日，赴美国（Brookhaven Natinal Laboratory），参加合作研究。
150. 许浒江，2004 年 11 月 15 日至 11 月 21 日，赴日本（日本 Spring-8），参加国际会议。
151. 方克明，2004 年 11 月 15 日至 11 月 21 日，赴日本（日本 Spring-8），参加国际会议。
152. 蔡建华，2004 年 11 月 15 日至 11 月 21 日，赴日本（日本 Spring-8），参加国际会议。
153. 沈文庆，2004 年 11 月 1 日至 11 月 7 日，赴日本（日本理化所），参加合作研究。
154. 李文新，2004 年 11 月 21 日至 11 月 25 日，赴香港（香港大学），参加国际会议。
155. 朱德彰，2004 年 11 月 21 日至 11 月 25 日，赴香港（香港大学），参加国际会议。
156. 樊春海，2004 年 11 月 21 日至 11 月 25 日，赴香港（香港大学），参加国际会议。

157. 郭晓冬，2004 年 11 月 23 日至 12 月 6 日，赴澳大利亚（院组织的赴德国财务管理培训），培训班。

158. 顾 强，2004 年 11 月 30 日至 12 月 13 日，赴日本（日本高能加速器研究机构（KEK）），参加合作研究。

159. 徐洪杰，2004 年 12 月 5 日至 12 月 14 日，赴日本（日本理化所、东京大学等），考察访问。

160. 赵振堂，2004 年 12 月 5 日至 12 月 14 日，赴日本（日本理化所、东京大学等），考察访问。

161. 朱志远，2004 年 12 月 6 日至 12 月 16 日，赴澳大利亚（BOOMERANG 同步辐射机构），考察访问。

162. 黄 敏，2004 年 12 月 6 日至 12 月 16 日，赴澳大利亚（BOOMERANG 同步辐射机构），考察访问。

163. 沈竹林，2004 年 12 月 6 日至 12 月 16 日，赴澳大利亚（BOOMERANG 同步辐射机构），考察访问。

164. 刘德康，2004 年 12 月 7 日至 12 月 12 日，赴日本（日本高能加速器研究机构（KEK）），参加国际会议。

165. 严培明，2004 年 12 月 16 日至 12 月 24 日，赴英国（Diamond LightSource Limited），考察访问。

166. 张福余，2004 年 12 月 16 日至 12 月 24 日，赴英国（Diamond LightSource Limited），考察访问。

167. 金伯良，2004 年 12 月 16 日至 12 月 24 日，赴英国（Diamond LightSource Limited），考察访问。

168. 李德明，2004 年 12 月 16 日至 12 月 24 日，赴英国（Diamond LightSource Limited），考察访问。

169. 王纳秀，2004 年 12 月 31 日至 2005 年 3 月 31 日，赴法国（欧洲同步辐射装置（ESRF）），参加合作研究。

附录 2

2003—2004 年度港台和外国学者来访情况

1. 赵玉民，日本 saitama 大学物理系，2003 年 1 月 21 日，
2. Akira Kira，SPring-8，2003 年 3 月 20 日至 2 月 22 日，签署合作协议。
3. Hideo Ohno，SPring-8，2003 年 3 月 20 日至 2 月 22 日，签署合作协议。
4. Haruo Ohkuma，SPring-8，2003 年 3 月 20 日至 2 月 22 日，签署合作协议。
5. Wataru Matsumoto，SPring-8，2003 年 3 月 20 日至 2 月 22 日，签署合作协议。
6. 冷用斌，美国 BNL 国家实验室，2003 年 2 月 17 日，
7. S. Ohtani，东京电气通讯大学激光研究所，2003 年 2 月 25 日至月 1 日，来所
8. Kobayashi，日本 KEK，2003 年 3 月 3 日至 3 月 5 日，
9. Ohsumi，日本 KEK，2003 年 3 月 3 日至 3 月 5 日，
10. Shinichi Kurokawa，日本 KEK，2003 年 3 月 17 日至 3 月 20 日，
11. Noboru Yamamoto，日本 KEK，2003 年 3 月 17 日至 3 月 20 日，
12. Kenji Hosoyama，日本 KEK，2003 年 3 月 17 日至 3 月 20 日，
13. Kaiichi Haga，日本 KEK，2003 年 3 月 17 日至 3 月 20 日，
14. Masao Kuriki，日本 KEK，2003 年 3 月 17 日至 3 月 20 日，
15. Masayuki Tsukada，日本 KEK，2003 年 3 月 17 日至 3 月 20 日，
16. Takeshi Saiki，日本 KEK，2003 年 3 月 17 日至 3 月 20 日，
17. Hiroshi Fukuda，日本 KEK，2003 年 3 月 17 日至 3 月 20 日，
18. Furuta，日本 KEK，2003 年 3 月 17 日至 2003 年 3 月 20 日，
19. Behect Alpat，意大利 Perugia INFA，2003 年 3 月 22 日至 3 月 25 日,
20. Prof. Behect Alpat，意大利 Perugia INFN，2003 年 3 月 24 日，
21. 安腾正海，日本 KEK，2003 年 3 月 31 日至 2003 年 4 月 1 日，
22. 张小威，日本 KEK，2003 年 3 月 31 日，
23. Dr. Geary Eppley，美国 Rice University, Texas, 2003 年 9 月 26 日，
24. 黄志戎，斯坦福直线加速器中心，2003 年 10 月 27，
25 Dr.Olexander.L. Fainchtein，乌克兰哈尔科夫钢铁能源研究设计院，2003 年 11 月 18 日，来所
26. A.S.Savenkov，乌克兰哈尔科夫钢铁能源研究设计院，2003 年 11 月 18 日，
27. Prof. Keiichiro Nasu，日本 KEK，2003 年 2003 年 12 月 11 日至 12 月 12 日，来所
28. 陈景升，新加坡 ASTAR-DSI 研究所，2003 年 11 月 21 日，
29. Masayuki Kumada(熊田雅之)，日本加速器物理工学部放射医学研究所，2003 年 12 月 16 日，
30. M. Ando，日本 KEK，2004 年 2 月 12 日至 2004 年 3 月 5 日，上海光源合作研究（SSRF 应用合研、SSRF 光束线站设计）。
31. Gerasimenko N.N，Russia，2004 年 3 月 9 日，上海光源合作研究（国际会议）。

32. Yasunori Tanimoto，日本 KEK PF，2004 年 2 月 28 日至 3 月 6 日，上海光源合作研究（真空控制系统）。
33. H.Mastumoto，日本 KEK，2004 年 5 月 16 日至 5 月 22 日，上海光源合作研究（100MeV 直线加速器调制器的调试试验）。
34. H. Baba，日本 KEK，2004 年 5 月 16 日至 2004 年 5 月 22 日，上海光源合作研究（100MeV 直线加速器调制器的调试试验）。
35. Yoshihiko Hatano，日本 东京技术研究所 2004 年 2 月 24 日至 2 月 28 日，来所学术交流（做了两场报告）
36. 余理华，美国 Brookhaven National Lab（BNL），2004 年 3 月 25 日至 4 月 9 日，HGHG FEL。
37. Bernd Johannsen，德国 FZR，2004 年 4 月 24 日至 4 月 28 日，商议合作（签订合作协议）。
38. Wolfhard Moeller，德国 FZR，2004 年 4 月 24 日至 4 月 28 日，商议合作（签订合作协议）。
39. Gert Bernhard，德国 FZR，2004 年 4 月 24 日至 4 月 28 日，商议合作（签订合作协议）。
40. Jean Peter，法国 法国科研中心，2004 年 5 月 4 日至 5 月 5 日，2004 年 5 月 9 日至 2004 年 5 月 12 日，学术交流（参加有关物理学术会议）。
41. 李宝安，美国 阿肯色州立大学，2004 年 5 月 8 日至 5 月 10 日，
41. Tadashi Matsushita，日本 KEK PF 所长，2004 年 5 月 10 日至 5 月 11 日，学术交流（discuss the design of SSRF）。
42. Zhang Xiaowei，日本 KEK PF， 2004 年 5 月 10 日至 5 月 11 日，学术交流（discuss the design of SSRF）。
43. Shunji Goto，SPring-8，2004 年 5 月 10 日至 5 月 11 日，学术交流（discuss the design of SSRF）。
44. Jeff Wang，美国 John Hopkins University，2004 年 4 月 20 日至 4 月 22 日，商议合作。
45. Vincent Serrano Guerra，法国，2004 年 4 月 2 日至 4 月 6 日，合作研究。
46. 李济晨，英国 曼彻斯特大学，2004 年 2 月 5 日至 2 月 6 日，商议合作。
47. Tadashi Matsushita，日本 Core-university ，2004 年 6 月 18 日至 6 月 20 日，商议合作。
48 YORIKIYO NAGASHIMA，日本 Core-university，2004 年 6 月 18 日至 6 月 20 日，商议合作。
49. TOSHIAKI OTA，日本 Core-university，2004 年 6 月 18 日至 6 月 20 日，商议合作。
50. AKIRA NODA，日本 Core-university ，2004 年 6 月 18 日至 6 月 20 日，商议合作。
51. TATSUYA TSUJI，日本 Core-university ，2004 年 6 月 18 日至 6 月 20 日，商议合作。
52. SHINICHI KUROKAWA，日本 Core-university ，2004 年 6 月 18 日至 6 月 20 日，商议合作。
53. SAKAE UCHIKOSHI，日本 Core-university ，2004 年 6 月 18 日至 6 月 20 日，商议合作。

54. SHINJI IWAMI，日本 Core-university ，2004 年 6 月 18 日至 6 月 20 日，商议合作。
55. HIDEAKI YAMAGUCHI， JSPS，日本 Core-university ，2004 年 6 月 18 日至 6 月 20 日，商议合作。
56. James K.Gimzewski，英国 加州大学洛杉矶分校，2004 年 5 月 26 日至 2004 年 5 月 30 日，学术交流。
57. Kazumichi Namikawa，日本 东京学芸大学，2004 年 5 月 30 日至 6 月 1 日，上海光源学术交流。
58. Robert M. Sweet，美国 Brookhaven National Lab，2004 年 6 月 10 日至 6 月 12 日，上海光源学术交流。
59. 黄焕中，美国 加州大学洛杉矶分校，2004 年 6 月 21 日至 7 月 8 日，合作研究。
60. Leo W. M. Lau，香港 香港大学，2004 年 6 月 20 日至 6 月 21 日，商议合作。
61. SP Wong，香港 香港大学，2004 年 6 月 20 日至 6 月 21 日，商议合作。
62. Robert Hettel，美国 SLAC，2004 年 6 月 22 日至 6 月 27 日，
63. 翁武忠，美国 BNL，2004 年 6 月 18 日至 7 月 3 日，
64. 高杰，法国 国家研究中心直线加速器实验室，2004 年 6 月 23 日至 6 月 26 日，上海光源合作研究。
65. Eckoldt Hans-joerg，德国 DESY，2004 年 6 月 14 日至 2004 年 6 月 17 日，上海光源学术交流。
66. 赵际勇（中国），美国 APS，2004 年 7 月 1 日至 2004 年 7 月 2 日，上海光源学术交流。
67. T. Mukherjee，印度 Bhabha 原子能研究所，2004 年 10 月 21 日至 10 月 28 日，学术交流（参加中国辐射化学学会第七届年会）
68. Hama，日本 早稻田大学，2004 年 10 月 21 日至 10 月 2 日，学术交流（参加中国辐射化学学会第七届年会）。
69. Washio，日本 早稻田大学，2004 年 10 月 21 日至 10 月 2 日，学术交流（参加中国辐射化学学会第七届年会）。
70. Katsumura，日本 东京大学，2004 年 10 月 21 日至 10 月 2 日，学术交流（参加中国辐射化学学会第七届年会）。
71. 台安，美国 加州大学洛杉矶分校，2004 年 7 月 19 日至 7 月 22 日，合作研究 Kazutoshi
72. Suzuki，日本 NationalInstitute of Radiological Sciences，2004 年 9 月 19 日至 9 月 21 日，
73. 学术交流（参加第六届中日双边放射性药物化学研讨会）。
74. J.Rafelski，美国 Arizona 大学，2004 年 8 月 18 日至 8 月 20 日，学术交流。
75. 王新年，美国 LBL，2004 年 8 月 17 日至 8 月 20 日，学术交流（考察访问）。张琳，
76. 法国 ESRF，2004 年 8 月 12 日至 8 月 16 日，上海光源合作研究。
77. James Joseph Sebek，美国 SLAC，2004 年 10 月 28 日至 11 月 8 日，上海光源合作研究。
78. Jung Ho Je，韩国 浦项科技大学，2004 年 9 月 24 日至 9 月 7 日，学术交流。Bruce
79. Hamilton，英国 曼切斯特科技研究所，2004 年 7 月 17 日，上海光源学术交流。

80. Sugiyama，日本 Ritsumeikan 大学 2004 年 7 月 12 日至 7 月 14 日，上海光源学术交流。

81. 黄厚诚，英国 Diamond Light Source，2004 年 9 月 16 日至 9 月 18 日，上海光源学术交流。

82. Alam J. Heeger，美国 加州大学 Santa Barbara，2004 年 10 月 8 日，学术交流。

83. Derun Li 李德润，美国 Lawrence Berkeley，2004 年 9 月 18 日至 9 月 22 日，上海光源学术交流。

84. John Byrd，美国 Lawrence Berkeley，2004 年 9 月 18 日至 9 月 22 日，上海光源学术交流。

85. Robert Hettel，美国 SLAC，2004 年 8 月 25 日至 8 月 28 日，上海光源合作研究（SSRF 初步设计报告预审会）。

86. Nu Xu （许怒），美国 Lawrence Berkely National Lab，2004 年 10 月 21 日至 10 月 22 日，学术交流。

87. Howard HU（胡浩川），美国 美国宾州大学，2004 年 7 月 3 日至 2004 年 7 月 5 日，学术交流。

88. Yuehong Qian（钱跃弘）中国，美国 美国普林斯顿大学，2004 年 8 月 10 日至 8 月 18 日，商议合作。

89. Philip L. Gardner，加拿大 TRIUMF，2004 年 10 月 22 日，学术交流。

90. Jochen Schneider，德国 Deutsches Elektronen-Synchrotron，2004 年 10 月 14 日至 2004 年 10 月 17 日，上海光源学术交流。

91. Hermann Franz，德国 Deutsches Elektronen-Synchrotron，2004 年 10 月 14 日至 10 月 17 日，上海光源学术交流。

92. Seiichi Tagawa，日本大阪大学，2004 年 10 月 21 日至 10 月 24 日，学术交流。（参加 6th 辐射研究与辐射工艺学会）。

93. Geary Eppley，美国 Rice University，2004 年 10 月 22 日，合作研究（ RHIC-STAR 飞行时间探测器的讨论）。

94. Kiman Ha，韩国 Pohang Accelerator Laboratory，2004 年 11 月 17 日至 11 月 19 日，上海光源合作研究（数字电源技术交流）。

95. Ponciano Rodriguez，美国 SLAC，2004 年 10 月 14 日至 10 月 17 日，上海光源合作研究（讨论 SSRF 接地系统）。

96. Toshio Kasuga，日本 KEK，2004 年 11 月 15 日至 2004 年 11 月 17 日，上海光源合作研究（Core-Uni.计划及 05/2 筑波研讨会）。

97. Kawata，日本 KEK，2004 年 11 月 15 日至 11 月 17 日，上海光源合作研究（Core-Uni.计划及 05/2 筑波研讨会）。

98. Mitsuhashi，日本 KEK，2004 年 11 月 15 日至 11 月 17 日，上海光源合作研究 Core-Uni.计划及 05/2 筑波研讨会）。

99. James Clendenin，美国 SLAC acce. Department，2004 年 11 月 27 日至 11 月 30 日，上海光源合作研究（报告 SLAC 电子源、注入器等）。

100. 黄焕中，美国 美国 UCLA ，2004 年 12 月 9 日至 12 月 14 日，学术交流（访问有关 STAR 合作单位）。

101. Qian Yuehong，美国 普林斯顿大学，2004 年 8 月 5 日至 9 月 13 日，学术交流（工作）。

102. 黄焕中，美国 普林斯顿大学，2004 年 8 月 5 日至 9 月 13 日，学术交流（工作）。

103. Christopher Gough，瑞士 SLS，2004 年 11 月 27 日至 11 月 30 日，讨论 SSRF 注入引出脉冲磁铁设计，

104. Hiroshi OGAWA，日本 Saga University，2004 年 12 月 15 日，讨论合作并签署协议。

105. Masao KAMADA，日本 Saga University，2004 年 12 月 15 日，讨论合作并签署协议。

106. Qixin GUO，日本 Saga University，2004 年 12 月 15 日，讨论合作并签署协议。

107. Toru TANAKA，日本 Saga University，2004 年 12 月 15 日，讨论合作并签署协议。

108. Makoto WATANABE，日本 Saga University，2004 年 12 月 15 日，讨论合作并签署协议。

109. Dr.John Warren，英国 SRS 2004 年 12 月 22 日，学术交流

110. Dr.Ralph Eichler，瑞士 PSL 所长，2004 年 10 月 8 日至 10 月 11 日，讨论合作并签署协议。

111. 19 人，“QCD 和 RHIC 物理”国际研讨会。

112. 15 人，“纳米结构与粒子束的相互作用”国际研讨会。

113. M.Ando，日本 KEK，2004 年 12 月 18 日至 12 月 19 日，东方论坛。

114. K.Hyodo, 日本 PF，2004 年 12 月 18 日至 12 月 19 日，东方论坛。

115. 渡边诚，日本 佐贺大学，2004 年 12 月 18 日至 12 月 19 日，东方论坛。

116. 邓昌黎，美国 APS，2004 年 7 月 1 日至 7 月 2 日，学太交流（04 加速器物理卫星会议）

附录 3

2003-2004 年所内举办的学术报告会

序号	报告题目	报告人	报告时间
1	Asymptotic behavior of many-body systems by jmax-th pairing interaction	赵玉民(日本 saitama 大学物理系)	2003 年 1 月 20 日
2	Net charge fluctuation and QGP phase transition	萨本豪 研究员(中国原子能研究院)	2003 年 2 月 18 日
3	离子束分析及应用	王铁山副研究员(德国 Rossendorf 核研究中心)(EU-LSF)	2003 年 2 月 19 日
4	H absorption and diffusion in Pd/Ag alloys by DFT calculations	柯学志 博士(Technical University of Eindhoven Netherland)	2003 年 2 月 19 日
5	Influence of the Pauli principal on the dynamics of the Quark-Gluon Plasma	萨本豪 研究员(中国原子能研究院)	2003 年 2 月 20 日
6	强磁场科学和技术	高秉钧 研究员(中科院等离子体物理研究所)	2003 年 2 月 21 日
7	流变技术在材料研发中的应用	姚明龙 博士(美国 TA 公司亚太区)首席技术专家	2003 年 3 月 3 日
8	有限核系统液气相变的实验证据	马余刚 研究员	2003 年 3 月 7 日
9	AMS02 介绍	Prof. Behect Alpat Perugia INFN(意大利)	2003 年 3 月 24 日
10	2003 SINAP 纳米科学学术研讨会	胡钧等	2003 年 4 月 2-3 日
11	Theory and Applications of the Lattice Boltzmann Method (A new computational fluid mechanics)	Prof. YueHong Qian (Department of mechanics and aerospace, Princeton University, USA)	2003 年 4 月 15 日
12	1.Feeling of Cleveland; 2.Radioactive microspheres for cancer therapy.	于俊峰 博士	2003 年 4 月 16 日
13	2003 SINAP T-ray 应用研究研讨会	余笑寒等	2003 年 5 月 27-28 日
14	合成聚合物纳米结构材料的新途径	陈道勇 副教授(复旦大学高分子系)	2003 年 7 月 15 日
15	1. ICP-MS 应用 2. SEM 应用	1.谈明光 研究员 2.巩金龙 研究员	2003 年 7 月 15 日
16	Neutron Scattering in Europe and USA	李济晨 博士(Department of Physics, UMIST，England)	2003 年 7 月 24 日

序号	报告题目	报告人	报告时间
17	1.植物修复与植物过滤技术兼谈先进核分析技术在其中的应用 2.植物对放射性铯的吸收及其研究意义	唐世荣 教授(浙江大学)	2003 年 8 月 26 日
18	放射性药物研究进展	项景德 所长(江苏省原子医学研究所)	2003 年 9 月 3 日
19	磁性纳米线的 Mossbauer 研究	薛德胜 教授(兰州大学)	2003 年 9 月 18 日
20	中科院网络文献资源和服务内容介绍	杨械 副研究员(上海生命科学信息中心信息服务部主任)	2003 年 9 月 25 日
21	RICH-STAR Time of Flight (TOF) Project	Dr.GearyEppley (Rice University, Texas, USA)	2003 年 9 月 26 日
22	碲锌镉[CZT]材料及探测器	Dr. 李陇遐 Yinnel Tech Inc.	2003 年 9 月 29 日
23	关于新材料的计算物理研究	杨金龙 教授(中科大选键化学重点实验室) 龚新高 教授(复旦大学)	2003 年 10 月 20 日
25	1.The status of the LCLS projects 2.The properties of high-gain FELs 3.Towards to the fs FEL	黄志戎 教授(斯坦福直线加速器中心)	2003 年 10 月 27 日
24	万方数据资源系统介绍	庞来福 副总经理 (北京万方数据股份有限公司上海分公司)	2003 年 10 月 29 日
25	天然高分子材料改性	刘强 研究员(加拿大农业部食品科学研究中心)	2003 年 10 月 28 日
26	1.GLAUB 理论及应用 2.THz 研究介绍	赵耀林 博士 韩家广 硕士	2003 年 11 月 6 日
27	1.身份生物识别—从概念创新到技术实现 2.加速器的 PLC 控制	李勇平 研究员 龚培荣 副研究员	2003 年 11 月 12 日
28	High Anisotropy Perpendicular Recording Media and Cluster Beam Synthesized Nanostructured Meterials	陈景升博士(新加坡 ASTAR-DSI 研究所)	2003 年 11 月 21 日
29	表面活性剂在流体的行为模拟	陈煜 副教授(东京大学工学部，量子工程与系统科学系)	2003 年 11 月 20 日
30	The Max-Planck Institute Nuclear Physics: Current Research and Future Perspectives	Joachim Ullrich 教授(德国马普核物理所所长)	2003 年 12 月 5 日
31	高解析度电子显微学研究	杨奇斌 教授(湘潭大学现代物理研究所)	2003 年 12 月 3 日

序号	报告题目	报告人	报告时间
32	Theory for Photo-induced phase transition	Prof. Keiichiro Nasu, KEK, Japan	2003 年 12 月 11 日
33	Theory for Angle resolved photo-emission spectra	Prof. Keiichiro Nasu, KEK, Japan	2003 年 12 月 12 日
34	纳米尺度生物分子结构与电子传递研究及其在生物传感器中的应用	樊春海 博士(美国加州大学圣巴巴拉分校)	2004 年 1 月 2 日
35	生物信息学研究进展	盛其铮 (比利时鲁汶大学)	2004 年 1 月 16 日
36	快速老化模型小鼠 SAMP98 血清蛋白质组研究	郭淑杰 博士后(北京军事医药科学院毒物药物研究所)	2004 年 1 月 14 日
37	水和氢键	李济晨(英国曼彻斯特大学物理系)	2004 年 2 月 6 日
38	X 射线成像研讨会	安藤正海 教授等(日本 KEK)	2004 年 2 月 20 日
39	FADD 蛋白与细胞增殖的关系研究	华子春 教授(南京大学医药生物技术国家重点实验室主任、生命科学院副院长)	2004 年 2 月 24 日
40	1.Aspects of Recent Synchrotron Radiation Research and Facilities in the World 2. Photon Interactions with Matter-Ionization, Excitation, and Dissociation of Molecules	Prof. Y. Hatano(东京工业大学名誉教授)	2004 年 2 月 25 日
41	The experimental and theoretical study on sequence-dependent DNA structure	蔡禄 教授(内蒙古科技大学生命科学学院)	2004 年 3 月 3 日
42	1.核分析技术应用进展 2.有机卤族污染物的核分析研究	柴之芳 研究员(中国科学院高能所) 相馆	2004 年 3 月 24 日
43	材料芯片——进展与挑战	项晓东 博士(斯坦福研究所高级研究员、材料芯片发明人)	2004 年 3 月 25 日
44	高增益自由电子激光物理及实验	余理华 高级研究员(美国布鲁克海文国家实验室)	2004 年 3 月 29 日
45	上海市核学会核物理专业委员会 2004 SINAP 学术会议	Prof. Jean Peter IN2P3/ CNRS, (法国科研中心) Prof. Bao-An LiArkansas State University, USA 马余刚等	2004 年 5 月 10 日
46	日本高能物理研究所 (KEK) 光子工厂(PF)目前进展情况	Tadashi Matsushita 教授(日本光子工厂所长)	2004 年 5 月 11 日

序号	报告题目	报告人	报告时间
47	流变仪原理及其应用	谢雷东 副研究员(辐射技术应用研究中心)	2004 年 5 月 14 日
48	碳纳米管与过渡金属接触研究	张志滨 博士	2004 年 5 月 14 日
49	Ultrasensitive Quantitative Analysis of Biomolecules using Microfluidics and Single-molecule Detection	Jeff Tza-Huei Wang Whitaker Biomedical Engineering Institute，Johns Hopkins University	2004 年 5 月 21 日
50	Nanoscale Science with a Single Molecule and Single Cell	Prof. James Gimzewski (University of California, Los Angeles, Department of Chemistry & Biochemistry)	2004 年 5 月 27 日
51	Methods, apparatus, and software for macromolecular crystallography data collection and structure solving--the Brookhaven experience	Prof. Robert M. Sweet (Biology Department, Brookhaven National Labratory, USA)	2004 年 6 月 10 日
52	Introduction to DESY and the Power Supplies	Dr. Hans-Joerg Eckoldt (MKK Group, DESY, Germany)	2004 年 6 月 15 日
53	Toshiba's performance on synchrotron radiation sources (SPring-8 etc.) 100MeV linac: with 90MW klystron and two accelerator structures Booster ring: with 5-cell cavity d) Storage ring: RF System with 180kW Klystrons and normal conductivity cavities	Director Technical Executive Koji Namiki 等 (东芝电子管和器件公司)	2004 年 6 月 24 日
54	1.Experimental study on Insospin effect in heavy ion collisions at intermediate energies 2.Interaction of Heavy Ion with Biomolecules	1. 靳根明 研究员 2. 张丰收 研究员	2004 年 6 月 23 日
55	1.Power Supply RF System and Grounding System 2.Analytical Treatment of Dynamic Apertures due to multipoles and Wigglers in Storage Ring	1. Prof.Bob Hettel(SLAC USA 2. Prof. Gao Jie (Laboratoire de L'Acclerateur Lineaire, France)	2004 年 6 月 25 日
56	Beam Diagnosis System and Control System for Light Source	Prof. Bob Hettel (SLAC USA)	2004 年 6 月 24 日
57	Three-Dimensional Diffraction Microscopy and Its Applications	Dr. Miao Jianwei (Standford University)	2004 年 6 月 29 日

序号	报告题目	报告人	报告时间
58	Nuclear resonant inelastic X-ray scattering at APS: instruments and activities	Dr. Zhao Jiyong (美国 APS)	2004 年 7 月 2 日
59	The emerging physical pictures of nucleus-nucleus at Relativistic Heavy Ion Collider	黄焕中 教授 (美国加州大学 Los Angeles 分校; 上海应用物理所客座研究员)	2004 年 7 月 7 日
60	低温等离子体在材料科学中的应用	孙卓 教授(华东师范大学)	2004 年 7 月 8 日
61	MEMS Technology from Research to Commercialization Three-dimensional Micro/ Nanostructures Formed by Synchrotron Radiation Lithography	Prof. Sugiyama (Ritsumeikan University, Japan)	2004 年 7 月 13 日
62	Charm and Charmonium production at RHIC	台安 博士(美国加州大学 Los Angeles 分校)	2004 年 7 月 21 日
63	High Performance Computing in Shanghai Supercomputer Centre	袁行球 博士(上海超级计算机中心)	2004 年 8 月 12 日
64	Thermal Strangeness Production and Strange Resonances	Prof. Johann Rafelski (University of Arizona, Tucson, USA)	2004 年 8 月 19 日
65	Microragiography/Microtomography using synchrotron X-rays	Prof. Jung Ho Je (Pohang University of Sci. and Tech.)	2004 年 9 月 6 日
66	Third Generation Synchrotron Radiation Accelerator---Diamond Light Source, UK I : Introduction to the present status II: Mechanical and thermal design and optimization	Dr. Huang Houcheng (Diamond Light Source, UK)	2004 年 9 月 17 日
67	Nanoscience Using Synchrotron Radiation	Prof. Bruce Hamilton (University of Manchester Institute of Science and Technology, UK)	2004 年 9 月 17 日
68	1.Introduction of Radiopharmaceutical Studies at National Institute of Radiological Sciences, Japan 2.The Development of PET Tracers for Imaging Benzodi Azepine Receptor in Brain and Tumor	Dr. Kazutoshi Suzuki Ming-Rong Zhang	2004 年 9 月 21 日
69	Introduction of PSI and SLS	Prof. Dr. Ralph Eichler 所长 PSI (Paul Scherrer Institue, Switzerland)	2004 年 10 月 8 日

序号	报告题目	报告人	报告时间
70	Gene Sensors: The Detection of specific targeted Sequences on DNA	Prof. Alan J. Heeger (2000 年诺贝尔化学奖获得者，美国加州大学 Santa Barbara)	2004 年 10 月 8 日
71	Partonic Collectivity at RHIC	许怒(Nu Xu) 研究员 (美国 Lawrence Berkeley National Laboratory)	2004 年 10 月 22 日
72	1. The future of photon sciences at DESY 2. PETRA III - a new high brilliance synchrotron radiation source at DESY	1．P rof. Schneider 2．Dr. Franz (Deutsches Elektronen-Synchrotron,Germany)	2004 年 10 月 15 日
73	Brief Introduction of TRIUMF	Prof. Philip L. Gardner (TRIUMF, Canadian's National Laboratory for Particle and Nuclear Physics)	2004 年 10 月 22 日
74	1.科技发展与知识产权 2.申请自然科学基金的质量问题	沈文庆 院士	2004 年 10 月 28 日
75	同步辐射系列报告	何建华等	2004 年 11 月 9 日
76	科学大师的启示	沈文庆 院士	2004 年 11 月 12 日
77	The Linac Coherent Light Source Electron Beam	Prof. James. Clendenin (美国 SLAC)	2004 年 11 月 29 日
78	中长期科学技术规划—关于基础研究	沈文庆 院士	2004 年 12 月 15 日
79	Search for Pentaqaurk in STAR at RHIC	Prof. Huanzhong Huang (University of California at Los Angeles)	2004 年 12 月 22 日
80	In situ Diffraction at SRS	Dr. John Warren (from SRS, UK)	2004 年 12 月 22 日

附录 4

2003 年专利申请、授权项目一览表

序号	专利名称	申请号	专利号	专利类型
1	^{18}F 氟标记的苯并吡喃类化合物及其制备方法和作为多巴胺 D4 受体显像剂的应用	03115164.7		发明
2	管式超滤元件制造方法	03115298.8		发明
3	DNA 单分子有序化测序方法	03115428.X		发明
4	一种基于原子力显微镜的测量衬底上样品高度的装置	03228129.3		实用新型
5	单个生物大分子的分离方法	03115943.5		发明
6	侧向离子束诱导电荷显微分析技术	03129326.3		发明
7	管式超滤膜元件卷管、成膜同步连续制备工艺	03141410.9		发明
8	木材和竹板用酚醛数脂胶粘剂的制造方法	03141762.0		发明
9	免疫微阵列蛋白质芯片	03150532.5		发明
10	紫外光直接辐照真丝绸形成接枝共聚物的方法	03151467.7		发明
11	人造板中甲醛含量的快速无损分析方法	200310108145.5		发明
12	中草药真伪及质量鉴别的快速无损分析方法	200310108358.8		发明
13	膜生物反应器沉浸式平片滤膜元件	200320109218.8		实用新型
14	$[^{188}Re\ (H_2O)_3(CO)_3]^+$试剂盒及其制备方法	200310108525.9		发明
15	一种用于 DNA 操纵的云母衬底的制造方法	00116715.4	ZL00116715.4	发明
16	1-羟基亚乙基二膦酸盐药盒、制备方法及其应用	00115864.3	ZL00115864.3	发明
17	Re-188 硫化铼混悬液制剂药盒及其制备方法	00111447.6	ZL00111447.6	发明
18	大片段脱氧核糖核酸芯片及其制造方法	98110965.9	ZL98110965.9	发明

2004 年专利申请、授权项目一览表

序号	专利名称	专利申请号	授权专利号	专利类型
1	一种磁性纳米放射性药物及其制备方法	200410002030.2		发明
2	零磁通电流传感器电路	200410015916.0		发明
3	以动态组合模式“蘸笔”纳米刻蚀技术制造纳米图形的方法	200410016197.4		发明
4	碳纳米结构体转变为纳米金刚石的方法	200410016926.6		发明
5	用于人体腔道支架上的医用聚氨酯膜及其制备方法	200410017746.X		发明
6	快速制备 AFM 生物样品的方法	200410017432.X		发明
7	带有不同官能团的窄粒径分布磁性高分子纳米微球的制备方法和装置	200410017912.6		发明
8	C_{60} 的衍生物富勒醇在滋养毛发方面的应用	200410018372.3		发明
9	膜——生物反应器专用滤膜的测试装置	200420022771.2		实用新型
10	医用聚氨酯透气膜及其制备方法和应用	200410025032.3		发明
11	高分子薄膜与无机晶体涂层复合材料及其制备方法	200410025135.X		发明
12	一种硅烷化云母基底及其在蛋白质晶体生长中的应用	200410025134.5		发明
13	一种医用高分子超疏水膜的制备方法	200410025734.1		发明
14	X 射线相衬成像的方法和系统	200410053014.6		发明
15	电子加速器加速管保护环装置	200420090483.0		实用新型
16	工业用电子加速器引出窗	200420090481.1		实用新型
17	强流电子枪阴极装置	200420090482.6		实用新型

序号	专利名称	专利申请号	授权专利号	专利类型
18	分离并再放置纳米颗粒的方法	200410067418.0		发明
19	硫脲壳聚糖-Ag+络合物及其制备方法和用途	200410084798.9		发明
20	工业用电子加速器的扫描盒	200420110679.1		实用新型
21	电子加速器钛箔更换装置	200420110680.4		实用新型
22	一种壳聚糖超细粉末的制备方法	200410089449.6		发明
23	DNA 的荧光检测方法及其传感器	200410089533.8		发明
24	真丝绸的染色方法	200410093245.X		发明
25	检测含鸟嘌呤的 DNA 的电化学方法及利用其的防伪认证方法	200410099297.8		发明
26	辐射交联 150℃阻燃的聚烯烃热收缩材料		ZL99125748.0	发明
27	辐射交联低烟无卤阻燃低温收缩聚烯烃热收缩材料		ZL00115353.6	发明
28	三氟甲基磺酸乙-三甲基铵-4，5-二甲氧基苯甲醛的制备方法		ZL00125486.3	发明
29	一种 ^{32}P 放射性血管支架及其制作方法		ZL01105119.1	发明
30	钯-103 种子药物及其制备方法		ZL01105243.0	发明
31	衬底介导的膜蛋白脂双层中的重组方法		ZL01126362.8	发明
32	构建纳米图形和纳米结构的操纵方法		ZL02110540.5	发明
33	以 C_{60} 为载体的骨靶向治疗药物 C_{60}-AEDP 及其用途		ZL02136178.9	发明
34	一种基于原子力显微镜的测量衬底上样品高度的装置		ZL03228129.3	实用新型
35	膜生物反应器沉浸式平片滤膜元件		ZL200320109218.8	实用新型